ANL-6562
Reactor Technology
(TID-4500, 18th Ed.)
AEC Research and
Development Report

ARGONNE NATIONAL LABORATORY
9700 South Cass Avenue
Argonne, Illinois

BOILING WATER REACTOR TECHNOLOGY STATUS OF THE ART REPORT

VOLUME II. WATER CHEMISTRY AND CORROSION

by

C. R. Breden

Reactor Engineering Division

February, 1963

Operated by The University of Chicago
under
Contract W-31-109-eng-38
with the
U. S. Atomic Energy Commission

DISCLAIMER

FOREWORD

The Boiling Water Reactor Technology Status of the Art Report consists of three volumes that treat respectively the following major areas of boiling water reactor design:

Vol. I - Heat Transfer and Hydraulics (ANL-6561)
Vol. II - Water Chemistry and Corrosion (ANL-6562)
Vol. III - Engineering Design = Probably never to published. ANL-4/11/66

The objective is to provide the reader with information pertinent to the design and operation of boiling water reactor power plants. Nuclear instrumentation and reactor control are not covered in this Status of the Art Report as this subject is adequately covered in "Nuclear Reactor Control Engineering," a book by J. M. Harrer. Boiling reactor physics is not reviewed in this status report since a synoptic treatment would only duplicate material already published in ANL-5711, 5849, 6221, 6305, 6306 and the revised edition of ANL-5800. Radioisotope hazards analysis and safeguards are also not included since these and other related disciplines are the subject of timely, single-volume documents available in the open literature.

In compiling and evaluating the material in each volume, the authors also have been confronted with the problem of timeliness of data. It is anticipated that subsequent editions of each volume shall be published periodically, consistent with the degree of technological advance in the status of the art of boiling water reactors. Accordingly the attention of the reader is directed to the terminal date for compilation of data which appear in the front matter of each volume.

The writers wish to acknowledge the cooperation of the leading commercial developers of boiling water nuclear power plants -- Allis-Chalmers Manufacturing Company, General Electric Company, and General Nuclear Engineering Company -- for providing technical details on their respective power plants. Grateful recognition is also given to Mr. B. Dieter and members of the Technical Publications Department of Argonne National Laboratory in assisting the Reactor Engineering Division staff in the final preparation of these three volumes.

C. Victor Pearson
Editor
February 1, 1963

TABLE OF CONTENTS

VOLUME II: WATER CHEMISTRY AND CORROSION

TABLE OF CONTENTS

TABLE OF CONTENTS

TABLE OF CONTENTS

TABLE OF CONTENTS

TABLE OF CONTENTS

TABLE OF CONTENTS

LIST OF FIGURES

LIST OF FIGURES

LIST OF FIGURES

LIST OF FIGURES

LIST OF TABLES

LIST OF TABLES

LIST OF TABLES

ACKNOWLEDGMENTS

In an early stage of the writing of this report, preliminary contributions to material subsequently allocated to Volume II were made by A. P. Gavin, N. R. Grant, W. G. Knapp, R. H. Leyse, and S. B. Skladzien. In addition, later contributions were made as follows: A. P. Gavin wrote the description of the oxygen addition experiment in EBWR, and reviewed the sections on Water Decomposition and Water Chemistry; W. G. Knapp reviewed the section on Corrosion Product Deposits; and S. B. Skladzien reviewed the section on Radioactivity.

Grateful acknowledgment is due R. F. S. Robertson and Peter Dyne of Chalk River, Canada, who reviewed the section on Water Decomposition.

Special thanks are due to J. E. Draley and W. E. Ruther of the Argonne National Laboratory Metallurgy Division who reviewed the section on Materials Corrosion and brought up to date the subsection on aluminum alloy development.

VOLUME II

WATER CHEMISTRY AND CORROSION

by

C. R. Breden

1. INTRODUCTION

The use of water as a moderator-coolant in a power reactor creates basic problems of nuclear physics, hydraulics, and heat transfer, and also a number of associated problems.

Some of these associated problems are chemical in nature and can be covered by the terms "water chemistry." One of the most important of these problems is that of corrosion. Since we emphasize the importance of the corrosion aspect of the problem, in this volume, we have selected the somewhat redundant title "Water Chemistry and Corrosion."

The volume is based on investigations reported in the unclassified literature. The literature coverage is believed to be fairly complete into 1959, but less complete since then.

The material has been arbitrarily divided into five sections: Water Decomposition, Water Chemistry, Materials Corrosion, Corrosion Product Deposits and Radioactivity. Due to the overlapping of subject matter, the separation of material into the various sections is not always clearly defined. As an example, one section is labeled "Radioactivity" but part of the material on radioactivity resulting from activation of corrosion products is given in the section on Corrosion Product Deposits. Sometimes the decision regarding placement is based on convenience, other times it is a matter of emphasis.

One of the reasons for the overlapping of the different sections is the interrelationship among the various subjects. This is illustrated by water decomposition, which affects oxygen content, which affects corrosion, which affects corrosion products, which affect radioactivity, deposits, and water purity. This completes the cycle since water purity affects water decomposition.

The use of the term "Water Chemistry" for title of a section as well as in the overall title leaves something to be desired but was done simply for lack of a better section title. The material covered in the

section on water chemistry concerns the composition of materials in contact with the water and the methods used to minimize corrosion and maintain water quality. The other section titles are self-explanatory with possible exception of Radioactivity, and in this case some explanation may be in order as to why radioactivity was included in a volume on chemistry. The reason is because of the chemical aspects of the problem, i.e., the identity of the chemical elements involved and the desirability of maintaining chemical control.

One important chemical subject not included is that of decontamination. The primary reason for this is that at least into 1959, there had been no truly serious contamination incident in a boiling water reactor, and consequently there was little or no published information on this subject.

One last thought . . . this is really a progress report, and not a final report. Investigation will continue as long as there is room for improvement in learning how to live and operate with less expensive materials.

2. WATER DECOMPOSITION

2.1. Introduction

Water decomposition, as it applies to water-moderated and cooled high temperature power reactors, may be defined as the breakdown by radiation of the water molecule, H_2O (or D_2O), into radiolytic gas which is a mixture of two volumes of hydrogen (or deuterium) and one volume of oxygen, i.e., $2H_2$ (or $2D_2$) + O_2. At low temperatures, hydrogen peroxide, H_2O_2 (or D_2O_2) is found in addition to H_2 and O_2.

Water decomposition is of interest to the reactor engineer because the gas produced, if sufficient in quantity, can create problems related to nuclear physics, hydraulics, heat transfer, air-ejector design, and corrosion. In addition, it can produce explosion hazards, and, if the water is D_2O, the loss of D_2 may be a problem.

2.2. Theory

The definition of water decomposition given above tends to over-simplify the subject. The theory of the mechanism results from a vast amount of research carried out in order to understand the nature of the problem. Some reviews of particular interest, from the reactor engineer's point of view, are given in the list of references.[1-5]

Briefly, it is believed that, under ionizing radiation, the water molecule is split into free radicals. The reaction is expressed in chemical symbols:

$$H_2O \rightarrow H + OH \quad . \tag{2.1}$$

The various phenomena observed experimentally in water decomposition studies are believed to result from the reactions of these free radicals with themselves, and with other radicals, ions, or molecules.

The amount or degree of water decomposition is believed to result from an equilibrium condition between a forward reaction, tending to produce molecular products and a back reaction in which water is reformed.

Reactions involved in the forward reaction are: the reaction between two hydrogen radicals to form molecular hydrogen,

$$H + H \rightarrow H_2 \quad , \tag{2.2}$$

and the reaction between two hydroxyl radicals to form molecular hydrogen peroxide,

$$OH + OH \rightarrow H_2O_2 \quad . \tag{2.3}$$

The net result of reactions (2.1), (2.2) and (2.3) is the breakdown of water to form molecular hydrogen and molecular hydrogen peroxide,

$$2H_2O \rightarrow H_2 + H_2O_2 \quad . \tag{2.4}$$

Under irradiation, and even without irradiation at temperatures above about 150°C, hydrogen peroxide decomposes to form water and oxygen gas,

$$H_2O_2 \rightarrow H_2O + \frac{1}{2} O_2 \quad . \tag{2.5}$$

Radical reactions responsible for the back reactions, reforming water, are:

$$H + OH \rightarrow H_2O \quad , \tag{2.6}$$

$$H + H_2O_2 \rightarrow H_2O + OH \quad , \tag{2.7}$$

$$OH + H_2 \rightarrow H_2O + H \quad . \tag{2.8}$$

The net result of (2.7) and (2.8), which together constitute a chain reaction, is

$$H_2 + H_2O_2 \rightarrow 2H_2O \quad . \tag{2.9}$$

At low temperatures, H_2 and O_2 dissolved in water react under radiation to form H_2O_2; at 200°C and 250°C they were found to react stoichiometrically under γ-irradiation to form water at a rate independent of total dose and of pressure.[6]

$$2H_2 + O_2 \rightarrow 2H_2O \quad . \tag{2.10}$$

Similar behavior has been observed[7] in stainless steel autoclaves exposed to in-pile irradiation at temperatures ranging from 164°C to 260°C.

2.3. Factors Affecting Water Decomposition

1. Nature of Ionizing Radiation

One of the most important factors influencing water decomposition is the nature of the radiation. Energy is dissipated in the water by the stopping of fast charged particles which range from fission fragments, through α-particles, recoil protons (or deuterons) produced by inelastic neutron scattering, to fast electrons resulting from absorption of gamma rays and resulting from decay of fission products.

The primary chemical reaction can be written:

$$H_2O \rightsquigarrow H + OH + H_2 + H_2O_2 \quad . \tag{2.11}$$

The yields per 100 ev of energy absorbed are expressed as G(H), G(OH), $G(H_2)$ and $G(H_2O_2)$.

Although stoichiometry requires[5] that $G(H) + 2G(H_2) = G(OH) + 2G(H_2O_2)$, the yields of H and OH and also H_2 and H_2O_2 are not necessarily equal to each other.[8] The yields of H_2 and H_2O_2 are decreased by certain solutes which scavenge the precursors in the particle tracks.[9] The yields depend on the type of radiation, or more specifically, on the energy transferred to the solution per unit length along the track of the charged particle. The initial linear energy transfer (LET) parameter varies from ~5 x 10^4 kev/μ* of path for fission recoil particles to ~0.2 kev/μ for fast electrons. (Fig. 2.1).[5]

---

*μ = Micron = 1 x 10^{-6} meter.

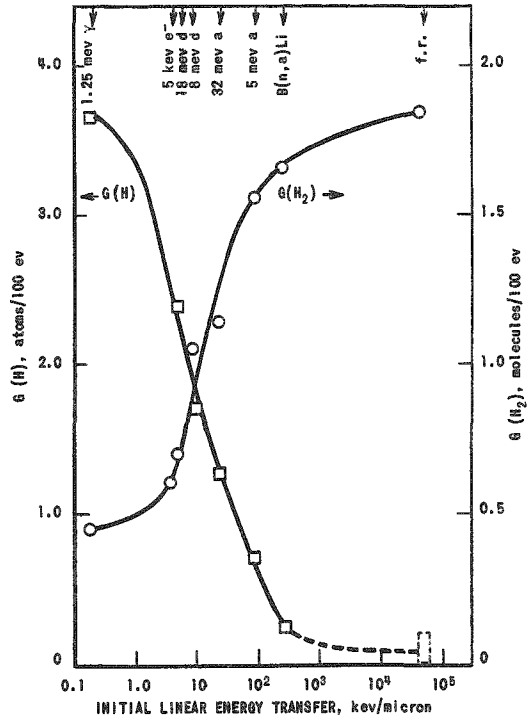

Fig. 2.1

Yields of (H) and (H_2) as a Function of Initial Linear Energy Transfer

The yields of $G(H_2)$ and $G(H_2O_2)$ are largest, i.e. net decomposition is greatest, for radiations such as fission recoil particles with large LET. The yields G(H) and G(OH) are largest, i.e., lowest net decomposition, for radiations such as fast electrons with small LET. The yields G(H) and $G(H_2)$ for recoil protons (or deuterons) produced in a reactor by the scattering of fast neutrons are intermediate between those for fast electrons and those for recoil particles. The net or average yield depends on the energy spectrum of the neutrons.

For gamma rays (or fast electrons) the steady-state pressure resulting from gaseous decomposition is nearly zero; whereas, for fission recoil particles, the steady-state pressure may be several thousand psi. The distribution of total energy among different types of ionizing radiations differs among reactors. For instance, in the Oak Ridge Graphite Reactor where about two-thirds of the energy imparted to ordinary water is by neutron scattering and about one-third by absorption of gamma rays, the yield $G(H_2)$ is about 1.1.[5]

2. Energy of Radiation

The energy of radiation influences the yields through the LET parameter. For example, for any type of particle, LET increases with a decrease in energy and results in an increase in $G(H_2)$ and a decrease in G(H).[5]

3. Radiation Intensity or Dose Rate

The effect of dose rate of 1.5 Mev electrons was studied[10] in the range up to 4×10^{20} ev/gram-min on steady state concentrations of H_2 and H_2O_2 in the irradiation of pure degassed water. It was found that under the conditions employed increasing the intensity favored the radical-radical reactions leading to decomposition products, over the radical-product back reactions.[5]

4. Temperature

Temperature has little or no effect on the forward reaction, but an increase in temperature favors the back reaction, and reaction (2.10). As a result, higher temperature favors lower net decomposition.(11)

As was mentioned previously, the breakdown of molecular hydrogen peroxide occurs at temperatures of about 150°C.

5. Substitution of Deuterium for Hydrogen

Limited data indicate that for decomposition produced by gamma rays, $G(D_2)$ is about 25% less than $G(H_2)$ and G(D) is about 25% greater than G(H).(5)

For densely ionizing radiation, resulting from B^{10} (n,α) Li^7, $G(H_2) = G(D_2)$.(4)

6. Effects of Ionic Impurities

Ionic impurities have no effect on the forward reaction producing molecular products. Some ionic impurities, however, have been found to promote water decomposition by reducing the back reaction, acting as radical scavengers. Particularly effective examples are Br^-, Cl^-, and I^-, whose action may be illustrated by

$$OH + Br^- \rightarrow Br + OH^- \qquad (2.12)$$

$$H + Br \rightarrow Br^- + H^+ \qquad (2.13)$$

$$H^+ + OH^- \rightarrow H_2O \qquad (2.14)$$

with the net result

$$H + OH \rightarrow H_2O \quad .$$

When this occurs the radicals are not available for the back reactions (2.7) and (2.8).

Other ions, which can act as radical scavengers in solution, are cations which can exist in two valent states in solution such as Fe^{++}, Cu^+ and Ce^{++++}. These cations must be present in acid solution to prevent hydrolysis.(4)

Some ions, such as OH^- when present as KOH, and PO_4^{---} when present as H_3PO_4, show little effect.(11)

H_3BO_3 irradiated in CP-3', in concentrations up to 0.02 M (M = molar), showed no effect on water decomposition. At higher concentrations, decomposition occurred at a rate of 1.83 mM (micro molar) H_2 and H_2O_2 per minute per molar boric acid.(12)

H_2SO_4 irradiated in Oak Ridge, resulted in high peroxide concentrations, suggesting that a persulfuric acid may have been formed which is more stable to radiation than H_2O_2.(11)

H^+ ions (low pH) do not affect $G(H_2)$ but do affect $G(H_2O_2)$, H_2O_2 being far less stable in basic solution. The net effect is that in acid solution H_2O_2 appears as a decomposition product while in basic or neutral solution O_2 is the product.(4)

The effect of pH appears to depend on the nature of the impurities and the particular reactions involved. For instance constant yields of hydrogen gas were obtained(13) by x-ray irradiation of deaerated solutions of nitrite, arsenite, selenite, ferrocyanide, iodide, and bromide, regardless of solute concentration or of pH from 2 to 11.

On the other hand in the presence of Cl^- ion, the concentration of H^+ ions has a marked effect. For a given chloride ion concentration, water decomposition increases with increasing hydrogen ion concentration, and for a given hydrogen ion concentration, decomposition increases with chloride ion concentration.(11)

Other cases have been noted(14) where water decomposition reactions show a marked dependence on pH.

7. Effects of Decomposition Products

The relative amounts of H_2, O_2, and H_2O_2 present influence the water decomposition.

An excess of H_2 increases or favors the back reaction, thus decreasing net decomposition.(11) When pure water containing only dissolved H_2 was irradiated in the Oak Ridge Reactor, no O_2 or H_2O_2 could be detected.(15) And, if H_2 is bubbled through dilute H_2O_2 solutions under irradiation, the H_2O_2 rapidly decreases to an undetectable level.(6)

Excess H_2 also stabilizes water to α-irradiation. In CP-3' irradiation of boric acid solutions, it was found that if a H_2 concentration of 8×10^{-5} M is present initially, the boric acid concentration can be increased to about 70×10^{-3} M with no net evolution of H_2 occurring. Hart(12) estimated that if a H_2 pressure of one atmosphere were maintained over the water, 0.5 M boric acid solutions could be irradiated in CP-3' without

decomposition. The presence of excess H_2 should help stabilize solutions of natural UO_2SO_4 to neutron irradiation, and also natural-uranium oxide slurries in which a smaller fraction of the fission fragments enter the water. It should have no effect, however, on enriched UO_2SO_4 solutions.[4]

An excess of O_2 or H_2O_2 decreases the back reaction and thus increases net decomposition.[11]

8. Effect of Undissolved Solids

Some undissolved solids, such as silicates or colloidal aluminum hydroxide, under certain circumstances appear to promote decomposition. The manner in which they function is not understood.[1] Some metallic substances, such as platinum, palladium, etc., have catalytic properties[2] toward reaction (2.10). Stainless steel corrosion products have also been reported to exert a catalytic effect in this reaction,[16] at least on the walls of the equipment.

9. Effect of Boiling

Normally, in water moderated reactors, decomposition of water is not a serious problem (if the water is pure) since there is a large reserve γ-ray flux available for promoting the recombination reaction (2.9). But during shaking, boiling, or bubbling, the hydrogen escapes from the aqueous phase and the radiation induced decomposition of hydrogen peroxide leads to oxygen evolution, (2.5). In gamma radiation experiments on pure water, Gordon and Hart[17] showed that bubbling had a marked effect. In completely filled cells, with no vapor space and with no bubbling or shaking, there was no net decomposition, $G(H_2)$ and $G(O_2)$ were equal to zero. With vapor space and with bubbling induced by CO_2 under steady-state irradiation conditions, $G(H_2) = 0.40 \pm 0.04$ and $G(O_2) = 0.20 \pm 0.02$ for γ-rays, which correspond closely to the established molecular hydrogen yields for these radiations. This indicates that the back-reaction is essentially absent during efficient bubbling. With the vapor space, but with no bubbling, the $G(H_2)$ dropped to 3% of the value with bubbling.

2.4. Water Decomposition in Pressurized Water Reactors

The subject of water decomposition in pressurized light water reactors can be summarized very briefly. In these reactors, as normally operated, there is essentially no net water decomposition.[18] The factors believed to be responsible for this include the following:

1. The high temperature favors the recombination or back reaction.

2. The high proportion of gamma flux favors the production of radicals over that of molecular products and so favors the back reaction, (2.9).

3. The steel system favors the thermal reaction, (2.10).

4. The excess H_2 maintained in the system favors the above reaction, (2.10), and also favors the back reaction, (2.9).

5. Reducing the O_2 content of the water tends to reduce net decomposition. Operating procedures to reduce O_2 content include: (1) use of hydrazine as an oxygen scavenger at startup; (2) reaction of O_2 with excess hydrogen according to equation (2.11), under the influence of heat and gamma flux at startup.

6. The absence of a vapor space above the moderator inhibits the escape of gaseous decomposition products and thus favors the back reaction.

7. High water purity, maintained by continuously passing a portion of the reactor water through a mixed bed ion-exchange, favors low net decomposition.[2]

8. Use of LiOH to supply OH^- ions has little or no effect on water decomposition.

9. Although not directly concerned with water decomposition, pressurized water reactor results on N_2 studies indicate that when H_2 and N_2 are both present in solution, ammonia (NH_3) is formed under reactor irradiation. When N_2 and O_2 are present, nitric acid (HNO_3) is formed. Since an alkaline condition minimizes corrosion and corrosion product problems, operation of the reactor is conducted so as to favor the formation of ammonia rather than nitric acid.[18]

Experience in CP-3' showed that in the presence of O_2 both N_2 and NH_3 may be oxidized under pile irradiation to nitric acid, resulting in increased corrosion product impurities and increased water decomposition.[2]

2.5. Water Decomposition in Boiling Water Reactors

1. BORAX-III

a. Normal Operation. BORAX-III[19] was the first of the BORAX experiments in which the steam generated was collected and led directly to a turbine. As a result, it was adaptable to studies on water decomposition. The first data on water decomposition obtained on BORAX-III are given[20a] in Table 2.1.

Table 2.1

WATER DECOMPOSITION - BORAX-III

Date	Power Level	Reactor Pressure	Gas cc/ Liter	Analysis (% by Volume)			
				CO_2	O_2	H_2	N_2 (by difference)
12/14/55	2.4 Mw	300 psig	75	0.0	29.0	54.0	17.0
12/15/55	2.4 Mw	300 psig	85	0.1	30.1	55.0	14.8
12/15/55	2.4 Mw	200 psig	75	0.2	29.8	50.6	19.4
12/15/55	4.8 Mw	300 psig	76	1.2	31.0	55.0	12.8
12/16/55	10.0 Mw	300 psig	76	0.0	31.0	59.0	10.0
		Avg.	77				

The values for quantities of gases collected per liter of condensed steam (avg. 77 cc/liter) do not include the gases dissolved in the water sample. The high amount of water decomposition, as compared to that in CP-5, came as a surprise. It was tentatively attributed to the high dissolved solids content at the time of sampling (greater than 100 ppm, primarily H_3BO_3).

Early in 1956, water decomposition data were obtained under varying water conditions.[19] Part of it was taken during an extensive study of DF (Decontamination Factor).* The reactor water, after the initial clean-up of the boric acid, had a specific resistance of 490,000 ohm-cm and a pH of 6.4. During the DF study, the pH gradually decreased to 5.2. The specific resistance decreased to 150,000 ohm-cm. After the DF studies, the anion bed was placed in service. This raised the resistivity to 750,000 ohm-cm and the pH to 6.75. The data obtained during this period of operation are plotted in Fig. 2.2 as evolved gas vs pH of reactor water. During this period of gradually improving water quality and

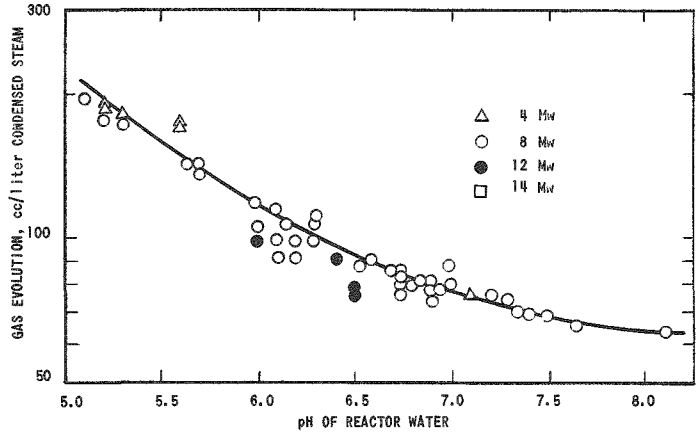

Fig. 2.2

Gas Evolution vs pH of Reactor Water in BORAX-III

* Decontamination Factor (DF), is a measure of impurity removal resulting when water goes through a process step. In this report it is used for two separate processes: (a) passage of water through an ion-exchanger, and (b) passage of water into steam: DF = impurity content before process step / impurity content after process step.

increasing pH, the non-condensate gases in the steam phase of the cycle decreased from 197 cc to 72 cc per liter of condensed steam. The data do not include the amount of gases dissolved in the condensed steam samples. This is estimated to be a constant of about 6 cc/liter, which would increase the results in the lower end of the curve by less than 10%.*

It is interesting to note that the first values obtained, 77 cc/liter, with about 100 ppm boric acid, were not significantly different from later values obtained with high purity water, confirming earlier results[12] that H_3BO_3 in these concentrations does not markedly affect water decomposition. The composition of the gases varied only slightly throughout all tests, being approximately 31% O_2, 60% H_2 and 9% N. Although the data correlate with pH, the evidence does not justify the conclusion that pH, as such, is the important factor. As was mentioned in Section 2.3.6. certain ionic impurities have a marked effect in inhibiting the back reaction. The degree to which ionic impurities affected the BORAX experiments is not known, since the pH was almost always adjusted by removal of ions with ion exchange resins and not by addition of known ions.

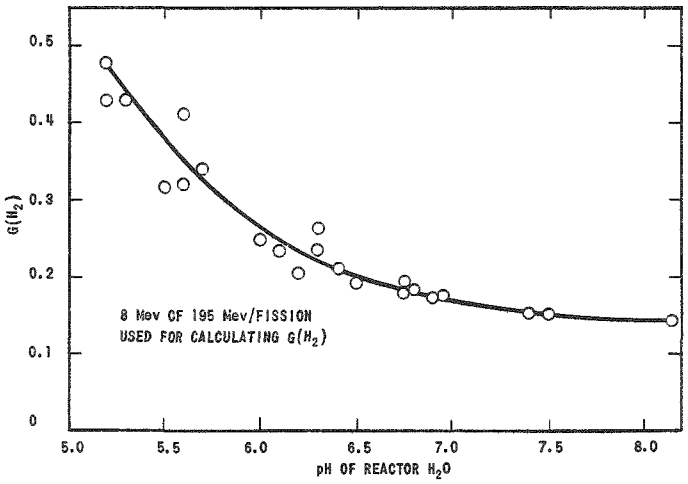

Fig. 2.3
$G(H_2)$ vs pH of Reactor Water in BORAX-III

In Fig. 2.3 the gas evolution data at 8 Mw have been recalculated to give the yield of hydrogen molecules, $G(H_2)$ per 100 ev absorbed in the water, which is plotted against pH of reactor water. For this calculation, it has been assumed that 8 Mev out of the 195 Mev per fission is used in water decomposition. It will be noted that the $G(H_2)$ value ranges roughly from about 0.2 at pH 7 to about 0.5 at pH 5.2. If the $G(H_2)$ value for the liberation rate, with no recombination, is 1.0 as has been estimated, the $G(H_2)$ range in Fig. 2.3 (0.2 to 0.5) indicates that only 50 to 80% of the decomposition gases undergo recombination to form water.

It was suggested that this low rate of recombination in a boiling water reactor, as contrasted with that in a non-boiling system,

---

*Records do not indicate if correction has been made to STP (Standard Temperature and Pressure). Correction for the 5,000 ft elevation at NRTS would lower the value by about 20%.

may be a result of the boiling process sweeping out decomposition gases, H_2 and O_2 before they could recombine to form H_2O.

Experimental evidence by Gordon and Hart[17] confirmed this view. (See Sec. 2.3.9.).

The evolution rates shown in Fig. 2.2 represent a range of 25 to 80 ppm of oxygen in the steam.

The increased decomposition became of considerable concern for several reasons. The most important reason was the possibility of accelerated corrosion from the increased oxygen concentration.

b. Effect of Additives In view of the effectiveness of added hydrogen in reducing water decomposition in pressurized water reactors, experiments were made to see if hydrogen additions to the water in BORAX-III would reduce the oxygen content of the steam. Several other additives were also tried in a preliminary manner to determine their effect on water decomposition.[20b] The results are given below.

Addition	Change in Water Decomposition
KCl, 4 gm	Increased 10%
NH_4OH, 4 cc	Increased 10%
N_2, 166 cc/liter of Condensed Steam	No effect
O_2, 26 cc/liter of Condensed Steam	Slight increase
KOH	Decreased as pH increased
H_2	Decreased in proportion to rate of addition

The preliminary test with addition of hydrogen looked sufficiently encouraging to justify further tests. The first additions were made through the feedwater sparger, at the top of the downcomer region. Later additions were made by introducing the gas through the drain line at the bottom of the reactor vessel, from which it bubbled up through the core. The hydrogen addition through the sparger was much more effective than additions through the bottom drain. (See Fig. 2.4). The greater effectiveness of sparger additions was attributed to more complete solution, better mixing, and prolonged radiation exposure time. However, hydrogen, as used in BORAX-III, was not recommended since the amount required created an excessive load on the exhaust system and probably could not be justified economically. Amounts of hydrogen needed to eliminate decomposition and reduce O_2 levels below that in the feedwater were

in excess of 180 cc H_2/liter. To see if the added H_2 reduced corrosion, total iron determinations were made of the condensate during normal operations and during the test period when hydrogen was added to the feedwater. Although the data are not conclusive, a decrease in total iron was noted when hydrogen was added (0.16 ppm to 0.05 ppm).

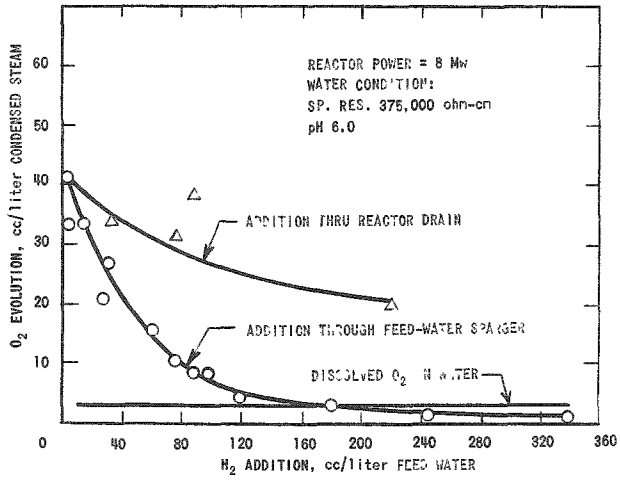

Fig. 2.4

Oxygen Evolution vs Hydrogen Addition in BORAX-III

2. EBWR

a. Normal Operation. The first data on water decomposition in EBWR are given in Table 2.2.

Table 2.2

EBWR WATER DECOMPOSITION DATA

Date	Time	Power Level, Mw	Reactor Water Quality			Gas Yield, cc/liter[a]	Condensed Steam Gas Analysis			Air Ejector Gas Flow, cfm[b]	Air Ejector Gas Analysis		
			pH	Resistivity Determined, ohm-cm	Conductivity Recorded, μmhos		O_2, %	H_2, %	Inert Gas, %		O_2, %	H_2, %	Inert Gas, %
12/23/56[c]	0115	20	7.0	180,000		50	22.7	47.0	30.3[d]		25.2	32.8	42.0
12/23/56[e]	2015	20	7.0	180,000		69	20.4	44.5	35.1[d]		22.6	27.2(?)	50.2
12/29/56[f]	2210	20	5.2	90,000		53	30.2	55.9	13.9		29.4	56.1	16.1
1/11/57[g]	1630	20	5.0(?)	410,000		47.5	29.7	68.6	1.7				
1/30/57	1715	20	7.05	900,000		66	31.0	63.4	5.6		30.4	53.9	15.7
2/11/57	1917	20	7.0	760,000		52.5	30.0	66.2	3.8		28.2	47.3	24.5
2/11/57	2330	20	7.0	600,000		46	29.2	62.4	8.4		28.9	44.6	26.5
2/12/57	1300	20	7.15	640,000		45.7	29.3	69.2	1.5				
2/12/57	2020	20	7.2		0.8	47.8	30.2	67.3	2.5		29.5	48.0	22.5
2/13/57	1030	20	7.1		0.9	58.5	31.6	66.6	1.8				
2/13/57	1920	20	7.08		0.9	55	30.0	66.0	4.0		29.9	47.5	22.6
2/14/57	1200	20	7.1		1.0	57.8	31.1	66.5	1.8		29.9	49.7	20.4
2/14/57	2110	20	7.02		1.0	63.3	32.5	67.5	0.0	1.2	29.7	51.8	18.5
2/18/57	1115	20	7.3		0.8	59.8	31.7	67.0	< 1.3	1.0	30.5	56.0	13.5
2/20/57	1000	20	6.9		0.9	58.0	31.7	66.2	2.0	0.92	30.9	56.1	13.0
Average of samples of 1/11/57 through 2/20/57						55.1	30.7	66.4	2.9		29.7	50.5	19.7

[a]Not corrected for gases dissolved in the condensed steam.

[b]Not corrected for gas density; values reported are for air at 80°F in cubic feet per minute.

[c]This sample was steam bypassed to the condenser.

[d]Values are high owing to transfer of sample or actual nitrogen in system.

[e]This sample was steam going to the turbine.

[f]Boric acid in the reactor water was 0.748 g/liter for this sample.

[g]Only 8.3 ppm boric acid was in the reactor water for this sample.

The results showed a rather wide spread from 47.5 cc to 69 cc gas/liter and averaged 55.1 cc gas/liter of condensed steam (uncorrected for H_2 and O_2 dissolved in the condensed steam sample). The average of the twelve analyses used gave 30.7% O_2, 66.4% H_2, and 2.9% inerts. This decomposition was about three-fourths that obtained from BORAX-III, namely 77 cc gas/liter analyzing 32% O_2, 60% H_2, and 8% inerts with water at pH 7.0.* The pressure and temperature in EBWR were 600 psig and 488°F (253°C) as compared to 300 psig and 420°F (216°C) in BORAX.

The results obtained December 29, 1956, are of interest because they indicate that the presence of 0.748 gm boric acid/liter of water (pH 5.2 and resistivity 90,000 ohm-cm) had no significant effect on water decomposition.(21) The decomposition, 53 cc total gas/liter of condensed steam at 20 Mwt, was very close to the 55.1 cc/liter average. This confirms earlier fundamental studies(12) (Sec. 2.3.6.) which showed that concentrations up to 0.02 M, (1.237 gm H_3BO_3/liter) have no effect on water decomposition.

Since radiolytic gas consists of two volumes of hydrogen and one volume of oxygen, $2H_2 + O_2$, the simplest measure of the amount of water decomposition is the total volume of radiolytic gas or the volume of hydrogen, or oxygen (since the ratio is stoichiometric) associated with a definite volume of condensed steam.* This should be distinguished from the rate of water decomposition, which is commonly reported in terms of volume of oxygen, hydrogen, or radiolytic gas at STP evolved per unit of time, e.g., cc/sec, or liters/min, vs reactor power. Some times the rate is reported as weight of O_2 or H_2 per megawatt hour. The amount of decomposition was the measure used to evaluate water decomposition in the early work at BORAX and EBWR. It was believed to be independent of power at the power levels employed.

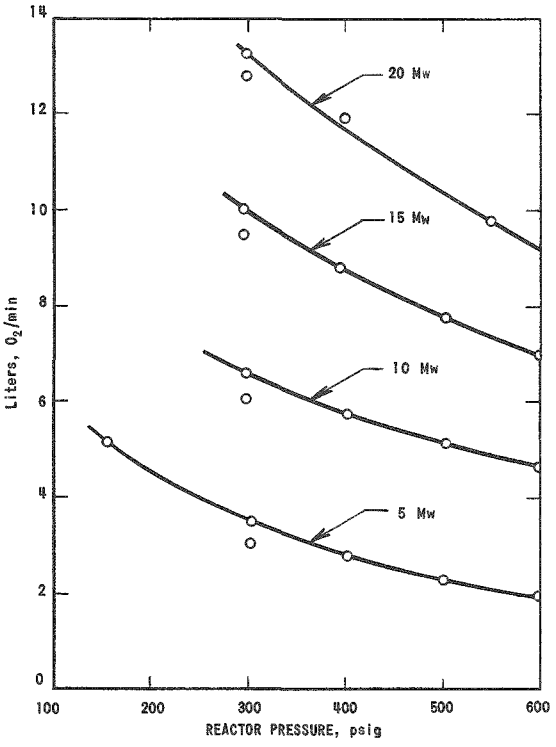

Fig. 2.5

Water Decomposition Rate in EBWR

Experiments(22-24) in EBWR, at different power levels and pressures, showed that up to 40 Mw, the rate of water decomposition increased in a linear manner with reactor power. The rate of decomposition at any power level decreased with increase in reactor pressure. Figures 2.5(23) and 2.6(24)

*See footnote p. 11.

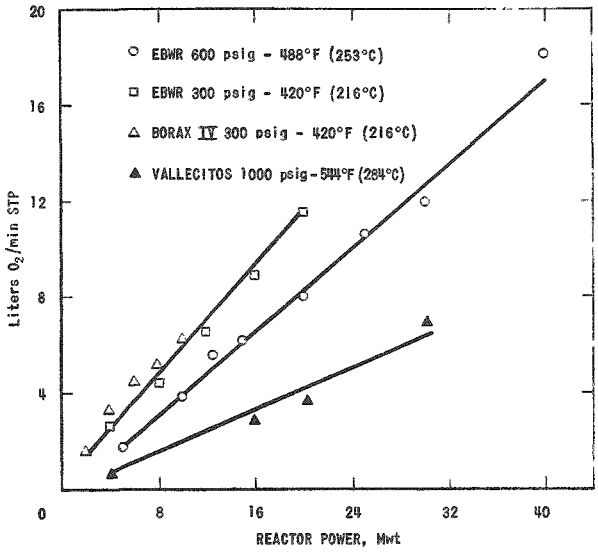

Fig. 2.6

Reactor Power vs Decomposition Rate, EBWR, BORAX-IV, VBWR

summarize the results.* Numerical values obtained for the specific rates in Fig. 2.6 were 0.4 liters O_2 (STP)/min - Mwt at 600 psig and 0.6 liters O_2 (STP)/min - Mwt at 300 psig. Assuming that 8 Mev of the total energy per fission is absorbed in water dissociation, the GH_2 values are 0.15 and 0.21, respectively.[24]

b. Effect of Hydrogen Addition. In BORAX-III the addition of gaseous hydrogen to the reactor water was shown to have a marked effect in reducing net dissociation (Sec. 2.5.1.b). Similar results have been observed also in BORAX-IV (Sec. 2.5.3.b) and in ALPR (Sec. 2.5.4.b).**

In the EBWR experiments,[25,26] hydrogen gas was metered into the reactor feedwater side stream from the purification system. After an equilibrating period of 20 min, samples of steam, condensate, and feedwater were analyzed. Gas samples were analyzed for oxygen, hydrogen, and inerts, and the liquid samples for oxygen. The results are graphically shown in Fig. 2.7, which shows the steady-state oxygen concentrations in cc/liter of condensed steam at 10 Mw and 20 Mw as a function of hydrogen additions. Data from BORAX-IV and ALPR are shown for purposes of comparison. Two conclusions reached from these experiments were:

(1) The BORAX reactor required much more added hydrogen to give a specific reduction in net decomposition than did EBWR or ALPR.

(2) Although small amounts of hydrogen caused a sharp decrease in water decomposition, the effectiveness of additional amounts diminished rapidly, and the data imply that it may be impractical to reduce the oxygen content below $\frac{1}{2}$-1 ppm of the steam by this method.

---

*Vallecitos curve added to Fig. 2.6 by C. R. Breden

**Chronologically some of these EBWR studies came after the BORAX-IV and ALPR investigations to be described later. Grouping them reactor-wise rather than chronologically was a matter of convenience.

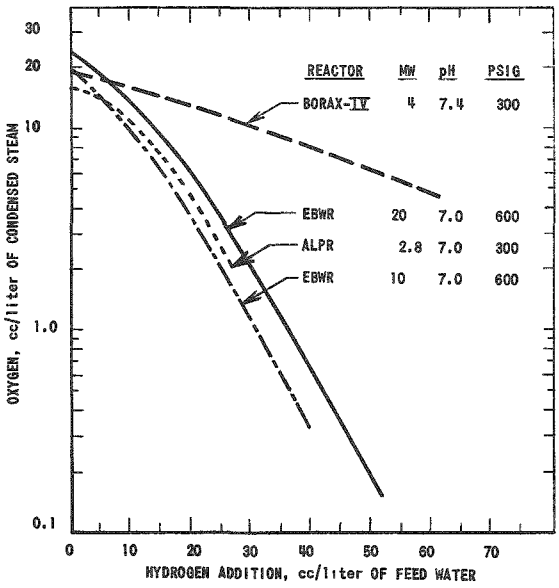

Fig. 2.7

Effect of H_2 Addition on Water Decomposition BORAX-IV, EBWR, ALPR

c. Effect of Oxygen Addition. Early static experiments described in Sec. 2.2 indicated that added oxygen would increase net decomposition. Addition of 26 cc O_2/liter of water in BORAX-III gave a slight increase (see Sec. 2.5.1.b).

(1) CP-5. During the building of EBWR the question rose as to whether the decomposition would gradually increase with increase in oxygen contamination in the feedwater or whether it would increase slowly at first and then reach a point where the rate of decomposition would rise rapidly. To investigate this matter, an experiment was performed in CP-5 to observe the rate of decomposition as a factor of oxygen contamination.(27) CP-5 is a D_2O reactor which at the time was operating at 113°F (45°C) with a power output of one megawatt. It is equipped with a catalytic recombiner for the radiolytic gases in the helium blanket. Bottled oxygen was metered into the reactor feedwater line. The temperature of the carrier gas, helium, was monitored before and after passing through the recombiner. Any increase in the ΔT (temperature change) across the recombiner was considered to be an increase in decomposition since the increase was caused by the quantity of D_2 and O_2 being combined per unit time.

The results are given in Table 2.3, which shows that the O_2 concentration was varied from 0.760 ppm O_2 to 2.21 ppm O_2 by the addition of a total of 1.50 cc O_2 per liter of heavy water. A corresponding increase in the ΔT of 2°C was observed indicating a 100% increase in decomposition. From these results the following conclusions were drawn:

(a) The presence of oxygen in the reactor water increases the rate of decomposition.

(b) Up to a concentration of 2.21 ppm O_2 in the reactor water there was no indication of a point of inflection where decomposition would suddenly increase many fold.

(c) In a boiling reactor it would be most advisable to have completely deaerated feedwater.

These conclusions are confirmed through similar work done by P. I. Dolin and B. U. Ershler[28] of the USSR who shut off the recombiner in a system such as CP-5 and watched the increase in decomposition as a function of time.

Table 2.3

OXYGEN ADDITION TO CP-5

ΔT (Normal Reactor Operation); ΔT_U = 24C*
ΔT (Pile Down); ΔT_D = 22C
$\Delta T_U - \Delta T_D$ = 2C

Time, min	O_2 add., cc/liter	ΔT, C	$\Delta T_U - \Delta T_D$, C	Remarks
0	-	21.0	0	Reactor down. O_2 conc.: 0.760 ppm.
90	-	23.0	2	Reactor up - at steady state.
93-104	0.250	-	-	
105	-	23.5	2.5	
120	-	23.9	2.9	
124-35	0.250	23.9	2.9	
180	-	24.0	3.0	
195	-	-		Reactor down.
300-11	0.250	23.0	2.0	Reactor up - at steady state.
330	-	23.1	2.1	
360-71	0.250	24.1	3.1	
390-401	0.250	24.3	3.3	
405	-	24.3	3.3	
420-31	0.250	24.2	3.2	
435	-	24.3	3.3	
450	-	24.5	3.5	O_2 conc.: 2.21 ppm.
465	-	24.6	3.6	
480	-	24.8	3.8	
495	-	25.0	4.0	
510	-	25.0	4.0	

Analysis of Carrier Gas at Start of Run:

He	99.7 %
D_2	0.03%
N_2	0.1 %
O_2	0.16%

*Average of values taken over 15 days of operation prior to experiment.

(2) EBWR. On June 26, 1959 the following experiments with oxygen addition to EBWR were performed.*

*This experiment description was written by A. P. Gavin.

Oxygen was added to the feedwater at various rates indicated in Table 2.4. Each addition rate was maintained until tests indicated that the rate of gas production was constant. This amounted to approximately ten minutes at each of the three rates. The reactor power was at 20 Mw and 600 psi during the addition period. Steam samples were taken from the steam dome by means of a $\frac{1}{8}$-inch stainless steel tube which penetrated the vessel lid. The total amount of gas produced per unit volume of condensed steam was determined by the use of a special stripping apparatus attached to this sample line. Samples of the gas from this apparatus were taken in glass bulbs for later analysis by mass spectroscopy.

Table 2.4

OXYGEN ADDITION TO EBWR

All Values cc/liter Condensed Steam

O_2 Addition Rate	0	24.7	48.5	123.2
H_2	44.8	61.1	64.7	91.0
O_2	22.4	48.2	64.3	155
Net O_2	22.4	23.5	15.8	32
Vol H_2/Vol O_2	2	2.6	4.1	2.8

The data show a definite increase in decomposition with increased oxygen addition as is indicated by the increase in the amount of both hydrogen and oxygen per unit volume of condensed steam. The results do not indicate stoichiometric balance and thus indicate that either there was a secondary reaction which consumed some of the oxygen or that there was some error in the experimental procedure. It is possible that steady state conditions were not reached in the limited time each addition rate was maintained.

Although this test does definitely indicate that increased oxygen content in the feedwater increases net water decomposition, it does not give sufficient data to establish reliable values for the amount of decomposition which could be expected if a reactor were run steadily with such an increased oxygen content in the feedwater.

d. Effect of Other Additives. The addition of nitrogen gas to EBWR feedwater produced no noticeable change in decomposition rate, reactor water conditions, or plant activities.[26] Similar results had been found in BORAX-III (see Sec. 2.5.1.b).

The reported breakdown of hydrazine (N_2H_4) to nitrogen and hydrogen under certain temperature and radiation conditions suggested its possible use in place of hydrogen to reduce water decomposition. Addition of about 3 ppm hydrazine to EBWR reactor feedwater resulted in a

sharp rise in conductivity of the water in the reactor and hotwell and in activities measured at several points in the system.[26] Decomposition decreased slightly and then increased to a value considerably above the initial value. The pH of the hotwell increased slightly while that of the reactor decreased to a value of about 5.2. No hydrazine was detected in the reactor water, and nitrate concentration in the reactor water increased from less than 0.1 to 0.8 ppm.

These results indicated that ammonia was produced in the reactor during the injection period and was carried over the steam; and that nitrate ions were formed in the reactor water and retained there. Addition of 0.5 ppm ammonia gave similar results.[26]

e. Other Experiments. The effect of the boiling process in increasing decomposition by reducing recombination has been mentioned previously, (see Sec. 2.3.9). By a simulated boiling process Gordon and Hart[17] essentially eliminated the recombination reaction and obtained almost theoretical yields of water decomposition products under gamma radiation at room temperature.

Although the rate of water decomposition in EBWR at 600 psi and 20 Mw is high (8 liters O_2/min, Fig. 2.6), it is believed that this rate would be increased to about 30 liters/min if recombination were completely eliminated and the theoretical yield of water decomposition products obtained.

If the factors responsible for this difference between observed and predicted net decomposition were understood, it could possibly influence future boiling water reactor design.

Two possible mechanisms have been suggested: (a) The stripping action involved in boiling does not free all of the hydrogen and oxygen from the water. Some gas remains in solution in the water at the top of the downcomer region, and, due to γ-flux, undergoes recombination by the time it gets to the bottom of the core. (b) Recombination is more efficient when the gases are in the vapor phase than when they are in the water phase.

These hypotheses appeared susceptible to simple experimental verification as follows: If (a) is correct, the concentration of dissolved H_2 and O_2 in the water should be higher at the top of the downcomer region than at the bottom. If (b) is correct, a sample of gas from the vapor space above the core led directly to the outside should show higher H_2 and O_2 content than a gas sample led down and up through the core before passing to the outside.

Experimental results obtained according to (a) showed O_2 concentration to be about 0.2 to 0.4 ppm at the top of the downcomer, decreasing to less than 0.1 ppm at the bottom. These values are sufficient to account for the difference between measured rate and the theoretical value. The results of one test made according to (b) showed no significant recombination in the vapor phase.

These results are far from conclusive, but they tend to indicate (a) rather than (b) as the more probable mechanism.

f. Catalytic Recombination. The original EBWR design requirements included provision for possible future operation with heavy water. Possible losses of deuterium as a result of water decomposition called for inclusion of a catalytic recombiner for the exhaust gases from the air ejector.

The original calculation for radiolytic gas production in EBWR, an extrapolation of the CP-5 value, was 48 liters of hydrogen per hour. The results from BORAX-III indicated that the value would be much higher (1140 liters of H_2 per hour). When the stoichiometric quantity of radiolytic oxygen is added to the hydrogen, the total amount of radiolytic gas is 1,710 liters/hr (1.0 cfm). This gas is explosive. When the 0.25 cfm estimated air in-leakage is added to it, the resulting mixture would still be in the explosive range. By passing this gas through a recombiner, a possible explosion hazard in the line to the stack could be eliminated.

Still another reason for recombining the gases before passing them to the stack is that the volume of such gases, if not recombined, would decrease the holdup time in the stack for decay of radioactive fission product gases in event of fuel element cladding penetration.

The particular requirements that called for development work in this application of a recombiner came from the following:

(1) Very limited pressure, 2-5 psi, was available for flow through the system. The recombiner would be physically very close to equipment vital to plant operation.

(2) Safety precautions called for operation of the unit from outside the containment shell.

(3) For economic operation on heavy water, efficiency should be of the order of 99%.

An experimental program was carried out.[26,29] Attempts to use explosive gas mixtures directly, with platinized alumina catalyst and flame arresters, were not successful. Limited tests with a flame recombiner were not promising.

The most promising results were obtained by diluting the gas with steam to approximately 5% hydrogen, adding 2-3 degrees of superheat to the inlet steam, and operating the catalyst bed below the ignition temperature of the gas mixture. An added requirement was that the exhaust temperature must be limited to safeguard equipment in the vapor recovery system. It was found that, over the range of about 3 to $8\frac{1}{4}\%$ H_2, efficiencies of about 99% were obtained.

The system as installed in EBWR is illustrated in Fig. 2.8. Briefly, reactor steam is passed through a superheater, metered, mixed with air-ejector exhaust gases, passed through a catalyst chamber filled with platinized alumina pellets in the form of $\frac{1}{8}$ in. x $\frac{1}{8}$ in. right cylinders and passed through a condenser cooler. Condensed steam is returned to the system, and cooled non-condensable gases pass through a flowmeter to the stack. Air-operated valves bypass the gases around the catalyst bed to the stack in case of unsafe operating conditions.

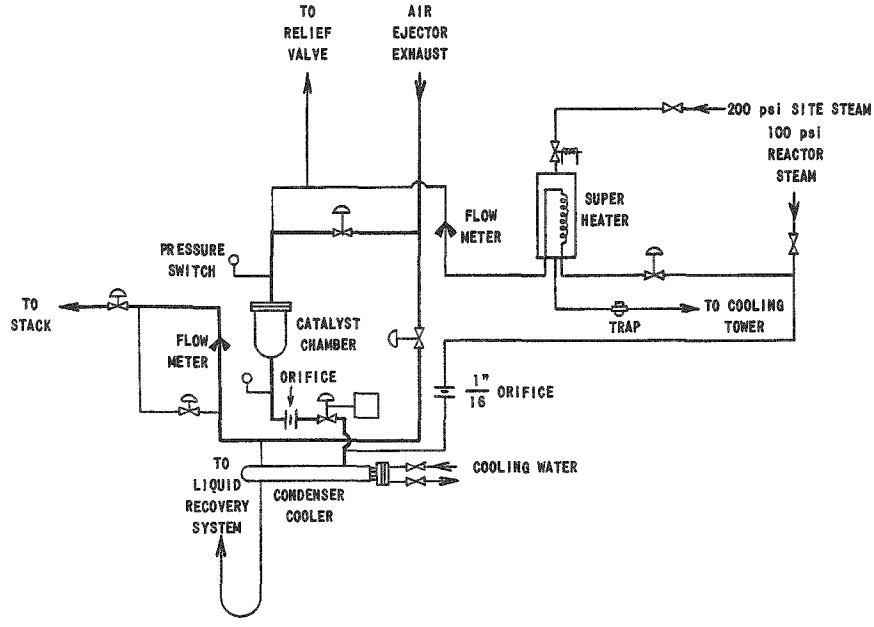

Fig. 2.8

EBWR Recombiner Flow Diagram

The recombiner was operated successfully for a period of time with estimated 99% efficiency. One minor explosion occurred in the exhaust line, as a result, it is believed, of catalyst fines being carried into it from the catalyst bed. It is believed that this particular problem has been circumvented by bleeding a small volume of diluting steam through the exhaust line between the catalyst bed and the cooler.

Use of the recombiner has been discontinued because sufficient need for it has not developed Heavy water has not been used, and no fuel element has failed

3. BORAX-IV

a. Early Experiments. BORAX-IV experiments were performed by two groups of workers Some results by the first group (see Fig. 2.6) show that at 300 psig, 420°F (216°C), water decomposition rates increase in a nearly linear manner with reactor power, for the range of about 2 to 10 Mwt, and check quite well with EBWR rates at this pressure.[24]

(1) Addition of Phosphoric Acid The use of phosphoric acid (H_3PO_4) preferably at pH 3 5 has been proposed as an inhibitor of aluminum corrosion in high temperature water.[30] A preliminary two-day test was made in BORAX-IV to study the effect of added H_3PO_4 on water decomposition and activity in the reactor water and steam systems.[31] With the reactor operating at 3 Mwt, and with the reactor water being bypassed through a cation-bed ion exchanger, H_3PO_4 was added in five portions at intervals until a total of 201 cc had been added (47.5 ppm PO_4^{---})

The observed effects of the H_3PO_4 addition were as follows: The pH of the reactor water dropped from 6 4 to 3 5 by the time all of the H_3PO_4 was added During this same interval of time the pH of the steam dropped from 6 3 to 6 1 This indicated that the actual carryover of the acid was low. One analytical determination, made just before the final H_3PO_4 addition confirmed this, showing 0 072 ppm PO_4^{---} in the steam. The resistivity of the reactor water dropped from 600,000 ohm-cm to 7500 ohm-cm, and the resistivity of the steam dropped from 2.1×10^6 ohm-cm to $1\ 5 \times 10^3$ ohm-cm Water decomposition, in cc total gas per liter of condensed steam increased from 129 to 291 (2 25 times).* The activity level of external components was increased by a factor of 2 in the air-ejector to a factor of 8 on the steam pipes and turbine casing. Carryover of P^{32} in the steam was observed. The total radioactivity DF (decontamination factor = activity of reactor water/ activity of steam) was about $1\ 3 \times 10^4$ whereas the P^{32} DF varied from 1.6×10^2 to 1.4×10^3 This lower DF was expected after seeing the decrease in pH of the steam.

(2) Addition of Morpholine. Morpholine is a volatile, organic-nitrogen, basic compound used in many conventional boilers to maintain high pH in the steam and condensate systems to minimize steel

*See footnote p 11.

corrosion. A preliminary test in BORAX-IV was made to study its effect on water decomposition and plant activity level. Observed results of 5 ppm morpholine addition were as follows:[31]

The water decomposition, in cc total gas per liter of condensed steam, increased from 155 to 187. Gas analysis showed 1% CO_2. The pH of the steam dropped from 6.3 to 5.2. The resistivity of the steam decreased from 1.8×10^6 ohm-cm to 0.25×10^6 ohm-cm. The pH, 5.8, and resistivity, 0.6×10^6 ohm-cm, of the reactor water did not change markedly during the test. A factor, the significance of which cannot be evaluated, was that the mixed-bed ion exchanger was operated during the first part of the test, while during the latter part, the mixed bed was turned off and the cation bed was turned on. During the test, activity levels on the steam line, air ejector, and condenser hot well increased by a factor of 4.

The drop of pH in the steam, instead of an increase as would occur in a conventional boiler plant after addition of hydrazine, and the high CO_2 concentration in the steam show that morpholine is decomposed by irradiation.

b. Later Experiments. Later experiments, by Whitham and Smith[32] are described below:

(1) Effect of Water Conditions. The radiolytic gas formation rate was studied as a function of power for a variety of water conditions. Particular emphasis was placed on pH control since previous experiences showed water conditions must be held constant for a period of hours prior to sampling to gather consistent data. The samples used for analysis consisted of the entrained gases separated from a known volume of condensed steam. An average composition of the separated gas may be regarded as O_2, 31%; H_2, 62%; inert gases, 7%; and a trace of CO_2. The presence of CO_2 can be explained by the decomposition of organic materials in the radiation field or by carbonates introduced by condenser leakage. The inert fraction consists essentially of nitrogen. A standard Winkler analysis of the condensed steam was used to measure the amount of dissolved oxygen present in the condensate sample. This correction proved to be of the order of 6 to 7 ppm. Variations in the dissolved oxygen content were attributed to variations in the sample temperature. Measurements of the dissolved hydrogen content were not attempted.

From the typical analysis given above, it is clear that H_2 and O_2 occur in the 2:1 ratio predicted from stoichiometric considerations.

Measurements carried out under different water conditions (pH and resistivity) indicate that while the total gas evolution rate varies with water conditions, the ratio of H_2 to O_2 remained the same.

Measurements were made to study the total gas evolution rate as a function of reactor power for various pH values. The data as taken are summarized in Fig. 2.9.* For a given power the gas evolution rate increases as the pH decreases, i.e., as the reactor water becomes more acidic. Presumably, hydrogen ion combines with the reaction intermediates, either to promote the forward reaction or to retard the back reaction. The latter seems more likely. Since the volume of steam produced is directly proportional to power, it is apparent from Fig. 2.10 that the quantity of gas produced per unit of power decreases as the reactor power increases.

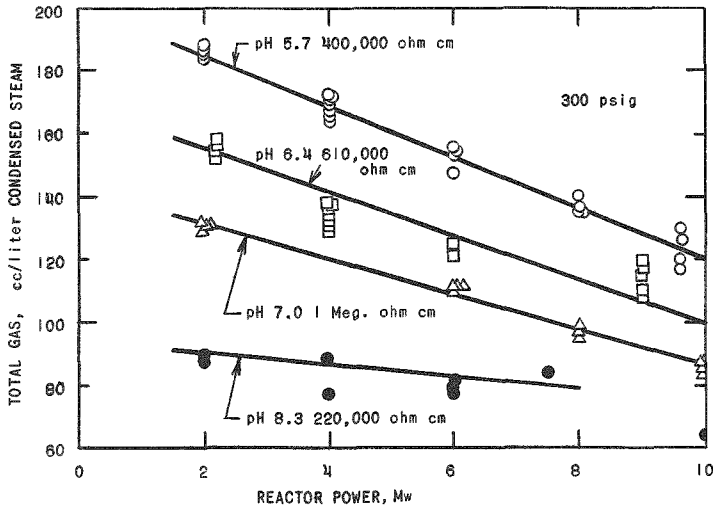

Fig. 2.9

Total Decomposition vs Reactor Power in BORAX-IV

The decrease in the specific decomposition rate with increasing power is consistent with the observations of Dolin and Ershler.(28) They have pointed out that the proportionality constant relating radiolysis rate and the amount of radiation absorbed is itself a function of reactor power. The fact that a limiting decomposition rate is eventually reached may be understood in terms of two effects: (1) a forward reaction (Eqs. 2.4 and 2.5) depending mainly on reactor power, and (2) a reverse reaction (Eq. 2.9) depending on the concentration of H_2 and O_2 dissolved in the water. A steady state is eventually reached when the amount of gas formed in the forward reactions is just

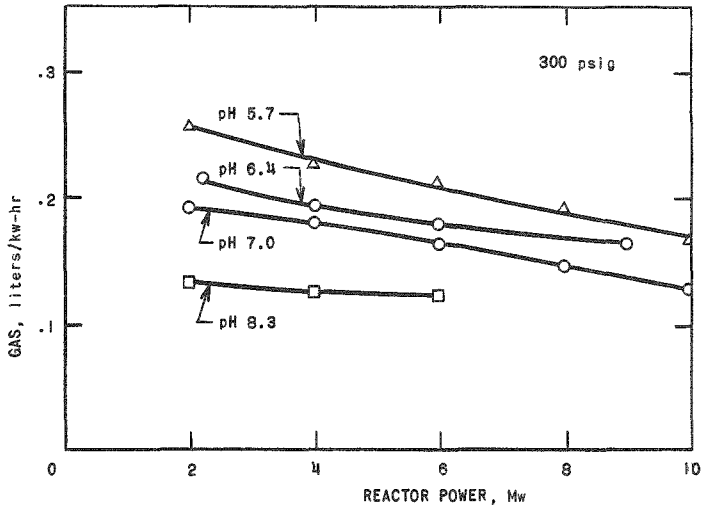

Fig. 2.10

Specific Rate of Radiolysis at Various Reactor Powers, BORAX-IV

*All gas data were taken at 5000 ft altitude and have not been corrected to sea level conditions. Correcting the volumes to standard conditions would reduce the volume approximately 20%.

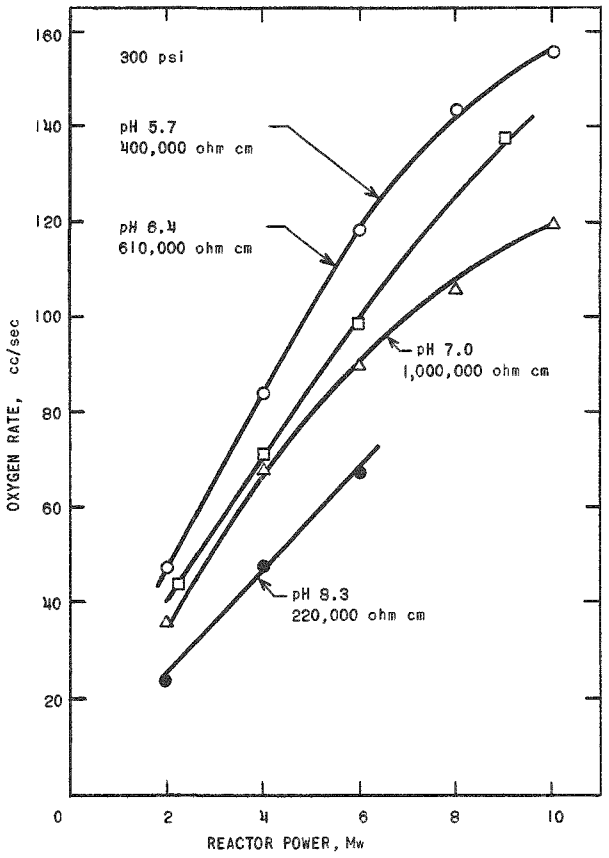

Fig. 2.11

Oxygen Formation Rate at Various Reactor Powers, BORAX-IV

equal to the amount of gas destroyed in the back reaction. The data summarized in Figs. 2.9, 2.10, and 2.11 support this interpretation.

During another series of tests at constant power on two occasions,* the pH of the reactor water was lowered to 4 by acid additions. Gas rates and radiation levels in the steam line were measured during the ensuing clean-up with the resin columns. Figures 2.12 and 2.13 show the results of these tests. The spread between the curves in Fig. 2.12 illustrates the difficulty in obtaining reproducible data from tests in which operating conditions are apparently identical. Figure 2.13 gives a graphic representation of the steam activity associated with an increase in dissociation rate. From this graph it is quite apparent that the activity of the turbine system is directly related to the decomposition rate in the reactor.

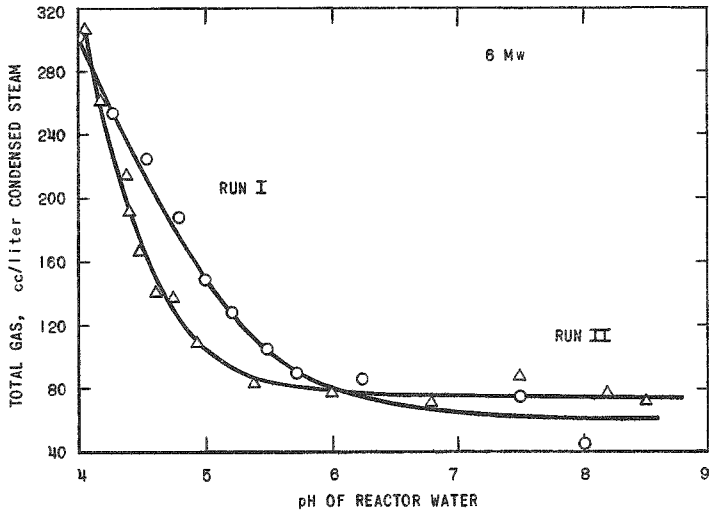

Fig. 2.12

Total Gas as Function of pH, BORAX-IV

*The acids were not identified in the reference, but a preliminary abstract of the paper mentioned sulfuric or phosphoric acids.

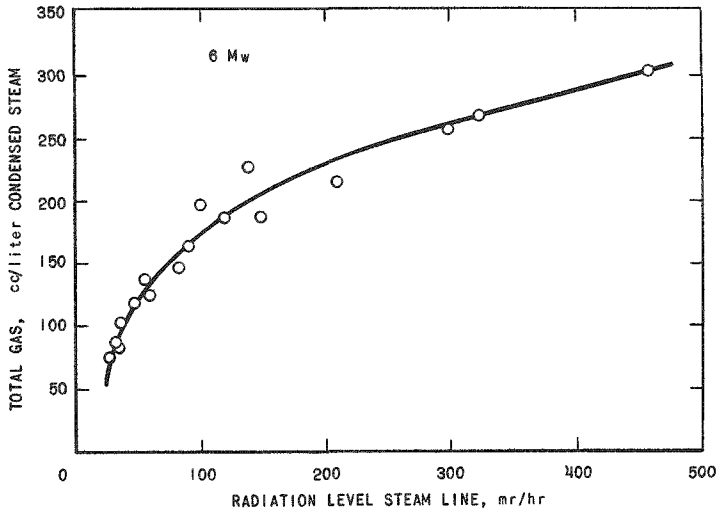

Fig. 2.13

Radiation Level of the Steam Line vs
Total Gas, BORAX-IV

(2) Effect of Hydrogen Addition. Two possibilities for reducing the free oxygen content have been considered. One concerns the catalytic recombination of O_2 and H_2 with a platinized catalytic bed in the steam line. This approach was rejected as impractical in view of the bed poisoning in an atmosphere of saturated steam. By superheating the steam, the bed thickness could be reduced in thickness to the extent that this method would prove practical.

The second possibility, the addition of hydrogen to the reactor water, was investigated experimentally. Hydrogen gas was forced into the feedwater line which enters the reactor vessel about 1 ft below the top of the fuel chimneys and which distributes the water in a ring shaped sparger through holes bored in the lower surface. In preparation for this test an S-10 "oxygen scavenger" resin column was placed in operation in the condensate return line to remove completely oxygen from the condensate return. Under normal operating conditions, without the S-10 column, this line returns water containing about 4 ppm of dissolved oxygen to the reactor. The atmospheric feedwater tank was valved so low-pressure argon would blanket the tank and eliminate oxygen absorption.

For each hydrogen addition rate, samples of steam condensate were collected and analyzed for total gas, hydrogen, oxygen and inert gas content. The results of these tests carried out at pH levels of 4.75, 6.1 and 7.4 are given in Figs. 2.14, 2.15, and 2.16. The results at pH 4.75 are important because they show the effect of hydrogen ion concentration on the back reaction. Additions at pH 6.1 and 7.4 show that sufficient hydrogen reduced the oxygen content of the steam to a low value.

These results are in accord with the water decomposition model discussed previously (see Sec. 2.2). Increasing the concentration of H_2 accelerates reaction (2.8) relative to reaction (2.5) and less free oxygen is liberated.

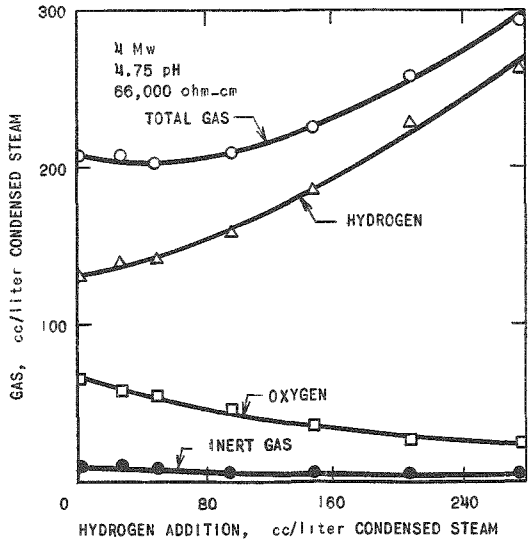

Fig. 2.14

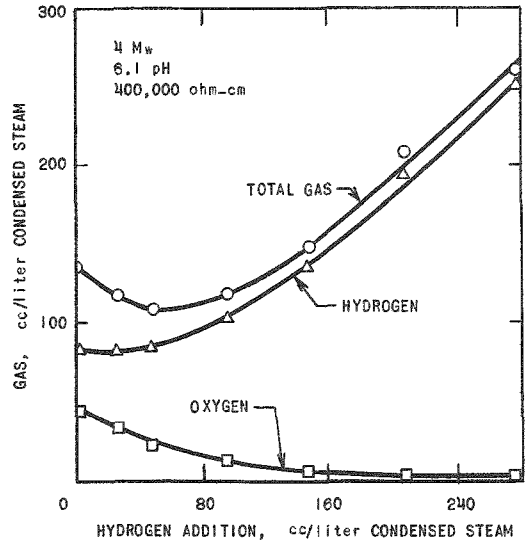

Fig. 2.15

The Effect of Hydrogen Additions on the Oxygen Content of the Steam, BORAX-IV

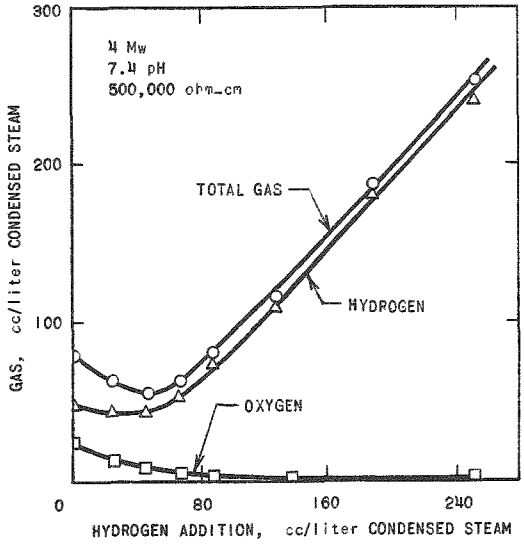

Fig. 2.16

The Effect of Hydrogen Additions on the Oxygen Content of the Steam, BORAX-IV

While these tests proved successful in decreasing the oxygen concentration, the economics of adding hydrogen at a rate of 24 liter/min at 4 Mev are questionable. Additions at other locations such as the steam dome or at the bottom of the reactor might prove more efficient. Alternatively, hydrogen from air-ejector exhaust could be recirculated into the feedwater. This approach, however, has the obvious disadvantage that nitrogen from the turbine leakage would slowly increase in concentration with time and would eventually require discharging or chemical removal.

(3) Effect of Oxygen Addition. Oxygen additions to feedwater gave no change in decomposition rate or steam activity.

(4) Effect of Salt Additions. To study the effects caused in the gas evolution rate by dissolved impurities, several chemical salts were added to the reactor water after which samples of steam condensate were analyzed for total gas content. With the resin bed clean-up loop closed and with pH and the reactor power constant, KNO_3 was added incrementally to the reactor water. Samples of steam condensate collected shortly after each addition showed only a slight increase in total gas content. With Na_2SO_4 a slight decrease in the total gas content was noted.

The results of these tests are summarized in Fig. 2.17 in which the volume of total gas per liter of steam condensate is plotted as a function of water quality (resistivity). From this it is evident that soluble salts, as such, have only a minor effect on the gas evolution rate. To augment these specific tests, the operating data were examined and the gas rates vs specific resistances were plotted, for constant pH values. This plot showed water quality had little effect on radiolytic gas rates. The effects of chlorides and other halides which are known to act with the free radical intermediates were not studied since the presence of these elements in a stainless steel system could lead to problems of stress corrosion.

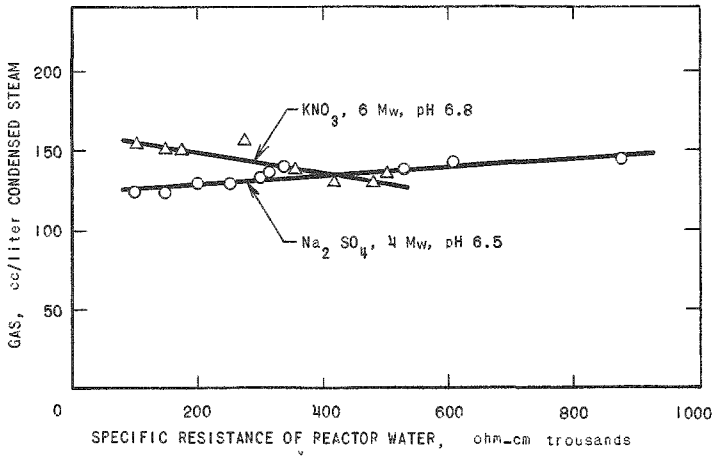

Fig. 2.17

The Effect of Water Quality on Total Gas Formation Rate, BORAX-IV

4. ALPR

a. Normal Operation. During the first week of the ALPR plant performance test, some water decomposition data were taken.(33) Water conditions prevailing at the time were as follows:

pH, slightly less than	7.0
resistivity	660,000 ohm-cm
O_2 reactor water	0.10-0.15 ppm
O_2 feedwater	0.2 ppm

The water decomposition data at several power levels are given in Table 2.5.

Table 2.5

ALPR WATER DECOMPOSITION DATA

Steam Flow, lbs/hr	Reactor Power, Mwt	cc Radiolytic Gas/L Condensate[1]	O_2 in Condensate,[2] ppm	Gas Analysis, %			cc O_2/L[3] Condensate	Liters[4] O_2/min
				O_2	H_2	Inert		
4,000	1.33	51.0	3.6	31.3	66.8	1.9	16.2	0.502
7,850	2.65	51.1	3.4	29.1	69.4	1.5	15.2	0.902
7,600	2.53	48.5	4.3	29.8	68.1	2.1	15.4	0.850
7,800	2.60	49.3	4.1	31.1	68.2	0.7	16.1	0.947
7,550	2.52	50.7	4.1	30.7	68.5	0.8	16.3	0.943
5,580	1.86	50.0	4.2	31.1	68.1	0.8	16.3	0.685
8,000	2.67	49.2	4.4	30.9	68.6	0.5	16.2	0.978
						Average	15.95	

[1]Free (undissolved) gas associated with sample of condensate. Although records do not indicate, it is believed (A. P. Gavin) correction was made for STP.

[2]Dissolved oxygen in sample of condensate. Calculation believed based on STP value.

[3]Based on sum of (1) and (2).

[4]Calculated by C. R. Breden.

Since the value cc O_2/liter of condensed steam is roughly constant, the rate of gas production is essentially a linear function of reactor power over this range of power. This is shown in Fig. 2.18* where the oxygen formed in liters/min is plotted against reactor power.

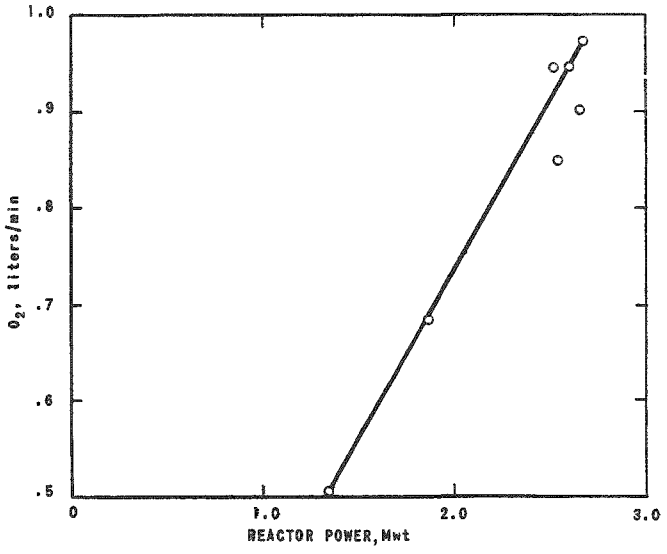

Fig. 2.18

Oxygen Formation vs Reactor Power, ALPR

b. Effect of Hydrogen Addition. To observe the effect of hydrogen addition on the retardation of decomposition, the following experiment was run. Bottled hydrogen gas was metered through a high pressure rotameter into the reactor feedwater line at the point where the effluent from the ion-exchange cleanup system and the feedwater meet. The oxygen content of the steam was suppressed to essentially zero with the addition of 32.8 cc H_2 per liter of feedwater. The data from the hydrogen addition is shown in Table 2.6 and Fig. 2.19.

*Made by C. R. Breden from data in Table 2.5.

Table 2.6

ALPR HYDROGEN ADDITION DATA

Steam Flow, lbs/hr	Mw	H_2 Addition Rate		cc Radiolytic Gas/liter Condensate	O_2 in Condensate, ppm	Gas Analysis, %			cc O_2/liter Condensate	Liter O_2/min*
		cc/liter Feedwater	Liters/min			O_2	H_2	Inert		
8,100	2.70	32.8	2.01	30.1	0.05	0.0	100.0	-	0.04	0.002
8,000	2.67	26.1	1.58	24.3	1.4	8.5	90.8	0.6	2.69	0.16
7,900	2.63	4.18	0.24	43.4	3.6	29.0	71.0	-	13.3	0.79
7,700	2.57	11.7	0.68	34.0	3.4	29.9	72.1	-	10.5	0.61
8,000	2.67	0.0	0.00	-	-	-	-	-	16.2	0.98

*Calculated by C. R. Breden.

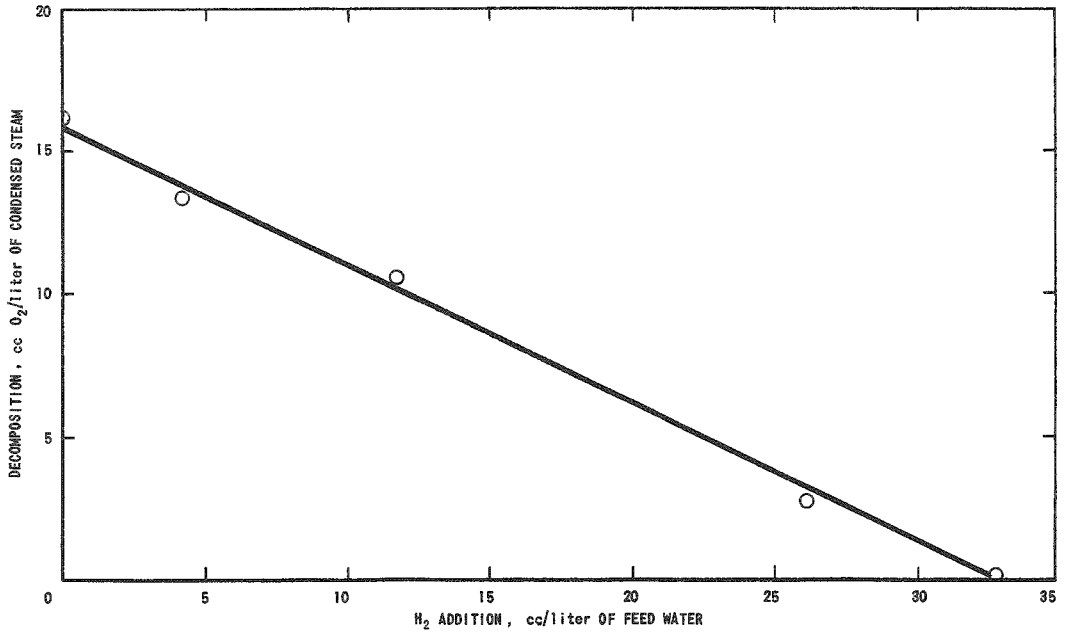

Fig. 2.19

Reactor Water Decomposition vs Hydrogen Addition, ALPR

The results obtained during the hydrogen addition parallel those obtained from BORAX and EBWR for similar experiments (see Sec. 2.6).

5. VBWR

The Vallecitos Boiling Water Reactor (VBWR) operates at higher pressure, 1000 psig and temperature, 544°F (284°C) than the other boiling water reactors so far discussed. Some of the water decomposition results reported[34,35] for this reactor have been incorporated in Fig. 2.6 by C. R. Breden. The results confirm EBWR conclusions that increased pressure favors the recombination reaction and results in less net decomposition. In a boiling water reactor, however, increased pressure is associated with increased temperature. For this reason, it is

difficult to make a sharp distinction between the two factors, temperature and pressure. One run at VBWR,[35] to test the effect of pressure (with corresponding change in temperature and steam density), confirmed this trend of less net water decomposition with increased reactor operating pressure.

The specific rate of water decomposition was found to increase slowly with reactor power. This trend is in agreement with that found at EBWR,[24] but is in contradiction with the decreasing effect found in BORAX-IV.[32]

Vallecitos investigators, as a result of in- and out-of-pile corrosion tests, have come to a conclusion of possibly great significance to boiling water reactor technology. In effect, their results indicate that the stoichiometric mixture of hydrogen and oxygen evolved from a boiling water reactor is less corrosive to carbon steel and stainless steel than the low oxygen, high hydrogen, high pH water environment of a pressurized water reactor. Enough confidence has been developed at Vallecitos in these reduced corrosion rates that an expected large program, to study both the inhibition of corrosion and the inhibition of corrosion-product deposition, has been curtailed.[35,36]

2.6 Discussion

Radiolytic water decomposition refers to the breakdown of light or heavy water under irradiation to its components, hydrogen (or deuterium), and oxygen, and at low temperatures, hydrogen peroxide (or deuterium peroxide).

If sufficient radiolytic gas is produced, it can create problems relating to nuclear physics, hydraulics, heat transfer, air-ejector design, and corrosion. In addition, it can produce explosion hazards, and if the water is D_2O, the loss of D_2 can be an economic problem.

The most important single factor affecting net decomposition is the nature of the radiation; the highest net decomposition being produced by heavy particles, specifically fission fragments. Because of this factor net decomposition is slight in water-moderated heterogeneous reactors where fission fragments are confined as compared to homogeneous reactors, where fission fragments are in contact with the water.[37]

Among the water-moderated heterogeneous reactors, where irradiation is largely made up of gammas and proton recoils from neutron scattering, the most important single factor affecting water decomposition is the purity of the water. While proton recoils tend to produce molecular products causing high net decomposition, the large excess of gamma

radiation favors the formation of free radicals and the back reaction reforming water. The overall result is low net decomposition as long as the water is pure. Certain impurities, if present, interfere with the back reaction by reacting with the free radicals.

A design characteristic that is a factor in water decomposition in these reactors is the presence of a gas space or void space in contact with the water. A gas space above the water is characteristic of low temperature reactors and also of boiling water reactors. It is normally absent in pressurized water reactors. In the low temperature reactors, the molecular water decomposition products are largely H_2 (or D_2) and H_2O_2 (or D_2O_2). A gas space favors escape of H_2 (or D_2) from the water decreasing the opportunity for recombination.[1,4,11] Another factor is that escape of hydrogen (or deuterium) in the gas or vapor phase results in the build-up of an excess of H_2O_2 (or D_2O_2) in the water phase. This also tends to inhibit the back reaction and favor net decomposition.[6,11,38] In low temperature reactors, this void effect is of only slight influence as long as the water remains pure, but becomes increasingly more important as impurities build up in the water.

With boiling water reactors, two types of void or gas space exist. One is the steam space above the core and the other is the steam void space in the core resulting from the formation of steam bubbles. In such reactors, water decomposition becomes significant even if water purity is high. At the temperature of the boiling water reactor, H_2O_2 is not stable and the free oxygen escapes into the voids along with the hydrogen.

In the boiling water reactor, there appear to be two mechanisms by which voids decrease recombination: (a) the escape of radiolytic gas into voids where less recombination occurs than in the water phase, and (b) the flow of steam out of the core by way of the voids produces a scrubbing or sweeping effect which carries the radiolytic gas out of the irradiation zone before it can recombine.

Evidence as to the relative efficiency of the recombination reaction in the vapor phase compared to its efficiency in the water phase appears to be contradictory. Static tests in silica at low temperature,[11] and at 200°C and 250°C[6] showed negligible reaction between hydrogen and oxygen in the vapor phase under irradiation. In static two-phase tests in stainless steel autoclaves at 164°C and 260°C, however, it was found that the recombination reaction occurred to a greater extent in the vapor phase.[7] It may be that under the latter conditions stainless-steel corrosion products on the walls of the autoclave were having a catalytic effect.[16] The fact that the reaction occurred most effectively at high temperatures, 164°C to 260°C, with little temperature effect between these two values tends to support this view.

The greater degree of recombination of H_2 and O_2 in the vapor phase of the stainless steel autoclaves as compared to that in the water phase does not appear to occur in the boiling water reactor, unless the scrubbing effect of the released steam completely overshadows it. One test indicating that little or no recombination occurs in the vapor phase in boiling reactors was the single experiment in EBWR described earlier where steam, carrying radiolytic gas, was passed through the core by means of a small tube between fuel plates. No recombination could be detected.

The operating pressure is an important factor influencing net decomposition in boiling water reactors in that net decomposition decreases with increasing pressure. Although increased saturation pressure in such reactors is associated with increased temperature, which also favors recombination, it seems likely that increased pressure is the more important of the two factors since the recombination reaction is one of condensation from three volumes to two volumes. However, Hochanadel[6] reported that at 200°C and 250°C recombination of H_2 and O_2 was independent of radiation dose and pressure, so the mechanism responsible is not clear.

One interesting aspect of the water decomposition problem is the reduction in decomposition that occurs in the presence of an excess of hydrogen. The addition of hydrogen in reactors to minimize water decomposition was predicted in early studies.[11] Its effectiveness has been demonstrated in pressurized water reactors where a concentration of 25-50 cc H_2 per kilogram of water results in almost negligible water decomposition.[18] In this type of reactor, an important factor favoring suppression of decomposition is undoubtedly the absence of voids throughout the primary system. Although addition of hydrogen to EBWR, BORAX-III and IV, and ALPR caused reduced decomposition, the amount of hydrogen required was generally much higher, and the suppression less complete than in pressurized water reactors.

To understand better the hydrogen addition of experiments, original data from EBWR (Ref. 25, Tables 2 and 3) and ALPR, (Table 2.6), were re-calculated in terms of liters O_2/min. For BORAX-III and IV values were taken from points on curves (Figs. 2.4, 2.14, 2.15, 2.16) and calculated to liters O_2/min.

The data plotted in this way (Figs. 2.20 and 2.21) suggest that the major factor involved is the stoichiometric recombination between the oxygen formed and the added hydrogen; as if the hydrogen added replaced that lost in decomposition. The simplest example is the curve for ALPR, where an oxygen production rate of one liter per minute is reduced to essentially zero by a hydrogen addition rate of two liters per minute.

Roughly the same ratios for recombination exist for other reactors at different power levels for the major proportion of oxygen; the last trace of oxygen is difficult to scavenge. In BORAX-III and IV the efficiency of this recombination, as indicated by the variation from the stoichiometric volume ratio between oxygen and hydrogen, is less than in EBWR at 10 and 20 Mw. Two different pressures were involved in these tests: ALPR, BORAX-III and BORAX-IV at 300 psig, and EBWR at 600 psig for both 10 and 20 Mw. The increased efficiency of recombination in EBWR may result from the increased pressure. Unfortunately, no data were taken in EBWR on the effect of hydrogen additions at lower pressures.

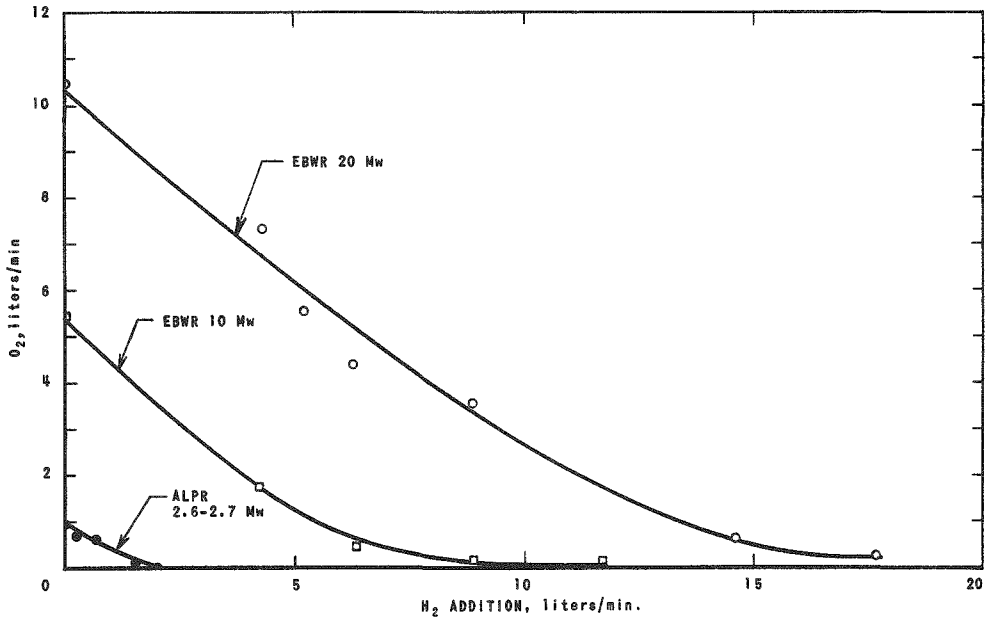

Fig. 2.20

Effect of Hydrogen Addition on Oxygen Production in ALPR and EBWR

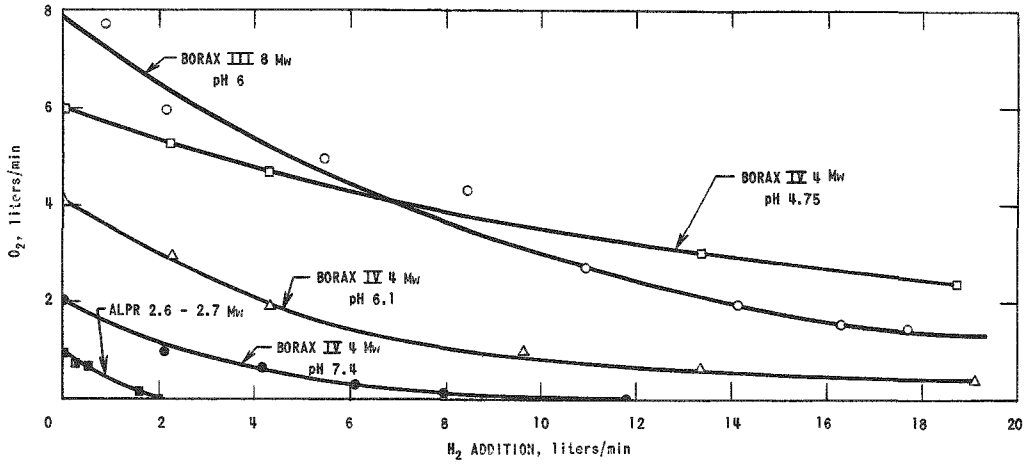

Fig. 2.21

Effect of Hydrogen Additions on Oxygen Production in ALPR, BORAX-III and BORAX-IV

Curves (Fig. 2.21) for BORAX-III and IV, except at pH 4.75, show parallel behavior. The efficiency of the recombination increases with decreased rate of oxygen production regardless of whether increased oxygen production is due to increased power (BORAX-III vs BORAX-IV pH 6.1) or the presence of undetermined impurity (compare curves pH 7.4 and pH 6.1 for BORAX-IV). The lack of parallelism between the BORAX-IV curve at pH 4.75 and the other curves in Fig. 2.21 may indicate that a different mechanism is the controlling factor at the low pH. Available data do not permit a distinction between the effect of low pH per se, and the effect of some specific impurity.

Because of the decreased efficiency of recombination shown by hydrogen addition and the quantity of hydrogen required with increased rates of oxygen production, hydrogen addition does not look attractive as a means of minimizing water decomposition in boiling water reactors.

The recirculation of evolved radiolytic gas through the core to achieve improved recombination has been suggested as a means of minimizing net decomposition but except for the EBWR test mentioned previously, this has never been tried. Failure of this particular test may have been because the gas was in the vapor phase rather than the water phase. The results of one experiment are not conclusive. More conclusive information on this possibility will be obtained when some of the proposed reactor superheat experiments are made.

Some other aspects of the water decomposition problem in boiling water reactors that need further work and clarification are as follows:

(1) What is the effect of oxygen concentration in the feedwater on decomposition in the reactor? Fundamental studies indicated that added oxygen would increase net decomposition. Reactor tests are not conclusive but seem to indicate a definite effect. Is it necessary to maintain low oxygen in the feedwater to minimize water decomposition? What are the controlling factors?

(2) Does the rate of water decomposition continue to increase with reactor power or does it level off or decrease as reported by certain investigators? What are the controlling factors?

(3) Is there a real effect of pH on water decomposition in reactors, or is the apparent effect due to some particular impurities? What are the factors involved?

The most important recent development in the field of water decomposition in boiling water reactors as mentioned previously is the idea proposed by the Vallecitos investigators that the stoichiometric mixture of hydrogen and oxygen evolved from a boiling water reactor is less corrosive to stainless steel, low alloy steel and carbon steel than the low oxygen, high hydrogen, high pH water environment of a pressurized water reactor. If this proves to be correct, water decomposition could become an asset rather than a liability as to its effect on corrosion. From this standpoint, attempts to minimize water decomposition, or to recombine the gases are unnecessary and even undesirable. But when other factors are controlling such as loss of D_2 from D_2O, methods of minimizing decomposition or recombining the gases remain important.

3. WATER CHEMISTRY

3.1. Introduction

Water Chemistry in this section is concerned primarily with water conditions as found in reactor systems, and the methods used to maintain these conditions. Since water conditions depend to a large extent on the materials in contact with the water, an attempt has been made to identify the materials in contact with reactor water and steam. The corrosion behavior of these materials and the problems resulting from the presence of corrosion products are dealt with in other sections. There is a certain amount of overlapping of the sections and the divisions of material among them in some cases is a matter of emphasis or convenience. The material in this (and following sections) has been compiled from unclassified reports on reactors that have operated.

3.2. Pressurized Water Reactors

From the standpoint of water chemistry, Boiling Water Reactors and Pressurized Water Reactors are high temperature water reactors. Pressurized Water Reactor development preceded that of Boiling Water Reactors and included a great amount of water chemistry investigation, some of the results of which are applicable to Boiling Water Reactors. For this reason, the water chemistry of Pressurized Water Reactors is reviewed in some detail.

1. Early PWR Systems

The early PWR Systems were made largely of stainless steel and used zirconium clad fuel. From the beginning, make-up water was high purity water, prepared by passing through mixed bed ion-exchangers.

At various stages of development[39] the make-up water was:

a) Deaerated by conventional steam deaeration followed by storage under a helium blanket. This procedure removes all dissolved gases except helium.

b) Deoxygenated by using a sodium sulfite regenerated ion-exchanger. This removed oxygen, but not argon and nitrogen.

c) Used without removing dissolved gases.

Experiences in the PWR development and operational program has been to keep the oxygen content of the primary water as low as possible, usually less than 0.05 ppm. The effects of dissolved oxygen on friction coefficients in mechanisms, the radiation-induced reactions with

N_2 to produce nitric acid, the corrosion of chrome-plated surfaces, and the adverse influence on the behavior of insoluble corrosion products, all make it desirable to maintain low oxygen concentrations.[18,39,40]

To maintain high purity water in the primary water system, a fraction of the primary water was continually bypassed through a Primary Water Purification System, operated at system pressure (see Fig. 3.1). In earliest systems, the mixed bed ion exchanger in hydrogen and hydroxyl ion forms was preceded and followed by sintered stainless steel filters. The purpose of the prefilter was to remove suspended impurities. The purpose of the after-filter was to remove resin fines. Due to the thermal sensitivity of the ion-exchange resin, the temperature of the water was reduced by heat exchangers to about 130°F (54°C).

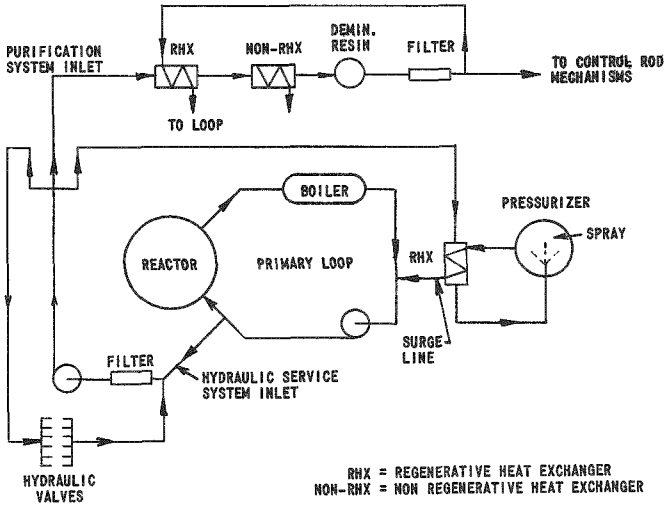

Fig. 3.1

PWR Primary Loop, Flow Diagram

An early in-pile loop experiment[40] indicated that fouling of zirconium clad fuel element had occurred by stainless steel corrosion products depositing on it. A similar fuel element in the out-of-pile portion of the loop showed no fouling. Although this experiment did not make clear whether heat flux or radiation was involved, other experiments showed that radiation was definitely a factor.[18,39] To insure that such a condition would not occur in the reactor, conventional means of corrosion inhibition and prevention of fouling were considered. For the most part these were inapplicable because of the adverse effects of radiation on chemical additives. Two experimental approaches were stressed. Hydrogen was added to the water as a possible means of inhibiting corrosion, and high pH (10) was tested as a means of minimizing liberation of corrosion products to the water. By the time the first plant was started, it had been decided to add hydrogen to the water. The advantages of high pH water were not considered sufficiently established to be applied at that time.

During the first year of operation the water to the primary system (original fill and makeup) was highly purified, i.e., demineralized and degassed. Hydrogen was maintained at a concentration of about 100 cc(STP)/kg water by periodic additions from cylinders. Water conditions considered typical during this early period are given[40] in Table 3.1.

Table 3.1

REPRESENTATIVE PWR WATER CONDITIONS

H_2 at 100 cc (STP)/kg

Filter and Demineralizer Operation, Normal

	Normal	Abnormal (Startup)
pH	7.5 - 8.5	8.5 - 9.3
Conductivity micromho/cm	0.3 - 1.5	3.7
Crud, ppm	0.05 - 0.25	0.5 - 1.8
Oxygen	(Essentially undetectable by standard Winkler test)	

Another manifestation of the high crud* content at startup was the fact that the filter plugged rapidly requiring frequent (sometimes hourly) back flushing.

Among the chemical phenomena observed in operation of the plant were the following:

a. Substantial concentrations of hydrogen reduced radiolytic dissociation of water to hydrogen and oxygen. Plant tests showed that as the hydrogen was reduced to 4-5 cc/kg water, oxygen appeared in the water to the extent of about 0.05 ppm.

b. The reverse reaction also occurred. If oxygen or air was added to the plant containing excess hydrogen, the oxygen combined rapidly with the hydrogen. This reaction also occurred if the power was off, due to the residual gamma radiation from the fission products formed in the fuel.

c. Under the influence of nuclear radiation, hydrogen and nitrogen in the primary water react to form ammonia. This reaction

*A laboratory developed term referring to corrosion products, wear particles, weld scale and other particulate matter carried by the water.

was demonstrated by addition of nitrogen while the plant was operating with an excess of hydrogen. During operation, the ion-exchanger removes the ammonia so that synthesis continues until the nitrogen is depleted.

d. In the absence of free hydrogen, nitrogen reacts with dissolved oxygen and water to form nitric acid as evidenced by a declining pH and the formation of nitrate ion.

Subsequent to this original test period, a program was started to simplify the water purification and control, the objectives were to eliminate feedwater deaeration, filters, and hydrogen addition.

Results of using non-deaerated water instead of deaerated water, along with excess hydrogen, were satisfactory. The oxygen from the air combines so rapidly with the hydrogen that it is never observed. The nitrogen in the air is converted to ammonia, which raises the pH. From the chemical point of view, the use of non-deaerated water (in a hydrogenated system) is actually advantageous in that the resulting moderately alkaline condition probably minimizes fouling. A radiation problem results however, because argon in the air is activated to radioactive argon-41.

Preliminary tests without the filter were encouraging. This was due to the fact that the ion-exchange resin bed acts as a filter.

Tests to reduce the amount of hydrogen showed that 30 cc/kg was substantially as effective as 100 cc/kg. Tests to eliminate hydrogen addition were not encouraging. As mentioned previously, when the hydrogen was reduced to 4-5 cc/kg, oxygen appeared in the water. When an excess of air was used, the oxygen depleted all the hydrogen and ammonia, and nitric acid was formed. The pH dropped from 9.5 to 5. The conductivity first declined as the hydroxyl ion was neutralized, and then increased with the formation of the hydrogen ion. Nitrate concentration increased verifying the formation of nitric acid. Soluble chromate increased, possibly from chromeplated surfaces, stainless steel, or dissolution of suspended corrosion products.

When the pH reached a low level, hydrogen was added. The result was a reduction of nitrate and chromate, and the pH returned to the alkaline side.

2. Later PWR Systems

a. Shippingport. Water conditions specified for the PWR (Shippingport)[41] were as follows:

pH	9.5 - 10.5 (LiOH)*
Dissolved Hydrogen	25 - 30 cc STP/kg H_2O
Dissolved Oxygen	Less than 0.1 ppm
Resistivity	Consistent with pH

Makeup water was degassed and demineralized. Hydrogen concentration of primary coolant water was maintained by addition from cylinders. The pH and specific resistance specified for the primary coolant water were maintained by continuous passage of the water through mixed bed demineralizers in the LiOH form in the PWR Reactor Coolant Purification System. With the specified hydrogen concentration, the oxygen content was below the specified limit during reactor operation; prior to operation of the reactor and the development of a high residual gamma flux in the core, it was planned to use hydrazine to remove oxygen in the water.

Most of these specifications are directly concerned with reducing corrosion and corrosion product problems. According to a survey,[42] the high pH reduces the already low uniform corrosion rate of stainless steel,[43] reduces pitting and crevice corrosion of stainless steel,[44,45] produces more tenacious corrosion product films,[41] reduces the yield of transportable crud,[18,46] tends to inhibit deposition,[47] and makes the crud more filterable.[48,49]

LiOH was selected in preference to NaOH, KOH or NH_4OH because it does not seem to aggravate caustic embrittlement, and stress corrosion cracking[42,50] as does KOH and NaOH, possibly due to reduced solubility; LiOH does not increase radiolytic decomposition whereas NH_4OH undergoes radiolytic decompositions.[51] Ion exchange resin in the base form is more effective with LiOH than with KOH or NH_4OH in maintaining pH control. The strong base form mixed-bed resin functions effectively both for maintaining coolant purity and for controlling pH.

Operational experience[52] has resulted in only minor changes in primary water specifications:

(1) Hydrogen concentration has been reduced to 15-60 cc STP/kg whenever steam temperature is above 200°F (93°C).

(2) Dissolved oxygen is less than 0.14 ppm at all times when the system temperature is above 200°F.

When starting the reactor from cold condition, it is necessary to scavenge oxygen before coolant temperature exceeds 200°F. Initially, oxygen was scavenged by adding an excess of 0.5 ppm hydrazine

*Measured at room temperature.

over that theoretically required to react with the amount of dissolved oxygen present. Later, this hydrazine addition step was omitted, and oxygen scavenging was accomplished, with the coolant temperature at 200°F, by addition of sufficient hydrogen. By making the reactor critical for $\frac{1}{2}$ hour, the flux caused the hydrogen to react with the oxygen. Deletion of hydrazine scavenge step reduced the time needed to heat the station by 3-6 hours.

Operation with reactor coolant at high pH, 9.5 - 10.5, has resulted in low crud levels in the coolant, at about 3-5 ppb (parts per billion). Data on surface contamination by deposition of activated corrosion products have been accumulated but have not been evaluated in terms of the higher pH.

It will be noted that no filters are employed in the bypass purification system; and the concept has been adhered to of maintaining low concentration of dissolved oxygen in the reactor coolant. The coolant purification system is provided with two by-pass purification demineralizers to remove dissolved and suspended solid material from the coolant steam. Each demineralizer serves two coolant loops. The flow through each demineralizer is 20,000 lbs/hr at 120°F (49°C). This amounts to a purification constant* of 1×10^{-4} seconds^{-1}. The effective volume of the bed is 23.5 cu ft with a flow loading of 7.5 gpm/ft^2 resin. The resins are Rohm and Haas IR-200 (XE-163) and IR-400 (XE-78) mixed in the proportion of 1.0 equivalent of hydroxyl ion in the anion resin to 1.0 equivalent of lithium ion in the cation resin. The mean particle size of the bed was set at 15-50 mesh.

The performance of the main purification system demineralizers is checked daily for DF $\left(\text{decontamination factor} = \frac{\text{inlet activity}}{\text{outlet activity}}\right)$ based on gamma activity after 15 minutes decay and after removal of noble gases by bubbling air through the sample. Original specifications called for discharge of the bed if the DF was less than 25 for any four consecutive days. An investigation showed that 50% of the influent gamma activity was due to 10.1 min N^{13} which is normally found as ammonia. The effluent activity could, at times, be attributed entirely to N^{13}. This raised a question as to the validity of the criteria for determining when the resin was exhausted. As a result, samples of the resin were taken from both demineralizers, designated as AC and BD respectively, just prior to the end of core life to determine the true efficiency of the resin for removing specific nuclides. The nuclides selected included anions and cations for both heavy and light fission fragments. The data are shown in Table 3.2.

---

* $\frac{\text{Rate of flow (mass) of coolant to demineralizer}}{\text{Total (mass) of coolant in system}}$

Table 3.2

DECONTAMINATION FACTORS FOR SPECIFIC NUCLIDES
ACROSS PWR PURIFICATION DEMINERALIZERS*

Nuclide	AC Purification Demin.				BD Purification Demin.				Half Life
	Inlet dpm/ml	Outlet dpm/ml	DF	Eff.† %	Inlet dpm/ml	Outlet dpm/ml	DF	Eff. %	
1. Bromine-83	875	1.2	730	99.9	880	0.6	1500	99.9	2.4 hr
2. Bromine-84	1780	Not Det.**	1000	-	1700	Not Det.	> 1000	-	30 min
3. Strontium-89	6.3	0.5	1.3	92.1	7.3	0.23	32	96.8	54 day
4. Strontium-90	1.3	Not Det.	-	-	1.3	Not Det.	-	-	20 yr
5. Strontium-91	350	Not Det.	> 1000	-	235	Not Det.	> 1000	-	9.7 hr
6. Strontium-92	200	Not Det.	> 1000	-	150	Not Det.	> 1000	-	2.7 hr
7. Iodine-131	230	1.7	140	99.3	230	1.4	160	99.3	8.1 day
8. Cesium-136	0.65	0.14	4.6	78.5	0.65	0.15	4.3	76.9	13.7 day
9. Cesium-137	16	18	0.89	-	16	7.5	2.1	53.1	33 yr
10. Barium-140	120	3.4	35	97.2	138	1.2	115	99.1	12.8 day

* Parameters:
pH - 10.0 @ 25°C
Reactor Power - 80%

** Not Detectable

†Demin. Eff. = $\left(\frac{\text{Inlet Act.} - \text{Outlet Act.}}{\text{Inlet Act.}}\right) \times 100$

The results can be grouped in three categories as follows:

DF greater than 500 - Br^{83}, Br^{84}, Sr^{91}, Sr^{92}

DF 500 - 25 - Sr^{89} (BD only), I^{131}, Ba^{140}

DF less than 25 - Sr^{89} (AC only), Cs^{136}, Cs^{137}

The large decontamination factors were associated with the short-lived component. This relationship indicated that both units still had a high efficiency for absorbing and holding both cations and anions for a period long enough to allow short lived nuclides to decay before they can reach the outlet. The small decontamination factors were associated with the two cesium nuclides and strontium-89 (across the AC unit). In the case of cesium-136, this was due in part to the lower exchange efficiency of cesium for lithium and possibly to its rather small concentration in the influent water. The data on cesium-137 showed a higher concentration in the effluent from the AC unit than in the influent. While the difference may be due to the analytical error of ±10% in each result, it is also probable that the resin in the AC purification demineralizer has a rather uniform concentration of this very long lived nuclide from top to bottom and is no longer capable of removing cesium-137 at this present equilibrium concentration level. The BD unit has not reached this point possibly due to the fact that it has less service time than the AC unit. The influence of service time may also explain why 54-day strontium-89 had a poorer decontamination factor across the AC unit.

These data indicated that (a) it was possible to obtain good decontamination factors for cation fission products with resin in the lithium form and with flows of 7.5 gpm/sq ft, (b) the service life of the

resin had a design expectancy of more than 90 days per unit; however, the AC unit showed no signs of exhaustion after two years service.

Among the small quantities of dissolved gases which enter the coolant in the makeup water is argon-40. It has a 0.53×10^{-24} cm^2 cross section for thermal neutrons; hence, considerable argon-41 is found in the coolant. Isotopes of nitrogen are also found but mode of formation is not clear. The 7.4 second nitrogen-16 which is the major contribution to gamma dosage during operation is formed by O^{16} (n,p) N^{16}. Fluorine-18 is probably formed from O^{18} (p,n) F^{18} and is observed generally in pressurized water reactor cooling water.

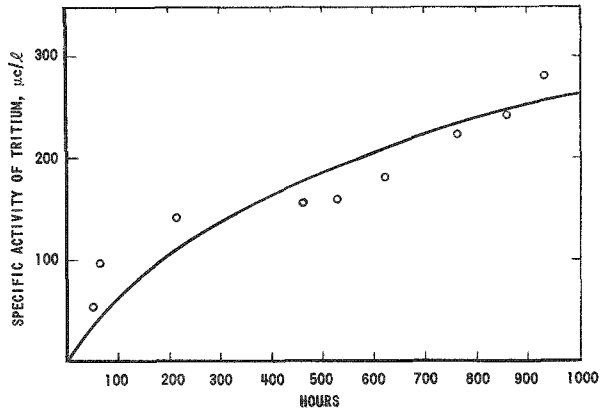

Fig. 3.2

Specific Activity of Tritium in PWR, Second 1000 hr Run

There has been concern over addition of lithium to the coolant as LiOH for pH control because of the cross section of the Li^6 (n, α) H^3 reaction. Figure 3.2 shows the activation trend during the second 1000-hour run. The maximum tritium concentration observed was 279 $\mu c/\ell$ (microcuries per liter) The major factor limiting the H^3 maximum concentration was plant leak rate. From the data collected, the effective neutron flux for tritium production was calculated and reported as $1.72 \pm 0.24 \times 10^{12}$ n/cm^2-sec at 68.79 megawatts gross electrical output.

b. APPR. The Army Package Power Reactor (APPR or SM-1) system is of interest because of the corrosion product reactivity build up problem to be described in Sec. 4.

This small (10 Mwt) reactor, producing about 200 kw of electricity, differs from the other PWRs described in that the major material of construction for all components in the primary system is AISI Type 304 stainless steel.(53) Unlike the other pressurized water reactors discussed, with fuel clad with zirconium or its alloys, the fuel in APPR was clad with Type 304L stainless steel. Minor materials of construction included stellite, 17-4 PH, Type 410 stainless, Haynes 25 alloy, etc.

High purity water is used in this reactor primary system. A combination condensate make-up and by-pass primary water purification system prepares high purity make-up water for the system and maintains it in the system (see Fig. 3.3). This system, in contrast to most by-pass purification systems, operates at a relatively low pressure.

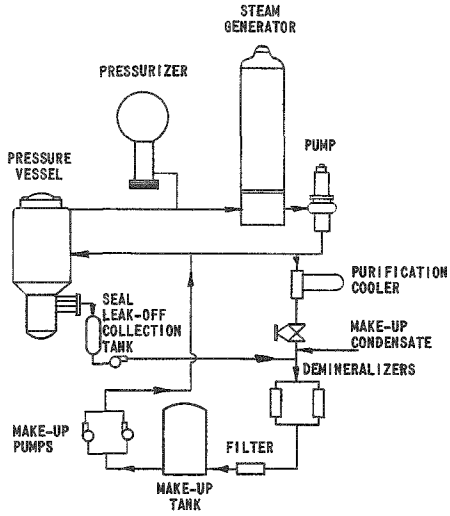

Fig. 3.3

APPR Primary System Flow Diagram

A portion, 0.07%, of the primary water flow from the steam generator, at about 430°F (221°C) and 1200 psig, is cooled to 120°F (49°C), throttled to about 100 psi, and passed (with or without make-up condensate as required) through one of two mixed-bed ion exchangers. It then passes through a sintered stainless steel filter to a 5000 gallon stainless steel make-up tank whence it is pumped back into the primary system by one of two positive displacement pumps.

A hydrogen blanket is maintained over the water in the make-up tank to prevent air in-leakage and to introduce sufficient hydrogen in the water to suppress radiolytic dissociation of the coolant. Regulating valves are set to maintain a hydrogen concentration of 28-30 cc/kg in the coolant.

At startup of the reactor hydrazine was added to react with any oxygen in the system. As the reactor power increased, hydrazine addition was suspended and hydrogen introduced to the system to maintain zero oxygen.

The presence of chlorides, a significant factor in stress corrosion, has never been a problem, the concentration has never been found to be over 0.1 ppm.

There has been no evidence of oxygen entering the 5000 gallon make-up tank. The hydrogen blanket pressure of 2-5 psi on the seal leak-off tank has not been completely effective. Water in this tank has contained up to 2.5-3.1 ppm dissolved oxygen. This inleakage has resulted in approximately 0.01-0.03 ppm O_2 in the make-up water. The recombination reaction with excess hydrogen under irradiation has been so efficient that oxygen is essentially undetectable in the main primary coolant during full power operation. Due to the radiation induced reaction between nitrogen and hydrogen to form ammonia, the inleakage of air produces about 0.01 ppm ammonia in the primary coolant. This ammonia is believed to be responsible for the slightly alkaline pH (7.5-8.5) of the primary water.

The mixed bed demineralizers consist of a mixture of strong sulfonic acid type cation resin in the H^+ cycle, and a strong basic type anion resin in the OH^- cycle. The bed depth is 36 inches; flow loadings generally have been low, even less than 1 gpm/ft^2 of bed surface.

Demineralizer effluent normally has a pH of 6.1-6.5 and a resistivity exceeding 2 megohm-cm measured in beakers exposed to the air. During the first half year of full power operation the resistivity of the primary system water consistently exceeded 600,000 ohm-cm without correction for presence of hydroxyl ion and ammonia.

3.3. Boiling Water Reactors

1. BORAX-III

BORAX-III was the first of the BORAX experiments to utilize steam produced for the production of electrical power and so was the first to be concerned with water quality.(19)

The fuel in BORAX-III was uranium-aluminum alloy clad with 2S aluminum. The use of aluminum meant that pH should be maintained on the acid side of neutrality to minimize corrosion. The problems connected with the reactor water were an important part of the BORAX-III program, the first step being to maintain water purity as high as consistent with the desired pH. As the purification system was set up originally, water from the reactor vessel was cooled from 421°F (216°C) to about 100°F (38°C), throttled from 312 to 17 psia, filtered through a 10 micron felted cartridge, passed through ion exchange columns, filtered again, and discharged to the feedwater storage tank. From this tank, to which make-up was also added, the water was pumped back into the reactor by means of the feedwater pump. (See Fig. 3.4.)

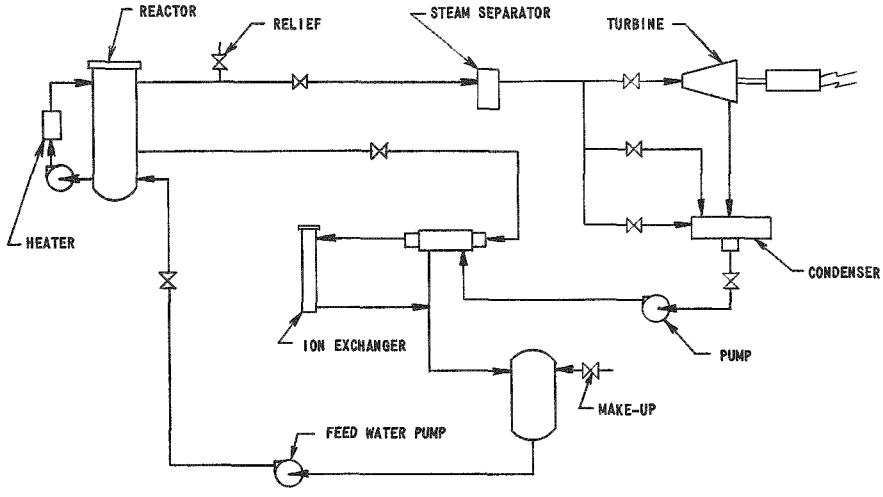

Fig. 3.4

BORAX-III Flow Diagram

In the first ion-exchanger combination, boric acid, added to supplement control rods during early phases of operation, was removed from the system by means of an anion exchange resin column. A mixed-bed

resin column was operated in parallel flow with the anion column to remove all types of ionic impurities to maintain a reasonably high level of water quality. The strong anion resin bed removed the boric acid but the pH of the water increased to 7-8, which approaches a range very corrosive to aluminum. Due to the mixed bed, the water did reach a reasonable level of purity because the resistivity reached 500,000 ohm-cm.

The second attempt at water quality control was through the use of separate anion and cation resin columns. The function of the anion resin was to remove the boric acid. The cation column released acid and lowered the pH to 5-6 which is closer to an optimum for the minimum corrosion rate of aluminum. The reactor water was controlled to a pH value as low as 5.0 but water quality decreased to a resistivity of 150,000 ohm-cm. A higher flow rate through the anion column increased the resistivity to 450,000 ohm-cm and the pH to over 6. A particular effort was made during this second series of tests to obtain megohm quality water but this was not reached. The columns did perform satisfactorily to allow the desired pH control.

The third series of tests involved cation and mixed-bed resin columns. Boric acid was not present in the water during this period. The cation resin column was operated continuously to hold the water in the desired slightly acid state. The mixed-bed resin columns were operated periodically to increase water quality. At one time a resistivity of 900,000 ohm-cm was reached at a pH 6.6. Normally the reactor water pH was maintained at 5.5 to 6.0 and the resistivity was 400,000 to 500,000 ohm-cm.

With the low pH requirement made necessary by the presence of aluminum, the mixed-bed resin and cation resin combination was the best of the combinations tried.

It was estimated that during the operating life of BORAX-III, the fuel was in boiling water at 420°F (215°C) for approximately 1170 hours. It was further estimated that during at least 100 hours the pH of the water was over 8. In addition to operation under boiling conditions, the fuel was in relatively stagnant water over 300°F (150°C) for 100-200 hours before and after the test runs.

These conditions are quite severe for the 2S aluminum cladding from the standpoints of temperature and pH. It is significant that a single loading of fuel was used over the nine-month test period. Although the presence of fission products in the water during the later stages of operation suggests a break in the aluminum cladding, it seems reasonable to assume that a low rate of aluminum corrosion occurred during the BORAX-III tests.

2. BORAX-IV

From the standpoint of water chemistry, BORAX-IV was not significantly different from BORAX-III. The combination of mixed-bed and cation exchangers operated with parallel flow, found best in BORAX-III was continued in BORAX-IV.[32] Instead of operating at a low pressure, however, as in the BORAX-III, the purification system in BORAX-IV was designed for reactor system pressure (see Fig. 3.5). Fuel cladding in BORAX-IV was the aluminum alloy M388 (Al, 1% Ni, 0.5% Fe, 0.2% Si) instead of 2S as used in BORAX-III; a pH range from 5-6 was maintained in the water to minimize corrosion.

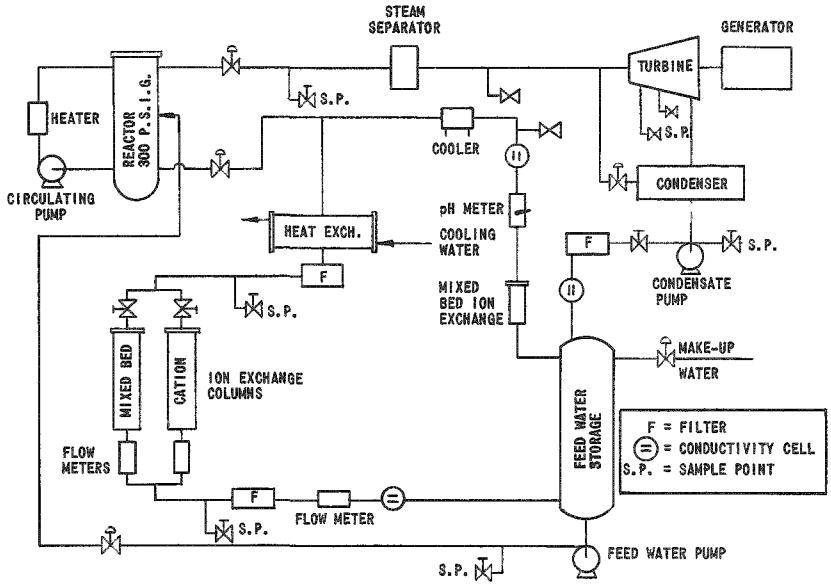

Fig. 3.5

BORAX-IV Flow Diagram

Extended periods of power operation have shown that reactor water quality can be maintained with a resistivity between 300,000 and 600,000 ohm-cm with a pH of 5.7 to 6.2. This was normally accomplished with a strong acid, hydrogen-cycle form cation exchange resin column operating in parallel with a strong acid-strong base mixed-bed resin column. The majority of the 10 gal/min flow went through the cation resin with sufficient parallel flow through the mixed bed to hold the quality of water at the desired level. If the quality of the water exceeded 600,000 ohm-cm, the pH of the system increased slowly. To prevent this the flow through the mixed bed was reduced or shut off for 10 to 15 hours. In this way, pH control with reasonable quality water was attained. Unfortunately, a certain amount of raw water continually leaked from the turbine condenser into the condensate return. The presence of carbonate impurities in the raw water tended to increase the pH of the reactor water. This effect was minimized to some extent during the cycling

through the cation column by release of hydrogen ions from the cation bed in exchange for cationic impurities from the raw water. These hydrogen ions lowered the pH.

From corrosion studies on M388 aluminum alloy, an optimum operating pH in the range 3.5 to 4.0 was indicated.[30] Unfortunately, at a pH of 3.5 and at an operating temperature of 420°F (216°C) some stainless steel corrosion is expected.[54] A satisfactory compromise seemed to be a pH of 5 since under these conditions stainless steel corrosion is negligible and 175,000 ohm-cm water can easily be maintained. The ionic solids associated with water of this quality are a source of some concern since it is quite likely that a small amount of radioactive solid material is carried over to the turbine system by the steam. The normal decontamination factor, $DF = \frac{\text{activity reactor water}}{\text{activity steam}}$, ranges from 10^3 to 10^4 for dried samples 6 to 8 hours after collection.

3. EBWR

a. Description. The Experimental Boiling Water Reactor (EBWR)[55] is a direct-cycle, light water-moderated and cooled boiling water reactor originally designed for 20-Mw thermal and 5-Mw electrical operation. The characteristics of this reactor have been so good that increase in power to 62 Mwt was possible. A subsequent decision was made to modify the heat-dissipation equipment to make possible its operation at powers up to 100 Mwt. The following discussion applies to operation before the 100 Mwt conversion.

Demineralized water boils in the core of the reactor, in contact with the fuel elements, to form steam which passes through a dryer to the turbine and on to a condenser. A steam air ejector removes noncondensable gases from the condenser. Condensed steam collected in the hotwell passes through full-flow cotton string filters back into the reactor.

Water from the reactor vessel, at velocities up to 10 gpm (0.63 liter/sec) is continually bypassed through a purification system. In the purification system reactor water is cooled, filtered through 2-micron particle size cotton string filters, passed through a mixed bed (Nalcite HCR and Nalcite SBR) ion exchanger, through a cotton string after-filter, regenerative cooler, and is pumped back into the reactor. A flow diagram of the reactor is shown in Fig. 3.6.

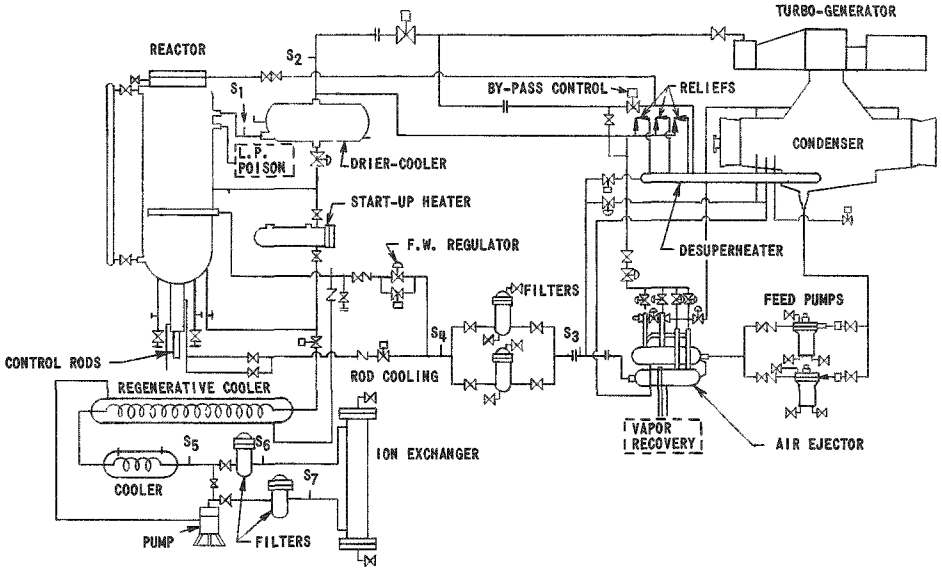

Fig. 3.6

EBWR Flow Diagram
(S_1 to S_7 = Sampling Points)

b. Materials. The pressure vessel is made from SA-212B carbon steel, with a Type-304 stainless steel 0.11-inch (0.28 cm) liner. Materials in the reactor vessel in contact with the primary water are:

Type-304 stainless steel - core support, shroud, and shock shield;
Type-304 stainless steel with 2% boron - control rods;
Type-304 stainless steel with 1% boron - thermal shield;
Zircaloy-2 - fuel cladding, and control rod followers;
Hafnium - control rods;
Aluminum-1% nickel alloy, (M-388)* - dummy fuel elements.

The material from the pressure vessel through the steam dryer is Type-304 stainless steel.

Piping from dryer to turbine is carbon steel lined with 0.005 inch (0.0127 cm) Kanigen nickel.** The turbine is made of conventional alloy materials; everything inside except the rotor, however, is coated with Kanigen nickel.

The condenser is of carbon steel with 6063-T831 aluminum tubes clad inside with 72S aluminum. The upper layer of tubes are protected from water erosion by stainless steel shields over the upper half.

*Developed by ANL Metallurgy Division; available commercially as Alcoa X-8001.

**Chemically deposited nickel containing 7% phosphorus; supplied by The General American Transportation Corporation, Chicago, Illinois.

Feedwater pumps are made of 4-6 and 12-14 chrome steels.

The shells of heat exchangers of the air ejector, through which all of the feedwater flows, are made of carbon steel, lined with 0.003 inch (0.0076 cm) of Kanigen nickel. Tubes in these exchangers are made from No. 16 BWG aluminum.

The feedwater filters, cotton string type with 2-micron particle size capacity, are supported in Type 304 stainless steel-lined steel vessels. The remainder of the feedwater system to the reactor vessel is stainless steel.

All of the metallic material in the purification system in contact with reactor water is stainless steel.

The fluid recovery system contains an aluminum sump tank and an aluminum tube cooler. Reactor water leaking past the seals on the feedwater pump and the seals on the control rods is collected in this tank along with condensed vapor leaking past other seals and is returned to the main condenser.

c. Water

(1) Design Conditions. The purification system, with its mixed-bed ion exchanger, was designed to maintain high-purity water in the reactor. The design figure was set at a resistivity of 1 megohm-cm (equivalent to 0.5-1.0 ppm total solids). Early calculations indicated that this quality could be maintained by a 4-gpm (0.252 liter/sec) flow through the purification system. The system was designed, however, for a 10-gpm (0.63 liter/sec) flow in case it should be necessary to remove boric acid.

The use of aluminum in dummy fuel elements, condenser, and air ejector coolers precluded the extended use of water of high pH.

(2) Prestartup Conditions. After placing the aluminum-nickel M388 dummy fuel elements in the reactor vessel, but before loading fuel, hydrostatic testing of the pressure vessel gasket was carried out by using tap water in the system. Tap water was used because sufficient quantities of pure water were not available. The tap water remained in the system for about two days. On reopening the vessel, extensive rusting of the vessel cladding was observed as a loose, reddish oxide film. Rather extensive corrosion of the aluminum-nickel dummy fuel elements was also observed.[56] This corrosion was characterized by some blistering and was aggravated by galvanic attack near rivets holding stainless steel and aluminum-nickel in contact. A spectrographic analysis of a sample of the corrosion product showed:

Element	% (Order of Magnitude)
Al	gg 1*
Fe	0.05
Mg	0.02
Ni	0.03
Si	0.1

(3) Early Operating Conditions. Shortly after the initial critical experiments a total of 11,250 gm of boric acid, a soluble neutron absorber, or poison, was added to the reactor water to obtain physics data; after a few days the reactor vessel was drained, flushed and refilled with demineralized water. The reactor water was circulated through the purification system to remove the remainder of the boric acid, but the amount remaining in the water was not determined.

About two weeks later, a total of 19.8 lb (9000 gm) of boric acid was added to simulate full-poisoned conditions. The pH of the water decreased to 5.2 and resistivity dropped to 90,000 ohm-cm. It had been planned originally to operate the reactor at 20 Mw for two days, but boric acid remained in the system for about two weeks. During this time the cleanup loop was not operated, and water conditions were very bad, i.e., pH 4.4, resistivity of 38,000 ohm-cm and a high "crud" content. No determination was made of insoluble solids.

The boric acid was taken out by the mixed-bed ion exchanger a little at a time, over a period of three days, at the end of which only 8.3 ppm remained of the original 748 ppm. Total operating time of the purification system was about 20 hr at 8.4 gpm (0.53 liter/sec). The efficiency of the ion-exchanger for the removal of the boric acid was about 98%.

The designed capacity of the water-cleanup system was found to be much greater than needed for continuous 20-Mw operation, since the resistivity of 38,000 ohm-cm was increased to 1,000,000 ohm-cm while operating at full power. No determination was made as to the minimum flow rate required to maintain water of 1 megohm resistivity. Later the filters and ion-exchange column were bypassed for 11 hr to increase the activity of the reactor water for DF data, and the resistivity decreased from 1,100,000 to 833,000 ohm-cm.

The boric acid carryover in the steam was higher than had been anticipated. The DF for boric acid was only 18 as compared with the radioactivity DF of about 4.5×10^3.

---

*gg = Much greater than, or predominant.

(4) Normal Operating Conditions. In the absence of boric acid, the resistivity was between 2 x 10^6 and 1 x 10^6 ohm-cm. The pH varied from 6.9 to 7.2, a result which agrees very well with predicted conditions (pH = 7.0 and resistivity of 1 x 10^6 ohm-cm).

Normal steady state oxygen levels at 600 psig and 20 Mw were as follows:(56)

Feedwater - 0.5 ppb (parts per billion)
Reactor Water - 0.24 ppm (parts per million)
Steam - 28 ppm

4. ALPR (Argonne Low Power Reactor)

a. Description. The ALPR (or SL-1) was a 3-Mwt, heterogeneous, highly enriched, uranium-fueled, natural-circulation boiling water reactor, cooled and moderated with light water. Steam at 300 psig, dry and saturated 421°F (216°C), was passed directly from the reactor to a conventional turbine-generator.(57) A flow diagram is shown in Fig. 3.7.

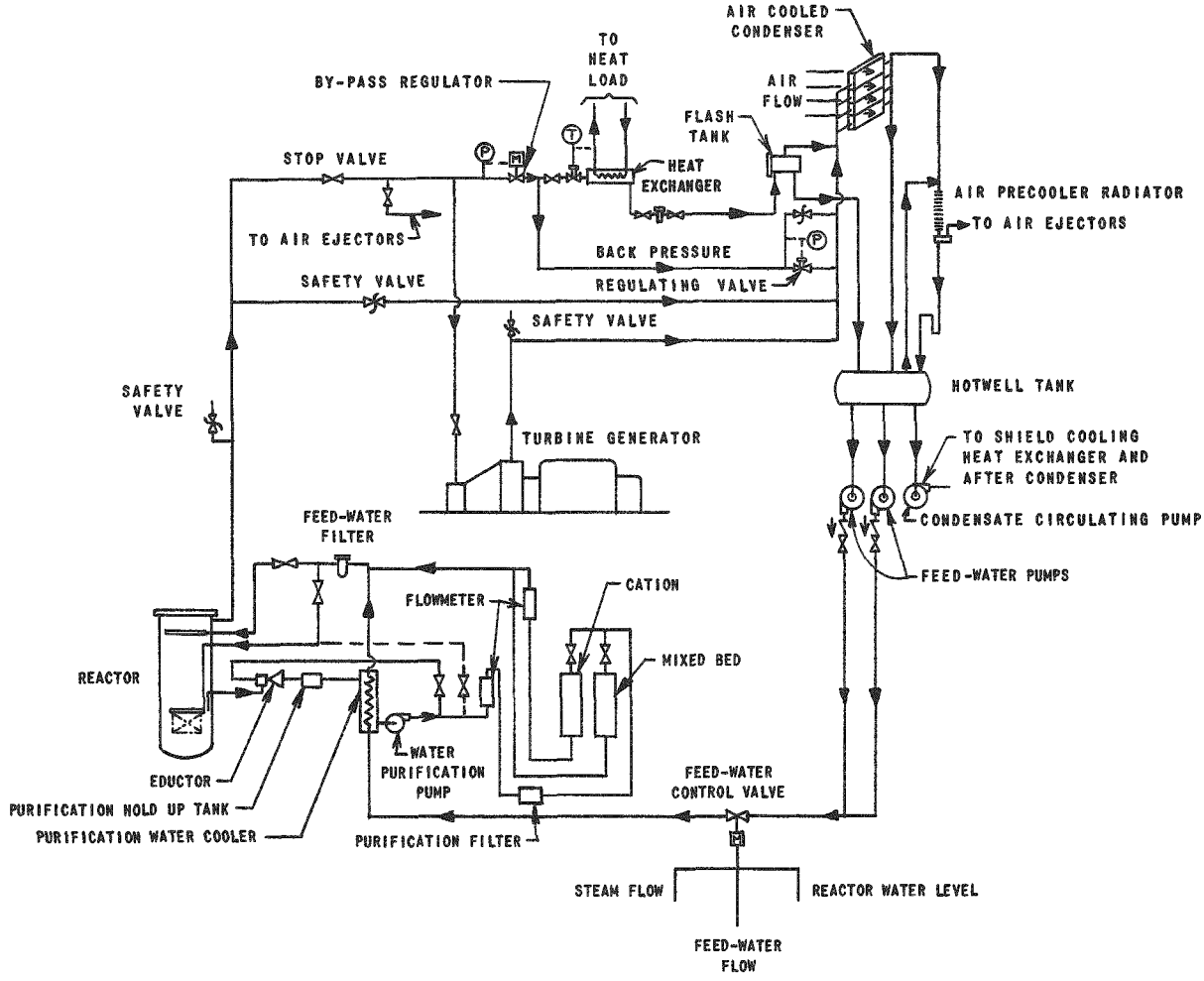

Fig. 3.7
ALPR (SL-1) Flow Diagram

b. Materials. Materials which were in contact with reactor water and steam were as follows:

Pressure vessel - carbon steel SA 212B clad with $\frac{3}{16}$ in. (0.48 cm) stainless steel - Type 304

Thermal shield - SS 304

Core Structure - Al - Ni (X8001)

Burnable poison strips - Al - Ni (X8001) containing B^{10}

Control rods - Cadmium, clad with Al - Ni (X8001)

Control rod drives - 17-4 PH stainless steel, chrome plate, stellite

Turbine - conventional materials

Condenser - 2S Al

Piping - SS 304

c. Water. Condensate was pumped from the hot well, through the reactor water-purification system cooler and feedwater filter, to the reactor vessel, where it was discharged through the feedwater spray ring.

A reactor water purification system was provided to maintain water quality. Water was pumped, at about 3 gpm from the reactor vessel through a heat exchanger purification filter, and ion exchange beds, to the feedwater line where it mixed with feedwater and passed through the feedwater filter to the reactor.

The purification system cooler, although designed for flows from 3-5 gpm was limited to cooling about 3 gpm purification stream water to 170°F (77°C).

The purification filter contained a single disposable cartridge of woven cotton material which was designed to remove particles down to 5 microns in size.

The two ion exchangers were designed for a maximum flow of 5 gpm, approximately 25 gpm/ft^2. Each bed was supported on a 50 mesh screen, with another screen above the bed.

The ion exchanger arrangement as initially designed, consisted of a cation column and a mixed bed column that could be operated either singly or in parallel. This combination had been satisfactory in BORAX-III for maintaining reactor water at pH 5-6 with associated high

resistivity, which are water conditions favorable to a low corrosion rate of 2S aluminum.[19] Unfortunately, limitations of the purification system heater exchanger prevented cooling of purification system water below 170°F (77°C). Since ion exchange resin manufacturers did not recommend the use of strong base anion resins above 140°F (60°C), the only alternative at the time appeared to be the use of a weak base anion resin which was stable up to 212°F (100°C). Since cation resins are reportedly stable to about 250°F (121°C), it was only the anion resin in the mixed bed that was under question. For these reasons the mixed bed was initially specified to contain equivalent parts of strongly acid cation resin in the H-form and weakly basic anion resin in the OH-form.

On November 6, 1958, the cation and mixed bed columns were charged with NR-1 and NR-11, respectively (Illinois Water Treatment Company designations for cation and mixed beds of the specified types).[58]

On December 8, less than one month after charging, depletion of the mixed bed resin was indicated when the resistivity of the reactor water was measured to be 0.9 megohm-cm at pH 6.3 and the resistivity of the purification system effluent 0.75 megohm-cm at pH 6.5. The mixed bed resin (NR-11) was then replaced December 9.

The life of NR-11 resin bed was considerably shorter than the anticipated life of approximately three months. Subsequent chemical analyses of raw water supply, demineralized water supply and reactor water showed excessive amounts of oil. This oil, inadvertently introduced in the raw water supply from an oil-lubricated bearing on a deep well pump, was deposited on the resin, and found to be the cause of the reduced resin life.

The difficulty caused by the oil apparently was more involved than its effect on the capacity of the ion exchange resin alone. In one test,[59] with the reactor cold, the quality of the ion-exchange effluent dropped to pH 4.2 and resistivity 42,000 ohm-cm, but after the reactor was brought up to temperature the pH was 6.5 and the resistivity 5 megohm-cm. There was also evidence that the oil emulsified the resin fines, causing them to pass the filters and enter the reactor.

Actual operation experience indicated that this type of mixed bed, containing a weakly basic anion resin, did not remove weak acids of organic origin, and did not maintain water of high quality (high resistivity). Satisfactory water quality could be maintained only by use of a single ion exchange column containing a mixture of strongly acid cation resin and strongly basic anion resin, [neutral pH and high quality water were recommended[60] for low corrosion of aluminum-nickel alloy X8001].

The limitation of 140°F (60°C) set for strongly basic anion resins is based on usage of this resin with frequent regeneration. Since it was not planned to regenerate ALPR resins, it was believed that the use of the resin at higher temperature should not be a problem. Evidence to support this view was based on accelerated laboratory tests[61] in which strong base-anion resins of the ALPR type were refluxed at temperatures up to 200°F (93°C). Results showed a basicity loss (a test for determining capacity of anion exchange resins to remove the anion of weak acids) of approximately 16% at the end of 750 hours.

Additional evidence[62] is derived from laboratory studies in which the basicity loss is roughly 13% after 6 months of operation at 200°F (93°C) for the type of resin similar to that recommended for ALPR. Although these accelerated laboratory tests are not necessarily directly applicable to ALPR operation, they do suggest the possibility of satisfactory operation at higher temperatures, between 170°F (77°C) and 200°F (93°C) for the strongly basic anion type mixed bed.

For these reasons, the ion exchange system that was finally specified[57] consists of a single mixed bed made up of equal parts of strongly basic anion resin and strongly acid cation resins. The specifications for these nuclear reactor grade resins are as follows:

(1) Strongly acidic, sulfonic cation exchange resin with a minimum exchange capacity of 4.7 milli-equivalents per dry gram of resin in the hydroxide form.

(2) Strongly basic, quarternary ammonium anion exchange resin with a minimum exchange capacity of 3.5 milli-equivalents per dry gram of resin in the hydroxide form.

The Illinois Water Treatment Company mixed resin NR-14, a mixture of strong base porous anion resin and the 8% cross-linked strongly acid cation resin, was recommended for ALPR applications as being able to withstand higher temperatures up to the specified 200°F (93°C) without damage, particularly since the resin is used only once. Use of this resin returned the water quality to satisfactory levels (pH 6.5; resistivity 1 megohm-cm).

For primary makeup water, raw (unchlorinated) well water was supplied to the demineralizer and the demineralized water was stored in the adjacent, overhead 1000-gal plant water storage tank. The system contained a $1\frac{1}{2}$ ft^3 resin capacity ion exchanger, a pre-filter and an after-filter. The resin used to demineralize the well water was Illinois Water Treatment Company Type TM-1, commercial grade. This resin was a mixture of a cation resin in the hydrogen form and an anion resin in the

hydroxyl form. No regeneration of resin was provided, primarily because the reactor was designed for remote installation, where water supplies, waste facilities, and man power for maintenance are limited.

5. VBWR

a. Description. The VBWR (Vallecitos Boiling Water Reactor)[34] is an enriched uranium boiling light water reactor, with a rated power capacity of 30 Mwt and 5 Mwe at a maximum pressure of 1000 psi. Provision is made to operate under a wide variety of experimental conditions, with single or dual cycle, natural or forced circulation and varying degrees of water purity and oxygen content.

The flow diagram is given in Fig. 3.8.

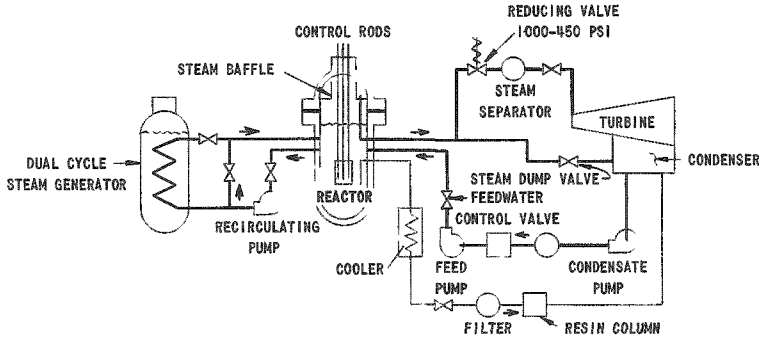

Fig. 3.8

VBWR Flow Diagram

b. Materials. The materials in contact with reactor water, steam, and condensate are:[34,63]

Fuel Plate Cladding	Stainless Steel 304L and Zircaloy
Pressure Vessel Lining	Stainless Steel 304L
Steam and Condensate Piping	Carbon Steel
Condenser Tubes	Phosphorized Admiralty

c. Water. The VBWR water circulates through a simple cleanup system consisting of a non-regenerative heat exchanger and a mixed bed demineralizer. The flow is returned to the suction of the feedwater pumps. During the first year of operation VBWR was used to investigate coolant chemistry problems associated with boiling water reactors and Dresden in particular.[35]

A comparison of the Dresden reactor water and feedwater quality specifications and normal experience at VBWR is given in Table 3.3.

Table 3.3

DRESDEN SPECIFICATIONS VS VBWR EXPERIENCE FOR REACTOR WATER AND FEEDWATER

Reactor Water	Dresden	VBWR
1. Additives	None	None
2. pH	7.2 ± 0.2	7.0 ± 0.2
3. Resistivity, megohm-cm	1	1
4. Total Solids, ppm	0.6	1-12
Feedwater		
1. Resistivity, megohm-cm	10	10 ± 1
2. Copper, ppm	0.002	0.01 ± 0.01
3. Iron, ppm	0.002	0.002 ± 0.001
4. Chloride, ppm	0.01	0.005 ± 0.005

In general, the Dresden specifications were maintained in VBWR with exception of the copper level and total solids. Some copper fittings exposed to the high temperature water in VBWR caused the former exception. The solids found in the VBWR water were silica obtained from inadequate treatment of cycled waste water, and at one time, boron carbide leached from a faulty control rod assembly.

Resistivity measures only the ionic content of the water. The high solids content found in combination with a high resistivity indicates that most of the solids are non-ionic. This emphasizes the importance of specifying both a total solids limit as well as a resistivity minimum for reactor water quality. The performance of the cleanup demineralizer as a filter, in large part, is also inferred.

It was realized that the primary coolant reference quality of one megohm-cm resistivity, neutral pH and no additives is not necessarily the optimum for a boiling water reactor. For example, tests carried out under the auspices of the NRB (Naval Reactors Branch, USAEC) for their PWR systems indicated that operation at high pH, above 9.5, produced less deposition on heat transfer surfaces than operation at neutral pH. It was also found that deposition and fouling were adversely affected by the presence of oxygen in the system.[64] Wroughton and Cohen[65] presented evidence that less corrosion product was introduced into the circulating water at the higher pH; and that the cleanup loop had access to only a small fraction of the corrosion product in the system.

No significant deposits on fuel elements, such as found in EBWR,[56] were noted in the first year's operation of the VBWR.

A loosely adhering copper-colored film was present on the zircaloy cladding of the test fuel, especially in the heat transfer areas. There has been no indication of a film buildup with time.

The hope that neutral, no additive coolant quality may continue to provide satisfactory performance has been strengthened indirectly by some recent 1000 hour out-of-pile corrosion tests.(35) The determination of corrosion product transferred to coolant, by calculation from weight of undescaled vs descaled corrosion coupons, indicates that in the case of both carbon steel and stainless steel a many-fold difference exists in favor of a boiling water system containing oxygen and hydrogen, as compared to a pressurized system containing only hydrogen, both operated at pH 7.

Full flow demineralization of the condensate returning from the condenser to the reactor was desirable for the Dresden plant for several reasons: (1) to minimize the total solids going to the reactor that could be irradiated and cause system activity problems; (2) to decrease the load on the reactor cleanup demineralizer resins that will be discarded because of the high radioactivity contained therein; (3) to permit the use of a copper-alloy condenser and Stellite-tipped blades on the turbine without the concern of the corrosion products getting back to the reactor; and (4) as a protection in case of a condenser leak to keep contamination from condenser cooling water out of the reactor coolant.

Because of the size of the equipment and the resin inventory required to handle the normal 3200 gpm flow of feedwater, utilizing normal design flow rates of about 5-6 gpm/ft^2 of resin bed surface would have resulted in a large costly installation.

A development program was started in 1955 to investigate the possibility of using faster than normal demineralizer flow rates. Results(66) showed higher flow rates, up to 75 gpm/ft^2 are technically and economically feasible with substantially complete removal of the metallic constituents (0.0 ppm cobalt and copper). Although with higher flow rates the operating capacity of the resins decreases and the pressure drop of the system and the pumping cost increase, the total equipment cost and space requirements decrease at a more rapid rate to give a lower initial capital investment and lower annual cost at higher flow rates. The economic gain levels off substantially with increase in flow rate above 50 gpm/ft^2 of resin bed. The following items regarding demineralization are of interest:

(1) As the flow rate through the bed is increased, the average leakage of any particular ion for a given break-through value increases and the operating capacity decreases.

(2) Increasing the concentration of the soluble corrosion products in the range studied has no effect on capacity to the same percentage leakage cut-offs.

(3) Varying the beds down to one foot in height gave no effect of column length due to loss of contact efficiency.

Performance data from the VBWR mixed-bed demineralizers have been very encouraging. The resin beds have operated satisfactorily up to the tested flow rates of 60 gpm/ft^2 of resin bed. The measured pressure drop did not increase with time and was in good agreement with corresponding calculated values utilizing the Kogeny-Carman type equation.(67)

The resin beds have passed 13,800,000 pounds of water/ft^3 of resin before requiring replacement. It is expected that better performance may be obtained in the Dresden installation where a lower anion load will exist from recirculated waste water.

6. Dresden

a. Description. The Dresden Nuclear Power Station(68) employs a boiling water reactor operating on a dual pressure thermal cycle, 965 psi saturated at the turbine primary admission and about 500 psi saturated at the secondary admission. The total flow of the two streams is about 2.6 x 10^6 pounds per hour. The net electrical output is 180,000 kilowatts.

b. Materials. The materials of construction affecting condensate and feedwater quality(69) are:

Pressure Vessel	ASTM-A-302, Grade B Carbon Steel clad with SS Type 304
Main Primary Circulating Piping	SS Type 304
Fuel	UO_2 pellets in Zircaloy Jacket, a few assemblies clad with SS Type 304
Control Rods	
Original	2.0% Boron Stainless Steel
Replacement	B_4C clad in SS Type 304
Steam Drum	Carbon Steel clad with Stainless Steel

Secondary Steam Generators	
Shell Side	Carbon Steel
Tube Side	Carbon Steel lined with Stainless Steel
Tube Bundles	Stainless Steel
Condensers	
Tubes	Phosphorized Admiralty
Tube Sheets	Carbon Steel
Shell	Carbon Steel
Hotwell Trays and Baffles	Stainless Steel
Extraction Piping, Flash Tanks, Heater Shells and Drain Lines	Carbon Steel
Low Pressure Feedwater Heater Tubes	70-30, Copper-Nickel
High Pressure Feedwater Heater Tubes	Monel
Turbine(70)	
Casings	
High Pressure	2 $\frac{1}{2}$ Cr-1 Mo
Intermediate Pressure	Carbon Steel
Exhaust Hood	Carbon Steel
Rotors	2 Ni-$\frac{1}{2}$ Mo
Diaphragms	
High Pressure	12 Cr or 2 $\frac{1}{4}$ Cr-1 Mo
Intermediate Pressure	12 Cr or 2 Cr or Ni-Resist
Low Pressure	Cast Iron
Buckets and Nozzle Partitions	Conventional
Packings	
Casings	12 Cr
Rotor Sleeves	12 Cr
Piping	Carbon Steel
Valves	
Primary and By-Pass	2 $\frac{1}{4}$ Cr-1 Mo
Secondary	Carbon Steel
Wheels	
Stages 16, 17, 18, 22, 23	1 Cr-$\frac{1}{2}$ Mo
Stages 19, 20, 21	3 Cr-$\frac{1}{2}$ Mo
Stages 24, 25	1 $\frac{3}{4}$ Ni-1 $\frac{1}{4}$ Cr-$\frac{1}{2}$ Mo-1 V

c. Water Treatment. The Dresden water treatment system[71] was designed to minimize adverse effects of contaminants of three types: (1) corrosion products from the cycle; (2) in-leakage of cooling water; and (3) dissolved gases. Of the three sources, the major contamination source is system corrosion products.

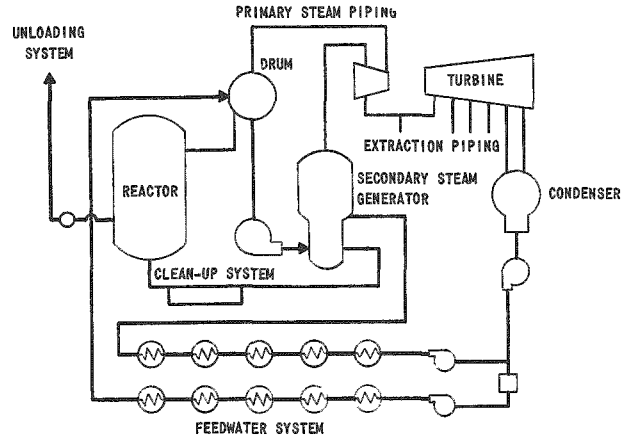

Fig. 3.9

Dresden, Schematic Diagram of Plant Cycle

The Dresden cycle is shown schematically in Fig. 3.9. An estimate was made of the maximum corrosion product concentrations to be expected throughout the cycle. Figure 3.10 is a schematic presentation of the cycle showing quantities of materials expected in various parts of the system. Quantities of fluid and contaminants or additives are given in units of pounds passing the indicated point per hour. Note that the full flow of feedwater to the reactor vessel is purified in mixed-bed demineralizers while the secondary feedwater is taken before demineralization. The primary reactor coolant is limited to a maximum of 0.5 ppm total solids. This solids level is maintained by bypass demineralization.

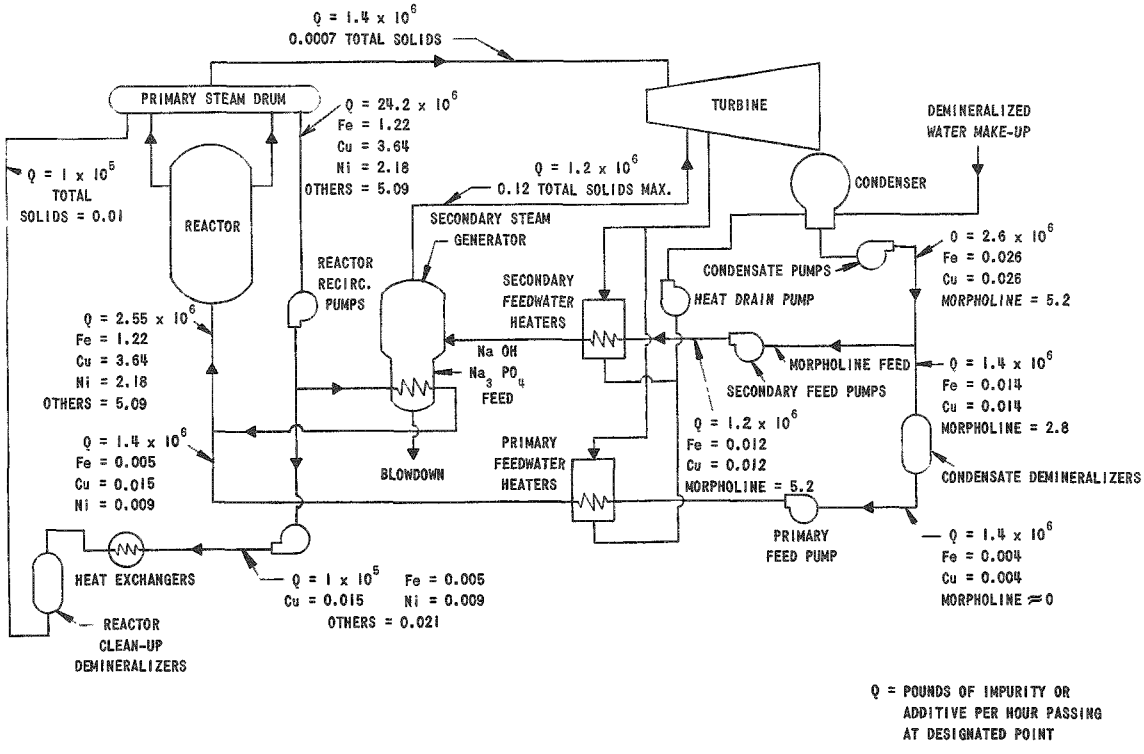

Fig. 3.10

Diagram of Dresden Cycle Impurities Balance

The concentration of solids in the secondary steam generators is maintained by a standard boiler blowdown system. Total solids in the shell side water of the generators is limited to 100 ppm.

A second source of system fluid contamination is leakage of the condenser cooling water. By means of a special condenser design, the designed leakages at tube to sheet joints was expected to be zero.

Gas concentration in the system is the third type of contamination to be minimized in the water treatment. Radiolytic decomposition of water in the reactor core results in a steam line oxygen concentration of up to 60 ppm. This and other gases plus any gaseous in-leakages are removed in the deaerating hotwell of the condenser.

The above are the three broad classifications of system fluid contamination. Methods of control and specific equipment used will be covered in some detail. To insure a minimum in-leakage with make-up water, complete demineralization is provided. Purity of this water is maintained by storage in aluminum tanks. Make-up water is sprayed into the condenser to insure deaeration.

(1) Main Condenser Design. In addition to providing degasification in the hotwell, the condenser incorporates a design feature to eliminate cooling water in-leakage. The condenser is of the single pass, divided water box type. Therefore, operation at reduced load can be maintained while one side of the condenser water box is opened for repair. To eliminate leakage of cooling water into the condenser, double tube sheets were provided. The space between these tube sheets is filled with demineralized water, with a static head higher than the cooling water pressure. Any rolled joint failure in either tube sheet roll will result in a loss of demineralized water from the between tube sheets space to the cooling water or to the hotwell.

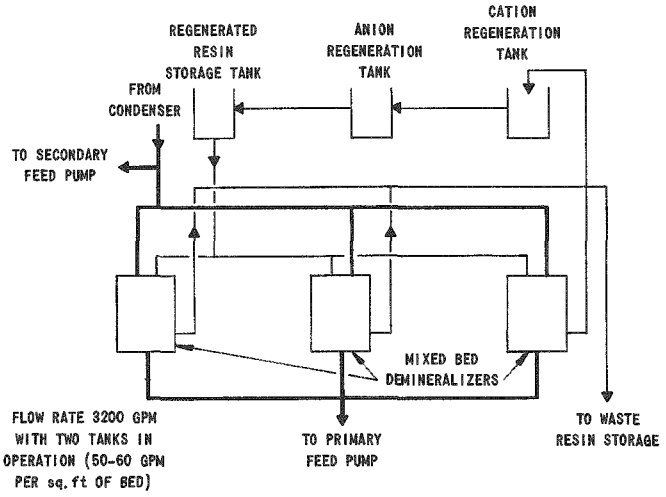

Fig. 3.11

Diagram of Dresden Condensate Demineralizer System

(2) Condensate Demineralizer. The condensate demineralizer system shown in Fig. 3.11 has some newly developed features. To maintain a maximum concentration of 0.5 ppm total solids in the reactor coolant, it was decided that the elimination of solids in the feedwater would be more satisfactory than to attempt to remove solids from the reactor.

Such a system reduces the amount of irradiated solids to be handled since most, if not all, of the corrosion products in the condensate system are not radioactive. Since the primary feedwater flow is about 3200 gpm, normal flow rate demineralization would have led to a very large installation. With normal flow rates of about 10 gpm/ft^2, 320 ft^2 of resin bed surface would have been required. However, since the total solids of the condensate are low, design flow rates for the condensate demineralizer were raised to 50 to 60 gpm/ft^2. The result is that the total primary flow can be carried on two 78-inch diameter exchangers operating in parallel. A third exchanger is provided as stand-by for resin transfer periods or times of high system contamination, such as may be caused by a fuel element rupture or complete failure of a condenser tube.

No filters are provided ahead of the demineralizers. The demineralizer beds operate as filters as well as ion-exchangers. The ratio of insolubles to solubles in the condensate stream was expected to vary from 4:1 to 1:2. Testing on steam plant condensate has shown that operation without prefilters at the 50-60 gpm/ft^2 design flow rates is completely satisfactory. Resin ion-exchange capacity and life were not appreciably reduced by the filtration load. Regeneration of the condensate demineralizer resins is not carried out in the ion-exchanger vessels. At the end of an operational cycle, the exchanger vessel is isolated and the resins are hydraulically transported to the cation regeneration tank shown in Fig. 3.11.

The resins are separated and rinsed in this tank before the anion resin is hydraulically transferred to the anion regeneration tank. The separated cation and anion resins can then be regenerated with sulfuric acid and sodium hydroxide respectively. The separate tank regeneration allows any special treatment necessary for each resin in addition to insuring complete isolation of regenerant solutions from the reactor cycle. The resins are finally transported to the resin storage tank for mixing and final rinsing.

Four resin charges are provided in the system with the spare charge kept in the regenerated resin storage tank. At the end of a service cycle, a given exchanger vessel will be out of service for not more than one hour. The spent resin is transported to the cation regeneration tank and a fresh charge of resin is immediately moved into the empty exchanger vessel. The spare resin charge allows extra time in regeneration for special treatment and procedures as may be found necessary. Resin losses will be made up by additions to the regenerated resin storage tank.

(3) Reactor Coolant Cleanup System. The purity of the reactor coolant must be maintained to insure good heat transfer characteristics and to minimize the quantity of irradiated solids. Reactor

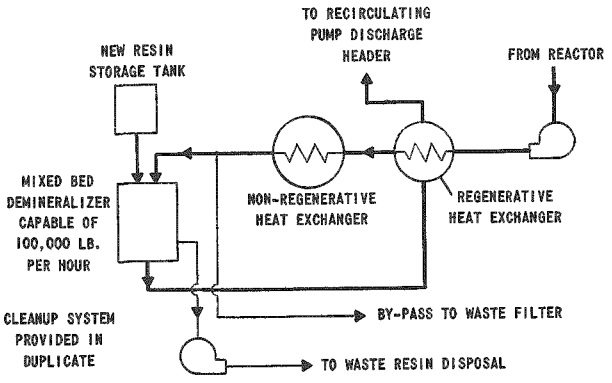

Fig. 3.12

Diagram of Dresden Reactor Water Cleanup System

water quality is maintained by means of a high pressure, bypass cleanup demineralizer shown in Fig. 3.12. The system shown is of 1250 psi design. The entire cleanup loop is provided in duplicate, each loop is of 100,000 lb/hr capacity. Water enters the system from the reactor recirculating pump discharge header. The cleanup recirculating pumps are of canned rotor design. By use of regenerative and non-regenerative coolers, 75 per cent of the heat entering the cleanup system is returned to the reactor circulating system. As in the condensate demineralizer units, no filters are used ahead of the resin beds. Conventional flow rates of about 10 gpm/ft^2 are employed in the cleanup demineralizer vessels, since the demineralizer vessels at these rates are small and are only a small part of the cleanup system cost. A bypass line to the waste system is provided to dump reactor coolant at times of high solids contamination. This loss of reactor coolant is made up by increased primary feedwater flow. Due to high radioactivity in the spent resins, no regeneration facilities are provided. Spent resins are pumped to permanent resin burial and new fully regenerated resins are charged to the high pressure ion-exchange vessel.

At the predicted corrosion rates, 100,000 lb/hr cleanup will maintain a reactor coolant concentration of about 0.4 ppm total solids. The operational limit was set at 0.5 ppm maximum. A factor of safety was provided in the system since both cleanup circuits can be operated simultaneously to give a cleanup rate of 200,000 lb-hr.

(4) Secondary Steam Generator Treatment. The secondary steam generators receive chemical treatment consistent with modern high pressure plant operation. Feedwater to the secondary heaters and generators is taken ahead of the primary condensate demineralizers. An upper concentration limit of 100 ppm was established for the shell side water of the generators. Such a limit is permissible since radiation and heat transfer rates are low in the generators as compared to the reactor. The steam generators are of shell and tube design mounted vertically. The tube side is stainless clad, with stainless steel tubes to maintain purity of the primary coolant. The shell side is of carbon steel. Blowdown of the secondary generator water was expected to be based on chloride concentration (0.1 ppm maximum) in order to avoid chloride stress corrosion of the stainless steel tube bundles. Provision was made for morpholine to be added at the secondary generator feed pumps to maintain a feedwater

pH of 8.8 to 9.0, thus minimizing corrosion in the feedwater system. Provision was made for trisodium phosphate and sodium hydroxide to be added directly to the shells. Limits of treatment have been set at 5 ppm phosphate and a water pH of 10.5 maximum.

(5) Operating Experience. The primary feedwater and reactor water quality specifications given for Dresden in Table 3.3 were established to prevent deposition on heat transfer surfaces in the reactor core and to minimize the load on the reactor cleanup demineralizers.

The condensate polishing equipment required to produce this high quality feedwater consists of three externally regenerated mixed-bed demineralizers, each containing 80 cu ft HCR - cation resin and 40 cu ft of nalcite SBR-P anion resin operated at 50 gpm/ft^2 of bed area.(60) There are no filters in this system; pilot plant studies had demonstrated that both suspended and dissolved solids present in condensate from high pressure steam generators could be removed throughout the depth of ion exchange beds operated at 30 to 100 gpm/ft^2 without excessive pressure loss or resin degradation, provided the equipment was properly designed for this service. Filters for removing suspended solids ahead of the demineralizers would have introduced additional pressure loss, created a troublesome waste disposal problem and more than doubled the space required for the installation.

Since the resin beds serve a dual purpose, removing suspended solids as well as dissolved ionic solids, provision was made for removing suspended solids from the beds as well as regeneration. At the end of an operating run, exhausted resin is removed through the connection at the bottom of the demineralizer to external regeneration equipment. The exhausted, mixed resin is separated into two layers by backwashing and the anion resin is transferred to its own regeneration tank. Each resin is then scrubbed with air, backwashed, regenerated if necessary, and transferred to the mixing and storage tank. Separate tanks for the cation and anion resins insure maximum removal of suspended solids and facilitate any special treatment required to restore maximum capacity. Most of the suspended solids deposited on the resins during operation are loosened during transfer from the demineralizer to the cation regeneration tank and eliminated by the backwash which hydraulically separates the resins. Additional suspended solids are removed by air scrubbing and backwashing in the two regeneration tanks. Chemical regeneration is required only when the resins are exhausted to dissolved solids.

Before startup the entire system, with the exception of the turbine and the upper portion of the neck of the condenser, was cleaned with citric acid. Metals in the cycle included brass, cupronickel,

monel, carbon steel, and stainless steel. The total water volume of the component parts of the system cleaned was 430,000 gallons and approximately eight tons of iron oxide and 0.14 tons of copper oxide were removed from the system. Details of the cleaning procedure have been described.(72)

Three months elapsed between acid cleaning and initial operation. Pre-operational tests conducted during this period made it difficult to protect the system from corrosion and this resulted in rather high turbidities during initial startup.

As the reactor was brought up to temperature and normal flow was established, the heater drains, turbine, etc. contributed a heavy load of suspended solids to the polishers. It is significant that the tremendous load of suspended solids did not result in plugging or channeling the beds. The resins simply lost capacity for suspended solids removal and were no longer effective. At a flow rate of 1300 gpm per unit (40 gpm/ft^2) the pressure loss across the system was only 36 psi after the beds were exhausted on the basis of suspended solids.

During the initial startup and the 50 per cent power run, the quality of the unpolished condensate varied over a wide range, as would be expected during any station startup, but these variations had little effect on polished condensate quality after the first few days. Average values of iron and copper are given in the first two lines in Table 3.4.

Table 3.4

AVERAGE TOTAL Fe AND Cu IN DRESDEN FEEDWATER BEFORE AND AFTER POLISHING

(Parts Per Billion)

	Fe In	Fe Out	% Removal	Cu In	Cu Out	% Removal
April 15-21, 1960	1,086	498	54	313	137	56
April 22-May 1	163	49	70	59	15	74
June 20-30	184	17	91	61	7	88
July 1-4	32	8	75	31	3	90

Table 3.5 gives maximum, minimum and average values for the conductivity, pH, chloride, iron, and copper of the reactor water from April 15 through May 1, 1960.

During the full power run starting June 20, 1960, operation of the condensate polishing equipment, for the first time since the initial startup, may be considered reasonably "normal." Variation in the concentration of impurities in the influent had little effect on effluent quality and flow variations were handled without incident. The last two lines in Table 3.4 give average values for these data.

Table 3.5

DRESDEN REACTOR WATER QUALITY APRIL 15 - MAY 1, 1960

	Maximum	Minimum	Average
Conductivity - m mhos	7.9	0.76	2.5
pH	6.5	5.1	5.7
Chloride-ppb	169	10	70
Total Iron-ppb	80	3	30
Total Copper-ppb	300	18	83

With continued operation, the quality of the water throughout the system improved, as impurities associated with initial startup were reduced to normal levels. The conductivity of the condensate before and after polishing averaged 0.5 and 0.2 micromhos, respectively, in July compared to 0.21 and 0.10 respectively in November. The reactor water averaged 1.4 micromhos in July and 0.56 micromhos in November.

The dissolved solids load on the condensate demineralizers has been very light. The resins have not been exhausted to dissolved solids and each of the four resin charges has been chemically regenerated only three or four times since the station first produced steam in April, 1960, although several regenerations were conducted before that time.

Since April, 1960, each of the four resin charges in the polishing system has made eight round trips for physical cleaning without chemical regeneration. This does not include several transfers conducted to check out the equipment during pre-operational tests and to clean the resin prior to startup.

Over 400,000,000 gallons of condensate have been polished, and at no time has it been necessary to bypass unpolished condensate to the reactor. Performance of the demineralizers as ion exchangers has been excellent. Performance in removal of suspended solids has been very good as evidenced by millipore filter discs, and, perhaps more important, by the small quantity of corrosion products found in the reactor after shutdown following the full power run and commercial service.

3.4. Conclusions

The use of ion-exchange bed cleanup loops in water-cooled and moderated reactors to remove ionic, particulate, and colloidal

impurities has become almost universal standard practice. This practice minimizes water decomposition, radioactivity hazard to personnel, and other problems resulting from crud deposition

In Pressurized Water Reactors using zirconium alloy clad fuel, the use of ion-exchange resins is supplemented or modified by alkali regeneration to maintain the water at high pH. This has served to minimize stainless steel corrosion and crud problems.

In Pressurized Water Reactors using stainless steel clad fuel (APPR), high pH control has not been tried but the activity buildup problem has been of such a nature that the use of high pH control has been proposed.

So far as the writer is aware, high pH control has not been applied to Boiling Water Reactor operation, so any advantage from its use in such reactors remains to be determined. Limited data indicate that Boiling Water Reactor environment (neutral pH and stoichiometric ratios of water decomposition gases) is less corrosive to stainless and other steels than Pressurized Water Reactor environment (high pH, high hydrogen and essentially no oxygen).

The high pH, favorable to stainless and other steels in Pressurized Water Reactors, is incompatible with aluminum. Low pH, in Pressurized Water Reactors reportedly increases corrosion, activity, and crud problems. Operation of Boiling Reactors at low pH has been limited to BORAX-III and BORAX-IV in which aluminum was used extensively. The nature of these experiments was not such as to make possible comparable evaluation of the corrosion, activity, and crud problems with those in Pressurized Water Reactors.

Use of full flow demineralization of condensate, as used in Dresden to remove both ionic and particulate matter, appears to be a practical way to minimize the crud activity problem. By preventing inactive corrosion products originating in the steam system from entering the reactor and becoming activated, condensate demineralization reduces the load of active corrosion products picked up by the reactor cleanup loop demineralizer. Maximum economy is favored by high flow rates through the condensate bed, and by provision for cleaning as well as regeneration. Due to the activity picked up by the reactor cleanup demineralizer, the latter cannot be regenerated.

4. CORROSION OF MATERIALS

4.1. Introduction

Section 4 is concerned with the corrosion behavior of materials in reactor or simulated reactor environment, as contrasted with problems resulting from the presence of corrosion products in reactor systems.

Section 4.2 summarizes the corrosion behavior background of the more important materials used in the primary system of EBWR, the reasons for their selection and in some cases the consequences of their use. Many of these materials are used in other boiling water reactors and pressurized water reactors also.

Section 4.3 summarizes corrosion investigations of materials for Dresden.

Section 4.4 summarizes corrosion investigations of aluminum alloys developed for high temperature water reactor use.

4.2. EBWR Materials

1. Type 304 Stainless Steel

The use of 18-8 stainless steel in contact with the primary coolant water in a boiling water reactor is a logical extension of its application in pressurized water reactors. Its use stemmed from a development program sponsored by the Naval Reactors Branch Division of Reactor Development of the U.S. Atomic Energy Commission. A great many materials were investigated in this program and much of the corrosion data as well as guides to application have been summarized in "The Corrosion and Wear Handbook for Water Cooled Reactors."[49]

Although early pressurized water reactors used Type-347 stainless steel (SS Type-347) widely, it was found early in the above program that the columbium, Cb, (or niobium, Nb) stabilized grade of 18-8 stainless steel was unnecessary as long as high purity water was maintained.[49] Because Type-304 stainless steel (SS Type-304) was considered acceptable from the corrosion standpoint for use in contact with high-temperature, high-purity water and because it was more attractive from the standpoints of availability and cost than other 18-8 stainless steel alloys, it was selected for wide use in EBWR.

Type-304 stainless steel was used in EBWR as lining for the pressure vessel, much of the core structure, piping to steam dryer, steam dryer and emergency cooler, purification system piping and components, and feedwater piping.

The 18-8 stainless steels because of their high corrosion resistance are widely used in water reactors for structural purposes, piping, components in contact with primary water and as a cladding material for carbon steel pressure vessels, and a cladding for fuel. Corrosion and other properties of stainless steels pertaining to their use in reactors are described in recent summaries.[73,74]

The use of any stainless steel in a reactor causes a problem from the activation of corrosion products. The problem that developed in EBWR as a result of activation of corrosion products is described in Section 5.

A result of using SS Type-304 in EBWR that has been discovered in examination of control rods removed since shutdown for 100 Mw conversion is the failure of a number of rivets used in fabrication. Failure has been attributed tentatively to stress corrosion cracking induced by using trichloroethylene in degreasing the control rods before subjecting them to high-temperature water.[75]

2. Zircaloy-2

Zircaloy-2 was the material used for fuel cladding and control rod followers in EBWR. It is a zirconium alloy containing 1.5% tin, 0.12% iron, 0.10% chromium and 0.05% nickel.[76] Use of zirconium and its alloys came from the development program sponsored by NRB mentioned previously to find reactor materials suitable for use in high-temperature water reactors. The corrosion resistance and low neutron cross section make zirconium and its alloys desirable for use in fuel cladding and core structural purposes.[77] The corrosion rate of Zircaloy-2 is less than 0.05 mg/cm^2-mo up to 600°F (316°C) water for tests conducted up to three years. One phenomenon of the corrosion behavior of this alloy was a breakaway type of corrosion. This is a sudden upward change in rate. In 680°F (360°C) water, it occurs after 50 days. The weight gain at breakaway is usually from 0.40 to 0.50 mg/cm^2. (One mil of metal penetration is equal to about 16 mg/cm^2 weight gain.)

The reason for selecting Zircaloy-2 as the cladding material for the fuel in EBWR is inextricably bound to the selection of U-5 Zr-1.5 Nb as the reference fuel material, (Sec. 4.2.3.). In essence, Zircaloy-2 offered maximum corrosion resistance, and at the same time maximum compatibility with the fuel alloy from the standpoint of hot roll bonding. On the other hand, a factor in selecting the reference fuel alloy was the close match in rolling properties with those of Zircaloy-2, specifically the absence of intermetallic compounds in the zirconium-uranium system.[78] Zircaloy-2 was chosen over high purity zirconium crystal bar because the latter was characterized by higher cost, more erratic corrosion behavior in high temperature water, and poorer rolling properties caused by its low hardness level. Zirconium ingot from sponge was unacceptable because of its high and erratic corrosion rate.

Other than finding Zr^{95} activity occasionally in reactor water deposits, there has been no evidence of zirconium corrosion causing any problem in EBWR.

3. EBWR Fuel

The alloy, U-5 w/o Zr-1.5 w/o Nb, was used as fuel in EBWR. It came[79] from a program to develop a corrosion resistant uranium alloy. This alloy, when subjected to its optimum heat treatment for corrosion resistance, gave corrosion rates in 290°C water averaging about 6 mg/cm^2-day. Whereas unalloyed uranium has shown corrosion rates in 260°C water estimated at about 64,000 mg/cm^2-day.[80] Irradiation tests[81] on this alloy, however, showed that as little as 0.74% total atom burnup destroyed much of the improved corrosion resistance given by alloying additions and heat treatment. In addition to loss of corrosion resistance under irradiation, the alloy in the super-saturated alpha condition showed very poor dimensional stability under irradiation. Kittel and Paine[82] found growth rates as high as 470 microinches/inch-ppm burnup. These investigators found, however, that with the proper heat treatment the irradiation stability of this alloy could be improved. The recommended heat treatment for dimensionable stability under irradiation consisted of a gamma solution treatment followed by an isothermal quench into the high alpha plus gamma temperature range, holding at this temperature and then air cooling. This treatment reduced the irradiation growth rate of the alloy from 470 microinches/inch-ppm burnup to 5.4 microinches/inch-ppm burnup. This heat treatment, like irradiation, was found to destroy most of the corrosion resistance of the alloy. Attempts to find a duplex heat treatment, by superimposing the optimum heat treatment for corrosion resistance over that for stability, failed to produce an irradiation stable and corrosion resistant structure.

Although one of the original objectives of the alloy development, corrosion resistance, was gone, the alloy was retained for fuel for EBWR because of its close match in rolling characteristics to those of Zircaloy-2 cladding material. Since the heat treatments for corrosion resistance and dimensional stability were incompatible, the decision was made to heat treat for dimensionable stability and depend on the cladding for corrosion protection.

The specific heat treatment used on the plates consisted of heating to 825°C ± 5°C, holding for 1 hour, quenching in lead at 640°C ± 5°C, holding at this temperature for 22-23 hours, removing, and air cooling.

All of the fuel plates passed in other acceptance tests were subjected to autoclave tests in 550°F (288°C) demineralized water for 9 to 15 days before they were fabricated into subassemblies; as subassemblies they were again given another similar autoclave test. Out of over 1,000 plates tested only three failed by rupturing in the autoclave. All three failures occurred within three days from the beginning of the test as indicated

by a buildup of gas (hydrogen) pressure in the autoclave. From the appearance of the plates, it is believed that failure was initiated at the bond area between the core and the side strip, due to the presence of an undetectable flaw in the cladding at this point, permitting water to reach the fuel alloy. It is believed that corrosion hydrogen that could not escape through the defect, accelerated the attack of the fuel.(83)

During the life of EBWR to date, there has been no fuel element failure. The small amount of fission products found have been attributed to other causes (see Sec. 6). Evidently vulnerable cladding defects not found otherwise were found, and the plates eliminated, in the autoclave test.

In June 1958 and November 1959, fuel elements T-23 and ET-51, which had been in the reactor (see Sec. 5) for periods of one year and two and one-third years, respectively, were disassembled and sampled. Samples of the irradiated fuel alloy core were corrosion tested in water at 260° to 270°C along with unirradiated control;(84) the results are given in Table 4.1. A marked improvement in the corrosion resistance with burnup in the range of 0.005% to 0.09% (atom percent, a/o) burnup is noted.

Table 4.1

CORROSION RATE VS. BURNUP, EBWR FUEL ALLOY

Burnup a/o	Corrosion Rate Mg/cm^2-day
0.000	9470
0.005	2500
0.009	2780
0.017	2310
0.024	1880
0.088	1890
0.11	5160

At present there is no positive explanation for this improvement in corrosion resistance with irradiation. It has been suggested(84) that the thermal spikes caused by irradiation may have an effect of changing the structure from the dimensionably stable, isothermally transformed structure to the corrosion resistant quenched gamma, with the effect of additional burnup being similar to the over-aging, which would lower the improved corrosion resistance. Supporting this hypothesis is the experimentally observed fact that the hardness values obtained on the irradiated core are comparable to those obtained on unirradiated material by quenching from the gamma phase.

4. Boron Stainless Steel

The high cost of hafnium and its general low availability was responsible for the investigation of alternate materials for control rods. This, and the need for a thermal shield for the EBWR pressure vessel, resulted in a development program on boron stainless steel.(85) An alloy of

1% boron in essentially SS Type-304 stainless steel was developed for the thermal shield, and an alloy of 2% boron in SS Type-304 was developed for the control rods.

The early, 1949, boron stainless steels, 1%, 2%, and 3% boron in Type-304 were too brittle for use and showed poor corrosion resistance in 600°F(316°C) static water. The newer materials, up to 2% boron could be fabricated[86] and showed sufficient corrosion resistance in preliminary tests to justify their use in EBWR. The corrosion test program initiated during the development period was continued after EBWR started.[87] Results of long-term dynamic tests are summarized in Table 4.2.

Table 4.2

DYNAMIC CORROSION AT 22 FT/SEC OF BORON STAINLESS STEEL IN DEGASSED WATER AT 288° AND 274°C

Source	Sample No	Type of Weld	Nominal Composition %			Analyzed % B	Total Test Time Hrs	Over-all Wt Change mg/cm²	Wt Change Rate mg/cm² mo	Hours that Rate was Constant	Final Appearance
			Cr	Ni	B						
KAPL	A-4403a b	-	18	14	1 6 2 5	NA	8118	-0 3280 0 3027	+0 0036 +0 0042	5000 3000	Adherent black coating Adherent black coating
Electric Steel Foundry Co	A-4463	Welded with 308 SS rod Cross section of weld	18	8	2 18	1 5 1 49	6753	-0 0464 +0 0230	+0 0292	5000	Adherent lustrous blue-black coating Loose black coating on edges
Superior Steel Co	A-4480	-	18	11	1	0 96 1 01	5999	+0 0487 +0 1006	+0 0066	3000	Thin loose black coating heavier on edges over adherent black tarnish
Universal Cyclops	A 4483a	Welded with 308 SS rod Cross section of weld	18	15	1 2	0 68 0 63	5999	-0 0494 +0 1276	+0 0208	3000	Adherent brown-black tarnish purple on weld Loose black coating on edges
	A-4483d	Sample cut from welded slab out of heat zone parallel to rolling direction					5999	+0 0988 +0 1028	+0 0046	1500	Adherent brown-black tarnish Loose black coating on edges
	A-4538c d	-	18 1	14 8	1	1 16	5062	0 0998 -0 0876	0 0073	1200	Adherent black tarnish Loose black coating on edges
Crucible Steel Co (Heated to 1121°C forged at 1010°C and air cooled)	A-4494b	-	18 8	8 7	2	1 85	5999	0 0864 -0 0371	+0 0052	3000	Thin loose black coating over adherent black tarnish
Same as above then heat treated at 1093°C for 1 hr and furnace cooled)	A-4494i j	-	18 8	8 7	2	1 96	5062	-0 1155 0 0716	0 0240	1200	Adherent blue-black to brown-black tarnish Some loose black-coating on edges
	A-4494x y	Welded with Arcos Chromend K rod lime coated Cross section of weld	18 8	8 7	2	1 85	5785	0 1187 -0 1186	+0 0067	2200	Adherent blue-black to brown black tarnish

*Last 4364 hours at 274° Previous time at 288°C

**Not analyzed

No significant corrosion problems have resulted as a result of using boron stainless in EBWR. Examination of boron steel control rods removed after shutdown for 100 Mw conversion has revealed no evidence of accelerated corrosion attack.[75]

5. Hafnium

Hafnium, used in 5 out of 9 control rods in EBWR, was another of the high-temperature water corrosion resistant materials that came from the NRB development program. Hafnium has a high neutron cross

section, desirable in a control rod material,[88] and has high corrosion resistance which eliminates the need for cladding. Cost of the material is high and the supply is limited particularly for material of satisfactory purity. These two factors are barriers to its wide use. It was selected for EBWR use because at the time it was the only proven control rod material for high temperature water use. The use of boron stainless steel for the remaining four rods was an experiment. Problems in procuring and fabricating satisfactory hafnium material have been described.[55] Fortunately, the corrosion resistance of hafnium is not as sensitive to the presence of impurities as is that of zirconium. Corrosion tests indicated that the material had a high corrosion resistance.

It has shown satisfactory corrosion behavior in EBWR; the only indication of corrosion observed is the presence of Hf activity in the water deposits, (see Sec. 6). It is believed that this resulted largely from erosion of the control rod in its channel.

6. Aluminum

Aluminum-6063-T831 (72S lined) was used for tubing in the EBWR main condenser. Originally it was planned to use conventional admiralty metal tubes but a study indicated a possible problem resulting from activation of copper corrosion product in the reactor water.

Corrosion of these aluminum tubes on the condensate side is believed to have been insignificant since no trace of aluminum was found in deposits on the feedwater filters, (see Sec. 5). The only definite corrosion problem that resulted from use of this material was failure of several tubes which corroded through on the cooling water side due to faulty treatment of cooling tower water. Since it does not involve corrosion in primary water or steam, it will not be discussed further.

7. Aluminum - 1% Nickel (M-388)

Aluminum - 1% nickel (M-388 later designated as X-8001) was used in fabricating the dummy fuel elements in EBWR. This alloy was developed by J. E. Draley and associates in a program to find a way to use aluminum in high temperature water reactors. A summary of the work done on this and related alloys is given in Sec. 4.4. Use of this alloy for dummy fuel elements in EBWR provided an opportunity to test the alloy in an actual reactor environment, without jeopardizing any critical components.

In the dummy fuel element, the M-388 was attached to stainless steel end pieces by means of stainless steel rivets. Previous to startup of the reactor, the dummy fuel elements were inserted before adding the fuel elements. The reactor was then filled with tap water to make hydrostatic tests. Although the tap water was in the reactor only a few days, some corrosion of the M-388 resulted with accelerated attack around the stainless steel rivets.

In July 1957 (after 1370 Mw days of operation), two dummy fuel elements were removed from the reactor to the storage pit and deposit samples taken (see Sec. 5). Subsequently, the two elements were subjected to cave examination.[89] Samples of the aluminum alloy were removed with a hole saw and the top and bottom adapters cut off on the aluminum side of the rivets.

The hole saw samples were descaled electrically in boric acid. Inspection showed no unusual corrosion. There was a slight amount of pitting, the largest pit being 0.3 mm in diameter and 0.1 mm deep. In general, the surface of aluminum outside the tube was more corroded than that inside, possibly due to the negligible flow of water inside. Actual weight changes could not be determined but the corrosion film had an average thickness of 0.001 inch.

An examination of the area around the stainless steel rivets on the top and bottom adapters was made at low magnification, as shown in Fig. 4.1 and 4.2. It was evident that the aluminum had undergone galvanic attack in the region adjacent to the rivets. The degree of galvanic corrosion, however was only slightly worse than had been noted on dummy assemblies after their original contact with tap water described above. It is believed that most of the pitting observed probably also occurred at this time.

In December 1958, two dummy fuel assemblies were removed from EBWR and immediately transferred to a cave in Building 301. They had been in the reactor since its original loading, about one year at operating temperature. These dummy assemblies[90] were covered with a loose corrosion coating that varied in color from a dark brown to a medium gray. Under this loose coating was an adherent speckled brown coating. The loose coating was missing from parts of the assemblies, but it had adhered well around the rivets in the side producing a splotched effect. An x-ray examination of the loose coating on a hole saw specimen showed it to be essentially all boehmite ($\alpha Al_2O_3 \cdot H_2O$) with only one additional line which was not identified.

Three transverse specimens of the aluminum tube wall were examined under the microscope. About 0.056-0.057 inch of uncorroded aluminum remained. If the original plate was 0.0625 inch, as specified, about 3+ mils per side had corroded away in the year of exposure to high temperature water (about two years total life). This rate of corrosion was considered to be in reasonably good agreement with the $1\frac{1}{2}$ mils per year obtained in static autoclave tests in 260°C helium saturated water.

In addition to the uniform attack, two shallow pits (about 0.02 inch diameter by 0.002 inch maximum depth) were noted in the sections examined. These pits may have resulted from initial rolling inclusions or the poor water quality previously mentioned. They have not been found in static autoclave specimens. No sign of catastrophic "blister" attack, characteristic of conventional aluminum alloys in 260°C water was noted.

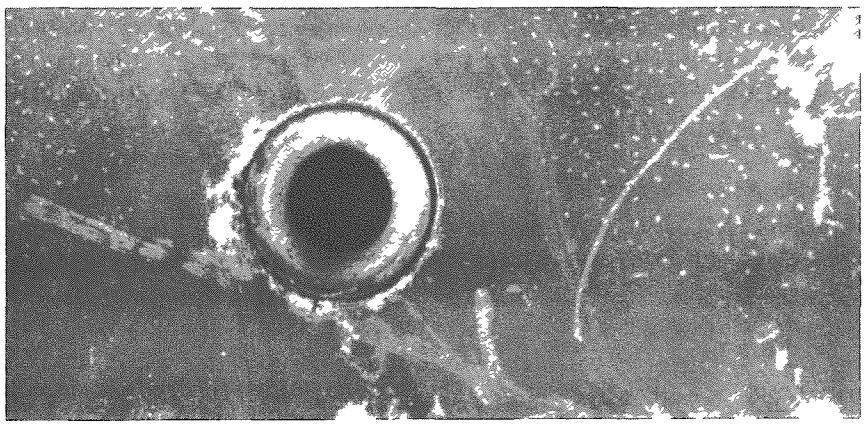

FRONT - 4X

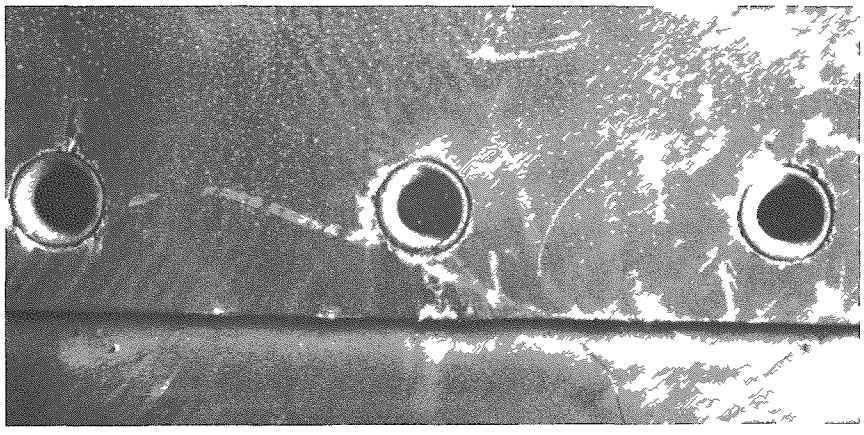

FRONT - 2X

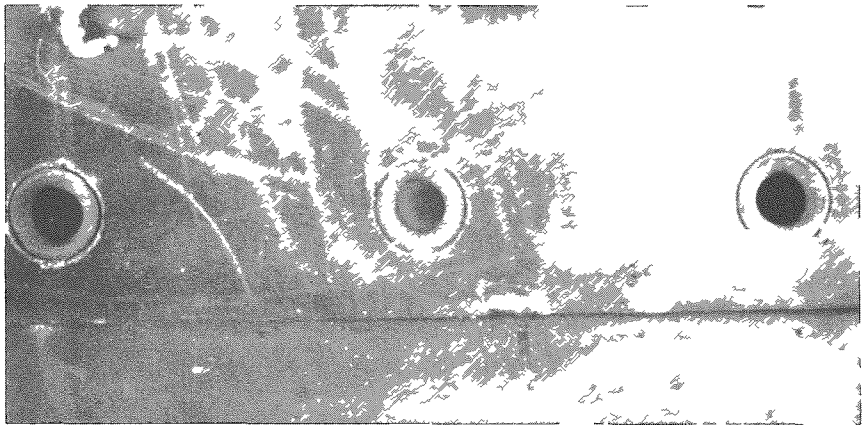

BACK - 2X

Fig. 4.1

EBWR Dummy Assembly from Core Position D13
112-1709

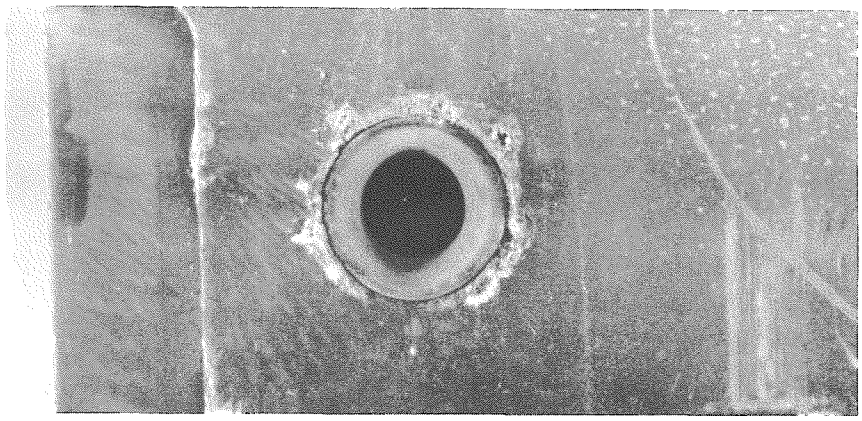

BACK - 4X

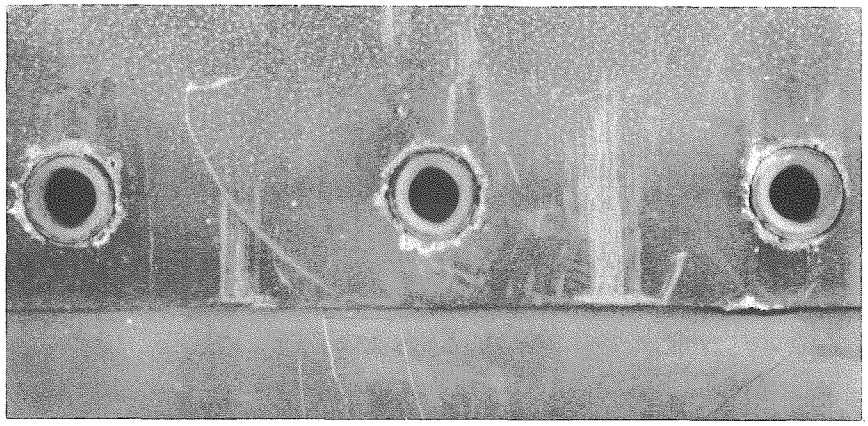

BACK - 2X

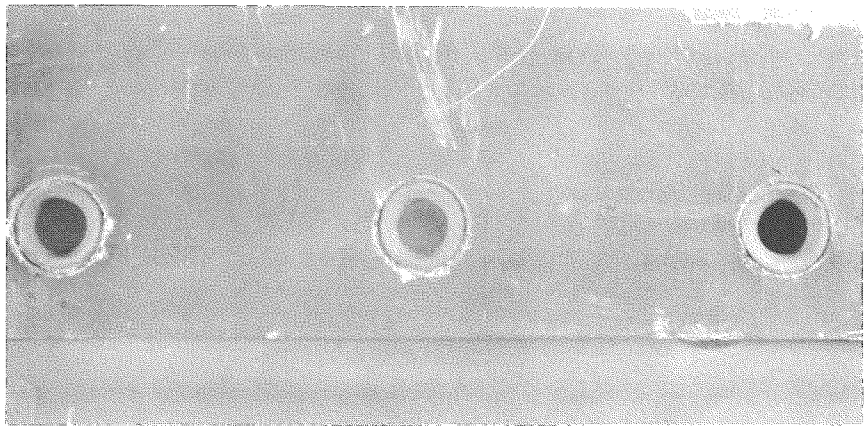

FRONT - 2X

Fig. 4.2

EBWR Dummy Assembly from Core Position K2
112-1708

Although the aluminum alloy M-388 showed no evidence of structural failure or the catastrophic intergranular attack in EBWR, a corrosion problem attributed to its use is described in the section on corrosion product deposits, (see Sec. 5).

8. Carbon and Low Alloy Steels

Carbon and low alloy steels were used in the steam system of EBWR. The reason for lining the steam system with Kanigen nickel, as described in Sec. 2, was because of the unexpectedly high oxygen content of boiling water reactor steam demonstrated by BORAX-III.

To determine the effect of the high oxygen steam upon the turbine internals if Kanigen nickel had not been used, samples of six types of structural materials used in the turbine were placed in the steam line between the reactor and the steam dryer in November 1957.[91] Representative samples were withdrawn for examination three times during the following nineteen months.

Alloy designation, description of the materials and typical applications are given in Table 4.3. Table 4.4 summarizes descaled weight loss data for the samples obtained after each of the three test periods along with data describing time of exposure and hours of operation.

Table 4.3

EBWR STEAM CORROSION SPECIMENS

No.	Designation	Material	Turbine Part
1	ASTM A-113-SSC	Structural steel	Diaphragm web
2	AISI 4140	Steel	Wheels
3	Type 403 stainless steel	13% chromium-stainless steel	Buckets
4		1% chromium $\frac{1}{2}$% molybdenum steel	Shaft
5		Low carbon steel	Diaphragm band
6		13% chromium-stainless steel, non-hardening	Nozzle element

Table 4.4

EBWR STEAM CORROSION SAMPLE RESULTS

Period	Inclusive Dates	Reactor Operation Time				Alloy and Sample No.	Metal Loss (mg/cm^2)
		For the Period		Total			
		hr	Mw-hr	hr	Mw-hr		
1	11/2/57-4/6/58	2,249	41,861	2,249	41,861	1C	2.05
						2A	1.14
						3A	0.22
						4D	1.24
						5A	2.76
						6A	0.31
2	4/11/58-11/8/58	3,522	67,272	5,771	109,133	1A	2.98
						2C	1.47
						3C	0.19
						4A	1.33
						5C	3.70
						6C	0.18
3	4/29/59-7/3/59	798	16,178	6,569	125,311	1D	4.19
						2D	3.58
						3D	0.46
						4C	16.90
						5D	3.23
						6D	0.25
		798	16,178	798	16,178	1E*	11.68
						2E	11.97
						3E	0.23
						4H	9.70
						5G	15.58

*These five samples placed in holder at start of third period.

The corrosion resistance of the chromium-containing alloys, as to be expected, increased with chromium content.

The appearance of the samples after the first period was satisfactory, and the corrosion rates over the first two periods, were good, (see Fig. 4.3). The corrosion behavior of all six materials was relatively good until the last month of operation prior to shutdown for 100 Mw conversion. During the last period pitting and accelerated attack of the low alloy samples occurred. The new samples placed in the holder at the start of the last month were even worse than those which had been in the system since the start of the test, indicating that the oxide on the old samples afforded some protection against attack. The reason for the accelerated attack during the last month is unknown, but may be a result of two known

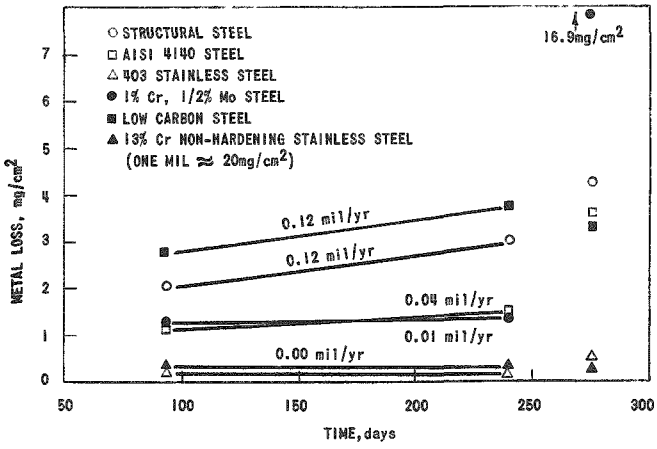

Fig. 4.3

Results of EBWR Steam Line Corrosion Test

operational factors: (1) the addition of oxygen to the reactor water for a two-hour period a week before final shutdown (which seems rather inadequate to explain the results); and (2) submerging of the steam line samples in air-saturated reactor water at room temperature for five weeks prior to startup for the last month of operation. Since the reactor had not been operated for five weeks previous to loading of the samples, the water quality may have been questionable. The final impression is that the accelerated attack resulted from some factor associated with shutdown rather than normal operation, (see effect of shutdowns on blocking of feedwater filter - Sec. 5).

9. Kanigen Nickel

The decision to line the steam piping, turbine (except rotor), and air-ejector heat exchanger shells with Kanigen nickel was made after the plant was nearly finished. The reason for it, as described in Sec. 2, was the high oxygen content of the steam due to water decomposition in BORAX-III. The decision was based largely on the following:

(1) Conventional boiler practice was insistent on keeping oxygen at as low a level as possible.

(2) No evidence could be found of a turbine being operated on saturated steam having a high oxygen content.

(3) The Kanigen nickel process was available as a method of lining components already fabricated, and was reported to offer high corrosion resistance.

Previous corrosion experience at ANL had been limited to high temperature water (not steam) tests on Kanigen nickel when applied to 2S aluminum. Although out-of-pile tests showed some promise, the in-pile tests showed a definite tendency for the plate to come off the aluminum under irradiation.[92]

Subsequent to EBWR startup, and, as part of another reactor program, high-temperature water (not steam) static and dynamic tests were started on 1, 3 and 5 mil Kanigen plate deposited on $2\frac{1}{4}$% Cr-1% Mo steel. Tested along with them were carbon steel samples plated with 3, 8 and 13 mils of electrically deposited nickel, and welded carbon steel samples electrically plated with 8 mils of nickel.

The static autoclave tests were made in degassed and air saturated water at 500, 600 and 680°F (260, 316, and 360°C). Dynamic tests were made at 550°F (288°C) in a corrosion loop at a velocity of about 25 ft/sec in degassed water.

In the autoclave tests, the Kanigen plate showed good corrosion resistance at all three temperatures in degassed and air saturated water. The electrically plated samples showed erratic behavior, in that they corroded relatively rapidly in 500 and 680°F air saturated water, but did as well as the Kanigen at the other conditions. One welded sample in 680°F air saturated water lost the plating near the weld area after 3611 hours.

In the dynamic test at 550°F, 25 fps velocity the Kanigen samples corroded at about 0.5 mils/year up to 5000 hours when they suddenly started to lose their plate on the leading edges. The electrically plated samples corroded at 1 to 1.5 mils/year, but the plate was still intact at 5000 hours.[93]

During the June-July, 1957 shutdown, the exhaust end of the turbine casing and last row of turbine blades were inspected. The Kanigen plate on the casing appeared to be in good condition. In December 1957, no detectable wear could be noted on the diaphragms, and the rest of the plating was still in good condition. There was some rust on the rotor at both the HP (high pressure) and LP (low pressure) seals in the air pressure and air vacuum regions. When this rust was removed, only very slight pitting was present. In May, 1958, mechanical failure of a turbine blade[94] necessitated opening the casing and removing the diaphragms (Kanigen plated) and rotor (not plated). Detailed microscopic examination of the surface of the (rotor) blades showed no evidence of stress corrosion, general corrosion, intergranular attack or other types of surface attack, and the general surface condition was found to be similar to other blades returned from service under standard steam conditions. There is no evidence that boiling reactor steam has had any adverse effect on the blade material. Examination of the diaphragms at this time showed that the Kanigen nickel plate had been completely removed in the high velocity areas due to erosion and/or corrosion (Fig. 4.4). The base metal exposed showed no visible evidence of attack. A lack of bonding was evidenced in some spots in the low-pressure stages of the diaphragms by a flaking tendency, with no signs of attack of base metal underneath.

In September, 1958, an examination[95] was made of the Kanigen nickel-plate coating in a vertical section of the main steam line just before it enters the turbine throttle valve. Since welding had been carried out in this area, both heat-treated and non-heat-treated Kanigen nickel plate were present.

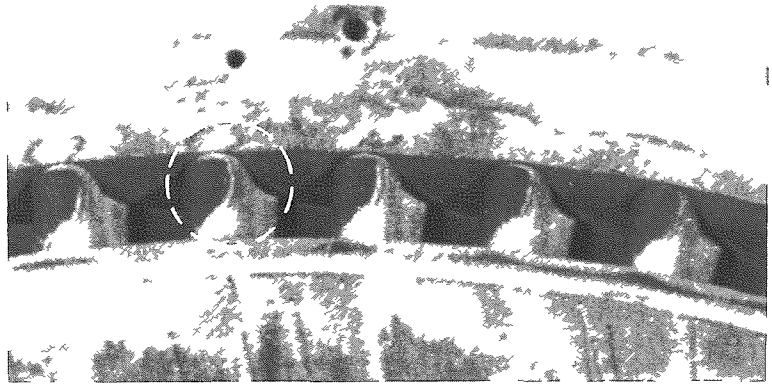

Fig. 4.4

Section of Turbine Diaphragm Showing Typical Loss of Nickel Plate from Nozzles
112-1707

Knoop hardness determinations showed the heat-treated Kanigen to be harder than the non-heat-treated Kanigen, 8700 vs 7800, respectively. Very little erosion occurred in the heat-treated zones, but considerable erosion occurred in the non-heat-treated areas.

An undesirable characteristic of the hardened (heat treated) Kanigen plate was the presence of cracks which penetrated through to the base metal. These cracks could afford ample opportunity for crevice corrosion, especially in the highly oxygenated steam (28 ppm O_2) of EBWR The general conclusion given was that the Kanigen nickel plating was not holding up under EBWR high-velocity steam conditions, but it appeared to be satisfactory in low-velocity steam.

In view of the small amount of corrosion on the rotor, which was not coated with Kanigen nickel, and the low amount of corrosion on the coupons in the steam line until the last month, it is doubtful if the Kanigen nickel has served any useful purpose in EBWR during operation. As noted elsewhere (see Sec. 5), there is reason to believe that much of the corrosion of the carbon and low alloy steels in the steam system or the release of the corrosion products occurred during the shutdown periods. It is possible that the load of corrosion products in the feedwater might have been much higher following startups if the Kanigen nickel had not been used. Whether or not the advantages of its use outweigh the disadvantages due to cost and increased water-borne activity is certainly open to question.

4.3 Dresden

1. Carbon Steel

In the early stages of Dresden design, while it was known as the CEP (Commonwealth Edison Project), a study was made[96] by

W. L. Pearl, General Electric Company, of the possible use of carbon steel instead of stainless steel for the primary coolant system in contact with high temperature water, or steam and water mixtures. Up to this time all high temperature water-cooled reactor designs had used stainless steel for basic construction material, primarily to minimize problems of corrosion and corrosion products passing into the recirculating water system.

It was pointed out in the study that although the Pressurized Water Reactors developed under the auspices of the NRB of the AEC were successfully operating, there were problems associated with the use of stainless steel, such as (1) high cost, (2) limited availability, (3) fabrication difficulties, (4) necessity for using hydrogen, and (5) crud formation and removal.

Because of the problems associated with the use of stainless steel, a program was initiated by the NRB to evaluate carbon steel as an alternate material for application in high-temperature high-pressure water reactor systems.

a. Some of the advantages of use of carbon steel as a substitute for stainless steel in primary system components were:

(1) Lower material cost;

(2) Lower thermal expansion - simplifies the design of key items, such as steam generator, pressure vessel, piping, etc.;

(3) Greater thermal conductivity - increases heat transfer per unit area;

(4) Greater availability in quantity and shelf items;

(5) Manufacturing experience in pressure vessels, piping, etc. is broader and techniques are well established.

Up to the time of the CEP survey, February 1956, the NRB program had been limited to out-of-pile testing and the known facts regarding carbon steel out-of-pile corrosion[97,98] could be summarized[96] as follows:

b. Factors having no significant effect:

(1) Variations in alkalinity in the range pH 10.5-11.5;

(2) Variations in alkalinity in the range pH 7-9.5;

(3) Difference in composition of material over the range of carbon steels investigated;

(4) Difference in surface finish over the range of surface finish used;

(5) Variations in H_2 concentration in high alkalinity water pH 10.5-11.5 at least when O_2 concentrations are low;

(6) Variations in resistivity in the range of 10^4 to 10^6 ohms-cm;

(7) Variations in velocity in the range 15-35 ft/sec;

(8) Variations in testing temperature in the range 500-600°F (260-316°C) at pressures well above saturation;

(9) Thermocycling between 200°F (93°C) and 600°F (316°C) at a rate of one cycle per day (8 hrs at 200°F, and 16 hrs at 600°F);

(10) Whether the test facility is stainless steel or carbon steel;

(11) Whether the alkalinity is obtained with Li or NH_3, as long as it is in the range of pH 10.5-11.5;

(12) Differences in specimen size and shape over the range used;

(13) Type and operation of demineralizer over the range of variables considered.

c. Factors that had a significant effect on the rate of corrosion:

(1) Increase in alkalinity from the range pH 7-9.5 to range of pH 10.5-11.5. This effect was probably the most significant noted;

(2) Hydrogen concentrations in neutral water;

(3) Specimen handling technique during intermediate loop shutdowns;

(4) Mixing of new specimens in the same test section with corroded specimens.

A general conclusion suggested in the CEP survey by the results of the NRB experimental program was that there was nothing to indicate that carbon steel would be unacceptable as a substitute for stainless steel. Although insufficient data were available to insure final success, the continued favorable results of the intensive test program made the calculated risk of such substitution less formidable.

By including carbon steel in an early design concept of the dual cycle boiling water reactor, the advantages and problems resulting from its use were more clearly emphasized.

d. Major problems that remained to be solved, without too great a risk in a dual cycle boiling reactor, as determined by this survey were:

(1) Effect of oxygen - both the effect of the oxygen concentration on carbon steel corrosion under operating conditions, and determining the amounts of oxygen that will be present in the system must be accomplished early in the program before carbon steel can be given further consideration.

(2) Effect of high corrosion rate - the maximum allowable total solids that can be present in the coolant must be determined early - to indicate the magnitude of the water treatment system.

(3) Effect of high initial crud release - must be designed for, as well as the effect of, the lower more steady state crud conditions. The deposition of the crud is of major importance whether it deposits on fuel elements, deposits on primary loop components, or remains suspended in the water.

(4) The effect of cycling and opening the system on the stable corrosion film - the stability of the coating of scale that develops by corrosion during the normal operation must be evaluated for various transient conditions of flow and thermal cycling, exposure to aerated water, etc.

(5) Development of methods for tube cleaning and system decontamination - this problem has not been adequately solved for stainless steel systems.

As a result of the survey, and the importance of the problems that remained to be solved before carbon steel could be seriously considered, the following recommendations were made: (1) That no further consideration be given to the use of carbon steel for the CEP plant; (2) If the problems remaining can be resolved satisfactorily, the possibility of conversion of a specific component to carbon steel can be investigated based on the gains that still can be realized at that time; (3) It was recommended further that an intensive carbon steel development program with emphasis on those areas applicable to the dual-cycle boiling reactor be undertaken to complement the NRB program.

2. Steam System Materials

In developing the design for the Dresden Reactor Power Plant, the designers encountered the problem of high oxygen content of the steam resulting from the relatively high rate of water decomposition found in a boiling water reactor, (see Sec. 2). Another characteristic of boiling

reactor steam not found in conventional boiler plant practice was the presence of about $\frac{1}{2}$% moisture. Still another factor not found in conventional plants was the radioactivity in the steam. Fortunately, this radioactivity carryover with steam was not expected to be a serious problem. However, there was very little information on the erosive action of wet high-pressure steam (with or without oxygen) and only scattered data on the effect of oxygen on the corrosion of metals in high-temperature water-steam mixtures. To acquire experience in these two fields, General Electric undertook a two-part experimental program.[99] The first part was a series of tests to aid in the selection of materials for the Dresden turbine; the second, a more fundamental study on the effects of temperature, pressure, oxygen, velocity, and pH on erosion and corrosion by water-steam mixtures.

The overall problem was analyzed as consisting of two parts: (1) corrosion of turbine materials in high-temperature steam-water-oxygen mixtures particularly with respect to pitting and crevice attack resulting from oxygen concentration cells, and (2) erosion by wet oxygenated high-pressure steam. The latter was visualized as occurring by three processes possibly arising from the same mechanism.

(a) Surface or washing erosion. This is the eroding of a metal by high-velocity water flowing along a surface as in a nozzle. Available information indicated this would be minor with 12 Cr steel.

(b) "Wire drawing" or channel erosion. Wet steam leaking with high velocity past narrow restrictions can cause deep undercutting of metal. There is little information on this type of erosion.

(c) Impact erosion. This is caused by the impingement of water droplets against a surface at high velocity and is a familiar occurrence in the last stage buckets of condensing turbines. In a high-pressure turbine, both the high steam density and relatively low bucket velocities would tend to minimize the impact velocity and hence the damage.

In order to obtain the desired information as quickly as possible, three tests were devised based on available facilities:

Test 1 - Erosion and corrosion with wet steam; 350 psia and 430°F (221°C) max; pH 6.8; with 0.05, 80 and 110 ppm oxygen.

Test 2 - Erosion and corrosion tests with wet steam using desuper-heated steam from the 14th stage of a turbine; 43 psia and 272°F (133°C) 70-110 ppm O_2 pH 8.8-9.5.

Test 3 - Pitting, crevice, and galvanic corrosion tests in water and steam in autoclaves, 545°F (285°C), (1015 psia), 50 and 199 ppm O_2 (initially), pH 7.

Materials used in these tests are described in Table 4.5. For complete details of the tests and the results, the original reference[99] should be consulted; only part of the results are given here along with the conclusions:

a. Erosion in Wet Steam. In Tests 1 and 2, erosion of the wire drawing or channel type was assessed by measuring the depth of the deepest pit on each specimen. Under the conditions of Test 1, increasing the oxygen concentration did not increase the erosion rate, except in the case of BTH leaded bronze which also was the only alloy which showed a simultaneous increase in corrosion rate.

The maximum pitting depth in Test 1 (1000 hr) was about twice that in Test 2 (1900 hr) reflecting the greater severity of Test 1 (higher temperature, higher velocity, and lower pH). However, the relative erosion resistance of the alloys remains the same in these tests.

The condition in Test 2, where the steam is required to turn suddenly, simulates conditions of leakage past diaphragms and shell ledges. These ledges frequently erode in marine turbines which operate with saturated steam unless they are faced with special alloys.

Resistance to erosion as determined by depth measurements follows roughly the order of expected corrosion behavior; that is, stainless steels are most resistant, low alloy steels intermediate, and carbon steel and cast iron least resistant. Chemical composition is more important than hardness, but with any particular alloy, increasing the hardness may be beneficial.

In 1000 hr tests with wet steam flowing at about 850 ft/sec (6% moisture, 0.05 and 80 ppm O_2) there was no visible "washing erosion" of Types 347 and 405 stainless steel nozzles. One gouge may have been due to a solid particle. Impact specimens (Types 347 and 403 stainless steel) placed two inches from the discharge of these nozzles, suffered some roughing as expected, possibly from solids. There was no difference between the Type-347 stainless steel and the hardened Type-403 stainless specimens; and no significant effect of oxygen on either the nozzle or impingement specimens.

Turbine buckets normally are protected with erosion shields when the tip velocity and moisture exceed 1000 ft/sec and 4%, respectively. The possible need for additional shielding in the Dresden turbine, where velocities may be below 1000 ft/sec, but moisture above 4%, is being determined with different apparatus.

b. General Corrosion in Wet Steam. Weight losses in 1000 hr (after cleaning) have been converted to corrosion rates using "exposed" areas. The results are shown graphically in Fig. 4.5. There is a

Table 4.5

DRESDEN MATERIALS TESTED[99]

Type	Condition	Test no. 1	2	3	Hardness, Bhn	Chemical composition, % C	Cr	Mo	Ni	Fe	Others
Carbon steel											
ASTM A106	Seamless pipe	x	x	...	126	0.23	...	...	...	Bal.	...
ASTM A212	Boiler plate	x	...	...	179	0.31	...	...	...	Bal.	...
ASTM A201	Boiler plate	x	...	x	103	0.20	...	...	...	Bal.	...
ASTM A27 Cast	N 1925 F, T 1200 F	x	...	x	126	0.25	...	...	...	Bal.	0.50 Si
ASTM A27 Cast	N 1925 F, T 1200 F	...	x	...	146	0.25	...	...	...	Bal.	0.50 Si
Low-alloy steel											
½ Mo (ASTM 204)	Firebox quality	x	...	...	131	0 20	...	0 5	...	Bal.	...
½ Mo Cast	N 1700 F, T 1200 F	x	...	...	131	0 20	...	0.5	...	Bal.	...
1 Cr, ½ Mo Forged	A 1550 F, T 1100 F	...	...	x	223	0 40	1.0	0 5	...	Bal.	...
1 Cr, ½ Mo, ¼ V ASTM A193–B16	HR T 1200 F	...	...	x	262	0 40	1.0	0 5	...	Bal.	0.25 V
1 Cr, 1 Mo, ¼ V Cast ASTM A389–C24	N 1925 F, T 1200 F	x	...	...	207	0 20	1.0	1.0	...	Bal.	0.20 V
1 Cr, 1¼ Mo, ¼ V Forged A293–Class 8	A 1750 F, T 1250 F	x	...	...	248	0.30	1.0	1.2	...	Bal.	0.25 V
2 Ni, ½ Mo, Forged ASTM A293–Class 2	A 1550 F, T 1100 F	...	...	x	248	0.30	...	0 5	2 0	Bal.	0.02 V
2½ Ni, ½ Mo Forged ASTM A293–Class 2	A 1750 F, T 1250 F	x	...	x	229	0.30	...	0.5	2.5	Bal.	0.05 V
2½ Ni, ½ Mo Forged ASTM A293–Class 2	& SR, 1100 F	...	x	...	262	0.30	...	0.5	2.5	Bal.	0.05 V
2 Cr Cast	Ann. 1650 F	x	...	x	229	0.15	2.0	...	...	Bal.	...
2¼ Cr, 1 Mo Forged ASTM A155	Ann. 1650 F FC to 500 F	x	...	x	143	0.15	2.25	1.0	...	Bal.	...
Nitrided steel											
Nitralloy[d] (ASTM A352–Class A)	HR Bar (Base)	x	...	x	60Rc	0.42	1.6	0.4	..	Bal.	1.0 Al
EML[e] nitrided	HR Bar (Base)	x	...	...	62Rc	0.15	19.0	...	12.0	Bal.	1.10 Cb + Ta
ASTM Type 410 stainless nitrided	HT Bar (Base)	x	...	...	62Rc	0.15	12 0	...	...	Bal.	...
Cast iron											
ASTM A48 cast	SR 1200 F	...	x	x	179	2.75	...	...	.	Bal.	2.0 Si
Ni-Resist #3[b]	SR 1150 F	...	...	x	97	2.75	3.0	...	30.0	Bal.	...
Ductile Ni-Resist #3[b]	SR 1150 F	x	x	...	166	2.40	2 5	...	30.0	Bal.	0.08 Mg
Stainless steel											
ASTM Type 304	CR Bar	...	...	x	241	0.08	18.0	...	8 5	Bal.	...
ASTM Type 304L	CR Sheet	x	...	...	163	0.03	18.0	...	8.0	Bal.	...
ASTM Type 304L (Sen)	Sen 1250 F	x	..	...	156	0.03	18.0	...	8.0	Bal.	...
ASTM Type 304L	HR Bar	...	x	...	143	0.03	18.0	...	8 0	Bal.	...
ASTM Type 304L (Sen)	Sen 1250 F	...	x	...	149	0.03	18.0	...	8 0	Bal.	...
ASTM Type 347	A-1800 F & OQ	x	...	x	162	0.10	18.0	...	8 0	Bal.	Cb-10X C
ASTM Type 403	HR & T 1200 F	...	x	...	235	0.12	12.5	...	...	Bal.	0 5 Si
ASTM Type 403	CR & HT to hardness	x	x	x	217	0.12	12 5	...	...	Bal.	0.5 Si
ASTM Type 405	HR Plate	x	...	x	202	0.12	12.5	...	...	Bal.	0.20 Al
ASTM Type 410	HT Bar to hardness	x	...	...	241	0.12	12.5	...	0.8	Bal.	1.0 Si
12 Cr, Mo, W, V	OQ, 1400 F, T 1200 F	...	...	x	311	0.21	13 0	1 0	...	Bal.	1.0 W, ¼ V
12 Cr, Mo	HR Plate	x	...	x	217	0.09	13.0	1.5	...	Bal.	...
12 Cr, Cb	HR Plate	x	...	...	223	0 08	13.5	...	...	Bal.	0.35 Cb
Nonferrous alloys											
90/10 Cupro-nickel	HR Bar	...	x	...	107	...	...	...	10.0	1.15	88.6 Cu
90/10 Cupro-nickel	Ann Sheet	x	...	...	43	...	...	...	10.0	1.15	88.2 Cu
80/20 Cupro-nickel	Ann Sheet	x	...	...	40	...	...	...	20.0	0.03	80 Cu
70/30 Cupro-nickel	Ann Sheet	x	...	...	46	...	...	...	30.0	0.55	69 Cu
Monel[b]	CR Sheet	x	...	...	121	...	...	...	66.5	2.0	29 Cu
Monel[b]	HR Bar	x	x	...	143	...	...	...	66.5	2.0	29 Cu
BTH Pb bronze[e]	CC	x	x	x	50	...	...	...	12.0	0.76	65 Cu, 2.5 Sn, 5 Pb, 14 Zn
Stellite #1[c]	HR Strip	x	...	...	401	2.5	30.0	...	3.0	...	12.0 W, 52 Co
Stellite #6[c]	HR Strip	x	x	...	401	1.0	29.0	...	3.0	...	4.5 W, 60 Co
KEL-F[f]	Elastomer 3700-336 (amine cured) Co-polymer of trifluorochloroethylene and vinylidene fluoride										

[a] Trade name of Midvale Steel Co.
[b] Trade name of International Nickel Co.
[c] Trade name of Haynes Stellite Co.
[d] Trade name of Nitralloy Corp.
[e] Special General Electric Co. alloy
[f] Trade name of M. W. Kellogg Co.

A, Austenized
CR, Cold rolled
FC, Furnace cooled
HR, Hot rolled
HT, Heat-treated
CC, Centrifugally cast
N, Normalized
OQ, Oil quenched
Sen, Sensitized
SR, Stressed relieved
T, Tempered
Ann, Annealed

marked increase in corrosion rates of high copper cupro-nickel alloys (BTH leaded bronze; 70/30, 80/20, and 90/10 cupro-nickels) with increase in oxygen from 0.05 to 110 ppm. This effect of oxygen becomes greater with increasing temperature. Under the same conditions, Monel (a high nickel cupro-nickel alloy), low-alloy steel, and Ductile Ni-Resist No. 3, show moderate increase in corrosion with added oxygen. With carbon steels, oxygen increases the corrosion rate greatly at lower temperatures, but has little effect at higher temperature. In autoclave tests at 545°F (285°C) with oxygen, BTH leaded bronze underwent dezincification.

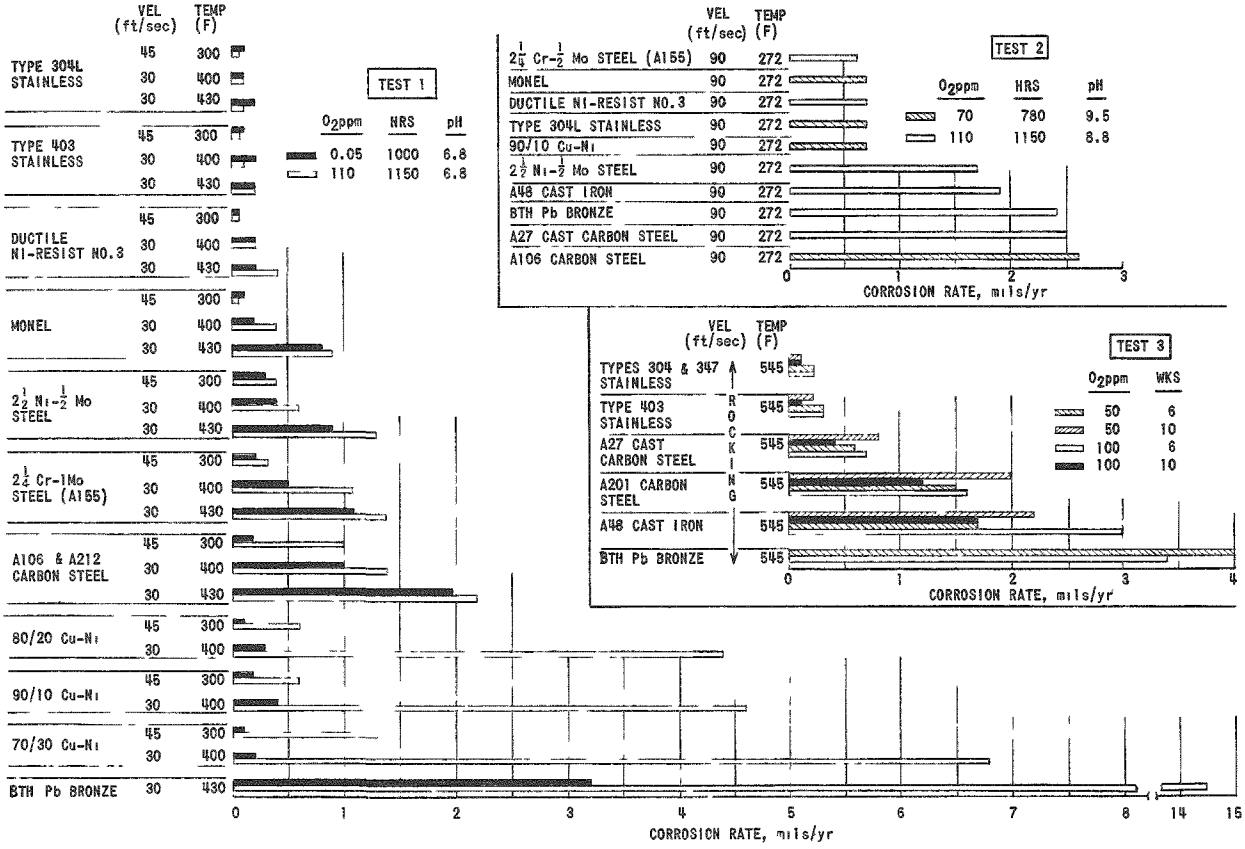

Fig. 4.5

Corrosion Rates of Materials, (descaled)

Austenitic and martensitic stainless steels showed no significant effect of oxygen in Test 1 [up to 430°F, (221°C)]. In the rocking autoclave tests [Test 3, 545°F (285°C)] there was no difference in the results with oxygen initially at 50 ppm and 100 ppm in six weeks. After cleaning these specimens and re-exposing them for an additional ten weeks, the corrosion was more severe with 50 ppm than with 100 ppm oxygen for all metals.

In autoclave tests, rates in water tended to be lowest; those in condensing vapor were intermediate; and those under alternating (rocking) conditions were highest. This may be due in part to differences in effective oxygen concentrations - specimens submerged in water developed less red oxide than the others. The rocking results may have included a velocity effect. Couples of dissimilar metals, which included combinations of stainless steel, low-alloy steels, carbon steel, and cast iron showed no noticeable galvanic effects.

The effects of velocity and pH cannot be distinguished in these tests. For instance, in Test 2, after 1150 hr, the corrosion rate of carbon steel at pH 9 and 90 ft/sec was about twice that in Test 1 at pH 7 and 45 ft/sec. In tests at 600°F (316°C) with steel capsules filled with distilled water, Bloom[100] found that the effect of ammonia was to increase the corrosion of carbon steel by a factor of two at 1000 hr. This effect disappeared as the exposure time was increased; e.g., 150 days. There was no effect if NaOH was used. However, in earlier tests (with no oxygen) the addition of morpholine to steam decreased the corrosion rates of carbon and low-alloy steels. Douglas,[101] in autoclave tests at 600°F with no oxygen, obtained no effect on the corrosion rate of iron with additions of NaOH. It is probable, therefore, that the increased corrosion in Test 2 is due to the higher velocity.

There was no intergranular corrosion of Type-304L stainless steel at 430°F with oxygen in 1000 hr (Test 1) even when sensitized (heat treated under conditions producing carbide precipitation at grain boundaries). Nor was there any cracking around heavily-stamped crosses.

c. Pitting. In the dynamic tests with wet steam at 430°F, pH 6.8, with oxygen, carbon steel pitted to a maximum depth of about 0.002 inch at the periphery of crevices. In the exposed areas, the pitting was scattered and about one-tenth as deep. The depth of attack increased with increase in temperature between 300°F and 430°F. Without oxygen, the crevice pitting at 430°F was minor (0.0003 in.). Low-alloy steels showed the same behavior to a lesser extent (0.0008 in. at 430°F with oxygen, negligible pitting without oxygen). The stainless steels, cupro-nickels, Monel, and Ductile Ni-Resist No. 3 developed minor pits with oxygen and none without.

There was no pitting at crevices or exposed areas of corrosion in Test 2 at 272°F (133°C), pH 9, with oxygen.

In the autoclave tests (545°F, with oxygen) the extent of general pitting paralleled the weight loss, indicating the major loss of metal was by pitting attack. Again, the austenitic stainless steels were most resistant; then followed ferritic stainless steel, low-alloy and carbon steel, and cast iron. Pitting on the exposed surfaces of the couples was more extensive (but not deeper) than on the contact and crevice areas.

Deposits of iron oxides from solution, and easier access to oxygen, may explain this. Heavier deposits led to larger, but not deeper, pits. This was especially noticeable on the stainless-steel specimens since they pitted less frequently. Pitting at the 0.002 in. wide crevices was largely confined to the mouths of the crevice.

In one study of the data obtained after exposure to steam-water oxygen at 545°F for a total of 16 weeks, the average penetration was calculated from the loss in weight (after descaling and correlating with the deepest pit on each specimen). The depths of the deepest pit varied less from alloy to alloy than did the average penetration value. For cast iron and low-alloy steels, the deepest pit was from ten to eighty times deeper than the average penetration. For stainless steel, the deepest pit was from forty to two-hundred times deeper than the average penetration, reflecting the greater general corrosion resistance of the stainless steels. As noted previously, the average penetration may be taken as a rough guide to the number of deep pits.

In cast iron and cast steel, a few very deep pits were observed. These might have been associated with inclusions or pin-hole porosity.

In some cases, the depth of the deepest pit, rather than some average value, is of primary interest. Representative portions of the pitting data for Types-347, 403, 1 Cr-$\frac{1}{2}$Mo, A48, and A201 were analyzed by the method of variance for possible differences in the maximum depth occurring.

(a) on different surfaces (external, contact, crevice).

(b) on different portions of a surface; e.g., near or removed from edges and screw heads.

(c) with exposure to water, condensing steam, and with alternating conditions (rocking).

(d) with 50 ppm and 100 ppm O_2 (initially).

(e) with different metals.

For practical purposes, the only significant differences were due to the metals themselves. The results of one analysis are shown in Fig. 4.6 which shows the variation,

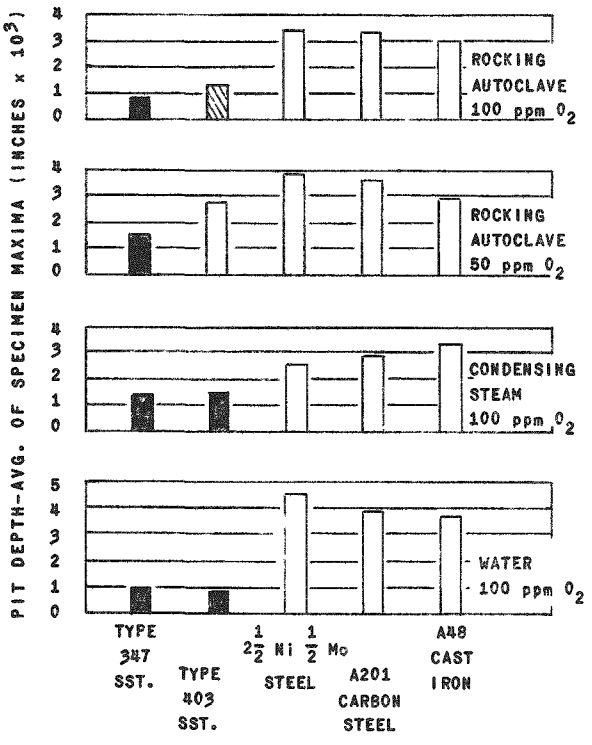

Fig. 4.6

Average of Maximum Depth of Pitting

among five materials, of the average maximum depth of pitting under four different test conditions. The different shadings in Type-403 stainless steel indicate significant differences. Type-347 stainless was the most versatile metal, appearing best under most conditions. Low-alloy steel, carbon steel and cast iron fell into one indistinguishable group. Type-403 stainless was intermediate, falling most often with Type-347, but sometimes with the low alloys. In this group, Type-403 stainless alone showed some effect due to oxygen. A greater number of specimens might have revealed other examples of oxygen effect.

Because of the small number of specimens, the maximum depth that might have occurred for a large number of specimens was estimated by extrapolation of these data by statistical means (extreme-value theory). A comparison of average penetration, average of the maximum measured, and the pit depth not to be exceeded more than 1% of the time, is shown in Fig. 4.7 for the cases involved. There is not enough experience with pitting to indicate how significant such extrapolations are. Besides questions of the applicability of the particular distribution assumed here, errors in the pit depth measurements are not known; there were no independent checks on these values.

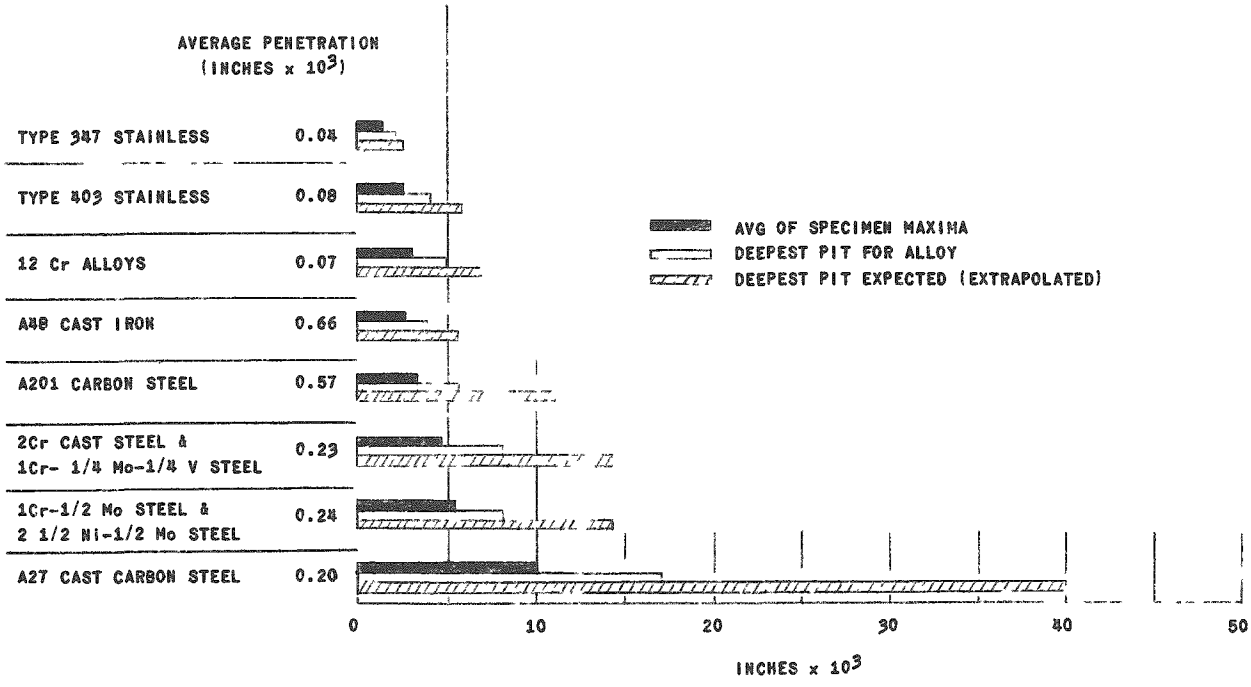

Fig. 4.7

Depth of Pitting

d. Conclusions. Conclusions reached were as follows:

(1) On the basis of this preliminary evaluation, erosion and corrosion of a turbine in a boiling-water nuclear power system can be maintained within tolerable limits with proper design and the selection of special materials for critical areas. This evaluation is being supplemented by continuing laboratory tests, and by the operation of a 500-kw turbine directly connected to a 10,000-kw boiling-water reactor at the Vallecitos Atomic Laboratory (Atomic Power Equipment Department).

(2) In wet steam with low (0.05 ppm) and high (100 ppm) oxygen, stainless steels, Monel, and Stellite 6 were most resistant to "wire drawing" erosion. Ductile Ni-Resist 3, low nickel steels, and low chromium steels offered better resistance than low molybdenum and carbon steels; plain cast iron was the least resistant material tested.

(3) In wet steam at pH 7 and 430°F (221°C), there was no effect of oxygen on erosion in tests with high and low oxygen concentrations, except for BTH leaded bronze. With low oxygen, BTH leaded bronze resembled low chromium steel in erosion: with high oxygen, it resembled plain cast iron.

(4) In wet steam at 300-430°F (149-221°C), and pH 7, with low and high oxygen, stainless steel, Stellite No. 1, and Ductile Ni-Resist No. 3 were most resistant to corrosion. Monel and low-alloy steels were superior to carbon steel. BTH leaded bronze was the least resistant material tested. At lower temperatures (300-400°F) (149-204°C) and low oxygen, the cupro-nickels were comparable to the most resistant materials; at high oxygen, they very rapidly approached the extreme corrosion rate of BTH leaded bronze.

(5) At 300-430°F, pH 7, increasing the oxygen level from low to high increased the corrosion rate of all materials tested except stainless steel. In the case of carbon steel, this effect of oxygen on corrosion diminished rapidly with increasing temperature. With the cupro-nickels, the effect of oxygen was much more severe at 400°F than at 300°F.

(6) Corrosion rates of all the materials tested, at 300-430°F, pH 7, high and low oxygen, increased with temperature, the logarithm of the corrosion rates varying approximately linearly with the reciprocal of the absolute temperature.

(7) At 430°F, pH 7, with high oxygen, there was no intergranular corrosion of sensitized Types 304 and 304L stainless steel specimens in 1000 hours nor were there any cracks around heavily-stamped crosses.

(8) With low oxygen, at 300-430°F, pH 7, there was no pitting observed except with carbon steel, where the effect was minor. With high oxygen, all materials pitted especially at crevices. Stainless steel and Stellite No. 1 were most resistant. Monel, cupro-nickel, and BTH leaded bronze were better than low-alloy steel. Carbon steel pitted most severely of the alloys tested.

(9) In autoclave tests in steam-water-oxygen mixtures (545°F, 1015 psia, 50 and 100 ppm O_2), run for six and ten weeks, the rates of corrosion decreased with time. The maximum depth of pitting, however, did not increase significantly.

(10) In the autoclave tests, the order of resistance, as measured by the maximum depth of pitting, was the same as for resistance to general corrosion. There was less difference in the maximum pitting depths among the ferrous alloys tested than there was in the corresponding weight losses.

(11) There were no significant galvanic or crevice effects in the autoclave tests. Naturally-formed deposits of iron oxides were more effective in promoting pitting on all classes of steel tested than were artificial 0.002 in. crevices.

(12) Cast iron and low-carbon cast steel were subject to occasional very deep pits in the autoclave tests. These may be related to inclusions and/or pin-hole porosity.

4.4 Aluminum Alloys for Use with High Temperature Water

The following survey of reported investigations of aluminum alloys for high-temperature water use was prepared in 1959.[102] It has been supplemented by more recent references.

1. Introduction

Aluminum alloys, particularly 2S (1100), have been favored as a fuel cladding material in water cooled reactors operated at low temperature because of their low nuclear absorption cross section, low cost, and adequate corrosion resistance. However, at higher temperatures difficulties occur due to an increase in corrosion rate with temperature. The static corrosion rate curve[103,104] changes from about 0.05 to 1.3 mils per year from 120°F to 200°C. Above 200°C catastrophic intergranular attack may occur instead of the uniform corrosion characteristic of the lower temperature. The uniform type of attack appears to be influenced by pH, since at each temperature, there seems to be a pH of minimum attack, ranging from about pH 6.5 below 100°C to about pH 3 at 300°C.[103-105]

As a result of further investigation into methods of improving the corrosion behavior of aluminum alloys at elevated temperature, Draley and Ruther[106,107] found that intergranular attack could be eliminated or minimized by the use of a metal with low hydrogen overvoltage such as nickel in one of three methods: by introducing a nickel salt into the water; by plating the aluminum with metallic nickel; or by introducing the nickel into the aluminum as an alloy constituent producing a finely dispersed second phase. A theory covering the effects was propounded. Other metals found beneficial were Cu, Co, Fe and Pt; however, Ni was considered the best. They found in distilled water static tests on a 1% nickel alloy in 2S aluminum uniform corrosion rates at different temperatures as follows:

250°C	1 mil per year
290°C	$1\frac{1}{2}$ mils per year
315°C	3 mils per year
350°C	9 mils per year

Of the three methods of protection proposed by Draley and Ruther, both the nickel plate and nickel alloy appeared more attractive for reactor application than the use of nickel salts, and were subjected to an extended series of dynamic engineering-type tests[92,108-114] over a period of several years by Argonne National Laboratory, Reactor Engineering Division (ANL-RED). The nickel plate was found to fail where the coating was faulty[92,108,109] and tended to come off when exposed to neutron flux.[92] For these reasons, further testing of nickel plate was discontinued.

The dynamic tests on Al-Ni alloys showed a marked velocity effect.[109] Semi-static test sections in dynamic loops showed corrosion rates very close to those found in static autoclave tests but the rates increased with increased velocities. At 7 ft/sec rates were higher than in semi-static tests and at 16-21 ft/sec the rates were still higher. It was also observed that samples exposed to 16-21 ft/sec tests showed an accelerated erosion-corrosion attack on leading edges and other local areas of still higher velocity.[109]

Another observation[110] that defied explanation for a long time was the difference in corrosion rates in 260°C high velocity tests between originally loaded samples and the replacement samples. Another baffling characteristic of the dynamic high velocity tests at 260°C was the lack of reproducibility of results between supposedly identical runs, both at ANL and elsewhere.

The promising results with Al-Ni alloy and others obtained by Draley and Ruther in static tests on high-temperature water were confirmed by other investigators[115-120] in U.S., Canada, and England. The

interest in this country was reflected in the activity of the Aluminum Alloy Task Group which, from its inception in 1955 to December 1957, was sponsored by the Naval Reactors Branch, Division of Reactor Development, USAEC, and subsequently by the Fuels and Materials Development Branch, Division of Reactor Development, USAEC.

The purpose of the Group was to reduce unnecessary duplication and to expedite interchange of information between organizations actively engaged in the development of aluminum alloys resistant to high temperature water. Although some of the reports are not readily available, they constitute a valuable source of information to those who do have access to them.[121] Much of the information has been published subsequently.

Development activity has been aimed in several general directions as follows:

a. Development of alloys of improved corrosion resistance.[30,117-120,122-124]

b. Development of corrosion resistant alloys of improved mechanical properties.[124-126]

c. To understand better the nature of the protective film.[119,122,127,130]

d. Learn more regarding the corrosion mechanism.[122,128]

e. Investigation of effects of water environment on corrosion behavior.[120,122-124,129-132]

f. Evaluation of effects of test geometry.[119,122,133]

g. Study of effects of irradiation.[92,111,112,119,133]

It should be understood that there is a great deal of overlapping among the references listed under the above categories.

As an aid in the evaluation of Al-Ni for reactor application, results of tests at Argonne National Laboratory (ANL), Westinghouse Atomic Power Division (WAPD), Hanford, and Chalk River in which corrosion rates were determined are summarized in Tables 4.6, 4.7, 4.8, and 4.9.

Information for the first three tables came largely from the Aluminum Alloy Task Group reports.[121] The Chalk River data in Table 4.9 came from references indicated in the table.

2. Tests at Argonne National Laboratory, Reactor Engineering Division (ANL-RED)

The RED results in Table 4.6 in combination with those in the references suggest the following conclusions:

a. The corrosion rate at 316°C is higher than that at 260°C.

b. The corrosion rate increases with the velocity.

c. The corrosion rate for replacement samples is higher than that for original samples. The difference between them is greater at 260°C than at 316°C.

d. The corrosion rate at about pH 5 is lower than that at about pH 7.

e. The corrosion rate is higher in the absence of hydrogen than when it is present.

f. The corrosion rate at 246°C appears higher than that at 260°C but it is believed that other factors had more effect than the 14 degree difference in temperature.

g. Under boiling heat transfer conditions [217°C and 25,000 Btu/(ft^2)(hr)] the rates obtained ranged from less than 1, to about 3 mils/yr. No significant pitting or other accelerated attack was observed.

h. The apparent effect of irradiation was to reduce slightly the corrosion from that found in the out-of-pile section. The high rates found were attributed to poor average water quality in one case, and to erosion effects in the other, combined with low Al/H_2O ratio, (aluminum surface / water volume).

i. The corrosion rates in dilute H_3PO_4 solutions were lower than those in H_2SO_4 of the same pH.

j. Dynamic corrosion rates at 260°C showed a greater range of values and some higher values than those at 316°C.

k. An important, but poorly understood factor, is the Al/H_2O ratio. The Al/H_2O ratio effect appears to be influenced by other conditions, such as pH, flow rate, temperature, etc. At pH >7 a high Al/H_2O ratio does not seem to be as effective as at a lower pH; and at low velocities the ratio had no effect.

l. Among the alloys proposed for high temperature water application, the differences due to alloy composition are generally less significant than those due to differences in water conditions.

m. While the use of H_3PO_4 markedly reduces the uniform corrosion rate of high temperature Al-alloys, long-term tests have been characterized by pitting attack at pH values ranging from 3.5 to 5.5 at 316°C. Alloys of different composition show differences in this respect. Also more attack of stainless steel occurs.

n. The high temperature Al-alloys appear to corrode by a spall-heal process that results in a considerable amount of aluminum oxide crud in the system. The amount of crud appears to be greater in systems maintained at low pH.

Table 4.6

ANL RESULTS ON X-8001 (M-388)

Loop	Run No.	Temp, °C	pH Range	Additive	H_2 cc/liter	Al/H_2O cm^2/liter	Type of Sample	Corrosion Rate mils/yr			Comments
								16-22 ft/sec	6-7 ft/sec	Semi-static[1]	
1	1	260	4.9-5.1	H_2SO_4[2]	N,[3]23-111	92	O[4]	2.0	1.4	1.2	
1	4	260	5.8-6.1	H_2SO_4[2]		25		10.3			Regular samples
1	4	260	5.8-6.1	H_2SO_4[2]		25		6.9			Pretreated samples
1	5	260	5.0-6.8	H_2SO_4[2]	N, 5-560	59	O	4.2	2.5		
1	5	260	5.0-6.8	H_2SO_4[2]	N, 5-560	59	R	7.3	4.0		
2	1	288	8.9-9.3	NH_4OH[2]	N, 100	0	O	7.1		2.6	
3	1	260	6.5-6.9	deion.	N, 41-540	73	O	2.0	1.5	1.5	
3	1	260	6.5-6.9		N, 40-350		R	5.9	6.1		
3	5	246	7.1-7.5		N, 30-320		O	8.7	2.7	1.2	
3	5	246	7.1-7.5		N, 30-320	71	R	17.4	4.5	1.9	
3	4	260	6.8-7.0		N, DG; 0-310	49	O	8.5	5.1		
3	4	260	6.8-7.0		A, 220-250		O	10.7	4.5		
4	1	260	5.3-6.3	H_3BO_3	A, 100		O	5.1			
4	2	260	6.3-6.9	deion.	DG	12	O	11.0			
4	2	260	6.3-6.9	deion.	DG		R	16.5			
3	6	260	7		N		O,R	6.3	1.9		
4	3	260	6.4-6.7		A, 150	8		11.0			
1	2	316	5.3-5.9	H_2SO_4[2]	N, 31-250	84	O	6.0	4.7	2.8	
1	2	316	5.3-5.9	H_2SO_4[2]	N, 31-250	84	R	8.6	3.2	3.5	
1	6	316	5-6	H_2SO_4[2]	N		R	13.6	7.4		
2	2	316	4.5	H_3PO_4[2]			O	0.77		0.36	
2	2	316	4.5	H_3PO_4[2]			R	very high			
3	2	316	6.8-7.0	deion.	A, 175-540	76	O	8.5	6.5	5.5	
3	2	316	6.8-7.0	deion.	A, 175-540	76	R	10.9	8.8		
3	7	316	5.5	H_3PO_4[2]			O	4.2	1.9	0.7	
3	8	316	5.5	H_3PO_4[2]			O	2.6	0.7		
3	8	316	5.5	H_3PO_4[2]			O	0.8	0.5		198 X alloy
4	8	316	7.0-7.4		DG	16	O	11.7			
4	8	316	7.0-7.4		DG	16	R	16.6			
4	9	316	7.2-7.3		DG	30		9.8-12.5			A series of ALCOA alloy.
Boiling rig #2	1,2,3	217	6.5-7.5	deion.	DG	92	clad tube		3.3		Vel. not known, natural circulation.
Boiling rig #3	1	217	6.5-7.5	deion.	DG	57-131	clad heater	1.7 1.2 0.9 0.4			6.7 watts/cm^2 } vel. not 3.3 watts/cm^2 } known, 1.7 watts/cm^2 } natural 0 watts/cm^2 } cir.
MTR-ANL-2	cartridge #7	252-260	6.2-7.8	deion.[5]	DG	3.5		11.6 17.4			15 ft/sec in-pile 2-9.8 x 10^{20} nvt. th. 15 ft/sec out-of-pile
MTR-ANL-2	cartridge #9	252-260	5.6-9.5	deion.	DG	4.4		16.7[6] 17.4			15 ft/sec in-pile 2.55-3.22 x 10^{20} nvt. th. out-of-pile

[1]Estimated flow 1/60 ft/sec.

[2]Acid added by means of ion exchange bed.

[3]N = natural hydrogen buildup; A = hydrogen added; DG = degassed.

[4]O = original sample; R = replacement samples.

[5]ion exchange bed was turned off part of time inadvertently.

[6]Considerable erosion effect observed.

o. Corrosion rate increases with flow. A definite erosion-corrosion effect becomes evident around high turbulent areas at leading or trailing edges and around clamps.

p. Velocity effects appear to be accelerated at pH values above 7.0.

3. Tests at Westinghouse Atomic Power Division (WAPD)

Some of the corrosion results obtained on X-8001 by WAPD[121] are summarized in Table 4.7. The WAPD results, all of which were obtained at 316°C or higher, suggest the following conclusions:

a. In pure water, corrosion rates at 360°C are slightly higher than those at 316°C, but there is not much difference between static tests in water or steam, and dynamic tests.

b. Corrosion rates at pH 3.5 are slightly lower than those at pH 7; and those at pH 7 are generally slightly lower than those at pH 8.5-9.0.

c. Corrosion rates in pH 3.5 solutions containing H_3PO_4 are lower than those containing nitric acid.

d. At 360°C, a break occurs after about 70-84 days in deionized water, after which the corrosion rate increases by about three times. After about 200 days, a second break occurs with another factor of 3 increase in corrosion rate.

e. Under nominally similar conditions, rates obtained at WAPD are in general lower than those obtained at ANL. However, in one test at pH 8.4-9.4, a rate of 62.5 mils/yr was obtained at 316°C.

4. Tests at Hanford Works

Some of the corrosion results obtained on X-8001 at Hanford[121] are summarized in Table 4.8. Some conclusions based on these results and on reference reports are as follows:

a. The corrosion rate depends on flow. Between 0 and 2 ft/sec the rate increases by twenty times. Between 2 and 12 ft/sec, there is no further change.

b. In long-term tests in deionized water at 350°C and 363°C, a break occurs after which the rate is accelerated.

c. Corrosion increases with the amount of irradiation received.

d. Corrosion rates at 260°C range from 0.3 mils/yr in pH 4.5 H_3PO_4 water solution to 109 mils/yr in high purity water.

Table 4.7

WAPD RESULTS ON X-8001 (M-388)

Temp. °C	Type of Test		pH	Addition	Corr. Rate mils/yr	Comments
360	Static	Water			4.0	
360	Static	Steam			4.7	
316	Static	Water			3	
360	Semi-Dynamic	Water	6.5-7.5		4	
360	Semi-Dynamic	Water	3.5	HNO_3	2	
360	Semi-Dynamic	Water	3.5	H_3PO_4	0.5	
360	Semi-Dynamic	Water	8.5-9.0	NH_4OH	3.4	
316	Dyn. 30 ft/sec	Water	8.5-9.0	NH_4OH	5.0	
343	Dyn. 20 ft/sec	Water	8.5-9.0	NH_4OH	8.4	
360	Static	Water			5.2	
316	Static	Water			6.0	
316	Dyn. 20 ft/sec	Water	8.5-9.0		6.7	
360	Static	Water			3.95 13.8	14-84 days 84-126 days
360	Static	Water			3.47 14.3	14-84 days 84-126 days
360	Static	Steam			4.6 13.0	14-70 days 70-112 days
316	Static	Water			2.6	
360	Dynamic	Water	7.0		5.0	
343	Dyn. 20 ft/sec	Water	8.5-9.0	NH_4OH	6	
343	Dyn. 20 ft/sec	Water	3.5	H_3PO_4	0	
343	Dyn. 4 ft/sec	Water	3.5	H_3PO_4	0	
360	Static		6.5-7.5	deion. water	3.27	14-98 days
					13.19 39.06	98-196 days 196-238 days
					5.40 8.55	14-70 days 70-182 days
					6.06 25.31	14-126 days 126-210 days
360	Static	Water-steam	6.5-7.5		4.55 12.60 30.10	7-80 days 80-140 days 140-210 days
316	Static	Water	6.5-7.5		2.10-4.53 6.08-6.23	7-210 days 77-224 days
360	Circulating 1.5 l/hr	Water	6.5-7.5	deion. water	5.6	14-95 days
316	Dynamic		8.5-9.4	NH_4OH	62.5 5.18	20 fps 1 fps

e. With a high ratio of metal surface to water, the corrosion rate is decreased.

f. It is believed that the lower rates under semistatic conditions are due to the higher concentration of corrosion products in the water in contact with the sample. The effect of increased flow is to reduce this concentration and thus increase the corrosion rate. The high rates obtained by Hanford as compared with those at ANL and WAPD are believed to be due to a low metal-to-water ratio at Hanford as compared with the high metal-water ratio at ANL and WAPD.

g. H_3PO_4 solutions of pH 3.5 attacked sensitized SS-304 at 150-180°C after 12-17 weeks.

h. 198X alloys prepared by ANL showed improved resistance over X-8001 and M-400 but Hanford melts were inferior to ANL melts.

i. High heat through-put appears to increase corrosion rate.

j. At pH = 4 (H_3PO_4) 249°C tests showed no attack of sensitized SS-304 up to five months.

k. Al/H_2O ratio and loop cleanup rate markedly influence corrosion rate.

l. The French alloy Al, 2.1% Fe, 0.7% Ni appears to be as good as ANL-198X.

m. For temperature increase 180°C to 250°C in dynamic tests, the corrosion rate increases 3.5 times, equivalent to a 20% increase for every 10°C rise.

n. The alloy A-203X showed very low uniform rates, but evidence of blistering at pH 4.5 (H_3PO_4) 300°C with Al/H_2O = surface area/volume = 119 cm^2/liter.

o. Experimental evidence indicates that a combination of pH 4.5 (H_3PO_4) and high Al/H_2O ratio is better than either alone.

p. Preliminary results indicate the possibility of a compatible carbon steel-aluminum alloy system at low pH values by using dichromate inhibitor and nitric acid to lower pH.

q. Dynamic loop tests at 200, 250, and 300°C indicate no replacement effect at 200°C but replacement effects at 250 and 300°C.

r. In these studies an increase in temperature from 200 to 300°C increased corrosion rate by a factor 2-3

s. Attempts to correlate corrosion rates at 200, 250 and 300°C based on the difference in solubility of the corrosion product indicated that observed rates were several times higher than predicted values. The presence of large amounts of aluminum oxide corrosion product in the form

of flakes during a run suggests an erosion effect rather than anomalous high solubility effect.

t. The pronounced beneficial effect of pretreatment by autoclaving may result from an aging of the corrosion product which renders it less soluble. The aging of aluminum oxide hydrates with resulting marked decrease in solubility is well known.

u. Based on static tests in 0.2 M acetate buffer, the pH of minimum corrosion at various temperatures is as follows:

300°C	<3.1
280°C	<3.1
255°C	4.0
205°C	4.9

v. At 260°C the corrosion rate of X-8001 was found to be 13.2 mils/yr. Under a heat flux of $1.39\text{-}1.4 \times 10^5$ Btu/(hr)(ft^2) and average surface temperatures of 268-270°C, tubes of X-8001 corroded at a rate of 21.6 mils/yr. Calculations showed that for every 9300 Btu/(hr)(ft^2), 2°F must be added to the calculated surface temperature to obtain the true corroding temperature. Film thickness determinations by eddy current and film weight calculations show it to be 2.5-2.7 mils with a density of 3.0 gm/cm^3. Thermal conductivity estimates for the film are 1.4-1.7 Btu/(hr)(ft)(°F).

w. There are three general types[132] of aluminum corrosion. The most destructive type: (a) below 50°C is pitting; (b) 50°C-250°C is uniform attack; and (c) above 250°C is intergranular attack.

In investigating the effects of various ions on uniform corrosion, it was found that pH was most important variable. Phosphate inhibited corrosion, citrate increased it. Corrosion rates were lowest at lowest flow rates; most important parameters of uniform Al corrosion are temperature, time, water composition and flow rate.

x. J. A. Ayres[133] attempted to predict the corrosion behavior of the high-temperature aluminum alloys in reactors by means of equations, graphs, etc. It was based on the corrosion rate being a logarithmic function of time; that corrosion increases with irradiation (reactor power); that optimum pH = 4.0; and two assumptions, i.e. (1) that the use of phosphate or other inhibitors in reactors will become practical and will decrease the corrosion rate by a factor of ten times over that found in the Hanford H-loop, and (2) by developing improved alloys and learning enough about the optimum loop conditions, the corrosion rate can be lowered by another factor of five.

Table 4.9

CHALK RIVER RESULTS OF DYNAMIC TESTS ON Al 0.5% Ni, 0.5% Fe, 0.2% Si

Temp. °C	Flow, ft/sec	pH	Additive	Corrosion Rate mils/yr	Comments	Reference
260	2-3	9.7	Li OH	7-10	Irradiation [1]	134
260	20	6.5-7.0	Deionized	17-20		
288	20	6.5-7.0	Deionized	100-120	Irrad.[3] heat flux [2]	119
260-288	20	6.5-7.0	Deionized	2	Prefilmed in 299°C static water	121, 122
				8	High Al/H_2O ratio	
				45	Low Al/H_2O ratio	
				45	Replacement samples	
300	Static		Deionized	1.2-2.1		122
260	Dynamic	6.5-7	Deionized	130		
260	Dynamic	6.5-7	Deionized	25	170, 360, 567 cm^2 Al/liter H_2O	122
						122
260	Dynamic	6.5-7	Trace diss. SiO_2	13	170	

[1] The slight amount of ionizing radiation employed appeared to reduce corrosion rate. The effect is not considered significant.

[2] Samples exposed to ~230,000 Btu/(ft^2)/(hr) showed about 10% estimated corrosion more than those exposed to ~35,000 Btu/(ft^2)/(hr).

[3] Slightly accelerated effect with enriched UO_2 fuel - not considered significant.

Table 4.8

HANFORD RESULTS ON M-388

Type of Test	In-pile	pH	Additive	Corrosion Rate mils/yr [1]												
				Temperature °C												
				363	350	280	260	250	240	230	225	220	200	180	160	150
Dynamic	Yes	5.5	Cation I.E.			103	70	54	46	31		24	14	7		
Dynamic	Yes	High purity						109	84			50	28	15		
Dynamic	Yes	4.5	H_2SO_4					52	42			24	14	7		
Dynamic	Yes	4.5	H_3PO_4						10			7	4	3		
Dynamic 2-4 ft/sec	No	-	$Al_2(SO_4)_3$					17.5								
Dynamic 2-4 ft/sec	No	-	High ratio Al/H_2O					6-8								
Dynamic	Yes	6.0	-										72	60	38	
Dynamic	Yes	5.0	-					44			24		12			
Dynamic 10-15 ft/sec	No	4.5	H_3PO_4 I.E.													0.6
Dynamic 10-15 ft/sec	No	3.5	H_3PO_4 I.E.													0.6
Dynamic 20 ft/sec	No	4.5	H_3PO_4 I.E.					0.3								
Static (low flow)	No	7.0	Deionized		2-2.5[2] 5.5-6[3]											
Static (low flow)	No	7.0	Deionized	3[4] 20[5]												

Type of Test	In-pile	pH	Additive	350	300	290	260	250	227	224	180	175	150	Comments
Dynamic 10-15 ft/sec		3.5-4.5	H_3PO_4										0.60	
Dynamic 20 ft/sec		4.5	H_3PO_4		1.3									
Dynamic		6-7	Deionized		24									
Dynamic		6-7	Deionized					5.4						High Al/H_2O ratio.
Static		6-7	Deionized	2.2										
Dynamic		8.5-9.5	NH_4OH			9.0								Low Al/H_2O ratio.
Dynamic		8.9	NH_4OH + $Al(NO_3)_3$					8.8						
Dynamic		4.0	H_3PO_4								0.094			
Dynamic		4.0	H_3PO_4					0.33						
Dynamic		4.5	H_3PO_4			0.06								High Al/H_2O ratio.
Dynamic		4.5	H_3PO_4							1.1				In-pile.
Dynamic		4.5	H_3PO_4								120			In-pile very high heat flux A-2 alloy.
Dynamic		4.5	H_3PO_4						1.44					In-pile A-2 alloy.

[1] In most cases estimated values taken from graphs.
[2] Penetration after first 6 months.
[3] 49 weeks penetration.
[4] 1-9 weeks rate.
[5] 9-15 weeks rate.

On these bases, and excluding the mechanical factors, he concluded that aluminum may well be potential material for cladding fuel elements for reactors operating at outlet temperatures up to 350°C. He has taken observed corrosion rates and compared them with calculated rates. He concluded that the predicted values do not fit data from corrosion experiments in deionized water in static or low flow systems either at HAPO or elsewhere; neither does it fit data from corrosion experiments in deionized water in flow tubes or pilot plants at sites other than HAPO. He concedes that more accurate information is needed to make the predictions truly realistic.

5. Tests at Chalk River, Canada

a. The Chalk River results,(134) some of which are included in Table 4.9, confirmed the earlier work on high-temperature corrosion resistant alloys containing Cu, Fe and Ni but found improvement when Si, Bi, Zr and Ti were added.

The best alloys show acceptable rates 1.3-2.1 mils/yr in static tests at 300°C but under dynamic conditions at 18-20 ft/sec rates increase about sixty-five times to about 130 mils/yr. The low rates are reached in static tests only after corrosion films 10-20 μ in thickness are built up in at least two distinct layers and in a fifteen-week static run about 15% of the film is lost through spalling and dissolution.(122) The higher rates under dynamic conditions are believed to be due to a combined erosion-corrosion effect that may be due to differences in test temperature, details of sample design and mounting, and characteristics of individual loops. This may help to explain the differences in results found in different sites. Due to the accelerating effect of mechanical damage on corrosion it is difficult to establish corrosion rates at 18-20 ft/sec. Maximum corrosion rates for freely vibrating samples may be as high at 0.030 in./month, while rates for flat samples rigidly clamped have been as low as 0.020 in./yr.(119)

In regions of linear corrosion attack (dynamic 18-20 ft/sec) there was a continuous spalling and reformation of the corrosion films in an uneven manner. Pitting was observed and accelerated attack at leading edges. A 5X reduction in corrosion rate was observed by using 1000 ppm dissolved silica. The protection, however, was erratic. In loop tests it reduced the uniform corrosion and spalling of most specimens, but resulted in a severe localized pitting attack, particularly at leading edges.

Increasing the Al/H_2O ratio from 2 cm^2/liter to 170, 360, and 565 cm^2/liter decreased the corrosion rate from greater than 130 mils/yr to about 25 mils/yr, apparently by saturating the water with dissolved corrosion product and reducing film dissolution corrosion.

While methods of saturating the loop water have reduced corrosion by a factor of 5, there is still no explanation for the 10X increase over static tests.

6. Summary

a. Corrosion rates on Al-Ni alloys above 200°C are higher in dynamic tests than in static tests, and the higher the flow rate the higher the corrosion rate. Velocity effects are greater at pH values above 7.0 than below.

b. Under static and dynamic conditions, the corrosion rate increases with temperature.

c. At 360°C the corrosion in stagnant static autoclaves over a long period of time makes two transitions, each rate being about three times the previous rate.

d. The range or spread in corrosion rates observed in dynamic tests at 260°C has been greater than that at 316°C.

e. Other factors appear to have a greater effect than temperature between 260°C and 316°C in dynamic tests.

f. The difference in corrosion rates between original and replacement samples in a dynamic loop has been greater at 260°C than 316°C.

g. The corrosion rate in dynamic systems is higher above pH 7, i.e. 7-9 than below 7, i.e. 5-7.

h. The corrosion rate at a low pH produced by H_3PO_4 is lower than that of the same pH produced by HNO_3 or H_2SO_4.

i. The use of low pH by means of H_3PO_4 may introduce corrosion problems with stainless steel, pitting of Al-Ni and increased activity problems in a reactor. Development work would be required before it could be used in a reactor.*

j. The aluminum surface/water volume ratio is an important parameter in the corrosion rate of Al-Ni alloys. A high ratio is conducive to low rates and a low ratio to high rates. The ratio effect is more important below pH 7 than above pH 7. But it is not important at very low velocities.

k. Pretreatment by autoclaving appears to favor low rates, at least for a time. Further work is needed in this area.

l. Data on the effect of irradiation on the corrosion of Al-Ni alloys is contradictory. ANL and Chalk River have found the effect to be minor. Hanford finds the effect significant. Further work is desirable.

*Later developments have been described by Draley et al.(135)

m. Data on the effect of heat through-put is limited but both Chalk River and Hanford encountered excessive rates in tests with high heat transfer rates.

n. If the function of the increased aluminum surface to water volume ratio is to inhibit corrosion by saturating the water with aluminum oxide corrosion product, then operation of a cleanup loop should nullify the inhibition by removing the dissolved (or suspended) corrosion product. More investigation is required in this area.

o. Differences in composition in the Al-Ni alloys developed for use above 200°C show less effect on corrosion than differences in water conditions; but under optimum water conditions it is believed that the effect of differences in composition will become more apparent. More work is required in this area and in the fabrication of alloys such as A203, 198X, etc.

p. There is indication that some of the apparently abnormally high dynamic corrosion rates may result from an erosion effect of aluminum oxide corrosion product suspended in the water, and high flow rates.

7. ANL In-Pile Loop and Reactor Tests

Static and dynamic out-of-pile and in-pile tests of Al-Ni have been made to simulate fuel cladding behavior under reactor conditions. In addition to these tests Argonne has some actual experiences with Al-Ni alloy clad fuel elements in reactors, and also with a miniature model of a clad fuel element used in a reactor. Evaluation is incomplete but the results to date should be included in this survey.

a. A BORAX-IV Type Fuel Element UO_2-ThO_2 pellets in a X-8001 tube plate was tested in ANL-2 at MTR for 5 cycles (1607 hrs at 465°F). Test conditions were:

temperature	465°F (241°C)
pressure	600 psig
flow	12-13 ft/sec
maximum heat flux	800.000 Btu/(hr)(ft^2)
maximum burnup	1.5 w/o total core atoms
average burnup	0 5 w/o total core atoms
pH	6.0-7.4
resistivity	1.5-3.0 megohm cm

After the test the in-pile and out-of-pile plates were subject to film stripping to determine metal loss due to corrosion. Since the sample represented only one point the corrosion rate could not be determined but the metal loss

for the in-pile plate was 15.9 mg/cm^2 while that for an out-of-pile plate was 8.57 mg/cm^2. The in-pile plate with boiling on part of its surface was at higher average temperature than the out-of-pile plate. Since 6.9 mg/cm^2 = 1 mil, the two weight losses could represent maximum corrosion rates of 12.4 mils/yr for the in-pile plate in heat flux and irradiation and 6.7 mils/yr for the out-of-pile plate without heat flux and without irradiation.

The relatively good corrosion behavior shown in this experiment and in appearance of the samples in combination with the very low Al/H_2O ratio, 6 cm^2/liter, and relatively high flow rates compared to semi-static conditions do not appear to be in accord with the results of the summary given previously. It does tend to support the Chalk River and ANL results with reference to effect of irradiation and heat through-put.

b. BORAX-III Fuel Elements were Al-U alloy, 93.21% enriched, clad with 2S aluminum. Water temperature was 419°F (215°C) and pressure, 300 psig. Water resistivity averaged 400,000 ohm/cm and pH 6.0-6.5. Boric acid was present for about six months, 410 gm/1000 gal. Heat flux averaged 39,800-53,000 with a maximum of 92,800 Btu/(hr)(ft^2). Punchings from elements removed from the reactor after 600 Mwd operation showed the surface to be nonuniform with many surface pits and oxide blisters. None of the pits appeared to penetrate the cladding but analysis of the water from the casks suggested the presence of traces of fuel.(136)

The presence of boric acid throughout a considerable part of the total period may have helped to reduce the corrosion of the 2S aluminum.

c. BORAX-IV Fuel Elements were thoria-urania pellets in X-8001 tube plates. Operating conditions were 419°F (215°C), 300 psig. Water quality was maintained at 300,000-600,000 ohm cm and pH 5.7-6.2 by cation resin in hydrogen form operating in parallel with a mixed bed. Total operation was 980 Mwd/t (megawatt days per ton, about 2.3% total U^{235} burn-up). Total exposure was about 100 operating days at 215°C and about 20 decay days 66°C-93°C. Maximum heat flux was about 288,000 Btu/(hr)(ft^2). The run was terminated when evidence of fuel element rupture was obtained. Examination showed evidence of leakage in more than half of the elements.

Examination of two faulty elements in the cave at ANL showed seven leaks in twelve plates:

> "The results of the bubble testing indicate two significant facts. No leaks were evident at the silicon bonded areas and the areas that did leak were not severely corroded. All the leaks which were noted were either in the top collapsed sections or near the bottom of the plates."(137)

It is interesting to note that the fuel element failures all occurred over a short period of time after about a year of successful operation.

d. EBWR Dummy Fuel Elements. EBWR, at 600 psig, 489°F (254°C), contained 34 aluminum alloy X-8001 dummy fuel elements which were in the reactor for about $2\frac{1}{2}$ years, about $\frac{1}{2}$ of which was at operating temperature. The situation with regard to aluminum is confused because the condenser tubes are also aluminum. The line from the hotwell to the reactor, however, carries all of the water through full-flow cotton filters, and it does not seem likely that significant quantities of aluminum oxide enter the reactor from this source.

Although corrosion of the dummy elements did not appear excessive from examinations that have been made, estimated to be 3 mils/yr,[90] a definite crud problem exists in EBWR. The aluminum oxide corrosion product along with nickel, iron, etc., deposited on the fuel elements, gradually spalled off and was carried to low velocity parts of the system, particularly control rod thimbles causing an accessibility problem. The channels between fuel plates are gradually decreasing in size due to the scale buildup. Examination of a fuel element gave preliminary indications that the scale was about 5 mils thick in some areas.

e. ALPR Fuel Elements. ALPR operating at 420°F (216°C) and 300 psig has Al-17% U (93% enriched) fuel elements clad with, and silicon bonded to, X-8001 aluminum alloy. Operating time has been so short that no significant data on fuel element behavior are yet available.

8. Addendum, September 1962*

The above survey, as has been mentioned, was written in 1959. In the final editing (1962) some later results have been added without any claim for complete coverage of the literature.

Out of Pile Testing. The more important results of the investigations made by the Aluminum Alloy Task Group have been summarized by R. J. Lobsinger.[138] Grant described ANL-RED tests[54] not covered in an earlier report[114] and indicated that the limiting conditions under which X-8001 can be satisfactorily used as a fuel element cladding in a high-temperature water reactor have not been established. A somewhat similar conclusion was reached by Riskevics in a survey of high-temperature aluminum alloys for the Pathfinder reactor.[139] A new class of controlled impurity alloys has been reported by ANL,[140,141] HAPO,[142] and Aluminum Company of America.[143] These alloys have much improved high temperature (305°-360°C) corrosion resistance as compared with X-8001.

*Subsections 8 and 9 have been brought up to date and rewritten by J. E. Draley and W. E. Ruther.

Mechanisms of dynamic corrosion have been discussed by Dillon,[144] Draley and Ruther,[145] and Dickinson.[146]

A BORAX-IV type fuel plate, aluminum-nickel (M-388) alloy cladding over ceramic fuel, was irradiated to a maximum burnup of 7800 Mw days per ton in the ANL-2 loop at MTR.[147] (Preliminary results were given in Sec. 4.4.7.) During the irradiation, the plate was in water at 600 psig and 465°F (241°C) with local boiling in the highest neutron flux region and a maximum heat flux of 500,000 Btu/hr-ft^2.

The specimen performed satisfactorily in spite of two factors, making the test more severe than would be expected in an actual reactor. These factors were: (a) a high corrosion rate, approximately 10 mils/yr, attributed to a low ratio of aluminum surface to loop water volume; and (b) a 5 mil scale deposit in the highest flux region which caused an increased fuel temperature and resulted in melting of the lead bond between clad and ceramic fuel. The only detectable effect of this occurrence was a slight flattening of the plate in this area. The increased temperature of the cladding due to the high heat flux and a heavy oxide film buildup was also a factor which influenced the corrosion rate.

ALPR type fuel elements, 1100 Al-17.5 w/o U-2 w/o Ni clad with X-8001 were irradiated in the ANL-2 loop in MTR in 420°F (216°C) water flowing at 12 ft/sec, with a maximum heat flux of 690,000 Btu/hr-ft^2, conditions considerably more vigorous than existed in the SL-1 reactor.[148,149] One test was terminated when high activity level in the water showed that penetration of the cladding had occurred after 156 days of full power operation of MTR (227 day total). Post-irradiation examination revealed the presence of two blister-type defects on one side of the element in the region receiving the highest flux. Both blisters were filled with corrosion products. It was concluded that local corrosion attack caused penetrations of the cladding at these points. The local corrosion which produced the cladding penetration was attributed to operation of the loop with water at high pH (9-10) for a seven-day period prior to detection of the rupture. Thickness measurements taken before exposure and after removal of the oxide scale indicate a uniform corrosion rate for the in-pile plate from 10 to 15 mils/yr at the conditions of the test.

This high uniform corrosion rate was attributed to two factors: the small ratio of aluminum surface to loop water volume, estimated at 5.8 cm^2/liter of water; and operation with water at pH 10 for a period of one week prior to failure.

The thickness of the scale, up to about 7 mils per side, and its low thermal conductivity resulted in a swelling of the core material in the high burnup region, where the central temperature was estimated to

have been as high as 1000°F (538°C). Only very slight corrosion of the fuel alloy occurred during the two day period in which it was exposed to the high temperature water.

The ANL-2 loop was chemically cleaned and a second test with the same type element was successfully concluded after 223 days (125 days of full power operation) at the same conditions. No high pH values were recorded for this experiment. Average scale thickness was 7 mils, corrosion 4-5 mils. As before, the relatively high corrosion rate was attributed to the small "surface to volume" ratio of the test equipment. No swelling of the fuel element was noted.

BORAX-IV - The final report[150] on the failed BORAX-IV reactor fuel elements attributed the primary cause of the failure to collapse and overstressing of the unfueled portion of the aluminum alloy tube plates. Although the collapsing was believed to have occurred during early operation, leakage of fission products was not observed until after nearly a year of operation when leakage of about 30% of the elements was observed following startup after a $2\frac{1}{2}$ month shutdown period. The most probable cause of the leaks which developed during shutdown was believed to be corrosion in the cracks and crevices of the collapsed tubing (at low temperature?). Pitting of aluminum in reactor storage canals has been observed in many instances when the quality of the water deteriorates.

ALPR - The operating life of ALPR ended with an accident.[151] The corrosion behavior of the X-8001 alloy used as fuel element cladding was not involved in the accident. In fact, its corrosion behavior was reported to have been better than had been anticipated.

English, et al.,[152] subjected X-8001 and other alloys to short time tests (ten days) at flow velocities between 20 and 107 ft/sec and at temperatures between 170° and 290°C. At 260° and 290°, all alloys except X-8001 showed extensive subsurface attack. At 260°C and at velocities up to 67 ft/sec, the corrosion rate of X-8001 was high during the early part of a run and decreased to rates of between 5 and 15 mils/yr; at the highest velocity the corrosion rate was constant at 200 mils/yr.

The important effect of heat flux on the corrosion of aluminum has been investigated by Griess, et al.[153] The thermal conductivity of the corrosion product film on aluminum alloys 1100 and 6061, largely boehmite ($\alpha Al_2O_3 \cdot H_2O$), was found to be 1.3 ± 0.2 Btu/hr-ft°F. The rate at which the boehmite formed on the surface (and consequently the rate at which the aluminum temperature increased) was a function of the temperature at the specimen-water interface and the pH of the coolant. The lower the temperature and the lower the pH (in the range of 5.0 to 6.5 with HNO_3), the lower the rate of corrosion-product formation. Within the ranges investigated, pressure and flow-rate were without effect and the same results were obtained with 6061 and 1100 aluminum.

9. Discussion and Conclusions

The operating experience of the ALPR and the corrosion data from the EBWR suggest that the corrosion of X-8001 aluminum in a typical natural circulation boiling water reactor should not result in penetration under conditions of good water control. Out of reactor data for newer improved alloys indicate that no hazard exists up to at least a 360°C cladding temperature. It is not indicated that the use of acid or inhibitors is necessary. However the use of aluminum in a reactor does increase the crud problems and limits the choice of compatible materials in the primary circuit more than either zirconium or stainless steel. There is also a more critical requirement for control of water quality, to avoid high corrosion rates at operating temperature or pitting during extended shutdowns.

The aqueous corrosion behavior of aluminum alloys in dynamic (7-50 ft/sec) high temperature tests appears to be only qualitatively explained by existing hypotheses. The corrosion rate is apparently very sensitive to certain small amounts of corrosion product carried by the dynamic stream in true solution or in colloid form. Until the factors involved in this sensitivity are better understood, no blanket recommendation can be given. Each potential application should be evaluated by experimentally duplicating the conditions as nearly as possible. For reactors whose operating conditions are more rigorous from the point of view of aluminum corrosion than SL-1 and BORAX-IV, full scale reactor testing of all aluminum clad fuel would be necessary before it could be determined whether this cladding material would be satisfactory.

5. CORROSION PRODUCT DEPOSITS

5.1. Introduction

The use of water at high temperature as a coolant-moderator material in power reactors has introduced certain problems due to the corrosive action of water on the materials in contact with it. The problems we are concerned with in this section are those that may result when corrosion products are dispersed in the water. The problems are: (1) fouling of heat transfer or bearing surfaces, which could decrease efficiency and shorten operating life; and (2) the buildup of radioactivity in the system which could increase the personnel hazards in the operation or maintenance of the reactor.

5.2. Pressurized Water Reactors

A considerable amount of investigation in the field of corrosion product deposits has been carried out on pressurized water reactor systems. Since the results are to a large degree applicable to boiling water reactors, we will review them briefly.

From the initial studies on pressurized water reactors, it was realized that corrosion products introduced into the water could produce radioactivity problems. It was partly for this reason that the materials selected for the first reactors were among the most corrosion resistant available: zirconium and its alloys for fuel cladding, and 18-8 austenitic steel for essentially the remainder of the system in contact with the primary water. Early autoclave and loop corrosion tests showed that even 18-8 stainless steel contributed a significant amount of corrosion products to the water. When these corrosion products became mixed in a system with corrosion products from other materials and miscellaneous debris, such as wear particles from pump bearings and control rod drives, weld scale, etc., it became known as "crud." Crud usually refers to products that are carried by the water but may be deposited from the water.

1. Fouling

Although fouling has occurred to heat transfer surfaces in in-pile and out-of-pile loop tests,[39,40,49,154] no damage by fouling (up to 1959) has occurred to fuel elements or other heat transfer surfaces in any pressurized water reactor. This has been attributed to maintenance of high pH and low oxygen concentrations.

The only instance in a reactor where deposition of stainless steel corrosion products has caused difficulty has been on throttling valves, causing decreased flow. Its effect could be alleviated by periodically closing and opening the fouled valve.

2. Radioactivity Buildup

Reactivity buildup has been of more concern to PWR investigators than the fouling problem. Very briefly, certain corrosion products become highly radioactive due to exposure to reactor neutron flux. These products are dispersed and carried in the water until they deposit somewhere in the system. As these deposits build up, particularly in the part of the system outside the reactor vessel, they become more of a health hazard to operating and maintenance personnel. Short-lived activity produces only a temporary problem; it is the long-lived activity that causes concern. The basic problem is to obtain sufficient understanding of the mechanisms involved so that the rate and extent of the activity buildup can be predicted and controlled.

This problem has been subjected to a considerable amount of investigation,[39,47,49,59,155-161] but only recent (1959-1960) reported results at Shippingport and APPR (or SM-1) will be summarized here.

a. Shippingport vs APPR (SM-1). The PWR represented by Shippingport is characterized by zirconium alloy clad fuel and operation with the water at high pH. APPR (or SM-1) is characterized by fuel clad with stainless steel and water maintained at neutrality. The nature of activity buildup problem in the two reactors is somewhat different. . .

In 1960, Bergmann[162] compared SM-1 and Shippingport activity levels. Induced activities found in Shippingport crud and those observed in SM-1 crud after 1440 EFPH (equivalent full power hours) operation were as shown in Table 5.1.

Table 5.1

SHIPPINGPORT AND SM-1 ACTIVITIES COMPARED

Nuclide	Activity (dpm/mg crud)		Activity (% of Total)	
	Shippingport	SM-1	Shippingport	SM-1
Co^{60}	5.8×10^6	3.9×10^5	39.2	10.8
Co^{58}	2.5×10^6	21.0×10^5	16.9	58.0
Fe^{59}	1.8×10^6	5.0×10^5	12.1	13.8
Cr^{51}	2.2×10^6	4.9×10^5	14.8	13.5
Mn^{54}	0.8×10^6	1.4×10^5	5.4	3.9
Zr^{95}	0.97×10^6	-	6.5	-
Hf^{181}	0.76×10^6	-	5.1	-
	14.8×10^6	3.6×10^6		

The lower specific activity level at the SM-1 can be a result of the following: the main source of the activity in Shippingport apparently arises from corrosion and wear products deposited on in-flux surfaces; in the SM-1 the main source can be accounted for by corrosion in the activated in-flux components. Since the Shippingport is operated at high pH, the corrosion deposits could remain in flux longer than they do during operation at low pH. The longer the deposits remain in flux, the greater the specific activity would be.

The greater contribution of Co^{60} activity to the total activity of Shippingport when compared to the contribution in the SM-1 suggests that in addition to the cobalt present as an impurity in stainless steel, another source of Co^{60} such as wear products is significant in Shippingport. Many of the high cobalt areas in Shippingport are in the control rod mechanisms located above the reactor core. Wear products presumably drop down and deposit on in-flux surfaces. Deposits removed from in-flux Shippingport surfaces show an enrichment of chemical cobalt and thus support the theory. In addition, the differences in relative contribution of Co^{60} to total activity may be due to more Co^{58} found in the SM-1. Co^{58} is produced by fast neutron activation of Ni^{58}. The SM-1 has a fast-to-thermal flux ratio of seven; in Shippingport it is about one. Thus, more Co^{58} would be expected in the SM-1 than in Shippingport.

After 4000 EFPH, radiation levels in one of the Shippingport steam generators were measured using a Cutie Pie (a radiation monitoring instrument). Measurements with the instrument as close to the tube sheet as practical were 2 r/hr. Radiation levels in the SM-1 steam generator in the tube sheet after 7700 EFPH were 6.3 r/hr. To make a comparison of the dose rates, the values measured at the SM-1 should be corrected back to 4000 EFPH. At the SM-1, radiation levels on the outside of the steam generator increased about a factor of 2.5 from 4000 EFPH to 7700 EFPH. Assuming radiation levels inside the steam generator increased in the same manner, the dose rates at 4000 EFPH are estimated at 2.5 r/hr at the surface of the tube sheet. Since Shippingport dose rates were taken away from the tube sheet, the radiation levels are probably about the same.

Since the specific activity of the crud in the Shippingport in terms of Mev/min/mg* crud at 1440 EFPH is about six times that found in the SM-1 at the same time, similar radiation levels would not be expected. If the relative distribution of nuclides remained the same from 1440 EFPH to 4000 EFPH in both reactors, the data indicate that out-of-flux crud desposits in Shippingport are somewhat less than those in the SM-1. Since Shippingport has a lower crud level than that of the SM-1, a smaller

*Mev/min is a measure of the energy of radiation while the term dpm used in Table 5.1 is only a measure of activity in number of disintegrations per minute.

crud film thickness might be expected. In addition, the stainless steel corrosion and wear products in Shippingport have a relative greater area over which they can be distributed when compared to the SM-1. In Shippingport, about two-thirds of the area exposed to the primary coolant is stainless steel (the other third is Zircaloy-2); in the SM-1 all of the exposed area is stainless steel. If we assume that corrosion rate of Zircaloy-2 is negligible, the net effect of these relative areas would be to lower the crud film thickness in Shippingport in comparison to the SM-1.

b. APPR(SM-1). Some of the results of the APPR investigations may be summarized as follows:

The data have shown that Co^{60} is the major contributor to radiation levels in the SM-1. In contrast with the activity levels in the water borne crud of SM-1 after 1440 EFPH in Table 5.1 where Co^{58} predominates, in the deposited activity levels Co^{60} predominates after about twelve months of reactor operation,(163) because of its longer half life.

The Co^{60} activity in SM-1 arises from the cobalt in Haynes 25 alloy flux suppressors, and the cobalt impurity in stainless steel. After thirty-five months of operation at an average power level of 55%, deposited Co^{60} activity accounted for approximately 83% of the total radiation level (mr/hr) contributed by the long-lived gamma emitting nuclides. In the primary coolant, after thirty-two months, 40% of the total gamma activity (from induced nuclides) was due to the Co^{60} nuclide. However, the contribution of the primary coolant activity to the total radiation level is insignificant when compared to the contribution of the activity deposited on the walls of the system. The radiation level on the superheater side of the steam generator was about 1400 mr/hr after thirty-five months of reactor operation. The percentages of Co^{60} activity in the coolant and in the deposits were not the same. This indicates either that the nuclides are depositing irreversibly on the surfaces of the system (with no redispersal in the water), or that all nuclides (if they are redispersing) are not exchanging at the same rate. The ratio of Co^{58} to Co^{60} in the deposits shows that a major fraction of nuclides are irreversibly deposited. A thin film on the surfaces appears to be in equilibrium with the activity in the coolant.

Knowledge gained from the activity buildup program was applied to reactors in the Army Nuclear Power Program as follows:

(1) Since the major source of Co^{60} in the SM-1 is due to the Haynes 25 alloy flux suppressors and cobalt impurity in stainless steel, flux suppressors containing no cobalt are being used in the SM-1A, the PM-2A and Core II of the SM-1. Also, low cobalt stainless steel is being used as fuel element clad material in the core of the reactors.

(2) Activity levels in the SM-1 coolant were used as a basis for estimating activity levels in the SM-1A and SM-2. This information was necessary to determine the engineering requirements for preliminary design of a waste disposal system.

(3) Mathematical equations derived during the early part of this study were used to estimate frequency of and need for decontamination in the SM-2. Although the equations do not exactly portray the activity buildup in the SM-1, it is believed that with certain modifications they are sufficiently accurate for design purposes. The equations were also used to determine the optimum impurity level in the SM-2 fuel cladding and reflector.

As was mentioned previously, APPR, or SM-1, was operated with neutral water. Consequently there has been no experience in operating pressurized water reactors having stainless steel clad fuel with water at high pH.

As the result of a literature survey,[42] on the use of high pH, the following conclusions were reached:

(1) High pH coolant is desirable for control of induced radioactivity in pressurized water reactors with significant amounts of stainless steel present in the core.

(2) No significant hazards are introduced by use of high pH coolant with respect to plant integrity or operability.

(3) LiOH is the best choice of a base for this purpose.

(4) A strong base form mixed-bed resin functions effectively in the dual role of maintaining coolant purity and high pH.

c. Shippingport. The activity of water-borne particulate matter in Shippingport[52] has been followed since early plant life (Fig. 5.1).

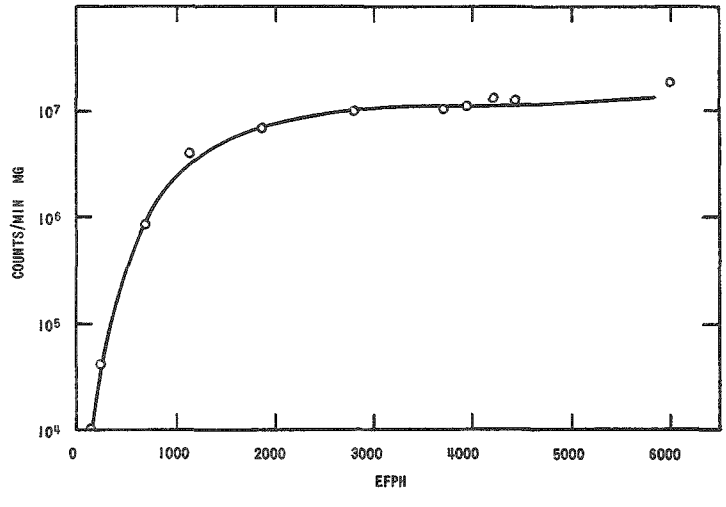

Fig. 5.1

Waterborne Crud Activity

By 1959 the specific activity had reached a saturation value of about 2×10^7 counts per minute per milligram (cpm/mg). The major contribution to this activity is 5.2 year Co^{60}. Chemical analysis of this crud indicated it contained 90%-95% iron as Fe_3O_4. The circulating crud concentration ranged between 3 and 5 ppb under steady state conditions; during startup some increases were seen. The highest crud burst observed was 61 ppb. Table 5.2 lists some typical radiochemical analyses of this material in disintegrations per minute per milligram (dpm/mg).

Table 5.2

RADIOCHEMICAL ANALYSIS OF CRUD SAMPLE

Date and Source**	Specific Activity - dpm/mg							Percent* of γ Activity Accounted
	Fe^{59}	Co^{58}	Co^{60}	Mn^{54}	Cr^{51}	Hf^{181}	Zr^{95}	
9/8/59 BD BIX	1.29×10^6		1.52×10^7	1.86×10^6	1.75×10^6	4.3×10^5	2.6×10^5	75
8/31/59 BD BIX	1.76×10^6		1.39×10^7	1.46×10^6	1.09×10^6	4.25×10^5	2.59×10^5	70
8/31/59 BD AIX	7.4×10^5		1.08×10^5	1.19×10^5	2.5×10^3	1.95×10^4	9.57×10^3	-
9/28/59 AC BIX	3.19×10^6	3.16×10^6	1.82×10^7	1.86×10^6	3.68×10^6	1.64×10^6	7.61×10^5	80

*Based on gross γ activity at 120 hours.
**Loop sampling point designations.

Further evidence of the extent of buildup of activity on the plant surfaces was obtained from the test pipe section, installed for deposit studies, referred to as the hairpin loop. The pipe samples were usually cut into 100 cm^2 sections, descaled using acids, and radiochemical analysis performed on the descaling solutions. There was never a weighable amount of loose crud found on the surfaces until the final performance of this test on a section which had been in service for about 3800 EFPH of operation. The specimen was brushed with a nylon brush and washed simultaneously with a high-velocity stream of water to remove loosely adherent material. This crud was weighed and its deposition on the surface calculated at 0.10 mg/cm^2. Radiation surveys of this section of the pipe using a Jordan probe-type monitor showed a radiation field of 100 mr/hr at the center of the Schedule 80, two inch pipe and 25 mr/hr on contact with the outer surface. All readings were taken twelve days after the samples were removed from the loop.

5.3. Boiling Water Reactors - EBWR

Corrosion product deposit investigations in boiling water reactors covered in this report are limited to those in EBWR.

1. Solids in the Water

The first investigation of solids in the EBWR reactor water system was made on samples taken May 28, 1957. Insoluble solids were collected by passing known water volumes through millipore filters. The pore size of the filters is not recorded. Similar surveys were made on June 18, June 21, and November 12, 1957. Only on the June 21 survey was a record made of the pore size of the filter, namely 10 microns. The results of the four surveys are given in Table 5.3.(56) Values for B, Ba, Cr, Mg, Zn, and Zr were given in most instances, but the amounts were so low that they were omitted from the table.

Table 5.3

SPECTROGRAPHIC ANALYSES OF INSOLUBLES CAUGHT ON MILLIPORE FILTERS

Element	Month and Day 1957	Micrograms per Liter*						
		Reactor Water			Feedwater		Steam	
		S-5(a)	After Prefilter S-6	After Ion Exchanger S-7	Before Filter S-3	After Filter S-4	Before Dryer S-1	After Dryer S-2
Al	5/28	19	8	3.2	3.6	-	3	1.8
	6/18	20	16	7	1.2	0.3	0.2	1.6
	6/21	6	-	-	-	-	0.7	1.5
	11/12	55	-	-	T(b)	0.5	-	0.5
Ca	5/28	0.8	0.4	0.9	1.2	-	2.5	2.3
	6/18	0.6	0.3	0.4	0.4	0.1	0.1	0.5
	6/21	0.2	-	-	-	-	0.3	0.6
	11/12	4	-	-	1.8	0.2	-	5
Cu	5/28	8	1.1	1.9	1.8	-	4	1.2
	6/18	1.2	1.1	0.8	0.4	0.1	T	0.8
	6/21	-	-	-	-	-	0.5	0.5
	11/12	7	-	-	5	T	-	0.5
Fe	5/28	77	42	16	30	-	12	14
	6/18	60	55	20	61	0.9	1.5	10
	6/21	1.6	-	-	-	-	2.9	6
	11/12	88	-	-	80	20	-	20
Mn	5/28	2.3	0.8	0.3	0.1	-	0.2	0.5
	6/18	0.3	0.3	0.1	0.1	T	T	0.6
	6/21	T	-	-	-	-	T	0.1
	11/12	2.5	-	-	0.7	0.2	-	0.5
Na	5/28	6	2.2	1.3	9	-	10	18
	6/18	0.1	0.6	0.2	0.1	0.1	T	0.2
	6/21	0.2	-	-	-	-	0.1	0.6
	11/12	-	-	-	-	-	-	-
Ni	5/28	25	11	6	1.2	-	1	0.1
	6/18	25	35	10	0.1	0.1	1.6	0.2
	6/21	1	-	-	-	-	0.4	0.5
	11/12	88	-	-	25	3.0	-	2.5
Pb	5/28	1.2	0.4	0.2	0.3	-	0.4	2.3
	6/18	0.4	0.1	0.3	0.2	0.1	T	10
	6/21	0.2	-	-	-	-	0.1	4
	11/12	-	-	-	-	-	-	-

(a) Sampling point on Fig. 3.6.
(b) Trace (0.1 μ gm/liter)

*Factor of 2 accuracy.

The following conclusions were made:

a. Very little chromium was found in the insoluble particulate manner, as compared to aluminum, iron and nickel. This suggests that most of the chromium corrosion product must be present in a soluble form.

b. Values obtained for aluminum, iron and nickel on June 21 samples were consistently lower than those on other sampling dates. Since this was the only group where the pore size of the filter was recorded, there is a possibility that a filter of smaller pore size was used in the other surveys.

c. Neglecting the June 26 results, the amount of iron in the water was about the same in May and June as in November. During this same interval, the amounts of aluminum and nickel increased.

d. Significant amounts of crud pass through the prefilter and to a lesser extent the ion exchanger.

e. A significant decontamination factor exists between reactor water and steam for particulate corrosion products.

f. The steam dryer alone does not seem to exert much of a decontaminating effect on suspended particulate matter.

g. The amount of suspended aluminum in the feedwater is less than that in the reactor water. None is removed by the feedwater filter, indicating that if aluminum comes from the condenser, it is in a dissolved form.

h. The amount of insoluble nickel in the feedwater is less than that in the reactor water. Some is removed by the feedwater filter.

i. The amount of suspended iron in the feedwater is nearly as great as in the reactor water. Significant amounts are removed by the feedwater filter.

In June 1957, water samples were taken from various parts of the system for investigation of total solids as contrasted to suspended or particulate solids. The small size of water samples and other problems in technique led to inconclusive results.

In 1959 a special device was developed(164) for determining the amount of total solids (suspended and dissolved) in reactor water. Water from any place in the primary system can be pumped into a weighed crucible in an autoclave which is operating at 100°F above the saturation

temperature. The steam is condensed, expanded to atmospheric pressure, and the total water flow measured. The device may be operated continuously with only occasional maintenance. A schematic outline of the device is given in Fig. 5.2.

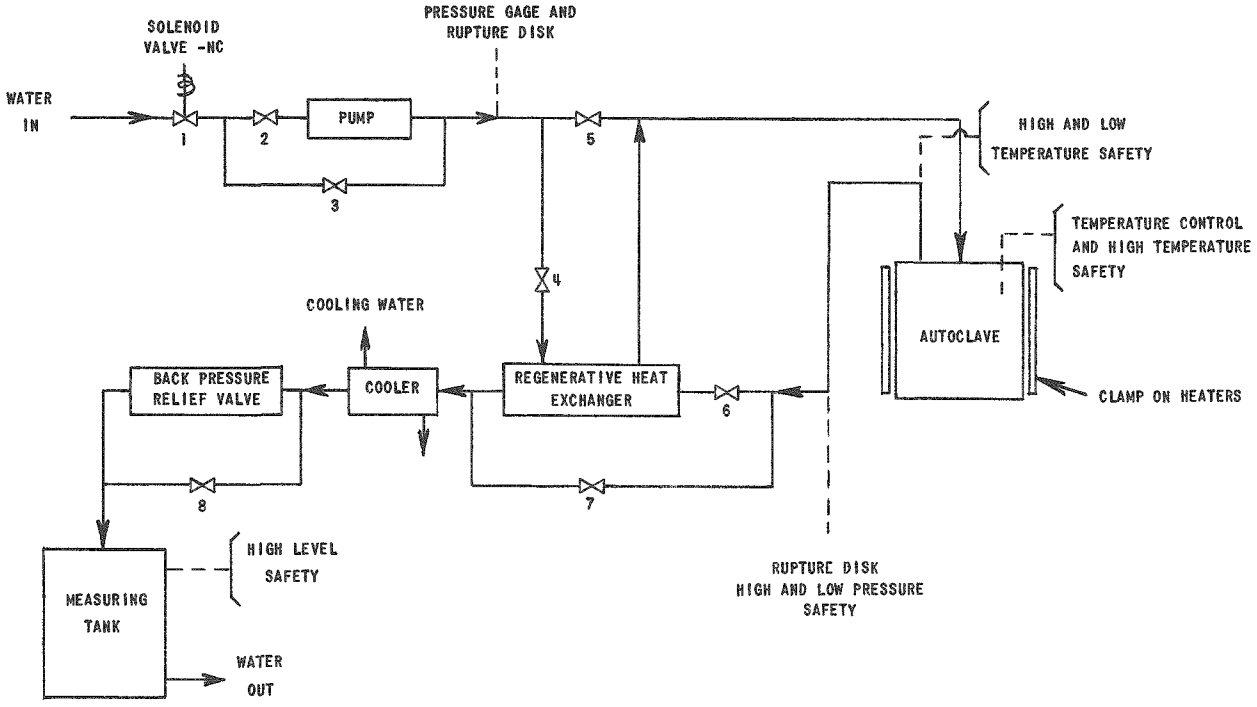

Fig. 5.2

System for Measurement of Suspended and Dissolved Solids

After installation of the equipment, one run was made on reactor water before final shutdown for the 100-Mw conversion. Evaporation of 107 liters of reactor water resulted in the collection of 7.7 mg, or a concentration of 0.07 ppm. Examination of the activity present by means of a 200-channel gamma-ray analyzer indicated Co^{58} and Co^{60} present in a ratio of about 10 to 1.

A wet chemical analysis for aluminum, iron and nickel gave the results summarized in Table 5.4 calculated on basis of the assumed composition designated in the table.

Table 5.4

WET CHEMICAL ANALYSIS OF REACTOR WATER SOLIDS

Element	Assumed Compound	Amount, mg		%	
		Element	Compound	Element	Compound
Al	$Al_2O_3 \cdot H_2O$	1.59	3.53	59	70
Fe	Fe_2O_3	0.68	0.97	25	19
Ni	NiO	0.43	0.54	16	11
		2.70	5.04	100	100

2. Nature and Distribution of Deposits

a. Purification System. During the boric acid run, in the EBWR, December 29, 1956 to January 11, 1957, the amount of insoluble "crud" in the reactor was high and most of the activity associated with the crud was deposited on the No. 1 prefilter. During this run the after-filter became radioactive also (2.0 r/hr at 4 in.). It is believed that colloidal particles which had passed through the prefilter and either had time, or in some way were caused, to agglomerate by going through the ion-exchange column were responsible for the activity picked up on the after-filter. Cartridges from the pre-filter were a dark red-brown color from deposited material, while those from the after-filter were a light brown color.(21)

A radiochemical analysis was made on a sample taken in February 1957 from the prefilter. Results showed:

Major activities were Fe^{59} and Co^{60};

Minor activities in decreasing amounts were Ni^{59}, Cr^{51}, Zr^{95}, Ce^{144}, and Zn^{65};

Trace activities, identification uncertain, were Sr^{89}, Ba^{140}, Mo^{99}, Cs^{138}, and possibly Nb^{95}.

In another examination of the prefilter, particularly the shorter-lived activity, an activity half life of about 3 hr was found. This corresponds to the 2.6 hr half life of Mn^{56} and checks with the fact that a primary activity in the reactor water was found to be Mn^{56}.

After cleaning up the boric acid and activities associated with removal of boric acid on an ion-exchange column, the activity of the ion-exchange column was checked at three ports in its shielded vessel. The activities were 1.9 r/hr at the top, 200 mr/hr at the center, and 100 mr/hr at the bottom port.

Later, another ion-exchange bed, which, after use, was removed after a 14-day decay period, exhibited the following dose rates:

Top of bed	1 r/hr at 6 in., hard
1 ft down	500 mr/hr at 2 in.
2 ft down	100 mr/hr at 2 in.

The primary radionuclides present on resins and filters were Co^{58}, Ba^{140}, La^{140}, Fe^{59}, and Co^{60}. Chromium-51 was found only on the anion resin, presumably as chromate ion. A high percentage of the particles of deposited material were less than 0.1 micron in diameter when examined by electron microscope.

During the $2\frac{1}{2}$ year operating life of the reactor prior to shutdown for 100 Mw conversion, ion-exchanger No. 1 was charged three times, No. 2 once. The last replacement for No. 1 occurred June 3, 1958, after one year's use in treating 1,064,600 gal of water. After 33 days decay the activity levels measured with a survey meter are given in Table 5.5.

Table 5.5

ACTIVITY LEVELS OF ION-EXCHANGE BED AFTER 33 DAYS DECAY

Position	Activity Level (mr/hr at 2 in.)
Directly above resin	22,000
Side of resin basket at top	17,000
One-fourth distance from top	7,000
One-half distance from top	500
One-fourth distance from bottom	170
Bottom	100

b. Feedwater Filters. In February 1957, No. 2 feedwater filter was changed for a second time after about 230 hr of operation. The activity level of the unloaded assembly of cartridges measured about 1.5 mr/hr. The maximum activity observed on the surface of these unshielded vessels was 15 mr/hr at 2 in. at 20 Mw.[21]

A sample of about 1 sq in. from the surface of one of the cotton string cartridges was spectrographically analyzed. After subtracting blanks on the filter itself, the results indicated the deposit to be 67% iron, 30% nickel, and the 3% balance of Mn, Cr, and Mo based on an accuracy within a factor of 2.

Filter cartridges were replaced four times in 1957 when pressure drop across the filter reached 30 psig. Subsequent experience has indicated that the frequency of replacing the cotton fiber cartridges depends on the number of times the vacuum is broken in the main condenser. Release of vacuum increases O_2 content of the primary system by addition of air and accelerates corrosion. During startup, corrosion products are picked up and tend to clog the filters. On a rough comparitive basis, it has been observed that one shutdown is equivalent to about 600 hr of continuous operation at 20 Mw. This indicates reduced maintenance will result from continued, rather than intermittent, power operation.

c. Steam Dryer. During the June-July shutdown in 1957, after 1370 Mw-days of thermal power production, the steam dryer was opened for inspection.(165) The radiation level in the dryer was between 5 and 6 mr/hr, and was primarily gamma activity. The walls of the vessel were, in general, free of deposit. Small areas had a brownish appearance, but no deposit sample could be obtained.

The emergency cooling coil in the lower half of the vessel did have some loosely adherent deposit, dark red-brown in color. This deposit, in general, was located on the upper surface of the tubes and a sample from the second row of tubes from the top was obtained for spectrographic and radiochemical analysis.

The results of the spectrographic analysis, accuracy within a factor of 2, are given in Table 5.6. The relative aluminum, chromium, iron and nickel contents should be noted for comparison with other water deposit analyses.

Table 5.6

SPECTROGRAPHIC ANALYSIS OF DEPOSIT FROM STEAM DRYER

Element	%	Element	%
Al	3	Mn	0.6
Cr	1.5	Na	0.2
Cu	0.1	Ni	1
Fe	Very large	Pb	0.1

The results of a radiochemical analysis (beta activity) are given in Table 5.7. Later examinations showed that the activity level increased to about 20 mr/hr inside the dryer (emergency cooling coil) and remained at about that level.

Table 5.7

RADIOCHEMICAL ANALYSIS OF DEPOSIT FROM STEAM DRYER

Element (Isotope)	Activity, % Total	Element (Isotope)	Activity, % Total
Co^{58}, Co^{60}	58	Cr^{51}	0.5
Fe^{59}	5	Ce^{144} and Pr	6
Ni^{63}	0.5	U	29 ± 50%, ppm
Gross β activity: 1.9×10^5 dpm/100 mg			

d. Startup Heater. In June 1958, during a preliminary hydrostatic test of the reactor vessel and its components, the startup heater leaked between gasketed flanges at a pressure of 600 psig.(166) On removing the head, radiation levels as high as 2 r/hr were observed.

A thick, hard, caked deposit of corrosion products was found between the flanges above the lower part of the gasket. It appeared likely that, with the large number of thermal cycles encountered by the startup heater, it expanded and contracted sufficiently to pack the accumulation and to finally separate the flanges to cause the leak.

Spectrochemical analysis gave the more important constituents as:

Al	0.3%	Fe	20%
Ba	4%	Mn	0.1%
Cr	0.8%	Ni	0.2%

The relative percentages of aluminum, chromium, iron, and nickel are of particular interest in comparing with other water deposit analyses.

e. Condenser. During the June-July 1957 shutdown, the condenser was examined.(167) Since the examination was a few weeks after reactor shutdown, the activity observed was due to longer-lived radioisotopes. The hotwell area, lower section, showed 1-2 mr/hr, while the upper portion, above the condenser tube banks, showed only 0.1-0.2 mr/hr. This difference was expected due to the more active washing action of the steam and condensate in the upper areas.

A radiation survey with a Juno meter showed that the major activity was gamma. Preliminary gamma-ray analyses of two samples of deposit showed the only measurable activity present 56 days after shutdown was Co^{58}. Quantitative figures obtained were 0.088 and 0.054 x 10^{-6} curie/gm of deposit ($\pm$ 20%). At the time of shutdown this would have been 0.15 and 0.09 x 10^{-6} curie/gm, respectively.

Condenser tube deposits in the lowest section of the tube bank (just above the hotwell) varied in color from dark reddish-brown to black. The layer was very thin and adherent, and appeared to be a discoloration film rather than a deposit. Scraping with a knife gave no sample.

An appreciable amount of deposit was present on the stainless steel shields on the top row of condenser tubes. Designating the two center sections of the condenser directly below the steam inlet as B and C, and the two end sections as A and D, the deposits (upper row of tubes in each case) were light brown in color and dull in appearance

(powdery type) in Sections A and D. They were not adherent and could be removed by wiping with a cloth. The deposits in Sections B and C were different, both in color and appearance. Most of the surface had a burnished copper or brass appearance, and behaved more like a scale. It could be scraped off, but not wiped off with a cloth. When the undersides of the shields were examined, the surface in contact with the aluminum showed occasional white spots, assumed to be aluminum oxide. No pitting of the aluminum was observed.

Deposit samples were taken from ten of the shields by scraping. Appearance, weights of samples and areas are given in Table 5.8. It will be noted that there is no good correlation between the amount of deposit and location or color. Except for one high and one low value, the range of densities was quite narrow and averaged 0.89 mg/in.^{2} (0.133 mg/cm^2).

Table 5.8

DEPOSITS FROM STEAM SIDE OF CONDENSER

Sample No.	Location in Condenser[a]			Color of Deposit	Amount of Deposit		
	Section	Bank[b]	Row[c]		Area Sampled (in.^{2})	Amount (gm)	Concentration (mg/in.^{2})
1	A	1	2	Burnished brass	21	0.0154	0.74
2	A	2	5	Dull light red-brown	11.3	0.0093	0.82
3	A	3	6	Dull light red-brown	22	0.0199	0.91
4	A	4	4	Half dull brown, half burnished brass	10	0.0044	0.44
5	B	1	5	Burnished brass	20	0.0230	1.15
6	B	2	8	Burnished brass	11.3	0.0083	0.73
7	B	4	4	Dull light red-brown	16.5	0.0127	0.77
8	C	2	6	Dull light red-brown	22	0.0166	0.76
9	D	1	2	Dull light red-brown	18	0.0182	0.01
10	D	3	6	Burnished brass	12	0.0192	1.6
							Avg. 0.89

Note: Deposit samples scraped off stainless steel shields

[a]All shields from top row of tubes.

[b]Counted from north side of condenser.

[c]Counted from south side of each bank.

Spectrographic analyses of individual and composite samples of the deposits are given in Table 5.9.

Table 5.9

SPECTROGRAPHIC ANALYSES OF DEPOSITS
FROM STEAM SIDE OF CONDENSER

Element	Condenser Tube Shield Samples			
	Dull Light Red-brown Color		Burnished Brass Appearance	
	Single Shield %	Composite of Four Shields %	Single Shield %	Composite of Four Shields %
Fe	VS[a]	VS	VS	VS
Al	1.5	3	2	2
Ni	1.5	3	3	4
Cr	0.02	0.15	0.02	0.2
Cu	0.1	0.3	0.1	0.2
Pb	1.5	1.5	2	3
Na	0.08	0.7	0.08	0.7
K	0.05	0.15	0.03	0.2
Ca	0.08	0.4	0.02	0.3
B	<0.1	0.2	<0.1	0.2

[a]VS - very strong, major constituent

X-ray diffraction examination showed the iron to be present largely as gamma $Fe_2O_3 \cdot H_2O$. The presence of iron is attributed to erosion-corrosion of the iron support members by the high-velocity steam. The high oxygen content in the steam accounts for the ferric rather than ferrous oxide which would normally be observed under low oxygen conditions in a condenser of this type.

f. Turbine. During the June-July, 1957 shutdown, the exhaust end of the turbine casing and last row of turbine blades were inspected.(165) The interior surface of the turbine casing, which is Kanigen nickel plated, was free of deposits and the plating appeared to be in good condition. The last row of blades was clean and the trailing edges of the blades showed no sign of erosion.

In December 1957 a more thorough examination was made of the turbine.(167) Activity level readings taken ten days after shutdown gave the following results in mr/hr:

No. 1 HP steam seal	2.0
First row blades	0.2
Remainder of blading	0.2 or lower
Admission valve stems	3.0
Nozzle inlets	5.0
Inlet side of trip throttle valve	2.0

The turbine in general appeared to be in excellent condition. No detectable wear or erosion could be noted on the blading or diaphragms. The blading was clean with only a small amount of deposit or discoloration noted. There was a small amount of greenish deposit on the No. 1 HP steam seal retainers and some also on top of the blade shrouds where the blade ends were peened.

There was some rust on the rotor at both the HP and LP seals in the air pressure and air vacuum regions. When this rust was removed, only very slight pitting was present. The nickel plating, covering in general everything but the rotor, was still in good condition.

For activity analyses,(167) samples were taken from the HP steam end gland, from first, fourth, ninth, and thirteenth rows of turbine blades, from the condenser, and from the steam pipe just before the steam throttle valve. The samples were removed by using a bearing scraper and actually removing metal plus deposited activity. The gross gamma activity from the samples was so low that they had to be analyzed in an iron room where whole-body gamma spectra are made on humans. This work was done by C. E. Miller of the Radiological Physics Division. The spectrum obtained from all samples was essentially that of Co^{58}.

The percentages of the long-lived activities found on the turbine at the time of shutdown was estimated to be as follows:

Co^{58}	92%
Ba^{140}-La^{140}	8%
Co^{60}-Cr^{51}-Fe^{59}	Trace

A rough calculation of the concentration of the Co^{58} activity at the various points sampled is given in Table 5.10.

Table 5.10

Co^{58} CONCENTRATION FOUND IN TURBINE

	Microcurie/in.^{2}
Steam end gland	108×10^{-4}
First row of blading	5.23×10^{-4}
Fifth row of blading	46×10^{-4}
Ninth row of blading	28.8×10^{-4}
Condenser tubes	0.206×10^{-4}

The observed activities can be explained as follows: The Co^{58}, Co^{60}, Cr^{51}, and Fe^{59} all exist in the reactor water. There is a known decontamination factor of about 5×10^3 between the reactor water and the steam for solid material. It has been observed that Co^{58} is the major long-lived gamma-emitting isotope in reactor water, and that there are smaller amounts of Cr^{51}, Co^{60}, and Fe^{59}. Hence, it is not impossible that these activities were deposited in the turbine by carryover with the steam. The Ba^{140}-La^{140} are brought to the steam system by Xe^{140} through the following chain:

$$Xe^{140} \xrightarrow[t_{1/2} = 16\ sec]{} Cs^{140} \xrightarrow[t_{1/2} = 66\ sec]{} Ba^{140} \xrightarrow[t_{1/2} = 12.8\ days]{} La^{140} \xrightarrow[t_{1/2} = 40.2\ hr]{} Ce^{140}$$

The short-lived Xe^{140}, being a gas, is stripped from the reactor water by the boiling and, on its way through the steam system, decays to Cs^{140}, which can then deposit on a surface and decay to Ba^{140}. This mechanism only works for gases short-lived enough to decay in the steam system before being removed by the air ejectors on the main condenser.

In May 1958 mechanical failure of a turbine blade(94) necessitated opening the casing and removing the diaphragms (Kanigen plated) and rotors (not Kanigen plated). A survey meter examination about five days after reactor shutdown showed the maximum detectable radioactivity level to be 2 mr/hr at 2 in.

Detailed microscopic examination of the surface of the (rotor) blades showed no evidence of stress corrosion, general corrosion, intergranular attack or other types of surface attack, and the general surface condition was found to be similar to other blades returned from service under standard steam conditions. There is no evidence that boiling water reactor steam has had any adverse effect on the blade material.

The surfaces of the blades were covered with a thin, brown-colored deposit. A green deposit was also observed on the surface on the blades, just under the shroud.

Radioactivity of the blades was very low. The beta plus gamma count did not exceed twice that of the background, as measured with a Geiger counter survey meter.

The brown deposit on the blades was a soft, nonmagnetic, amorphous solid consisting of major amounts of iron and nickel, and very small amounts of chromium, copper, lead, and zinc. The green deposit was also soft and nonmagnetic. X-ray diffraction patterns of the green deposit were similar, but not identical with those of the nickel hydroxides. Small amounts of iron and copper were also present in the green deposit.

g. Recirculation Nozzles and Control Rod Bushings. By spring of 1958, the activity in the subreactor room had built up to the extent that the general radiation level was about 500 mr/hr at head height on the control rod drive motor platform.(168)

Most of the activity came from three of the four six-inch diameter nozzles provided for forced circulation, which, pending their eventual use, had been capped. The water in the three nozzles showing high activity had been stagnant. That in the fourth nozzle had been circulating, because this nozzle was connected to the purification system and startup heater. The surface activity level at this nozzle was only 300 mr/hr, or essentially background.

The nine control rod bushings were also very active, with the center rod bushing having the maximum of 65 r/hr at contact.

The buildup of activity in these nozzles and bushings was due to the deposition of suspended corrosion products or crud in these stagnant areas. When the deposits were removed from the nozzles by a flushing procedure and from the bushings by disassembly, the activity level dropped from 50 r/hr to 4 r/hr at the nozzle and from 65 r at the control rod bushing to 2 r/hr.

About a "fistful" of crud was removed from each of the three stagnant nozzles. Both spectrographic and wet chemical analytical results on samples of this material are given in the first two columns of Table 5.11. Results of a wet chemical analysis made later are given in the third column. The predominant activity found in the crud was Co^{58}.

Table 5.11

ANALYTICAL RESULTS ON DEPOSIT FROM RECIRCULATING NOZZLE

Element	Spectrographic (%) 5-28-58	Wet Chemical (%)	
		5-28-58	12-22-58
Ni	20	4.5	11.3
Fe	15	7.7	14.0
Mn	0.4	-	-
Cr	0.15	-	-
Mg	0.04	-	-
Al	VS(a)	35(b)	26.3
Si	-	<1	

(a) Very strong, predominant.

(b) Aluminum determined on a separate sample

There are two observations that can be made on the results in this table:

Due to the limitation of the spectrographic analysis in accuracy to a factor of two, an incorrect impression is given as to the relative amounts of iron and nickel that are in the deposit.

Although the proportions of nickel, iron and aluminum are of the same order as in the two wet chemical analyses, the actual percentages are different, showing that the two samples do not have the same composition.

After final shutdown for 100-Mw conversion in July, 1959, the recirculation nozzles were cut off. The appearance of the corrosion product deposit in one of them is shown in Fig. 5.3.

Fig. 5.3

Corrosion Product Deposit in Recirculation Nozzle

The crud accumulating in the control rod bushings not only resulted in a buildup of activity in this area, but also caused mechanical interference with the movement of the rod. On one occasion it prevented the rod from going to its complete "in" position by about 2 in. and made necessary some changes in the design of the bushing.(169)

At several times since startup of the reactor, difficulties with the crud in the bushings occurred, and on some occasions samples of the deposits were taken for analysis. Some of the results of the spectrographic and wet chemical analyses are given in Table 5.12.

Table 5.12

ANALYSES OF DEPOSITS FROM CONTROL ROD BUSHINGS

Element	Spectrographic			Wet Chemical, 5-28-58 %
	1-7-57, Amount(a)	3-1-57, Amount(a)	10-2-57, %(b)	
Ag	M	-	-	-
Al	M	S	0.3	35(c)
Ca	M	-	43	-
Cr	VS	S	6	-
Cu	-	W	3.0	-
Fe	VS	VS	31	5
Mg	M	-	3	-
Mn	M	M	0.9	-
Mo	MW	M	8	-
Ni	VS	S	3	13.7
Pb	M	M	0.3	-
Sr	-	-	0 3	-
Ti	MS	M	-	-
Zr	MS	M	-	-
Si	-	-	-	<1

(a)VS = Very Strong, S = Strong, M = Moderate, and W = Weak Accuracy - order of magnitude.

(b)Accuracy - factor of 2

(c)Aluminum determined on separate sample.

The results in the first two columns, being determined on a different basis than the others, cannot be precisely compared with them. They do confirm other data in showing that in the deposits examined

earlier, the amount of aluminum was relatively less than the amounts of iron and nickel, whereas about a year later the aluminum was present in greatest amount. There is no satisfactory explanation of the high proportion of calcium in column three.

A control rod bushing deposit sample taken about August 13, 1957 was subjected to radiochemical analysis for β activity, with results given in Table 5.13.

Table 5.13

RADIOCHEMICAL ANALYSIS OF DEPOSIT FROM CONTROL ROD BUSHINGS

Radioisotope	% Total β Activity	Radioisotope	% Total β Activity
Co^{58}, Co^{60}	11	Cr^{51}	0.1
Fe^{59}	4	Ce^{144}, Pr	0.15
Ni^{63}	1		
Gross β Activity: 1.1×10^6 dpm/25.4 mg			

h. Fuel Elements

(1) First Fuel Element Deposit Examination. During the July 1957 shutdown (after 1370 Mw days of operation), one fuel element, ET-5 (for position see Fig. 5.4), and two dummy elements were transferred to the fuel storage pit for examination.(170) At this time samples of the deposits on these elements were taken. Observations were made to determine the nature of the deposits (adherent or nonadherent), and samples were submitted for spectrographic and radiochemical analyses.

Three samples were taken by underwater wiping with new cellulose sponges:

External surface of end fuel plate of fuel element (upper portion).

External surface of dummy element.

Internal surface of dummy element.

(a) Type of Deposit. All three deposits were nonadherent and readily removed by a single wipe of the sponge. The deposit on the fuel plates was reddish-brown in color and the dark grey zirconium oxide film appeared intact when the deposit was wiped off (Fig. 5.5). The deposit on the external surfaces of the dummy element was greenish-blue

when observed in the reactor core; however, when the dummy was moved to the storage pit the color was much lighter, and finally when the deposit was removed it was a dirty white color. The appearance of both the external and internal surfaces of the dummy was not bright when the deposit was wiped off. This would be expected since the aluminum alloy would have formed an oxide layer before the "crud" or corrosion product layer had been deposited.

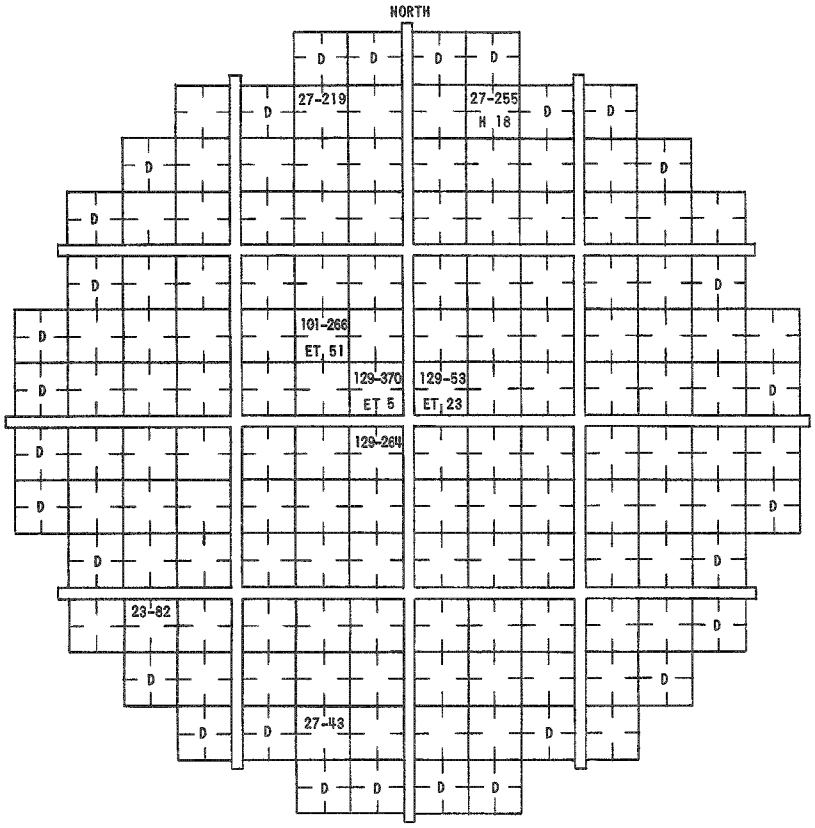

Fig. 5 4

Core Positions of Examined Fuel Elements, and Dummy Elements

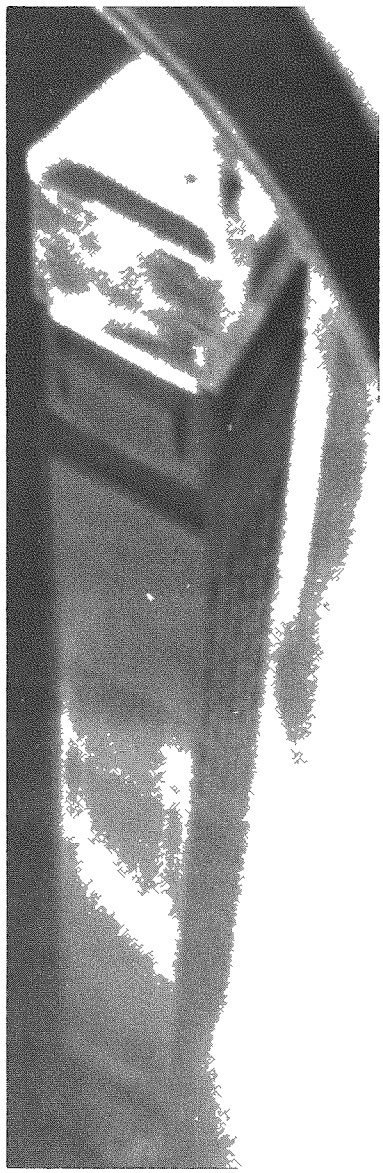

Fig 5.5

Fuel Assembly ET-5 Being Removed After 1370 Mwd Operation in EBWR

The deposits were very soft and flocculent in texture, and when washed off the sponge, appeared to be very finely divided. An attempt was made to determine the particle size of the fuel element deposit, but by the time the sample was photographed (in the electron microscope) the particles had agglomerated. Later, a sample of deposit from the external surface of the dummy element was prepared and an electron microscope photograph taken at 3100 X. Most of the particles appeared to be less than 1.5 microns in diameter. This deposit should be similar to that on the fuel element.

The physical characteristics of the deposit on the dummy elements changed after drying. When additional samples were taken later from the dummy elements, stored dry, the deposit was very adherent and had to be scraped off. Two external surfaces had a dark reddish-brown color and the other two sides had a mottled appearance, with light-colored dots which probably were the aluminum alloy corrosion products.

The amount of deposit on the fuel element could not be determined; however, that on the external and internal surfaces of the dummy element was determined. The amounts in mg/in.^{2} are given in Table 5.14. These values were determined by scraping off the deposit and are approximate figures.

Table 5.14

SPECTROGRAPHIC ANALYSES OF DEPOSITS FROM EBWR FUEL ELEMENT AND DUMMY ELEMENT

Constituents* (as elements)	Deposit from Fuel Plate of Fuel Element (%)	Deposit from External Surface of Dummy Fuel Element (%)	Deposit from Internal Surface of Dummy Fuel Element (%)
Iron	17	35	3
Nickel	14	13	16
Chromium	0.1	0.3	0.05
Aluminum	6	10	20
Copper	0.3	0.4	-
Lead	0.2	0.3	0.1
Boron	0.2	0.5	0.4
Manganese	0.2	0.3	0.04
Sodium	**	1	0.5
Potassium	**	0.1	0.1
Calcium	**	0.08	0.05
Magnesium	**	0.1	0.02
Zirconium	-	-	-
Amount of Deposit:	†	1.1 mg/in.^{2} 1.4 mg/in.^{2}	2.2 mg/in.^{2}
Color of Deposit:	Reddish-brown	Reddish-brown	Dirty white (wet) buff (dry) greenish-blue (viewed through reactor water)

*This table gives major components only - trace constituents not included.

**Sample contaminated by water from the fuel storage pit - determined values not valid.

†Sampled underwater - could not get amount of deposit per square inch.

Note: Factor of 2 accuracy. The individual metal component values do not total 100 as these values are of the metals only. The anions are not included in this analysis. Practically all of the metals were present as oxides and some of the oxides may have had water of crystallization present also.

(b) Spectrographic Analyses of Deposits. The analyses of the three deposits are given in Table 5.14. Both the fuel element deposit and the deposit from the external surface of the dummy fuel element consisted primarily of iron, nickel, and aluminum oxides in decreasing order of relative amounts present. The aluminum content of the deposit from the external surface of the aluminum dummy was higher than that from the Zircaloy clad fuel, as would be expected. The nickel content of all the deposits was considerably higher than would be expected, and is due to two factors:

(1) In the insoluble corrosion products of stainless steel, the nickel content is much higher than the chromium content because chromium is more soluble.

(2) The nickel pickup in the steam piping and turbine by the condensate must be quite high, as indicated by erosion of diaphragm nozzles (see Sec. 4).

The deposit from the internal surface of the dummy was quite different from the other two deposits, and the low iron content might be expected since the water in the dummies was stagnant and the deposit primarily due to the corrosion products of the aluminum alloy M-388. The high nickel content of this deposit is of significance in that the ratio of the aluminum to nickel in the deposit is not the same as in the alloy (1% Ni-99% Al).

(c) Radiochemical Analyses of Deposits. Only long-lived activities were determined, since the reactor had been shut down in June and samples for analyses were not taken until July.

A preliminary gamma-ray spectrometer analysis made on the deposit from the internal surface of the dummy element showed its major activities to be due to Co^{58} and Co^{60}, which are products of nuclear reactions to be given in Table 5.16. The measured activity was 91×10^{-6} curie/gm of Co^{58} and 3.5×10^{-6} curie/gm of Co^{60}.

The results of the analysis for beta activity are given in Table 5.15. They confirm the gamma analysis, indicating that the major activity was due to Co^{58} and Co^{60}.

Table 5.15

RADIOCHEMICAL ANALYSES OF FUEL ELEMENT AND DUMMY FUEL ELEMENT DEPOSITS

Source of Deposit	% of Total β Activity					Gross β Activity	Uranium
	$Co^{58,60}$	Fe^{59}	Ni^{63}	Cr^{51}	Ce^{144} and Pr		
Fuel Plate	72*	3	< 0.5	< 0.1	< 0.08	9.2×10^6 dpm/entire sample	-
Internal Surface of Dummy Fuel Element	49	3	< 0.5	< 0.1	< 0.14	4×10^6 dpm/59 mg	7 ± 3.5 ppm

*Examination by means of a gamma-ray spectrometer showed that the ratio of Co^{58} to Co^{60} was approximately 8 to 1 on October 7, 1957.

(d) General Comments. The amount of deposit present on the fuel elements was more than had been expected since the quality of the reactor water has been maintained at less than one-micromho conductivity during most of the reactor operation.

In view of the results of films examined later, it should be noted that at this time the external surface films on fuel element and dummy appeared to be nonadherent, and that they were composed largely of oxides of iron, nickel, and aluminum, in relative amounts decreasing in that order.

There was considerable speculation about having an accumulation of crud in the bottom of the reactor vessel. During the July shutdown, when the reactor was open, an attempt was made to determine whether there was a layer of loose deposit at the bottom. A probe (28 ft long) was put down through one of the outer dummy holes and water drawn up with a vacuum system. No deposit was drawn up. It could be that the probe which was quite flexible ($\frac{1}{4}$ in. stainless steel tubing) did not get past some of the plates located below the grid support plate.

(2) Second Fuel Element Deposit Examination. Examination of the EBWR core in January 1958, after about a year of operation, showed the presence of considerable scale on fuel element ET-5. This was evident by the flaking off of scale from it as it was lifted out of the core toward the surface of the water in the reactor for observation. Large flakes of scale could be seen floating away from the external plate and a relatively large area, estimated to be about 20 in.^{2}, in the highest heat flux zone from which the scale had flaked away could be observed (Fig. 5.6). Large flakes of scale could be seen resting on top of the assemblies still in the core. Attempts to remove more scale from this plate, around this area and elsewhere, and from the other (opposite) external plate by scraping with a piece of wood on the end

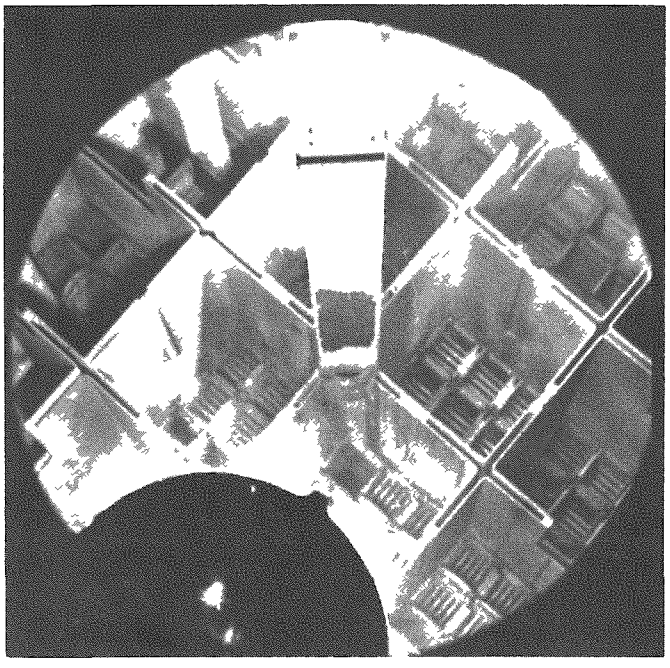

Fig. 5.6

Fuel Assembly ET-5, After One Year of Operation

of a long piece of pipe were unsuccessful. A piece of the loose scale was fished out and measured with a micrometer. It was found to be 0.003 in. in thickness. Spectrographic analysis of the scale showed 67% aluminum, 25% nickel, and 8% iron. X-ray analysis showed it to be at least 50% boehmite (α $Al_2O_3 \cdot H_2O$). The x-ray diffraction pattern was identical to that observed from samples of the corrosion layer on the aluminum-nickel dummy fuel elements. The aluminum is believed to have come from corrosion of the aluminum-1% nickel dummy fuel elements, the nickel largely from the aluminum-1% nickel, the stainless steel, and possibly from the Kanigen nickel plate on the turbine and piping, and the iron from the stainless steel corrosion products.

The long-lived activities found[171] on a sample of crud removed from an EBWR fuel plate during the Janury, 1958, shutdown along with their probable sources are given in Table 5.16.

Table 5.16

ACTIVITIES IN EBWR FUEL ELEMENT DEPOSIT

Nuclide	Half Life	Crud, dpm/mg	Probable Nuclear Reaction
Co^{58}	71 d	1.43×10^7	Ni^{58} (n,p) Co^{58}
Co^{60}	5.3 yr	1.66×10^6	Co^{59} (n,γ) Co^{60} Ni^{60} (n,p) Co^{60}
Fe^{59}	45 d	2.43×10^5	Fe^{58} (n,γ) Fe^{59}
Mn^{54}	300 d	2.08×10^5	Fe^{54} (n,p) Mn^{54}

(3) Third Fuel Element Deposit Examination. In January 1958, core loading No. 46 was changed to core loading No. 47. This involved replacing two natural uranium fuel elements, T23 and T21, in central positions 129-53 and 129-264, respectively, with enriched fuel elements ET18 and ET46 from core peripheral locations 27-219 and 23-82, respectively.

Fuel Element T-23 removed from position 129-53 was submitted to the Metallurgy Division for destructive examination. Preliminary findings[172] indicated a rather nonadherent scale; however (in contrast with the scale on ET-5 described above), no spalling was observed. Spectrographic analysis (factor of 2 accuracy) indicated major constituents as follows:

Aluminum	18%
Nickel	12%
Iron	6%

X-ray diffraction data indicated the scale was largely boehmite, and there was a second phase present, resembling aluminum-silicon monohydrate.

Although specific pre-irradiation thickness measurements on Plate 606 (from T-23) were not available, averaged data indicate that it increased by 4-5 mils maximum. This increase includes the sum of any volume increase plus corrosion product deposition during in-pile operation.(84)

After cutting Plate No. 606 into coupons, samples from varied flux regions were returned to the Reactor Engineering Division for corrosion product scale examination. Attempts were made to remove the scale by means of alternate oxalic acid-nitric acid treatments as used by WAPD(173) in descaling Zircaloy-clad specimens. Satisfactory results were not obtained, due, it is believed, to the high aluminum oxide content of the EBWR fuel element deposits. When this descaling treatment was supplemented by mechanical scraping, chipping, and brushing, the samples finally appeared to be free from scale.

In Fig. 5.7, the thickness of scale (mg/cm^2) as determined by weight loss was plotted against distance of the sample from the bottom of the plate.(174) In the same figure the per cent of maximum flux, as determined,(84) is plotted against distance from the bottom of the plate. There is quite good correlation between maximum scale thickness and maximum scale flux or burnup.

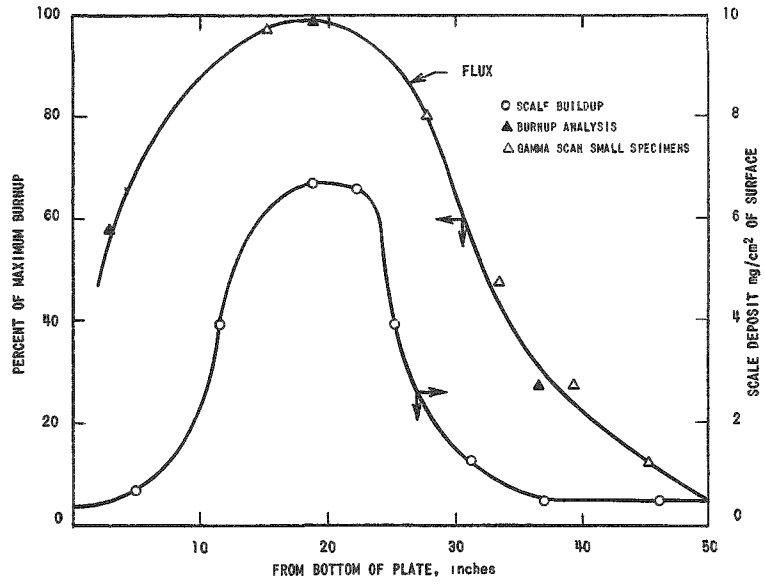

Fig. 5.7

Relation between Scale Buildup and Burnup After Operation for About One Year

(4) Fourth Fuel Element Deposit Examination. Fuel element ET-51 occupied position 101-266, next to 129-370 and diagonally second from the central control rod (see Fig. 5.4) from startup of the reactor in December 1956 until April 20, 1959, when it was removed. According to a flux survey made on loading No. 46 in February 1958, this position represented the highest flux on the diagonal radius in the reactor.(175)

In April 1959, while making a flux plot at 40 Mw, a cobalt wire became stuck in element ET-51 and could not be removed. Because of this, and because of the interest in destructively examining a fuel element with maximum burnup, the decision was made to remove ET-51 for examination. When examined by the Metallurgy Division, this element showed areas where scale had spalled off. In the course of cutting up the element, a considerable amount of scale flaked off.(84)

The thickness of the scale from the general zone of high heat flux was determined to be 0.0046 in. by measurement of photomicrographs of the scale in cross section. The thickness as measured with a micrometer was 0.005 in.,* based on several measurements.(176) Due to surface roughness, these values are larger than those established from photomicrographs.

The density of the scale, determined from weight measurements and volume calculation, was 2.5 gm/cm^3. Pieces of scale tested were found to be attracted by a magnet. Results of spectrographic and wet chemical analyses are given in Table 5.17. X-ray diffraction measurements indicated the presence of boehmite and of a second, unidentified phase.

Table 5.17

SUMMARY OF FUEL ELEMENT DEPOSIT ANALYSES

Fuel Element No.	Date of Sample	Type of Analysis	Al	B	Ca	Cr	Cu	Fe	K	Mg	Mn	Na	Ni	Pb	Si
ET-5	7-8-57	Spectrographic[a]	5	0.2	9	0.1	0.3	15	1.5	0.8	0.2	2	12	0.2	
ET-5	1-18-58	Spectrographic[a]	VS	1	0.2	0.5	2	10		0.3			25	0.1	
ET-5	1-18-58	Spectrographic[a]	VS		0.15	0.4		7		0.3			25		
ET-5	1-18-58	Wet chemical	35[b]					6.2					13.6		<1
Unknown	12-4-58	Spectrographic[a]	VS		0.04	0.2		17		0.03	0.2		14		
T-23	-	Spectrographic[a]	18					6					12		
ET-51	6-10-59	Spectrographic[a]	>50	0.1	0.003	0.04	1	6		0.2			16		
ET-51	6-10-59	Wet chemical	36.3					373					10.6		0.8

In per cent.
[a]Factor of 2 accuracy.
[b]Aluminum determined on a separate sample.

The most complete analytical information on the composition of the scale is given in Table 5.18.

*Scale specimens collected from the bottom of the reactor vessel after shutdown ranged up to 0.008 in. in thickness.

Table 5.18

ANALYSIS AND CALCULATED COMPOSITION OF EBWR FUEL ELEMENT SCALE

Element	Analysis (wt %)	Assumed Compound	X-Ray Identification	Calculated (wt %)
Al	36.3	$Al_2O_3 \cdot H_2O$	Boehmite	80.6
Ni	10.6	NiO	Not identified	12.6
Fe	3.9	Fe_3O_4	Not identified	5.1
Si	0.8	SiO_2	Not identified	1.6
			Total	99.9

(5) Visual Inspection of EBWR Fuel Assemblies. In July 1959, the fuel was removed from the reactor in preparation for 100 Mw conversion. Many of the assemblies showed patches where scale had flaked off, and the water was murky from suspended corrosion products. No further examination was made at that time. When the fuel was reloaded into the reactor (January 29 to March 3, 1960), each fuel assembly was visually inspected[177] as it was raised from the fuel storage pit into the transfer coffin. The purpose of this inspection was to determine how many of the elements exhibited flaking of scale on the two exposed plates; to note the position of the descale area; and to estimate the relative area and thickness of the scale.

Due to the high radiation level, and the light refraction in the water, the estimates are very rough. The core loading comprised 114 assemblies; 93 showed some degree of descaling, 20 showed none, and 1 was not inspected. The descaled areas ranged from a few square inches to one-half the total area of the plate. Most of the descaled areas were on the lower half of the fuel plate, where the heat generation rate is believed to be higher. The thickness of the scale, as judged from the appearance of the edges of the descaled patches, increased in the direction of the core center. This supports the view that scale formation increased with burnup, as shown in Fig. 5.7. Further support is given by the observation that two elements, irradiated for about three months, showed no evidence of descaling.

i. Dummy Fuel Elements. Results of chemical analyses of the first dummy fuel element deposits have been given in Table 5.14. Results of subsequent analyses[56] are summarized in Table 5.19. A rather wide scatter is shown, particularly with respect to aluminum, iron and nickel. In most instances, deposits in dummy fuel elements have a higher proportion of aluminum relative to nickel and iron than deposits in fuel elements. This is not unexpected since the dummy fuel elements are

made of aluminum alloy. Early deposits on fuel elements, however, showed a preponderance of nickel and iron over aluminum while later deposits showed aluminum to predominate over nickel and iron.

Table 5 19

ANALYSES OF DEPOSITS FROM DUMMY FUEL ELEMENTS

Date of Sample	Location of Sample	Degree of Accuracy	Al	B	Ba	Ca	Cr	Cu	Fe	K	Li	Mg	Mn	Na	Ni	P	Pb	Sn	Zn	Zr
8-12-57	Storage Pit Water (control)[a]	(b)	1 2	1 3	0 1	65	0 1	0 6	1 2	10		4	0 2	11	1		0 7	0 1	2	0 1
8-12-57	Outside of Element	(c)	10	0 5	0 04	0 08	0 3	0 4	35	0 1		0 1	0 3	1	13		0 3			
8-29-57	Inside of Element	(c)	20	0 4		0 05	0 05		3	0 1		0 02	0 04	0 5	16	<4	0 1			
10-22-57	Inside of Element	(c)	VS	0 4		0 04	0 06	1 5	2	0 02		0 03	0 03	0 4	6		<0 1			
10-22-57	Outside of Element	(c)	VS	0 4		0 15	0 1	0 1	6	0 05		0 06	0 06	0 4	2		<0 1			
12- 4-58	Uncertain	(b)	VS			0 08	0 08	0 7	17			0 03	0 2		14					

[a] Average of 2 determinations per cent calculated from results reported as mg/ml

[b] Order of Magnitude

[c] Factor of 2

Since fuel and dummy elements, from which deposit samples had been removed, had stood for varying periods of time in the water in the fuel storage pit, a sample of this water was analyzed as a control. In most instances the amounts of the various elements in the deposits, other than iron, nickel and aluminum, corresponded roughly with the amounts present in the water. Although there appeared to be no correlation between the calcium content of the water and that of the deposits from the dummy fuel elements, there was a correlation between the high calcium in the water and the calcium in one of the fuel element deposits analyses in Table 5.17.

In December 1958, two M-388 aluminum dummy fuel assemblies which had been exposed about one year at operating temperature were removed from EBWR to the hot cell facilities of Argonne National Laboratory.

They were covered with a loose corrosion coating that varied in color from a dark brown to a medium gray.[90] Under this loose coating, there was an adherent, speckled brown coating.

A sample of the loose coating, on x-ray analysis, was found to be essentially all boehmite (α $Al_2O_3 \cdot H_2O$), with only one additional x-ray line which was not identified.

j. Pressure Vessel. In February 1959, two 3-inch nozzles were installed in the pressure vessel. To do this, it was necessary to lower the water level in the vessel to 10 ft above the core and install a

temporary platform for the workmen. Above the water level, the walls gave measured gamma readings up to 150 mr/hr (hard and soft) at 2 in. The upper surface of the steam ring gave readings up to 750 mr/hr, whereas the lower surface gave lower readings. After wiping up the loose particulate deposit with wet rags, the readings from the walls and steam ring were reduced to 25 and 150 mr/hr, respectively. The ease with which the deposited activity is removed is worthy of note.

Samples of the deposits were analyzed spectrographically and radiochemically. The results are summarized in Tables 5.20 and 5.21.[178]

Table 5.20

SPECTROGRAPHIC ANALYSES* OF WALL AND STEAM RING DEPOSITS

Element	Deposit from Wall	Deposit from Top of Steam Ring	Deposit from Bottom of Steam Ring
Al	4	16	10
Ca	6	16	16
Cr	6	1.6	2.8
Cu	1.3	1.6	1.4
Fe	50	37	39
Mg	1.3	1.1	1.4
Mn	0.6	1.1	0.6
Mo	0.6	0.2	0.1
Ni	3.8	13	2.8
Pb	25	9.2	23
Ti	0.3	0.4	0.4
Zr	0.6	0.8	0.7

*In per cent, factor of 2 accuracy, assuming no other elements present.

Table 5.21

RADIOCHEMICAL ANALYSES OF WALL AND STEAM RING DEPOSITS

	Activity (dpm/mg Fe)			
	Co^{60}	Co^{58}	Fe^{59}	Co^{58}/Co^{60}
Top of Steam Ring	3.3×10^7	1.0×10^8	5.6×10^6	3.0
Bottom of Steam Ring	2.0×10^5	8.0×10^5	2.0×10^5	4.0
Wall of Vessel	1.1×10^6	3.9×10^6	6.2×10^5	3.5

It is evident from the results that the compositions of these deposits do not correlate too well among themselves or with other deposits that have been described, except for the high content of iron and nickel. The proportions of calcium and lead are unexpected; and aluminum shows a wide variation among these deposits, but is surprisingly low.

In Table 5.21, two observations are of interest (1) the high activity in the deposit on top of the steam ring as compared to that on the bottom side or vessel walls; and (2) the ratios of 3.4 to 1 between Co^{58} and Co^{60}.

When the core was removed in July 1959 for 100 Mw conversion, the water was murky due to the amount of suspended material from fuel element deposits, stirred up or released by the removal operation. The loose crud was removed from the pressure vessel by flushing with water from a hose down through valves on control rod thimbles and recirculation nozzles provided for the occasion. A manifold system carried the slurry through a full-flow filter to a sump, and then the retention tank. The filters were changed about a dozen times during the operation. No measurements were made, but an estimate was made that the amount was "less than a cubic foot."

Some observations made[179] with reference to deposited activity in the pressure vessel during shutdown for 100 Mw modification were as follows:

A radiation survey made inside the reactor vessel with the water level at the top of the thermal shield gave readings ranging from 75 mr/hr at the vessel top to 1000 mr/hr six inches above the core shroud. The inner surface of the shock shield measured up to 1500 mr/hr at two inches.

Washing the walls in the upper part (steam zone) of the pressure vessel with wet rags four times reduced the radiation from the surface by about 50%.

Washing the steam ring with wet rags removed an estimated 70%-80% of the activity. The highest percentage of activity on the steam ring was on the upper horizontal surface as compared with the lower surface.

Washing the shock shield four times reduced the activity by only about 10%. After removing the shock shield in sections from the pressure vessel activity measured showed up to 1250 mr/hr at two inches.

Chemical cleaning (H_3PO_4 + Versene) of sections of the shock shield removed from the reactor pressure vessel failed to give a noticeable reduction in activity.

Radiochemical analysis of grinding and cutting chips from the shock shield showed the presence of only Co^{58} and Co^{60} activities. The ratio between Co^{58} and Co^{60}, calculated back to per cent total activity at time of shutdown (July 15, 1959) was roughly between 4 to 1 and 5 to 1.(180)

k. Corrosion Specimens. In Sec. 4.2.8 a corrosion experiment was described in which corrosion samples of structural materials representative of those on the turbine were placed in a holder in the 6-inch steam line just before the dryer in November 1958. During the next nineteen months, samples were removed three times for examination of the corrosion rate. At the end of these examinations the samples were examined for activity deposits. The major activities were found to be Co^{58} and Co^{60} in a ratio of about 6 to 1.(91)

l. Deposition Coupons. In connection with fuel defect studies (to be described in Sec. 6), samples representative of structural materials were placed both in the steam line ahead of the dryer and also in the condenser to study the activity deposited on them. Results of examination by the Chemical Engineering Division may be summarized as follows:(181,182)

(1) First Defect Test. Duration of the test was 18,800 Mw-hr. Samples from top tubes in the condenser were examined as to nature of deposit and associated activities; the results are summarized in Table 5.22.

Table 5.22

NATURE OF DEPOSITS AND ACTIVITIES ON SAMPLES IN CONDENSER, FIRST DEFECT TEST

Metal	Appearance	Absorbed Activity, cpm/cm^2	Major Activities
Mild Steel	Pitted and streaked	764	Co^{58} and Cu^{64}
Stainless Steel	Brown film	300	Co^{58} and Cu^{64}
Copper	Brown film	330	Co^{58} and Cu^{64}

Approximately the same amounts of Cu^{64} activity were deposited on all samples, but a much larger amount of Co^{58} was absorbed on mild steel than on either copper or stainless steel. Both wet-ground and as-received surfaces on mild steel and stainless steel samples

were tested. Results showed about 10-15% less activity on wet-ground surfaces than on as-received surfaces.

(2) Second Defect Test. During the second defect test, which had a duration of 15 weeks and 51,214 Mw-hr, samples of eight structural materials were exposed in the steam line ahead of the steam dryer, and samples of five structural materials in the condenser.

The materials in the steam line were:

Structural steel ASTM A113;
AISI Type 4140;
13% chromium steel;
Chrome-moly steel containing, (%):

Carbon	0.45 (max)
Manganese	0.70-100
Silicon	0.20-0.35
Chromium	1.0-1.5
Molybdenum	0.45-0.65
Vanadium	0.15 (min);

Low carbon steel;
13% chrome nonhardening steel;
Type X-8001 aluminum-1% nickel;
Type A-198 aluminum-1% nickel-0.1% titanium.

Examination of activities on a single channel analyzer showed that about the same amount of gamma activity was absorbed on all of the steel specimens, but about twice as much gamma activity was absorbed on the aluminum alloy specimens as on the steel specimens.

Materials in the condenser were:

Type 304 stainless steel;
Mild steel;
Copper;
Type A-198 aluminum-1% nickel-0.1% titanium;
Type X-8001 aluminum-1% nickel.

The samples were examined very shortly after reactor shutdown in order to pick up short-lived activities. The total counting rate for each specimen at two different times was determined to give a semiquantitative measure of absorption of each active nuclide. The results are tabulated in Table 5.23. These results show that about ten times

as much F^{18} activity is absorbed on aluminum as on the next greatly absorbing specimen - mild steel; and that stainless steel absorbs the least activity.

Table 5.23

ACTIVITY ON SPECIMENS IN CONDENSER DURING SECOND DEFECT TEST

Material	cpm/sample	
	After 0 hr[a]	After 72 hr[b]
Type 304 stainless steel	210	100
Mild steel	780	70
Copper	380	130
Type A-198 aluminum	6040	250
Type X-8001 aluminum	6890	180

[a]Major activity = F^{18}.

[b]Major activity = Co^{58}.

No F^{18} activity was detected on samples from the first defect test because, being short-lived, it had decayed out by the time the samples were examined.

The failure to detect Co^{60} in the condenser is believed to be due to its lower concentration as compared to Co^{58} and to the lower level of activity found in the condenser as compared to that in the steam line.

It is of particular significance that no fission product activity was reported on any of these samples.

m. Plant Activity Levels After Shutdown. In order to get an indication of the activity levels reached as a result of deposition of activity with time, a survey was made March 25, 1960 by Health Physics.(56) This survey, which was made about nine months after shutdown for 100-Mw conversion, represents long-lived activity buildup around the plant following about two and one-half years of operation. The results obtained by survey meter are given in Table 5.24. Due to changes made below the reactor for 100-Mw conversion, no readings are reported in that area.

Table 5.24

EBWR BUILDING ACTIVITY SURVEY

(March 25, 1960)

	Hard Radiation	
	mr/hr	in.
4th Level - Main Floor		
Background: 1. Immediately inside airlock	0.08	
2. Between turbine and reactor	0.2	
3. Near storage well	0.17	
Main steam header:	0.17	1
Main steam chest:	0.11	1
Exhaust hood (max):	0.14	1
3rd Level - Condenser Floor		
Background: 1. At east stairs	0.5	
2. At west stairs	0.09	
3. Opposite air ejectors	0.3	
Steam dryer and emergency cooler:	1.3	1
Main steam line from dryer (top):	0.4	1
Relief steam line from dryer (bottom):	0.3	1
Feedwater filter No. 1:	1.5	1
Feedwater filter No. 2:	9	1
Air ejector after cooler:	0.3	1
Air ejector inter cooler:	0.3	1
Desuperheater (max):	0.4	1
2nd Level - Pump Floor		
Line from purification system on reactor face:	0.5	1
Startup heater:	16	1
Shield cooling manifold:	0.4	1
Rod cooling water line under manifold:	6	1
Air ejector discharge line:	0.2	1
Air ejector flow meter:	0.2	1
Twin strainer:	0.25	1
Feedwater pump No. 1:	0.18	1
Feedwater pump No. 2:	7	2
Feedwater pump filter No. 1:	7	2
Feedwater pump filter No. 2:	7	1
Background: 1. Between feedwater pump and face of reactor:	0.3	
2. East stairwell:	0.7	
1st Level - Basement		
Retention Tank No. 1:	22	2
Retention Tank No. 2:	20	2
Background: 1. West stairwell	2	
2. East stairwell	0.9	
Prefilter No. 1:	18	2
Prefilter No. 2:	5	1
Ion exchanger No. 1:	21	2
Ion exchanger No. 2:	17	2
After filter No. 1:	32	2
After filter No. 2:	100	2
Regenerative cooler No. 1: 1. left end	100	2
2. right end	15	2
Secondary cooler No. 1: 1. left end	310	2
2. right end	180	2
Regenerative cooler No. 2: 1. left end	130	2
2. right end	20	2
Secondary cooler No. 2: 1. left end	240	2
2. right end	100	2

3. Discussion

a. Effects of Depositions. Due to the decontamination factor between reactor water and steam, significant amounts of corrosion products carrying high levels of radioactivity do not escape the reactor vessel and its components and do not produce an accessibility problem in the steam system.

Although accumulation of corrosion products did occur in the control rod bushings to the point where they interfered with operation of the rod, redesign of the bushing eliminated the problem. Similarly buildup of corrosion products and high activity levels in connecting rod thimbles and recirculation nozzles was controlled by eliminating stagnant areas; this was accomplished most simply by maintaining a flow of water through them

Deposition of corrosion products on heat transfer surfaces of fuel elements is potentially the most serious problem encountered in EBWR.[183] The buildup of scale has a pronounced effect on the operating temperature of the individual fuel plates The maximum EBWR fuel centerline temperature has been calculated[184] as 767°F (408°C). This value was based on a total heat generation rate of 100 Mw, a maximum heat flux of 485,000 Btu/(hr)(ft^2), (153 watts/cm^2), and on the assumption there was no scale deposit on the surface of the fuel plate. It is evident that the thermal resistance of any scale will increase the centerline temperature by an amount essentially equal to the temperature drop through the added resistance, assuming no changes occur in heat flux or surface temperature. It is believed[185] that as the fuel temperature approaches 900°F (482°C), growth of the uranium alloy may promote swelling or distortion of the plate. [Evidence[84] shows some growth at 400°C in EBWR]

To make a good estimation of the maximum centerline temperature to be encountered, it was necessary to measure the thermal conductivity of the scale. The method of measuring thermal conductivity and the method of calculating fuel centerline temperatures, along with the results. are described in detail in ANL-6136.[56] Briefly, the measurements were made on pieces of dry scale 0.004-0.008 in. thick (0.010 to 0.020 cm), removed from the bottom of the reactor vessel during the July 1959 shutdown. Air and other gases of known thermal conductivity were used in the apparatus to minimize contact resistance between scale and metal, and at the same time, to simulate steam-filled voids in the scale. The value obtained for the thermal conductivity of the scale was 0.44 ± 0.09 Btu/(hr)(ft)(°F), [0.0076 ± 0.0015 watts/(cm)(°C)]. The calculated minimum and maximum centerline temperatures based on this value and on certain assumptions as to scale distribution and thickness are given in Table 5.25

Table 5.25

CALCULATED MINIMUM AND MAXIMUM CENTERLINE FUEL TEMPERATURE

Assumptions Regarding Scale			Temperature			
Thickness		Number of Surfaces Covered	Min		Max	
cm	in.		°C	°F	°C	°F
0.005	0.002	one	446	834	462	864
0.010	0.004	one	478	892	501	935
0.005	0.002	both	493	919	537	998
0.010	0.004	both	577	1070	665	1229
0.020	0.008	both	746	1375	922	1692

The highest temperature obtained (922°C) resulted from using the most pessimistic values of scale thickness and thermal conductivity. It was concluded that even the most optimistic calculation, using the thinnest scale specimen recovered (0.010 cm) gives a temperature bordering on 900°F (482°C). If the scale does not flake off the fuel plates at these elevated temperatures, and if fuel alloy growth occurs at temperatures above 482°C, then growth problems can be expected to develop as EBWR begins 100 Mw operation.

b. Attempts at Descaling. The difficulties that could result from the presence of scale on the EBWR fuel elements prompted a series of descaling experiments. Mention was made earlier to the failure of simple chemical agents, i.e., dilute oxalic and nitric acids, to remove the scale from fuel plate coupons. The failure was attributed to the presence of a large percentage of Al_2O_3. More drastic chemical agents were avoided because of their possible attack on Zircaloy-2.

Heating the plates at an elevated temperature was also investigated. It was thought that the water of hydration in boehmite might be involved in the adherence of the scale, and if this water of hydration was driven off by heating, the scale might flake off or become loose enough to brush off. Accordingly, coupons from fuel element ET-51 were heated to 850°F (454°C) in an argon atmosphere for 8 hr. As evidenced by Fig. 5.8, the scale did curl and flake off. A complete fuel element (H-18) was then blanketed in helium, heated to 454°C for 25 hr and allowed to cool slowly. No descaling occurred. The Zircaloy side plates, however, buckled out an estimated $\frac{1}{8}$ in. (0.32 cm) between weld points. The buckling was attributed to difference in creep behavior between the Zircaloy side plates and the fuel plates.

Fig. 5.8

Coupon from EBWR Fuel Assembly ET-51 Heated 8 hr at 454°C (850°F) in Argon

The test element had occupied a position of low thermal flux in the reactor and consequently had achieved a burnup of about 0.1 atom %. Failure of the thermal treatment to effect descaling was attributed to the thinness of the scale, less than 0.002 in. (0.005 cm). In any event, the extent of the buckling was great enough, with existing clearance limitation, to eliminate the element from further use in the reactor.

Slurry blasting was investigated in a preliminary manner. The technique is similar to sandblasting, except that a slurry of abrasive suspended in water, instead of dry abrasive, is fed into the gun. A description of the experiments and the results have been published.(186) In brief, two types of slurries were used: one contained sharp particles used for cutting, and the other contained rounded particles used for polishing or peening. Both slurries resulted in removal of base metal as well as the scale.

Assuming that removal of some base metal could be tolerated, there are still a great many problems to be resolved before the process could be applied to EBWR fuel elements. Some of these problems are discussed in the reference.

c. Factors Responsible for Scaling Problems. The amount of transport corrosion product scale found and the possible consequence of its presence on the fuel, makes it potentially a bigger problem

in the EBWR than it has been in any other reactor. The question immediately arises: What are the factors responsible for this problem in the EBWR? The scale in EBWR is largely $Al_2O_3 \cdot H_2O$ (boehmite), mixed with iron and nickel in an unidentified form, but presumably existing as oxides, and a little silicon, present apparently as hydrated aluminum silicate. Since samples are attracted by a magnet, some magnetite is believe to be present. The relative amounts of aluminum, nickel and iron are not constant, indicating the presence of a mixture of compounds rather than a single chemical compound. Probable sources of these elements are as follows:

Element	Source
Aluminum	Dummy fuel elements, and possibly, condenser tubes
Iron	Stainless steel and, possibly, carbon steel and alloy steel in the steam system
Nickel	Al-Ni alloy, stainless steel, and, possibly, Kanigen nickel plate in steam system
Silicon	Impurities in water and in structural materials

The nature of the corrosion product deposits in the EBWR differs in several respects from deposits in pressurized water reactors. In EBWR, the deposits are difficult to filter, and are insoluble in dilute oxalic and nitric acids. By comparison, the deposits in PWR systems are easily filtered (at optimum pH), and are soluble in the aforementioned acids. The difference is attributed to the presence of Al_2O_3 in the EBWR deposits.

In the EBWR, the deposits on fuel plates build up to a high thickness and then flake off. The mechanism might be thought similar to the deposition and subsequent "crud bursts" in the PWR systems. However, a more rigorous comparison would reveal a significant distinction between the two mechanisms. The "crud bursts" seems to be a redispersal of fine particulate matter occasioned by a change in water chemistry. The redispersed particles are distributed throughout the entire system. In contrast, the flaking process in the EBWR results in the temporary entrainment of large flakes by the reactor coolant. The entrainment is temporary since the flakes are broken up to some degree by the dynamic water However, the flakes in general are relatively large pieces that settle rapidly to the bottom of the reactor. This is supported by the observation that the activity level of deposits on filters and on ion exchanger beds has never approached the level measured on deposits in the control rod bushings and forced circulation nozzles Again, the predominant constituent of the flaked-off scale is Al_2O_3 (as boehmite). The high radioactivity level of the scale results from the $Al_2O_3 \cdot H_2O$ acting as a carrier for the iron, nickel, cobalt, etc. codepositing with them on the surface of the fuel plate, and setting up favorable conditions for maximum neutron activation.

The assumption that aluminum is responsible for the nature of the deposits in EBWR gives rise to the question: Why was this problem not experienced in BORAX and in ALPR where aluminum-clad fuel was used and, hence, more aluminum was present? Five factors are offered in explanation:

(1) The ratio of aluminum surface to water volume was higher in BORAX (estimated at 250-300 cm^2/liter), than in the EBWR (27.3 cm^2/liter). This would tend to lower the corrosion rate of aluminum in BORAX.

(2) The pH was maintained at a lower value in BORAX and ALPR, than in EBWR.

(3) In EBWR, the deposition of Al_2O_3 on the fuel elements removed Al_2O_3 from the water. In essence, this acted to refresh the water and, hence, promote further corrosion of the aluminum. The effect is similar to that obtained by refreshment of water through ion exchange operation.[144]

Factors (1) to (3) represent conditions that are conducive to a higher corrosion rate for aluminum in EBWR than in BORAX or ALPR. Unfortunately, data are not available for comparing corrosion rates in EBWR with those in BORAX or ALPR. A tentative corrosion rate of 0.003 in. (0.0076 cm)/yr has been estimated from samples representative of dummy fuel elements present in EBWR during the first year of operation. Analyses of the corrosion deposits showed less aluminum content during this period than observed during the later preconversion analyses.

(4) In BORAX the major core materials were aluminum and stainless steel. In the EBWR core both aluminum and stainless steel were present, but the surface area of Zircaloy fuel cladding was greater than either of the others. Early ANL corrosion studies in the Hanford in-pile loop[155] indicated heavier deposits of iron oxide on zirconium than on stainless steel. Other instances of selective deposition of corrosion products or activated corrosion products were noted in APPR[159] and EBWR.[56] If this is an example of selective adsorption, it is a common phenomenon and may be greatly affected by radiation.

Another factor that may be involved in the relationship between the Zircaloy and the Al_2O_3 deposited on it is the poor bond between them, particularly when affected by buildup of film thickness, and temperature changes during heating and cooling. Under certain conditions the weakness of the bond facilitates the flaking off of the scale. The black appearance of the fuel plate after the scale has flaked off is evidence that the weak bond is between the scale and the zirconium oxide, rather than between the scale and the Zircaloy.

Evidence that the flaking off of scale can result from the heating-cooling cycle was obtained the first time flaking off was observed. The reactor had cooled before the head was removed. As the fuel element was lifted out of the core, a large piece of scale was observed to loosen, detach, and float away. Had this piece of scale flaked off during reactor operation, the turbulent boiling water would have broken the flake into many small pieces.

(5) Radiation and heat fluxes were higher in the EBWR than in BORAX or ALPR. Shortly after the scale buildup and flaking off was observed in EBWR, an attempt was made to reproduce the phenomenon with heat transfer in the absence of radiation. The facility used was a radio-frequency induction-heated, harp-shaped stainless steel boiler.(187) A cold finger condenser was installed in the downcomer section to facilitate recirculation of the condensed steam. The heat transfer surface was a Zircaloy-2 jacket fitted closely around the alloy steel thimble containing the induction heating coil. Demineralized water, to which several grams of high-purity boehmite were added, was used in the boiler. The experiment ran for two weeks at 550°F (288°C), with about 500,000 Btu/(hr)(ft^2), (82 watts/cm^2) through the heat transfer surface. The very thin deposit produced was not typical of the scale observed in EBWR. The failure of this attempt to reproduce the scale buildup may be attributed to the absence of radiation; however, owing to the difficulties in reproducing all factors in a reactor environment, no definite conclusions could be drawn.

One distinction between in-pile and out-of-pile systems is the form taken by the Al_2O_3 as it deposits out of the water. Radiation effects can be expected to play a part in determining whether crystals or colloidal particles are formed. Out-of-pile loops at ANL in which aluminum-nickel alloys were tested over long periods of time were characterized by the presence of the needle crystals of aluminum oxide. The oxide was identified as alpha and beta $Al_2O_3 \cdot H_2O$ by x-ray diffraction. The crystals were typical of those grown from saturated solutions, and not deposits formed from suspended colloids.(114)

On the other hand, samples of deposits from EBWR, such as those obtained from the purification filters, top of ion exchanger bed, and millipore test filters,appeared to be largely colloidal in nature. This was supported by their visual appearance in an electron microscope and effect of buildup on pressure drop. Analyses of all samples showed high percentages of aluminum. X-ray diffraction examination gave the usual report: boehmite, with an unidentified second phase. Feedwater filter deposits (where radiation effects were of minor significance) showed no aluminum. This would indicate that either there was no aluminum corrosion product from the condenser tubes in the water, or if present, the product existed in solution not as colloidal or particulate matter.

In out-of-pile loop experiments, where pH has ranged from pH = 5 to pH = 9, crystalline alumina has been predominant. In EBWR primary water, where pH has averaged close to pH = 7.0, the alumina has been largely colloidal. These observations suggest that radiation effects may be involved in the transformation of soluble alumina (after nucleate-induced crystallization), to a colloidal form, as well as in the deposition of the colloidal particles.

d. Conclusions. The corrosion product transport problem in the EBWR results essentially from (1) introduction of aluminum oxide into the water by corrosion of the M-388 (Al-1% nickel) dummy fuel elements; and (2) deposition of the aluminum oxide on the Zircaloy-2 clad fuel elements as a result of radiation, (3) the Al_2O_3 acting as a carrier for Fe and Ni, supporting them on the fuel element for maximum neutron activation.

The extent of the problem is aggravated by factors tending to increase aluminum corrosion: (1) low surface to volume of water ratio; (2) neutral pH; and (3) a water refreshing effect due to removal of aluminum oxide from the water by deposition on the fuel plates. One important factor is the nature of the bond between the boehmite scale and the oxide film on the Zircaloy-2. A weak bond facilitates flaking of the scale after buildup and, as mentioned earlier, gives rise to accessibility problems.

Removal of the aluminum dummy elements is expected to reduce or eliminate further buildup of boehmite scale in EBWR during 100-Mw operation.

The amount of scale still present on the fuel elements could markedly shorten the life of the core through damage promoted by excessive fuel temperatures. Since no method of cleaning the elements appears feasible at this time, the self-descaling process represents the only mechanism operating in the interest of an extended core lifetime.

6. RADIOACTIVITY

6.1. Introduction

This section is compiled from unclassified reports of radioactivity investigations carried out on operating boiling water reactors. In contrast to Sec. 5 where the emphasis was on radioactivity due to neutron activation of corrosion products, the emphasis in Sec. 6 is on other types of radioactivity. Radioactivities of primary interest in Sec. 6 are those induced in water components (oxygen) and those due to fission products. Since the distinction is arbitrary, there is an overlap when the investigator reported radioactivity findings regardless of source. In such cases corrosion product activities are included with other activities in Sec. 6 if the primary interest is coolant radioactivity rather than some other attribute of corrosion products.

6.2. BORAX-III

1. Early Investigations

An early report(188) stated that the radioactivity of the steam in BORAX-III was principally N^{16}. The following dosage values for the radioactivity of the steam were characteristic: on the surface of a 6-inch line carrying 290 psi steam, 100 mr/hr; on the surface of the turbine casing 20 mr/hr; on the surface of the condenser hotwell, when the hotwell was filled with water, 150 mr/hr. These activities on shutdown of the plant died out to negligible values except for the hotwell where there was some longer-lived activity in the water.

The reactor water had an activity of 390 microcuries per liter. More than 0.8 of this radioactivity was due to Na^{24}. Because of the relatively large activity due to sodium, the plant was examined to determine the source of sodium. Two possible sources were identified.* The demineralizer which supplied make-up water to the plant produced water of about 1 ppm sodium. This was much too high for such a water supply. Also, there was evidence of some leakage in the condenser tubes. The cooling water for the condenser was raw well water having a very high sodium content. Rather small leaks in the condenser would supply enough raw water to account for the sodium activity in the reactor water.

The gases removed from the condenser by the steam ejectors were radioactive. The principal activity was short-lived N^{16}. There was, however, in this activity a component which was identified as A^{41}. Make-up water supplied to the reactor was not deaerated and it was the argon in this air which was the source of the radioactive A^{41}. The gas

*Apparently the investigators were not aware of the significance of the Al^{27} (n,α) Na^{24} reaction.

withdrawn from the condenser by the steam injector contained 1.4 microcuries per liter of A^{41}. The total A^{41} vented to the atmosphere per day was only 240 millicuries.

Later observations on N^{16} activity in BORAX-III(189) indicated that the N^{16} activity was present not only as gaseous N_2 but also as a compound such as NO or NO_2. This was deduced from effects of added base such as KOH which could react with acid compounds, or use of anion exchange resins which could react with anionic forms of N^{16}. Equilibrium of these various forms between water and steam would then determine the N^{16} radiation level in the steam system.

2. Radioactive Carryover

An outstanding difference between boiling water reactors and pressurized water reactors results from the decontamination factor introduced by the boiling process. This phase change, from water to steam, constitutes a separation process between volatile and non-volatile materials in the water. From a practical viewpoint, however, the separation process is not complete due to the carryover of water droplets with the steam. These water droplets carry dissolved and suspended solids present in the water. The magnitude of this carryover problem, particularly with respect to radioactivity, has been a matter of concern since the beginning of the boiling water reactor concept. Theoretical calculation was encouraging(190,191) but experimental verification was desired, and this was accomplished in 1957.(192) Preliminary out-of-pile tests, on a small laboratory boiling test unit, and on a 600 psig loop, using Cs^{137} as a tracer indicated that decontamination factors of 1×10^4 to 1×10^5 are possible at steam flow rates and heat fluxes comparable to reactor operation.

3. Entrainment Measurements

Measurements of entrainment were made on the BORAX-III reactor.(192) The activities carried by the steam and the condensate were sampled and compared to the activities in the reactor water. Steam samples were removed at isokinetic rates, throttled to about atmospheric pressure, and condensed. Care was taken to prevent knockout of moisture in the sampling process. The reactor water sample was obtained directly from a continuously circulating loop, run through a heat exchanger and throttled to atmospheric pressure. No flashing of the water was permitted.

During the test period the reactor was operated for about three days at each of four different power levels ranging from 4 to 14 Mw.

Samples were removed at approximately 8- to 12-hour intervals, evaporated and counted in a beta-gamma proportional counter.

The reactor water was continuously deionized and varied in specific resistance between 5×10^5 and 2×10^5 ohm-cm. It was maintained at a pH of 5 to 6 during the tests. The activation products dissolved in the water were derived from natural impurities, from corrosion products of the reactor and steam system, and from dissolved gases present in the water. The activity in the steam and condensate came from reactor water droplets carried as entrainment, and from volatile activation products. These were continually being swept out of the reactor water in the boiling process. To differentiate droplet entrainment from the carry-over of volatile activation products, the decay schemes of the reactor water, the steam, and the condensate were studied. The decay curves for the reactor water samples (log of activity vs time) exhibited considerable curvature for about the first twenty hours of decay. However, in the interval of 20 to 30 hours decay, the principal activity appeared to be due to 15-hour Na^{24}. The decay curves for the steam and condensate showed a similar, but not identical, decay scheme as a result of partition of volatiles between the reactor water and condensate. After some 20 hours decay of the steam and condensate samples, the rates of decay were constant with slopes characteristic of Na^{24}. Therefore, a decay interval between 20 to 30 hours was chosen as that representative of the activity associated with decontamination factors based on droplet entrainment.

Figure 6.1 shows a semilog plot of a set of data obtained at the 4-Mw operating level. Although the steam and condensate decay curves show similar curvature, the marked difference in the 1- to 20-hour decay rates between the reactor water and the condensate is readily apparent. However, after about 20 hours decay all these curves approach the slope of 15-hour Na^{24}. Figure 6.2 shows a semilog plot of a set of data obtained at the 14-Mw operating level. The decay range from 20 to 80 hours is covered. In the interval of 20 to 50 hours, the decay rates show half lives of about 15 hours. After about 50 hours decay, the slope begins to change so that the steam and condensate appear to decay at a slower rate than the reactor water. The presence of volatile products which are carried out of the reactor water with the steam is considered the principal mechanism for the differing decay rates. It is significant from the point of view of operation that at the time of sampling the condensed steam showed a higher activity than the reactor water. The activity in the steam rapidly decayed with about a 7-second half life indicative of N^{16}. Radiation survey instruments were used in this test.

Table 6.1 is a list of observed radioactive nuclides in the reactor water. The presence of Ba^{140}, Ce^{141}, and Ce^{144} which are daughters of the volatile fission products Xe^{140}, Xe^{141}, and Xe^{144}, respectively, are examples of how longer-lived activities could contribute to the differing decay rates of the overhead steam and the reactor water. The presence of fission products in the reactor water appeared to be the result of very slow leakage through the fuel element cladding.*

*Subsequent experience by other investigators indicates that the Al cladding may have picked up U from rolls used to roll fuel alloy.

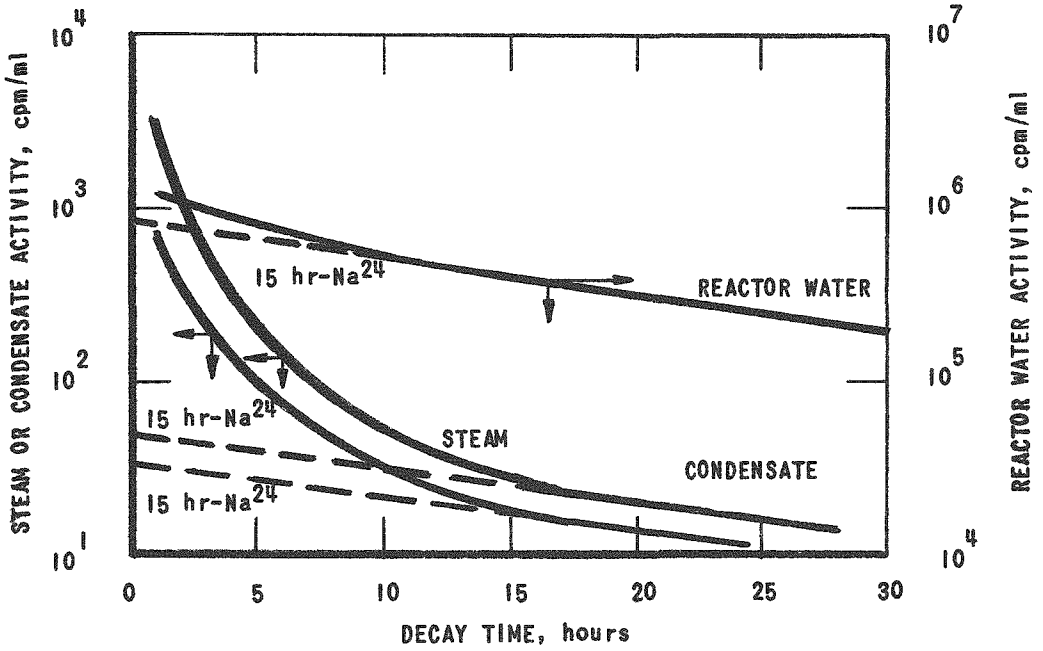

Fig. 6.1

BORAX-III Decay Curves for 1-30 Hour Period

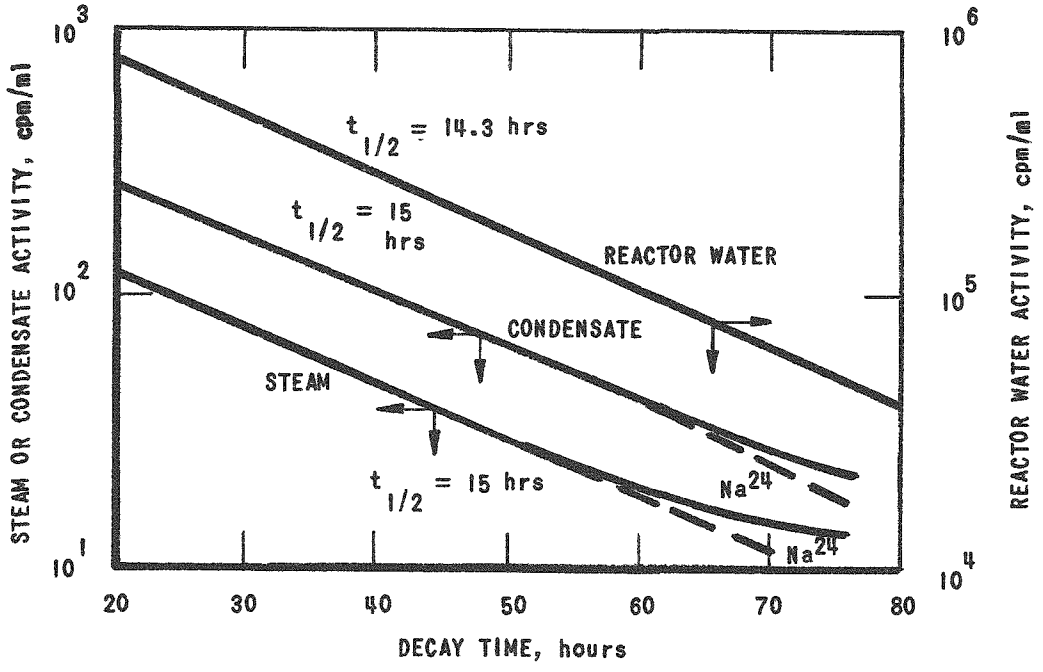

Fig. 6.2

BORAX-III Decay Curves for 20-80 Hour Period

Table 6.1

RADIOACTIVITIES OBSERVED IN BORAX-III REACTOR WATER AND FILTER

Element	Probable Formation	Half Life
N^{16}	$N^{15}(n,\gamma)$; $O^{16}(n,p)$	7.3 seconds
Cl^{38}	$Cl^{37}(n,\gamma)$	37.3 minutes
A^{41}	$A^{40}(n,\gamma)$	110 minutes
Mn^{56}	$Mn^{55}(n,\gamma)$	2.6 hours
Cu^{64}	$Cu^{63}(n,\gamma)$	12.8 hours
Na^{24}	$Na^{23}(n,\gamma)$; $Al^{27}(n,\alpha)$	15.0 hours
Cr^{51}	$Cr^{50}(n,\gamma)$	27 days
Fe^{59}	$Fe^{58}(n,\gamma)$	46 days
Sr^{89}	$Sr^{88}(n,\gamma)$	54 days
Ca^{45}	$Ca^{44}(n,\gamma)$	152 days
Zn^{65}	$Zn^{64}(n,\gamma)$	250 days
Fission Activities Observed in Reactor Water		
Mo^{99}		67 hours
Ba^{140}:	$Xe^{140} \xrightarrow{16\ sec} Cs^{140} \xrightarrow{66\ sec} Ba^{140}$	12.8 days
Ce^{141}:	$Xe^{141} \xrightarrow{3\ sec} Cs^{141} \xrightarrow{S} Ba^{141} \xrightarrow{18\ min} La^{141} \xrightarrow{3.7\ h} Ce^{141}$	32 days
Ru^{103}		41 days
Zr^{95}		65 days
Ce^{144}:	$Xe^{144} \xrightarrow{S} Cs^{144} \xrightarrow{S} Ba^{144} \xrightarrow{S} La^{144} \xrightarrow{S} Ce^{144}$	280 days
Ru^{106}		1 year

Note: S = short

No attempts were made to measure the extent of particulate matter in the reactor water for this series of runs. However, it was apparent that as a result of an effective filtering system, very little crud was present during operation. Samples of reactor water which were centrifuged showed little change in activity in the supernatant liquid.

Figure 6.3 shows the variation of decontamination factors with time based on the steam and condensate samples. Approximately one day following a change in power and for the duration of the test, the decontamination factors show little fluctuation. A trend can be seen at different power levels; for 14 and 12 Mw the decontamination factors average about 6×10^3, while at the 4- and 8-Mw levels the decontamination factors are about 1.5×10^4. These values correspond to 20 to 30 hours decay so that the decontamination factors are based on Na^{24} activity and are indicative of the droplet carry-over. Referring to the data at 12 Mw, it is noted that the decontamination factors based on steam samples taken before and after the moisture separator check very closely.

Figure 6.4 shows a graph of the decontamination factors obtained in the tests as a function of the velocity of the steam in feet per second in the free space above the boiling interface. The vertical lines indicate the range of decontamination factors based on the steam samples. The intersecting horizontal lines represent average values for samples permitted to decay for 20 to 30 hours. It is seen from the graph that between the power levels of 4 to 14 Mw and corresponding steam velocities in the reactor free space between 0.3 and 1.0 ft/sec, no sharp break in the curve or abrupt priming of reactor water occurs.

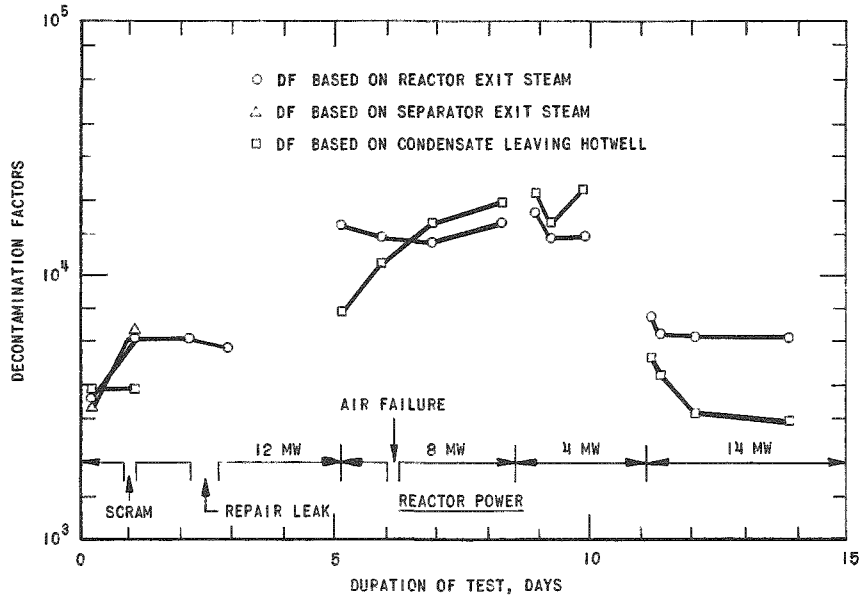

Fig. 6.3

BORAX-III Decontamination Factors for Steam and Condensate, 20-30 Hour Sample Decay

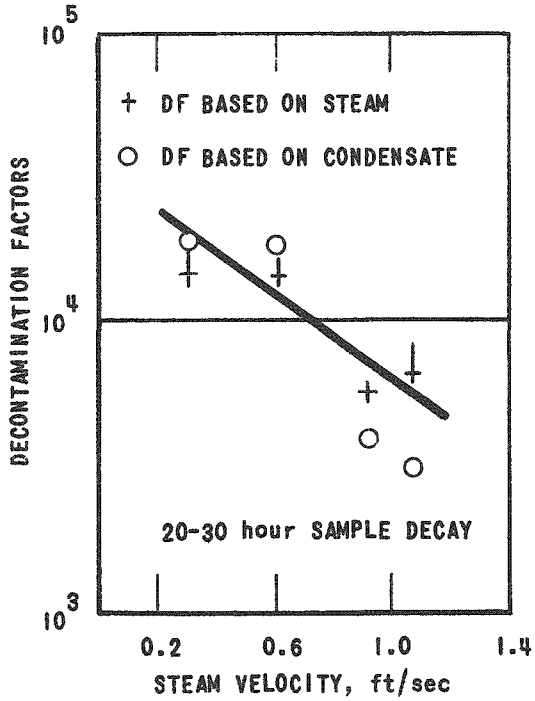

Fig. 6.4

BORAX-III Decontamination Factors for Steam and Condensate

A comparison of the decontamination factors based on the condensate with the points based on the steam indicates that they are of the same order of magnitude. It appears that, at least for short-lived activities, only a small amount of the entrainment is deposited in the external machinery.

Decontamination factors based on steam and reactor water samples permitted to decay for about 40 days do not exhibit any noticeable trend with power level and fall in the range 1 to 2 x 10^3. A mechanism for this behavior based on a partition of activities resulting from relatively long-lived volatile species has been mentioned.

Figure 6.6 shows the data obtained from the BORAX-III test, together with those obtained in the high pressure loop experiments and in the laboratory scale entrainment study apparatus described (in the reference). The data taken in the high

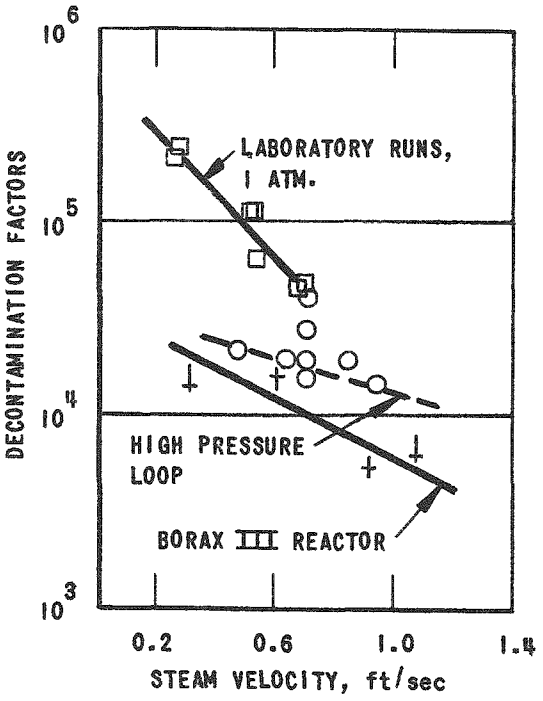

Fig. 6.5

BORAX-III Decontamination Factor vs Steam Velocity

pressure loop are from the uppermost sampler (about 42 inches from the boiling interface) at pressures from 150 to 600 psia. Although the data are scattered they exhibit a similar trend in the range of steam velocities observed. The three curves are displaced in respect to the range of decontamination factors observed. This displacement may be accounted for in part by wall effects in the experimental apparatus. The diameter of the cylindrical boiler was about 3 inches in the atmospheric runs and about 5 inches in boiling loop experiments. The diameter of the BORAX reactor vessel was $4\frac{1}{2}$ feet. Thus, considering the probable range and direction of the droplets leaving the boiling interface, it is reasonable to expect that in the smaller vessels a greater proportion of the droplets were impinged on the walls.

A later report indicated that the activity in the external circuit varied greatly during operation.(19) The reactor water conditions and the operating temperatures of the condenser markedly affected the activity at various points in the circuit. As the pH increased, the activity measured at the air ejector tended to decrease. A decrease in activity at the air ejector was noted with decreasing condenser temperature. Table 6.2 gives some of the activity levels throughout the system during operation. The water quality is the variable in the three test runs.

Table 6.2

RADIATION SURVEY OF BORAX-III STEAM CYCLE COMPONENTS

Reactor Power Level, Mw	8	8	8
Water, pH	5.7	6.7	8.1
Water Specific Resistance, ohm-cm	270,000	490,000	150,000
Survey Location			
Steam Line-Reactor Bldg, mr/hr	430	160	120
Turbine Inlet, mr/hr	145	55	30
Turbine Outlet, mr/hr	50	20	15
Air Ejector, mr/hr	245	210	85
Hotwell Bottom, mr/hr	290	100	50

In the later stages of BORAX-III operation, analysis of the gases from the condenser air ejector indicated the possibility of a break in the (aluminum) fuel plate cladding. The presence of fission products could indicate such a break.

Numerous analyses were made of contaminants in the air ejector gas, in the reactor water, and in solids collected on the filters. A^{41}, Kr^{85}, and Xe^{135} were identified in the air ejector gases. In some of the samples the ratios of these gases were such that air in-leakage into the system did not explain their presence. An analysis of a sample of reactor water identified Sr^{89}, Ba^{140}, La^{140}, and Mo^{99}. The gaseous fission products or the daughters of gaseous fission products, such as Sr^{89}, Ba^{140}, or La^{140}, might have been found outside the fuel because of diffusion through thin sections of cladding metal. Mo^{99} is not in this class and its presence could indicate a cladding failure. In a system having as many materials of construction as did BORAX-III, the molybdenum could have been picked up as a corrosion product and activated in the reactor core. Subsequent analysis of material from the cleanup circuit prefilter showed the presence of the fission products Zr^{95}, Ru^{103}, Ru^{106}, Ba^{140}, and Co^{144}, and also uranium was finally detected. The alpha count of the reactor water and filter cartridges was quite low. In addition, a rupture of the cladding metal should have released Xe^{133}. This was not detected.

The evidence suggested strongly that there was a rupture in the cladding. The evidence was not quantitatively strong enough to conclude that any major quantity of uranium was exposed to water. Also the rate of increasing exposure of uranium to the reactor water could not have been rapid. Even if the exposure of uranium had been due to corrosion of the aluminum cladding rather than a structural failure of the cladding, it still remains reasonable to assume that a low corrosion rate of aluminum occurred in the BORAX-III tests.

6.3. BORAX-IV

1. Early Investigations

Both aluminum nickel (M-388) and stainless steel were used in BORAX-IV.[32] Because the low pH, 3.5-4.0, favored by the M-388 is incompatible with stainless steel, a compromise pH of 5 was selected - it permits 175,000 ohm-cm water, and corrosion of stainless steel is negligible. The ionic solids associated with water of this quality were of concern due to the possibility that a small amount of radioactive solid material could be carried over into the turbine system by the steam. The normal decontamination factor $\left(\frac{\text{activity reactor water}}{\text{activity of steam}} = \text{DF}\right)$ was found to range from 10^3 to 10^4 for dried samples 6-8 hours after collection.

Typical water conditions and activity readings, for various power levels are summarized in Table 6.3.

Table 6.3

TYPICAL WATER CONDITIONS AND ACTIVITY READINGS FOR VARIOUS POWER LEVELS IN BORAX-IV

Reactor Power Mw	Reactor Water pH	Reactor Water Sp. Res. ohm-cm	Steam Line		Activity, mr/hr		
			Reactor	Turbine	Turbine	Turbine Hot Well	Turbine Air Ejector
3	6.4	60,000	40	10	2	8	25
4	6.5	880,000	60	20	4	17	60
6	6.8	500,000	150	65	18	90	330
8	6.7	500,000	175	80	24	110	225
8	5.8	300,000	400	175	45	260	250

2. Effects of Gas Additions on Steam Line Activity.

Various gases including N_2, H_2, O_2 and He were added through the feedwater sparger ring and their effects on the N^{16} carryover rate were studied by noting changes in the N^{16} activity in the steam.(32) Discrimination against other radioactive constituents was obtained by monitoring the main steam header with a NaI scintillation spectrometer biased in such a manner that only events with gamma energies in excess of 3.0 Mev were registered. All other species known to be present have gamma energies lower than 3.0 Mev and were, accordingly, not counted. From Fig. 6.6 which summarizes the results of various gas additions it is clear that little or no change in the N^{16} carryover is effected with N_2, O_2 or He. The addition of H_2, however, causes a significant increase in the carryover rate. From Fig. 6.7 it may be seen that a few seconds after H_2 is admitted to the water system the N^{16} activity increases sharply, passes through a maximum and approaches a new and higher equilibrium level. If the mechanism

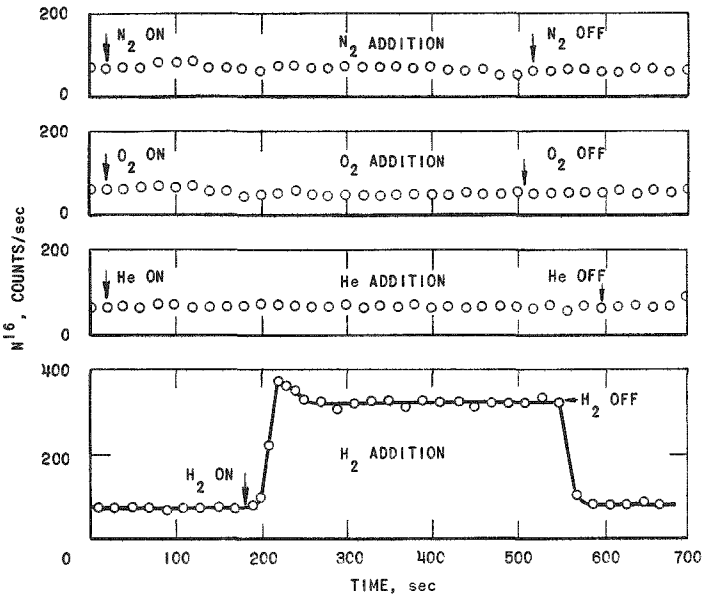

Fig. 6.6

N^{16} Activity in Steam During Gas Additions to BORAX-IV

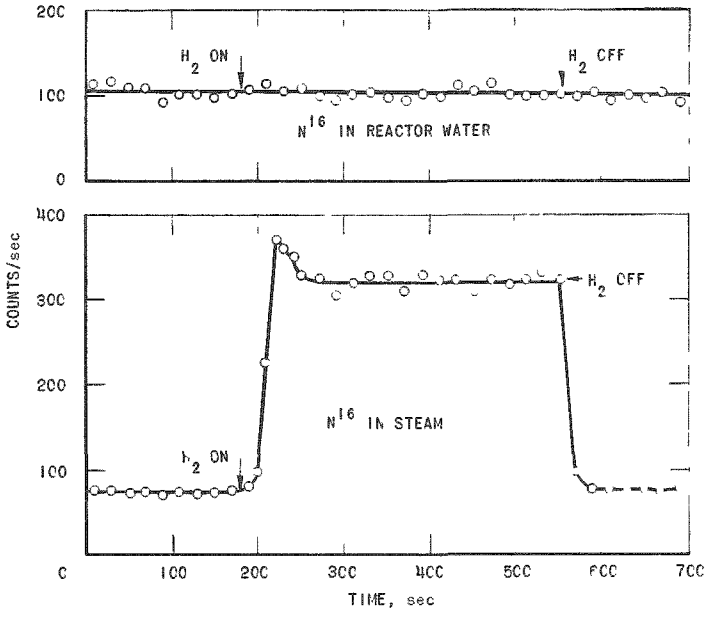

Fig. 6.7

N^{16} Activity in Steam and Reactor Water During Hydrogen Additions to BORAX-IV

responsible for N^{16} carryover is strictly a physical process, i.e., a sweeping effect, little or no difference between the results for the various gases should have been noted. The fact that H_2 effects a large change in the carryover rate while the other gases do not suggests that H_2 must act in a chemically specific manner.

Evidence that N^{16} is carried in chemical form has been obtained from an experiment in which steam condensate was passed through a mixed bed resin column. Decay measurements carried out on the resin bed showed about three half lives of N^{16} indicating that this species was the major activity fixed. Little or no N^{16} was detected in the effluent. The fixation with the resin strongly supports the conclusion that N^{16} is present in the steam condensate in ionic form.

From the H_2 addition curve in Fig. 6.7 which gives the counting rates of N^{16} observed before and after a H_2 addition for the gas and water phases, it is evident that the ratio of counting rates after and before H_2 addition is 1.00 for the water phase, and that the ratio of counting rates after and before H_2 addition is 4.28 for the steam. This indicates that the residence time of the N^{16} in the water phase has been shortened by a factor of 4.28. Since no change in the N^{16} level in the water phase was observed, it may be concluded that the residence time of N^{16} in the water phase is extremely long compared with its half-life. Only a very small fraction of N^{16} is released to the steam. From the experiments, two conclusions were drawn: (1) the decontamination factor for N^{16} is large, and (2) the residence time of N^{16} in the water phase is affected by the addition of H_2 presumably through chemical action. If other additives which act to increase the residence time can be found, problems associated with N^{16} carryover could conceivably be minimized.

Decay curves made on the steam after the reactor was scrammed showed a considerable amount of 30-second activity. This was interpreted to be O^{19}. Efforts to isolate the O^{19} (gamma spectrum) energy

peak from the N^{16} Compton background with a NaI scintillation spectrometer were unsuccessful.*

3. Fuel Defect Test.

A fuel defect test in BORAX-IV was described by Robertson and Hall.(195)

a. Introduction. BORAX-IV fuel elements were thoria-urania pellets bonded with lead in aluminum - 1% nickel tube plates. The effective cladding thickness was 0.016 in.; that of the lead sealer was 0.018 in.

On February 19, 1958, startup of the reactor was accompanied by about a 5X normal increase to 9 r/hr in hot well activity as power reached 10 Mwt. At this time considerable steam was coming from the reactor pump pit and exhaust stack so the reactor was shut down. The following day two of the electrical startup heaters were found to be ruptured. It was assumed that the high level of activity was caused by MgO and other impurities released into the water.

On February 25, another startup was accompanied by hot-well activity reaching 8 r/hr at 12 Mwt. The reactor was shut down and the activity decayed with a 33-minute half life to normal background levels. Cs^{138} was identified by half life and gamma-energy spectrum.

It was concluded that fuel rupture had occurred. The rapid decay to background levels indicated that the reactor could be operated for further evaluation. On March 11 and 12, 1958, the reactor was operated at 2.4 Mwt as an experiment to evaluate the effect of running a direct cycle boiling water reactor with a fuel element defect. This power level was chosen as the lowest which could be maintained and yet run the plant under equilibrium conditions.

b. Objectives. To determine the limiting factors on operation of this reactor with a fuel defect, the following measurements were made:

(1) activity levels of steam plant equipment;

*Note: O^{19} results from the reaction:(193)

$$O^{18}\ (n,\gamma)\ O^{19} + 4.24\ \text{Mev}$$

$$O^{19} \xrightarrow[29.4\ \text{sec}]{\beta} F^{19*} \xrightarrow[\text{inst}]{\gamma} F^{19}$$

The cross section for this reaction has been reported(194) as 22 mb.

(2) quantitative determination of Xe^{138} and Kr^{88} released through air ejector;

(3) analyses of reactor water, condensed steam before turbine, and condensed steam after the turbine (hotwell condensate) for fission products;

(4) area contamination down wind from the reactor.

c. Results. Results are described under eight different subdivisions as follows:

(1) Radiation Levels. Table 6.4 lists the radiation levels at various locations in the system at steady operation as determined with portable Juno Survey Meters. The last column shows the relatively low activity obtained during normal operation at 12 Mw when it was known that no defects were present. The activity levels in the last column are attributed to N^{16} since, on reactor shutdown, they decayed with a 7-second half life.

Table 6.4

RADIATION LEVELS DURING OPERATION OF BORAX-IV

Location	mr/hr		
	With Defect		No Defect
	2.4 Mw	6.0 Mw	12 Mw
Reactor Building			
Main Steam Line	500	500	250
Feedwater Filter	6,000	12,500	⩽50
Top of Reactor	160	210	⩽100
Main Door to Building	20	30	⩽10
Turbine Building			
Main Steam Line	250	400	200
Turbine Exhaust Casing	150	190	50
Air Ejector After Cooler	15,000	-	420
Air Ejector Exhaust Filter (A-C Type)	30,000	50,000	Not in Service
Hotwell	2,200	-	500
Main Door to Area	20	27	⩽10

It is obvious that during operation on March 11 and 12 radiation levels everywhere were significantly higher than normal. On reactor shutdown they no longer fell off rapidly, but decayed with a half life of roughly 30 minutes. However, after a period of 17 hours all radiation levels had decayed to their initial low values.

Measurements of internal radiation levels in the turbine exhaust casing showed that no activity had built up during this experiment.

(2) Down Wind Activities. Measurements of filter paper from air samples and the field survey for down wind activities were made approximately one hour after reactor shutdown. The observed activities decayed with a half life of 33 minutes. The values in Table 6.5 have been calculated back to time of reactor shutdown on the basis of the 33-minute half life.

Table 6.5

BORAX-IV FIELD MONITORING,
HIGH-VOLUME AIR SAMPLERS,
MARCH 12, 1958

Location	Activity
125 ft Downwind	350 mr/hr (average of 3 samplers)
500 ft Downwind	150 mr/hr (average of 3 samplers)

Field Survey

Along Downwind Centerline

(Normal Background, 0.03 mr/hr)

Distance From Gas Discharge Stack (ft)	Ground Surface Activities β and γ (mr/hr on contact)
125	4.0
200	2.7
300	1.6
500	3.0
750	1.8
1000	0.12

(3) Rates of Xe^{138} and Kr^{88} Release From Defective Fuel Elements. The samples of gases emitted from the air ejector were analyzed for Xe^{138} and Kr^{88}. Knowing the times involved, the activities of Xe^{138} and Kr^{88} in the original sample could be determined. From this and a knowledge of the flow rate of the gases through the air ejector, the rate of emission of Xe^{138} and Kr^{88} could be calculated. The emission rates (curies/min) were found to be 4.0 ± 2.0 and 0.7 ± 0.1, respectively.

(4) Radioactivities in Reactor Steam, Hotwell, and Reactor Water. Samples of reactor steam, reactor water, and hotwell condensate were taken during each period of operation at 2.4 Mw. Results, obtained by conventional radiochemical methods, are given in Table 6.6.

Table 6.6

RADIOACTIVITIES IN BORAX-IV REACTOR WATER, STEAM, AND CONDENSATE

Date	Time	Location	Cs^{138}	Cs^{137}	Ba^{140}	Sr^{89}	Sr^{90}	I^{131}	Mo^{99}
3-11-58	1107	Reactor Water						710	
3-11-58	1410	Reactor Water	2.2×10^6	1.1×10^4	4.3×10^3	1.1×10^4	420	4.0×10^3	
3-11-58	1508	Steam		19	120	1.2×10^3	neg	120	
3-11-58	1415	Condensate	2.2×10^6	16	60	570	neg	130	
3-12-58	1330	Reactor Water	1.3×10^6	1.2×10^4	7.5×10^3	1.7×10^4	484	3.1×10^3	1.6×10^4
3-12-58	1323	Steam	1.2×10^7	20	120	690	neg	90	neg
3-12-58	1325	Condensate	1.6×10^6	24	47	590	neg	70	neg

All activities expressed as disintegrations per minute per milliliter (dpm/ml) of water or condensed steam.
All activities corrected to sampling time.

N.B. (1) "neg" means < 10 dpm / ml.

(2) Uncertainty in above results is about ±30%.

The nuclides listed in Table 6.6 and Co^{58} contribute well over 90% of the observed gamma activity in the reactor water and the majority of the beta activity. Except for Co^{58} the same nuclides were present in the steam, but ratios of disintegration rates were different. Calculated back to reactor shutdown, the ratios in the water were Cs^{137}: Ba^{140}: Co^{58} = 2:1:0.6.

In the condensed steam the ratios were Cs^{137}: Ba^{140} = 1:14, somewhat higher than that indicated by Table 6.6, but values are in qualitative agreement. The very low counting rate in these samples made quantitative estimates difficult.

(5) Radioactivities Deposited on Metal Coupons. Before operation on March 11, 1958, the manhole cover of the turbine exhaust casing was opened and coupons of mild steel, stainless steel, aluminum, and copper were inserted in a special holder. On March 13 they were removed, taken to ANL, and examined for gamma-ray spectrum in a 256-channel gamma-ray pulse-height analyzer. The results are given in Table 6.7.

The gamma spectra of the various metal coupons removed from the turbine exhaust casing were very similar to the spectra of the reactor steam samples and showed the presence of only Ba^{140}, La^{140}, and Cs^{137}. These three nuclides contributed over 95% of the observed gamma-ray activity deposited on the coupons. It must be noted that Sr^{89} and Sr^{90} have no gamma rays and would not be detected in a gamma-ray spectrometer.

Table 6.7

RADIOACTIVITIES ON METAL COUPONS IN BORAX-IV

Metal	Activity/Coupon 137 hr after Reactor Shutdown (disintegrations/min)			Activity at Reactor Shutdown March 12, 1958 (μ curie/ft^2)		
	Ba^{140}	La^{140}	Cs^{137}	Ba^{140}	La^{140}	Cs^{137}
Mild Steel		7.4×10^3	775	0.42		0.032
Stainless Steel		6.6×10^3	890	0.37		0.037
Aluminum		5×10^3	635	0.28		0.026
Copper		4×10^3	510	0.22		0.021

The Ba^{140} peaks, although suitable for qualitative identification, were not suitable for quantitative interpretation. Ba^{140} activities could be calculated, however, on the assumption that at the time of reactor shutdown, La^{140} activities were low and that the La^{140} activity observed at counting time resulted from decay of Ba^{140}.

The general conclusion may be drawn that if the activity deposition on these specimens was representative of deposition in the turbine and condenser as a whole, the reactor operation on March 11 and 12 led to very low contamination by these nuclides.

(6) Calculation of U^{235} Equivalence of Fission Gas Release Rates. Based on certain assumptions as to behavior of fission products in water and the fact that the reactor had operated for a sufficiently long period of time for the fission gases precursors to be in radiochemical equilibrium, the mass of U^{235} which must be exposed to the water to release fission product gases at the observed rate, was calculated.

$$\text{Production Rate } R = M^{235} FY \text{ (atoms/sec)} \qquad (6.1)$$

where

M^{235} is mass of U^{235} in grams;

F is fission rate per gram of U^{235}, fission/(sec)(g U^{235});

Y is fission yield;

R is an experimentally measured value.

This is an oversimplified expression which ignores burnup of U^{235} and assumes that fission products come only from U^{235} fission. F and Y are known, hence M^{235} may be calculated. Table 6.8 shows the results for Xe^{138} and Kr^{88}.

Table 6.8

CALCULATION OF MINIMUM U^{235} EXPOSED IN BORAX-IV

Nuclide	Curie/Min	Atom/Sec	(R/Y) x 10^{13}	M^{235} (gm)
Xe^{138}	4.0 ± 2.0	(3.6 ± 1.8) x 10^{12}	(6.3 ± 3.2)	15.5 ± 7
Kr^{88}	0.7 ± 0.1	(6.2 ± 0.9) x 10^{12}	(17 ± 3)	42.5 ± 6.5

(7) U^{235} Equivalence of Other Fission Products

(a) I^{131} and Mo^{99}. The U^{235} equivalence of I^{131} and Mo^{99} in reactor water was calculated. The values for M^{235} (gm) were found to be 0.25 and 0.26 respectively. Values for the quotient R/Y were found to be 1 x 10^{12} and 1.1 x 10^{12} respectively. It will be noted that these values, both for M^{235} and for R/Y are very much lower than those for the fission gases.

(b) Cs^{137}, Sr^{89}, Ba^{140}. These three nuclides contributed over 50% of the long-lived activity present in the reactor water. They undoubtedly arise from the decay of the shorter-lived Xe and Kr precursors. Some of these precursors, the fraction depending on their half life, will be removed from the system via the air ejector exhaust system. The remainder will decay to the Cs or Sr which will deposit on equipment surfaces or will be returned to the reactor water via the condenser hotwell and feedwater pumps. It is difficult to make any significant calculations regarding these isotopes.

The most probable explanations for the presence of the large amount of these nuclides is that they were emitted as a burst of activity when the defect first occurred, or perhaps as bursts when the reactor was cycled at higher power during the period February 19 - 25, 1958.

From the foregoing it is clear that a simple mechanism of release of fission products from fission recoils cannot explain the observed results. The only significant radioactivities found were due either to fission gases or their decay products and that no significant amounts of nuclides without gaseous precursor were found.

It was also found that the function R/Y was not constant but decreased with decreasing half life of the fission gas.

This behavior is in accordance with that found in EBWR;(196) that is, this behavior may be explained by some diffusion controlled mechanism within the fuel element. Whether this

diffusion is through the oxide matrix or through the gap between the fuel and the sheath has not been established definitely. It is definite, however, that the time delay between the time of production of a fission gas atom within the fuel and the time when it reaches the defect is long enough that a large fraction of the very short-lived gaseous nuclides will have decayed before they reach the defect.

Thus, a small defect (or many small defects) must be presumed, behind which there is a reservoir in which gases can diffuse. Subsequent examination of a fuel element[141] has shown that defects had occurred in the void at the top of the fuel tubes. Thus, the desired mechanism is present, all the more so if it is assumed that the lead bond between the pellets and the aluminum-nickel sheath was porous.

The magnitude of the release rate of these gases, however, demands that many such defects were present in the fuel elements. Again, subsequent examination[141] showed that of 69 fuel elements, 22 contained defective plates.

(8) Decontamination Factors. In a boiling water reactor, concern has always been expressed regarding the extent to which activity will be transferred by the steam to the turbine and condenser. A decontamination factor (DF) may be expressed as the ratio of the activity per unit weight of reactor water to the activity in the same wieght of steam. The DF may be expressed for gross activity or, better, for individual nuclides.

Since fission product gases are effectively stripped from the reactor water, i.e., DF = 0, it is useless to use them, or their decay products, to measure DF's. In this experiment the only meaningful DF obtained was that for I^{131}. On March 11 it was $(4.0 \times 10^3)/120 = 33$, and on March 12 it was $(3.1 \times 10^3)/90 = 32$, both values taken at 2.4-Mw power.

These surprisingly low values indicate that some of the I^{131} in the reactor water was probably in the form of elemental iodine which is volatile rather than in an ionic form such as I^-, IO_3^-, or IO_4^-.

Previous work on the BORAX reactor[192] showed a DF of 5×10^3 for Na^{24} at powers of 12-14 Mw and higher for lower powers.

d. Discussion. To establish the radioactivity hazards from operation of a boiling water reactor, such as BORAX-IV, which contained defective ceramic-type fuel elements, three main questions must be answered:

Question (1). What is the source, nature, and magnitude of radioactivity released during operation?

Question (2). What is the nature and the level of subsequent contamination of the reactor system? Of the steam system, including the turbine, condenser, and piping leading to the stack? Only nuclides having half lives longer than 2-3 hours need be considered.

Question (3). To what extent will the surrounding countryside be contaminated by long-lived fission products emitted from the reactor stack?

In the following treatment, answers to these questions will be attempted with specific reference to the operation of BORAX-IV. The most significant results brought out by this experiment are:

Answer to Question (1). During the operation of the reactor with defective fuel, the main products which caused a high level of radioactivity in the system were the fission product gases and their decay products. Precursors such as radio-iodines were presumably retained within the sheath (or the fuel) and there was no evidence that significant amounts of other fission products such as Mo^{99} which have no gaseous precursor were released through the defect. The results also indicate that there is a delay mechanism in the fuel such that shorter-lived gases are emitted to a lesser degree than the longer-lived ones.

Table 6.9 shows all decay chains which produce radioactive fission product gases. The chains are arranged in the order of increasing half life of the fission gas. No chains involving stable gases have been included and several chains have been simplified in that branches of low yield involving short-lived activities have been neglected.

Examination of Table 6.9 shows that, if release of fission gas precursors through the defect is negligible, then the only chains which will contribute significantly to activity release and subsequent long-lived contamination are those which involve a gas of half life shorter than 3.9 min; i.e. those above the chain of mass number 137 in the table. In all others, although the release rate of the gas itself may be high, the decay products which will produce contamination are either very short-lived or so long-lived they may be considered stable.

A more quantitative estimation is based on the plot of R/Y vs $1/\sqrt{\lambda}$ (where R is the release rate of the gas in atom/sec, Y is the fission yield, and λ is the decay constant) as was found in EBWR, i.e. by using a plot based on two experimental points for Kr^{88} and Xe^{138} and the origin, release rates of other fission product gases can be calculated from this line.

Table 6.9

DECAY CHAINS INVOLVING RADIOACTIVE FISSION PRODUCT GASES

Mass No.	Precursors	Fission Gas	Daughters	Yield, %
143		Xe (1 s) →	Cs (short) → Ba (< 0.5 m) → La (18 m) → Ce (33 h) → Pr (13.7 d) → Nd (stable)	6
94		Kr (1.4 s) →	Rb (short) → Sr (2 m) → Y (16.5 m) → Zr (stable)	6.4
141		Xe (1.7 s) →	Cs (short) → Ba (18 m) → La (3.7 h) → Ce (33 d) → Pr (stable)	6
93		Kr (2.0 s) →	Rb (short) → Sr (7 m) → Y (10.5 h) → Zr (1.1 x 10^6 y)	6.5
92		Kr (3.0 s) →	Rb (80 s) → Sr (2.7 h) → Y (3.6 h) → Zr (stable)	6
91		Kr (10 s) →	Rb (1.67 m) → Sr (9.7 h) → Y (58 d) → Zr (stable); Rb (14 m) → Sr (9.7 h)	5.8
140		Xe (16 s) →	Cs (66 s) → Ba (12.8 d) → La (40.2 h) → Ce (stable)	6.4
90		Kr (33 s) →	Rb (2.7 m) → Sr (28 y) → Y (64.3 h) → Zr (stable)	5.8
139	I (2.7 s) →	Xe (41 s) →	Cs (9.5 m) → Ba (84 m) → La (stable)	6.6
89	Br (4.5 s) →	Kr (2.6 m) →	Rb (15.4 m) → Sr (51 d) → Y (stable)	4.8
137	I (24.0 s) →	Xe (3.9 m) →	Cs (30 y) → 0.92 Ba (2.57 m); 0.08 Ba (stable)	6.2
138	I (5.8 s) →	Xe (17 m) →	Cs (33 m) → Ba (stable)	5.7
87	Se (17 s) → Br (55 s) →	Kr (78 m) →	Rb (6 x 10^{10} y)	2.5
83	Se (68 s) → Br (2.4 h) →	Kr (114 m) → Kr (stable)		0.5
88	Br (15.5 s) →	Kr (2.8 h) →	Rb (18 m) → Sr (stable)	3.6
85	Se (40 s) → Br (3.0 m) →	Kr (4.4 h) → 0.775 Rb (stable); 0.225 Kr (10.3 y) → Rb (stable)		1.3
135	Te (< 0.5 m) → I (6.7 h) (0.3 / 0.7)	Xe (15.3 m); Xe (9.2 h) →	Cs (2.6 x 10^6 y) → Ba (stable)	6.4
133	Te (63 m) (0.72 / 0.28); I (20.8 h) (0.02 / 0.98); Te (2 m) → I (20.8 h)	Xe (2.3 d); Xe (5.27 d) →	Cs (stable)	6.6
131	Te (30 h) (0.15 / 0.85); I (8.05 d) (0.008 / 0.992); Te (24 m) → I (8.05 d)	Xe (12 d); Xe (stable)		2.9

Note: s = seconds, m = minutes, h = hours, d = days, y = years; metastable.

For purposes of calculation, the BORAX-IV reactor system was arbitrarily divided into five zones. As the gases were carried by the steam to the turbine and then by exhaust gases to the stack, they would spend a certain time in each zone; this time depended on the velocity of the carrier gas and the volume of the zone. From the residence time in each zone and release rate for each nuclide, the activity of each nuclide in each zone could be calculated. Details of the method of calculation are given in the reference by Robertson and Hall.(195)

Figure 6.8 shows a plot of the activity, in curies, due to fission gases in various parts of the system as calculated.

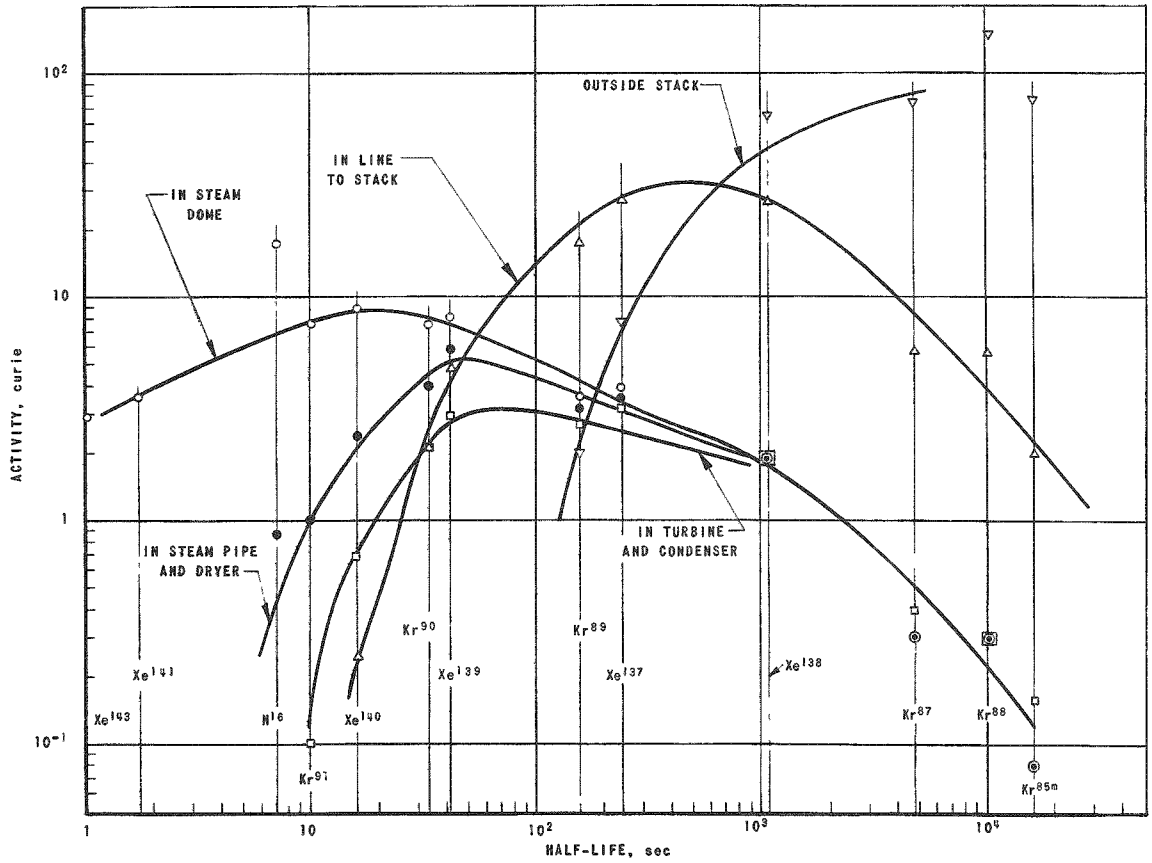

Fig. 6.8

Distribution of Fission Gases in BORAX-IV at 2.4 Mw

Some highlights of the results of the calculations are:

The very short-lived gases decayed completely in the steam dome, and the majority of the activity on the remainder of the system was due to fission gases having half-lives from 10 seconds to 1 hour, and to the decay products from these gases.

As expected, along the path taken by the gas from reactor to stack, the predominant fission gas activity became progressively longer-lived as the distance (and time) from the reactor increased.

During steady operation at 2.4 Mw, there were at least 12 curies of fission gases alone in the turbine and condenser. Short-lived daughters brought this up to well over 30 curies of activity.

Xenon^{138} was released from the BORAX-IV stack at a significantly higher rate than any other gas, hence, its daughter Cs^{138}

was the predominant short-lived activity outside the reactor. In the rest of the system Xe^{138} and Cs^{138} were overshadowed by other gases and their daughters during actual operation.

On shutdown, however, the shorter-lived nuclides decayed quite rapidly, and the longer-lived nuclides have no significant daughters. Thus, one-half hour or so after shutdown, Cs^{138} was the predominant activity, especially in the turbine and condenser and in the piping beyond the condenser.

Answer to Questions (2) and (3). Extent of Long-Lived Contamination. In making calculations regarding extent of contamination, it was assumed that all contamination resulted from long-lived daughters of fission gases. Results are given in Table 6.10. The discussion as to each zone follows:

Table 6.10

CALCULATED LONG-LIVED CONTAMINATION RESULTING FROM 8 HR OPERATION OF BORAX-IV AT 2.4 Mw

Nuclide	Half-life	1 Day after Shutdown					10 Days after Shutdown				
		Zone 1	Zone 2	Zone 3	Zone 4	Zone 5	Zone 1	Zone 2	Zone 3	Zone 4	Zone 5
Ce^{143}	33 hr	300	neg	neg	neg	neg	3	neg	neg	neg	neg
Pr^{143}	13.7 d	20	neg	neg	neg	neg	30	neg	neg	neg	neg
Ce^{141}	33 d	25	neg	neg	neg	neg	20	neg	neg	neg	neg
Sr^{91}	9.7 hr	790	100	10	neg	neg	neg	neg	neg	neg	neg
Y^{91}	58 d	25	3	0.5	neg	neg	27	3	0.5	neg	neg
Ba^{140}	12.8 d	150	41	12	4	neg	95	25	7	3	neg
La^{140}	40.2 hr	53	14	4	2	neg	110	29	8	3	neg
Sr^{90}	28 yr	0.17	0.09	0.05	0.06	1.2×10^{-6}	0.17	0.09	0.05	0.06	1.2×10^{-6}
Y^{90}	64.3 hr	0.04	0.02	0.01	0.01	neg	0.15	0.08	0.04	0.05	neg
Sr^{89}	51 d	16	14	12	78	9	14	12	10	66	8
Cs^{137}	30 yr	0.005	0.04	0.035	0.3	0.085	0.005	0.04	0.035	0.3	0.085
Total Millicuries		1380	170	40	85	9	300	70	25	72	8

All activities in millicuries

Zone 1 - Reactor Steam Dome
Zone 2 - Steam Pipe and Dryer
Zone 3 - Turbine and Condenser
Zone 4 - Piping to Stack
Zone 5 Outside Stack

Zone 1 - Reactor Vessel. Contamination in the reactor vessel came from three sources:

(a) First source was from decay of fission gases. The majority of the long-lived activity remained within the pressure vessel. The level, however, was low, in contrast to the corrosion products there. Activity of 1.4 curies at 2.4 Mw was negligible compared with the activities of the activated corrosion products which were there already.

(b) The second source was from fission gas decay products swept from piping, turbine, etc., and returned to the reactor via feedwater. It was known (Table 6.6) that the BORAX-IV feedwater contained Cs^{137}, Cs^{138}, Ba^{140}, and Sr^{89}. The net result of this was that the contamination in Zones 2 to 4 could be lower than indicated, but the activity in Zone 1 would not be increased greatly.

(c) The third source was the presence of nonvolatile components released from the fuel, (UO_2 + ThO_2 in BORAX-IV). These components evidently contributed to the activity of the BORAX-IV reactor water to a minor extent. This has also been found to be true for UO_2 ceramic fuels(197,198) with the exception that the latter seem to release large quantities of radio-iodines, comparable to the amounts of fission gas released. This did not appear to have been true during the BORAX-IV fuel defect test under investigation. ThO_2 may actually release radio-iodines to a lesser extent than does UO_2 or the radio-iodines may have been absorbed on Al or Al_2O_3 surfaces. It must be remembered that all UO_2 tests reported have been conducted in steel systems with no aluminum present.

Zone 2 - Steam Pipe; Zone 3 - Turbine and Condenser; Zone 4 - Piping to Stack. Table 6.10 shows that the main source of contamination in BORAX-IV in these zones came from Ba^{140}-La^{140}, Sr^{90}-Y^{90}, Sr^{89} and Cs^{137}. It is significant that these nuclides were the only ones found in the steam and condensate samples. These results indicate that contamination from such nuclides as Ce^{143}, Pr^{143}, Ce^{141} or Y^{91} was not serious in this part of the system.

It is of interest to note that almost one-half of all the Sr^{90} produced remained in the steam dome, the remainder being found mainly in the steam line, with some in the turbine and in the piping to the stack. Virtually none escaped from the stack. Sr^{89}, however, deposited mainly in the line to the stack.

It must be remembered that these two nuclides, which are most harmful from radiological health standpoint, were present on the walls of the steam pipe, in the turbine and condenser, and in the line to the stack in BORAX-IV. With direct cycle reactors of this type, such a condition must be expected when the steam system is opened up after reactor shutdown following operation with defective fuel.

Zone 5 - Contamination Released From Stack. During this fuel defect test very little long-lived contamination was released from the stack. Large amounts of short-lived activity, such as from Xe^{138} and Cs^{138} were released but in a few hours they decayed to negligible levels.

Large amounts of long-lived fission gases were released but were not considered a potential health hazard since they decayed to stable or very long-lived nuclides.

The most important contaminants released from the stack from a health standpoint were Sr^{90} and Sr^{89}. It is obvious that the 10-minute delay from the reactor to the stack was not enough, alone, to make the resulting outside contamination by Sr^{90} negligible. Some Sr^{89} did build up outside, but the amount that resulted from 8-hour operation of BORAX-IV at 2.4 Mw, 8 millicuries, was spread over a large area and did not pose a large problem.

e. Summary. The first important general conclusion from the results of the BORAX-IV fuel defect test is that it is perfectly feasible to operate a boiling reactor fueled with ceramic fuel with many defects in the fuel cladding, such as were present during this test.

Although radiation levels may be high during operation, it would appear that protracted operation would be feasible without serious contamination to equipment or to the surrounding countryside provided two criteria were met:

(1) The system should be free from leaks.

(2) The delay time from the reactor vessel to the exit from the stack should be longer than one hour.

With such a delay time the amounts of Sr^{89}, Sr^{90}, or Cs^{137} released from the stack would be negligibly small, even for a large number of defected elements. If the delay time were of the order of 24 hours, then the only significant activities released from the stack would be due to Xe^{135} and Xe^{133}.

The second important conclusion is that a means exists for estimating the activity released and the resulting contamination from operating a reactor with defective ceramic fuel. First of all, the only fission products which are released in significant quantities are fission gases. If a release rate for one gaseous nuclide can be measured or estimated, then the release rates of all other fission gases may be calculated. This calculation will lead to conservative results in that estimated release rates for very short-lived fission gases appear to be larger than they actually are. Then, if the reactor, steam, turbine and condenser, and off-gas systems are divided into a number of zones, and an average

time that a gas atom will spend therein is assigned to each zone, then the activities throughout the system at steady operation may be estimated and the long-lived contamination resulting from a known period of operation may be calculated both for the reactor system and for the surrounding countryside.

6.4. EBWR

1. Early Investigations.

In the earliest reports(21,199) on radioactivity present in EBWR, Zitek reported that the air ejector gases contained N^{16} with smaller amounts of fission gases (Xe^{135}, Xe^{138}, Kr^{88}, Kr^{89}, Kr^{90}, and A^{41}) and that the reactor water contained radioactive strontium in addition to Na^{24}. A gamma-ray spectrometer analysis of the water showed that 99% of the gamma activity could be accounted for in decreasing order of importance by: Mn^{56} 0.822 Mev, $t_{1/2}$ = 2.6 hr; Sr^{91} + Y^{91M}, 0.551 Mev, $t_{1/2}$ = 9.7 hr; and Na^{24}, 1.4 Mev, $t_{1/2}$ = 15 hr.

Soon after the original startup of the reactor, background higher than normal was noticed by several low-counting laboratories on the site. Samples of gas were taken from the air ejector discharge and reactor vent system and counted. Cs^{138} was identified immediately and the fission gases, Xe^{138}, Xe^{135}, Kr^{89}, Kr^{90}, and Kr^{91}, were identified later. Examination of reactor water samples on January 10, 1957, for Cs^{138}, Sr^{89}, Ba^{139}, and Mo^{99} gave positive results for all. From the analytical results on four samples it appeared that the production had reached equilibrium conditions. On the basis of the data obtained, it was concluded that the amount of fuel (uranium) in the reactor water was 59 mg.

The source of the uranium was concluded to be surface contamination of fuel elements which resulted from rupture of about three plates during autoclave testing previous to the loading of EBWR. Although the autoclaves were decontaminated, subsequent plates could have been contaminated, and it is not certain how well the plates which had been in the autoclave at the time of the failures were decontaminated.

Another possible source was the reported presence of about 1 ppm uranium in the Zircaloy-2 used for fuel cladding.

The results of a survey of the activities in and around EBWR, made by Goslovich and associates early in 1957,(200) are given in Tables 6.11 and 6.12.

It is of interest to note that the decontamination factor (ratio of water activity to condensed-steam activity) for F^{18} is only 4.33, indicating a high degree of volatility in the steam.

Table 6.11

CORROSION PRODUCT ACTIVITIES AT EBWR APRIL-MAY, 1957

Isotope	Half Life	γ rays (Mev)	Probable Formation	Concentration[a] x 10^{-2} μc/ml	Conc. MPC[e]
Reactor Water:					
Mn^{56}	2.6 hours	0.850 1.82 2.15	Fe^{56} (n,p) Mn^{55} (n,γ)	4.5	0.3
Na^{24}	15 hours	1.36 2.75	Al^{27} (n,α) Na^{23} (n,γ)	1.5	1.9
Co^{58}	72 days	0.81	Ni^{58} (n,p)	0.088	0.04
Co^{60}	5.2 years	1.17 1.33	Co^{59} (n,γ) Ni^{60} (n,p)	Trace	$\ll$MPC
F^{18}[b]	1.9 hours	0.51[c]	O^{18} (p,n)	1.3	0.01
Condenser Tubing Deposit:					
Co^{58}	72 days	0.81	Ni^{58} (n,p)	8.8	
Reactor Steam:[d]					
F^{18}	1.9 hours	0.51[c]	O^{18} (p,n)	0.3	
Co^{58}	72 days	0.81	Ni^{58} (n,p)	Trace	
Anion Resin:					
Cr^{51}	26 days	0.32	Cr^{50} (n,γ)	-	

[a] All concentrations, microcuries per milliliter (μc/ml), determined for 20 Mw over periods of 24 hr or longer.

[b] Comes from O^{18} in water; not a corrosion product.

[c] Annihilation quanta.

[d] Before steam dryer. Concentration per ml condensed steam.

[e] MPC = Maximum permissible concentration (Handbook 52 National Bureau of Standards - 1953)

Table 6.12

FISSION PRODUCT ACTIVITIES AT EBWR - APRIL-MAY, 1957

Isotope	Half Life	γ rays (Mev)	Decay Chain	Concentration (μc/ml)	Ratio Concentration / MPC
Air ejector gas:					
Cs^{138}	33 minutes	0.46 0.98 1.44	$Xe^{138} \rightarrow Cs^{138}$	7.4×10^{-3}	150
Xe^{135}	9.2 hours	0.250	$Xe^{135m} \rightarrow Xe^{135}$	3.2×10^{-4}	0.32
Kr^{85m}	4.5 hours	0.150	U fission	1.2×10^{-4}	
Air ejector filter:					
Ba^{139}	85 minutes	0.163	$Xe^{139} \rightarrow Cs^{139} \rightarrow Ba^{139}$	Trace	
Ion-exchange filter:					
Ba^{140}	13 days	1.60	$Xe^{140} \rightarrow Cs^{140} \rightarrow Ba^{140} \rightarrow La^{140}$	Trace	
Room Air:					
Cs^{138}	33 minutes			1.2×10^{-7}	0.002

Since all the fission product activities listed in Table 6.12 result from xenon and krypton, two high yield gaseous fission products, and since no other fission products were observed, Goslovich and associates concluded that the fission gases escaped through the Zircaloy cladding by diffusion, and that no appreciable uranium contamination existed on the outside of the EBWR fuel elements. The lack of agreement between this, and the Zitek conclusions regarding uranium contamination on EBWR fuel plates is believed to be based on Goslovich and associates not finding Mo^{99} or radio-iodines (non-gaseous fission gas precursors) in the water. For lack of better information, a difference in technique is suspected as the cause.

In a sample of water taken July 11, 1958,(201) about a year later, over 90% of the gamma-emitting nuclides present at the time the sample was taken could be accounted for as indicated in Table 6.13.

Table 6.13

ACTIVITIES IN EBWR REACTOR WATER
JULY 11, 1958

Nuclide	Half Life	Approx. % of Total
Na^{24}	1.5 hours	75
Mn^{56}	2.6 hours	20
Co^{58}	72 days	2
Cu^{64}	12.6 hours	3

A comparison of the specific activities of these nuclides with those calculated from the previous survey is shown in Table 6.14.

Table 6.14

EBWR REACTOR WATER ACTIVITIES COMPARED

Nuclide	Activity, dpm/ml	
	July 11, 1958	April-May, 1957
Na^{24}	1.6×10^5	3.3×10^4
Mn^{56}	6×10^4	1×10^5
Co^{58}	4×10^3	2×10^3

It thus appears that during the year the Na^{24} content of the reactor water increased by a factor of 5 and the Co^{58} increased by a factor of 2.

It should be noted that the actual concentrations of these impurities were negligibly small and would have been hard to detect by ordinary chemical means.

A sample of reactor steam was subjected to gamma-ray spectra analysis; the only significant activities were:

Photopeak	Half Life	Probable Nuclide
510 kev	114 minutes	F^{18}
510 kev	~10 minutes	N^{13}

The F^{18} isotope has been identified previously in the steam. N^{13} identification must be regarded as tentative as yet. The method of production is perhaps N^{14} (n,2n)N^{13}, the N^{14} coming from the small amounts of N_2 present in the reactor water.

Monitoring of delayed neutrons showed a marked dependence on flow rate, increasing sharply as the flow increased. Among the four channels monitored, no significant difference in the counting rate was observed from one channel to another at a given flow rate. This would indicate that the main contribution to the neutron counting rate was from the N^{17} (half life 4.14 sec) and that any contribution from the fission product halogens was negligible.

The reaction responsible for N^{17} is:(193)

O^{17} (n,p) N^{17} - 8.0 Mev:

$$N^{17} \xrightarrow[4.14\ \text{sec}]{\beta} O^{17} \xrightarrow[\text{inst}]{n} O^{16}$$

The O^{17} isotope occurs to the extent of 0.039% in the atmosphere. The average cross section of this reaction in a fission neutron spectrum has been reported to be 0.0052 mb,(202) and 0.0093 ± 0.0009 mb.(203)

2. Decontamination Factor.

During the early operating period of EBWR(21) attempts were made to measure the decontamination factor, as shown by the activity of the water before and after the prefilter, ion-exchanger, steam dryer, and condenser.

The values obtained, considered somewhat preliminary in nature, were as follows:

Samples to Show DF Between	Avg. DF	Number of Determinations
Reactor water, and steam before dryer	4,900	1
Reactor water, and steam after dryer	5,100	9
Reactor water, and condenser (hotwell)	2,330	8
Reactor water, and after prefilter	1.35	1
Reactor water, and after ion exchanger	120	1

In later measurements of the DF between the reactor water and the steam after the dryer, the average of 5.9×10^3 was obtained; and in a still later series using higher activity in the water, the average value of 4.7×10^3 was obtained.

In all tests the DF between reactor water and condensate from the condenser was lower than that of the steam. This was due to the fact that all drainage is dumped into the condenser.

In a later investigation,(204) sodium was added, to act as a tracer after neutron activation to Na^{24}, to determine the decontamination factor in EBWR at 20, 30 and 40 Mw of thermal power. Samples of reactor water, of condensed steam before the steam dryer and of condensed steam after the steam dryer were taken at the three different power levels. The data were interpreted, Table 6.15, as decontamination factors and apparent steam qualities.

Table 6.15

STEAM QUALITY AND CARRYOVER IN EBWR

Wt. % Moisture Steam			Decontamination Factor* Steam		
Thermal Power (Mwt)	Before Dryer	After Dryer	Before Dryer	After Dryer	Across Dryer
20	0.062	0.032	1600	3110	1.94
30	0.133	0.06	754	1660	2.2
40	23.2**	0.6	4.3	167	38.8

$$* \quad \frac{\text{Sodium Activity in Reactor Water}}{\text{Sodium Activity in Steam at Sample Point}} = DF$$

**The high moisture content at 40 Mwt is attributed to slugs of water leaving the reactor. This occurred because of high reactor water level during the test. (This footnote came from a later reference.(24))

Boiling decontamination at the highest power (40 Mw) proved very poor. The steam dryer, in this case operating at 200% of design, proved surprisingly effective. At lower powers (i.e., steam flow) the dryer does not appear to be necessary since entrainment is very small. Carryover in EBWR in the range tested increases with power. A later reference[24] attributes the high carryover at 40 Mw to high reactor water level during the test.

Decontamination factors between reactor water[201] and steam were obtained during the defect fuel test from the gamma-ray spectra. Values quoted in Table 6.16 are approximate because steam samples were not counted for a sufficiently long period. The Na^{24} value is in good agreement with those obtained previously.

Table 6.16

DECONTAMINATION FACTORS IN EBWR BASED ON Na^{24} AND Co^{58}

Nuclide	Reactor Water-Steam Photo Peak Counted	DF
Na^{24}	1.37 Mev	3.2×10^3
Co^{58}	.81 Mev	3.6×10^3

3. Radiochemical Studies

During the winter of 1958-59 radiochemical investigations[169] in EBWR gave the following results: The major long-lived activities which were found associated with crud taken from various locations in the reactor are given in Table 6.17. The values are given in terms of disintegrations per minute per milligram of iron.

Table 6.17

DEPOSITED CRUD ACTIVITIES IN EBWR

Source and Date	Activity (dpm/mg Fe)			
	Co^{58}	Co^{60}	Mn^{54}	Sb^{124}
Crud from Ion-exchange Prefilter, 11-7-58	6.0×10^6	9.0×10^5	4.1×10^6	1.1×10^6
Forced Circulation Thimbles, 11-7-58	2.7×10^7	1.3×10^7	4.2×10^6	5.4×10^5
Scale from Fuel Element, 12-4-58	3.5×10^8	9.6×10^7	3.7×10^6	6.3×10^6
Scale from Dummy Element, 12-4-58	3.8×10^7	4.1×10^7	1.2×10^7	1.0×10^6

All of the above crud samples yielded, in addition to the major activities listed, small amounts of Zr^{95} and Hf^{181}, the latter being the more predominant of the two. These two nuclides are assumed to result from activation of zirconium in the cladding and hafnium in the control rods. The source of the Sb^{124} is unknown.

The water borne activity found in EBWR is typical of that which would be found in a system containing significant amounts of aluminum. Examples of the short lived nuclides which characterize an aluminum and steel system are 2.4 minute Al^{28}, 2.6 hour Mn^{56}, and 15 hour Na^{24}.

Their mode of production is as follows:

$$Al^{27}\ (n, \alpha)\ Na^{24},\ t_{1/2} = 15 \text{ hours}$$

$$Al^{27}\ (n, \gamma)\ Al^{28},\ t_{1/2} = 2.3 \text{ minutes}$$

$$Mn^{55}\ (n, \gamma)\ Mn^{56},\ t_{1/2} = 2.58 \text{ hours}$$

EBWR water samples observed with an automatic recording 200-channel gamma scintillation spectrometer, following the decay of N^{16}, showed two major gamma peaks at 1.37 and 2.75 Mev which identify Na^{24} as the major activity.

The Na^{24} activity was not carried by particulate material present in the water. This was shown by passing the water sample through a millipore filter and observing the activity in the filtrate and that retained on the filter. A thoroughly washed filter was completely free of Na^{24} and the original amount of Na^{24} in the sample was accounted for in the filtrate. Figures 6.9a and 6.9b show typical decay curves of the gross activity in the reactor water, the activity remaining after filtering and the activity retained on the filter.

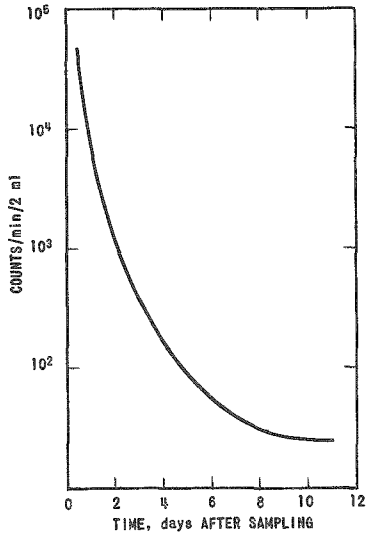

Fig. 6.9a

EBWR Reactor Water Activity Decay Curve

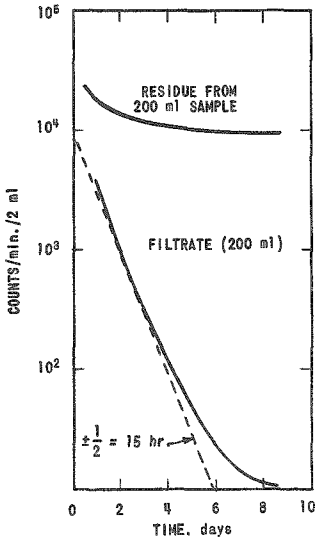

Fig. 6.9b

EBWR Reactor Water Activity Decay Curves, after Filtering

Radiochemical analysis of the insoluble material retained on the filter yielded Co^{58}, Co^{60}, Fe^{59}, Mn^{54} and Cr^{51} as the major active components. Although zirconium as Zircaloy-2 was widely used in the core, only trace amounts of Zr^{95} could be found in the system.

4. Nitrogen-16

The primary activity originating from water itself is N^{16}, produced by the following reaction:

$$O^{16}(n,p)\ N^{16} - 9.5\ \text{Mev}$$

$$N^{16} \xrightarrow[7.35\ \text{sec}]{\beta} O^{16*} \xrightarrow[\text{inst}]{\gamma} O^{16}$$

Only fast neutrons 10.0 Mev - 18 Mev are effective, with a maximum cross section of 89 mb at 14 Mev.(205) The average cross section for the fission neutron spectrum has been reported as 0.019 mb,(202) and 0.0185 ± 0.0015 mb.(203) The energies of the betas are 68% as 4.3 Mev, 26% as 10.4 Mev; the gammas: 73% as 6.13 Mev, and 5% as 7.12 Mev.(206) The O^{16} isotope occurs naturally to the extent of 99.76%.

During operation of a boiling water reactor the N^{16} accounts for most of the activity coming from parts of the system external to the pressure vessel. Compared to a pressurized water reactor, less shielding is required on the external piping system of a boiling water reactor because steam velocities are high and density is low relative to water. For the same power the pipes contain relatively little activated water.(207)

Due to the 7.4 second half life this activity has little effect on normal maintenance work after shutdown. Table 6.18 lists the surface activities attributed to N^{16} at various power levels for EBWR.(24)

Table 6.18

EQUIPMENT SURFACE ACTIVITIES IN EBWR ATTRIBUTED PRIMARILY TO N^{16}

Location	Activities, mr/hr			
	Reactor Power			
	10 Mwt	20 Mwt	40 Mwt	61.7 Mwt
Air Ejector after Cooler	90	400	4000	7000
Condenser Hot Well	10	40	240	580
Steam Dryer	80	150	600	720
Turbine Exhaust Casing	2	4	14	20
Feedwater Filters	8	10	50	100
Plant Air Exhaust	6	12	40	120

a. Calculation of Expected Dose Levels. During the design stage of EBWR shielding, calculations were made of expected dosage levels due to N^{16} activities. It was subsequently found that the results did not correlate well with actual measured operating values. This led to a study by Gibson and Kershaw(208) to find a more satisfactory method. A more successful method was found, based on a calculation procedure referred to as "Non-Sweep, Perfect-Mixing." For this procedure it was assumed that the activated N^{16} retains the same molecular form which it had prior to activation; that is, one pound of steam carries off an amount of N^{16} activity equal to the amount contained in one pound of reactor water. It was further assumed that in the steam dome of the reactor vessel, the N^{16} diffuses completely and reaches an average activity level before being discharged to the steam line. Figure 6.10 shows graphically the steam line measured activity, and calculated activity by the "Non-Sweep - Perfect-Mixing" calculation as a function of reactor heat load. It has been determined that by multiplying the calculated values of activity by a factor of 3.1, the actual measured values are obtained. The authors believe that due to the nature of the calculations, the multiplying factor of 3.1 is applicable to other boiling water reactors of the same general arrangement as EBWR, but that a suitable factor of safety should be used.

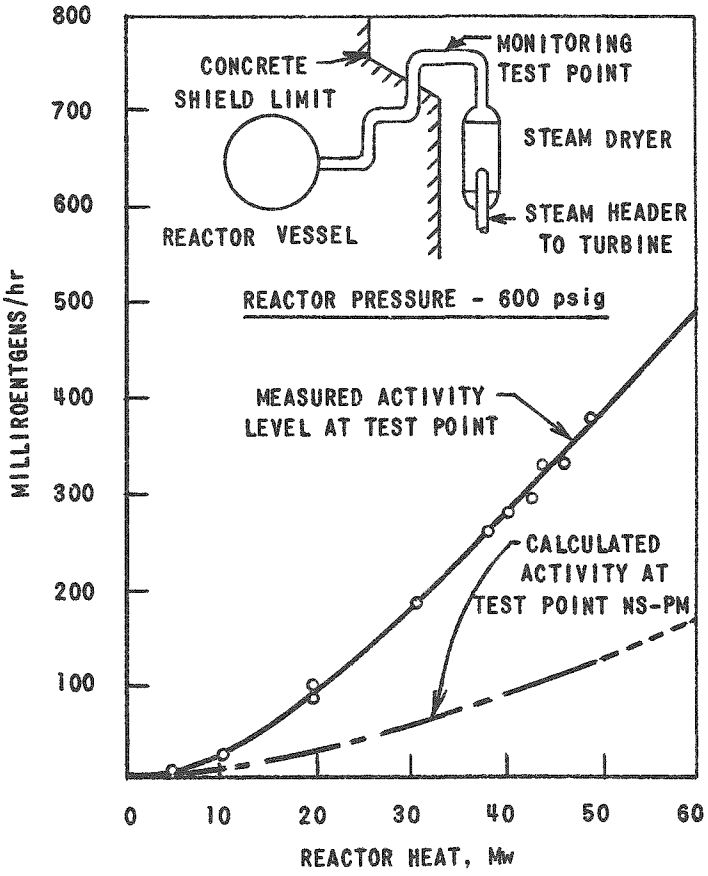

Fig. 6.10

Calculated vs Measured N^{16} Activity in EBWR

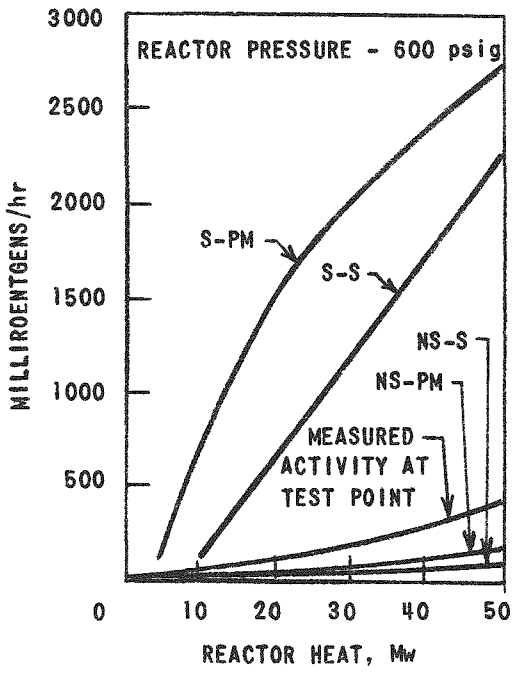

Fig. 6.11
Calculated N^{16} Activity Levels in EBWR Compared

Figure 6.11 shows graphically the results of all methods of calculations performed, and shows that the results do not correlate very well with the measured curve, with the exception of the "Non-Sweep, Perfect-Mixing" case.

The four calculation procedures are defined as follows:

(1) Sweep, Perfect-Mixing (S-PM). This type of calculation assumes that all of the N^{16} generated in the core is swept out of the water, and leaves the core with the steam. The "Perfect-Mixing" implies that in the steam dome of the reactor vessel, the N^{16} diffuses completely and reaches an average activity before discharging to the steam line.

(2) Sweep, Slug-Flow (S-S). This type of calculation is identical with (1) above except that in passing through the reactor steam dome, the steam is assumed to decay by a factor of $e^{-\lambda t}$. (λ is decay constant, t is time since irradiation, e is logarithm base.)

(3) Non-Sweep, Perfect-Mixing (NS-PM). The assumption in this calculation is that the activated N^{16} retains the same molecular form which it had prior to activation; that is, one pound of steam carries off an amount of N^{16} activity equal to the amount contained in one pound of reactor water. "Perfect-Mixing" is defined the same as in (1) above.

(4) Non-Sweep, Slug-Flow (NS-S). Same as (3) above for NS, and same as (2) above for S.

An examination of the effect of various parameters, such as average fast virgin flux (fission spectrum before collision), recirculation ratio, exit voids, etc., indicated that except for the flux, fairly large errors can be tolerated in these parameters without materially affecting the results. The average fast virgin flux is not known accurately and may be as much as 40% low; this will affect the results as a straight multiplying factor.

An attempt was made to obtain correlation between reactor pressure and N^{16} activity, but the measured data were too incomplete to justify inclusion in the report. The report should be consulted for the mathematics used. The high degree of success in correlating predicted dosage rates with measured operating values resulted from using a "non-sweep" mechanism. This affords some insight into the N^{16} distribution, indicating that a high percentage of the N^{16} activity remains with the water rather than being stripped out with the steam.

b. Activity Distribution. Mittl and Theys(209,210) investigated N^{16} activity distribution in the EBWR.

(1) Experimental. In order to understand the mechanism controlling the amount of N^{16} in the steam vs that in the water, measurements were made of the absolute concentration in the water and steam within the reactor vessel. To measure the activity in the water (or steam) a continuous sample was brought outside the reactor vessel by sampling tubes. After cooling, the sample passed to a flat coil in front of a scintillation counter. The pulses produced in the counter were analyzed in a single channel pulse height analyzer and the activity of N^{16} was discriminated. The pulses counted were those whose energy was greater than 4.5 Mev. Verification that the counting rate was caused by N^{16} was obtained from a spectrum of the radiation and the half life of the activity obtained from the decay curve.

In order to determine the concentration of N^{16} per gram of coolant for a given point in the reactor vessel, a standard Co^{60} solution was introduced into the counting coil, and a calibration made with adjustment for γ-ray energies.

It was necessary to apply certain corrections to the count rate indicated by the scintillation counter. These corrections concerned the time required for the sample to flow from the probe to the counter, the decay of N^{16} during the flow through the counting core, and the non-condensable gas content of the sample. In determining the relative amounts of anion and cation species of N^{16}, three beds, anion, cation, and inactive, were employed. Since the particle and bed sizes were equivalent in the three cases, the differences in flow delay time and resulting decay were minimized.

Experiments were made over a range of reactor pressures and power levels and included the use of several known chemical additives. Since N^{16} was known to be produced in the core by a nuclear reaction, Mittl and Theys believed that it must appear as a recoil atom with varying degrees of ionization. As such it was expected to exist in combination with oxygen and hydrogen atoms present in the coolant. Since the reactor water was of high purity with a conductivity of 2 μmhos, it

seemed unlikely that the N^{16} would be combined with any impurity. Some chemical forms that seemed probable, for combination between N^{16} and oxygen and hydrogen, were as follows:

Anion species, NO_2^-, NO_3^-;

Cation species, NH_4^+;

Neutral species, NO, NO_2.

Since the N^{16} concentration was very low, it seemed unlikely that an ion contained more than one of the radioactive nuclides.

(2) Results. It was concluded that after its production N^{16} combines mainly in an anion form which remains in the water. The N^{16} was detected only as a cation and neutral species in the steam. Any anion species which might have been present in the steam could not be determined without the experimental accuracy. No neutral species containing N^{16} could be detected in the water. The concentration of the latter in water was relatively small due to the recirculation ratio of about 50 to 1 at 20 Mw and the almost complete stripping of the gaseous compounds.

Under normal operating conditions N^{16} was present in the water as anion and cation species in the ratio of about 7 to 1, see Figure 6.12. In the steam, the ratio of neutral to cation species decreased with increasing reactor power, see Figure 6.13.

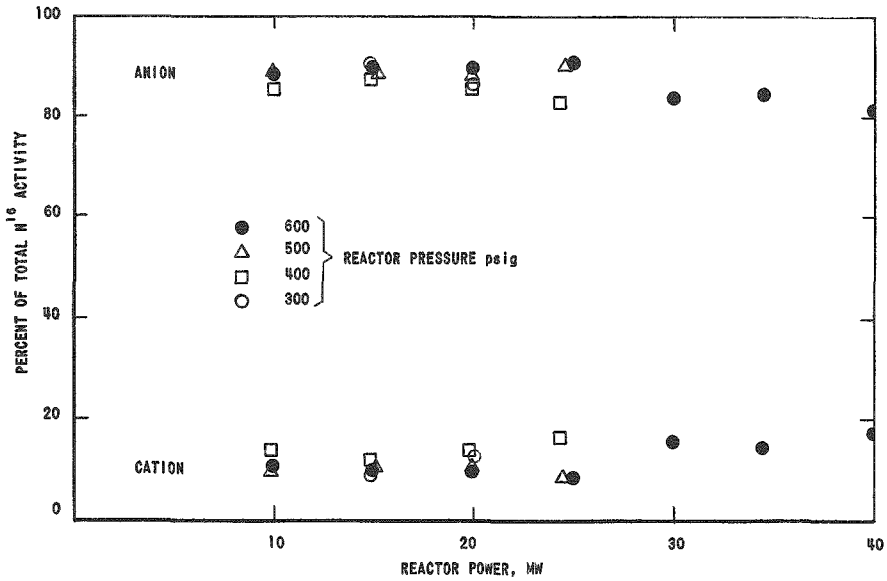

Fig. 6.12

Per Cent of Cation and Anion Species of N^{16} in EBWR Reactor Water 52 inches above Fuel

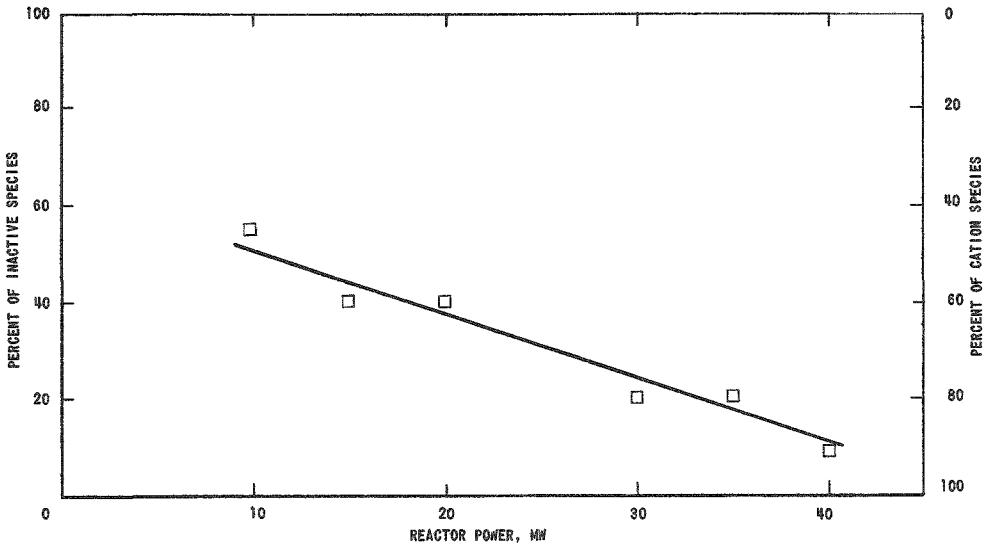

Fig. 6.13

Per Cent of Inactive and Cation Species of N^{16} in EBWR Steam 92 inches above Fuel

(a) Effect of Chemical Additions. Various additives were introduced into the reactor feedwater to study their effect on the distribution of N^{16} between anion and cation species and their partition between water and steam. Nitrogen, oxygen and argon had no apparent effect on the ionic form of N^{16} and hence on steam activity.

The addition of hydrogen, hydrazine, and ammonia decreased the ratio of anion to cation species in the water. In each case the activity in the steam and plant increased above the normal value. The increase in steam activity with hydrogen addition at two different power levels is shown in Figure 6.14. At 20 Mw, 600 psig, and 489°F reactor operation, the addition of 40 cc H_2/liter of feedwater resulted in a shift to nearly equal proportions of anion and cation species in water. At the same time the steam activity, as well as the steam and condensate system monitor indications, increased by a factor of four. No change was observed in the total water activity since the amount of N^{16} in the steam was still a small fraction of the amount produced.

(b) Effect of Power, Pressure and Water Level. Concentrations of N^{16} at specific points in the reactor water above the core, and in the steam contained in the upper portion of the reactor vessel were determined as a function of reactor power. In the water, 52 inches above the fuel, the concentration was approximately proportional to reactor power, see Figure 6.15; in the steam, 92 inches above the fuel, the concentration was proportional to the square of the power, see Figure 6.16.

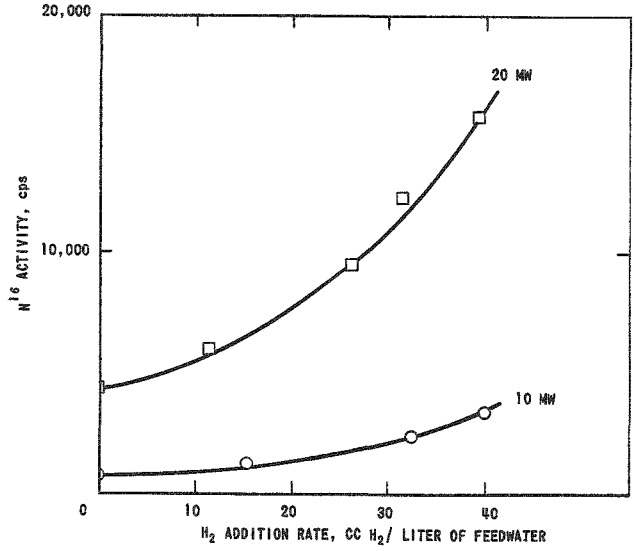

Fig. 6.14

Effect of Hydrogen Addition on N^{16} Activity in EBWR Steam 112 inches above Fuel

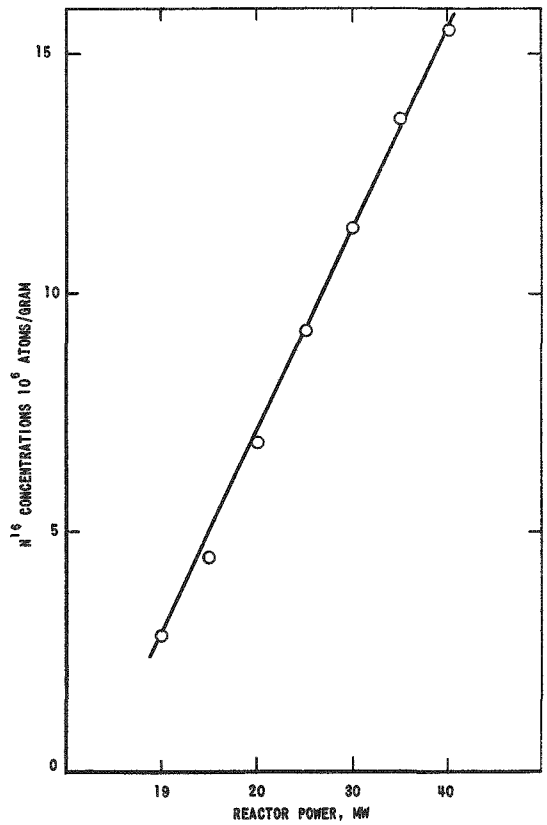

Fig. 6.15

N^{16} Concentration in EBWR Reactor Water 52 inches above Fuel

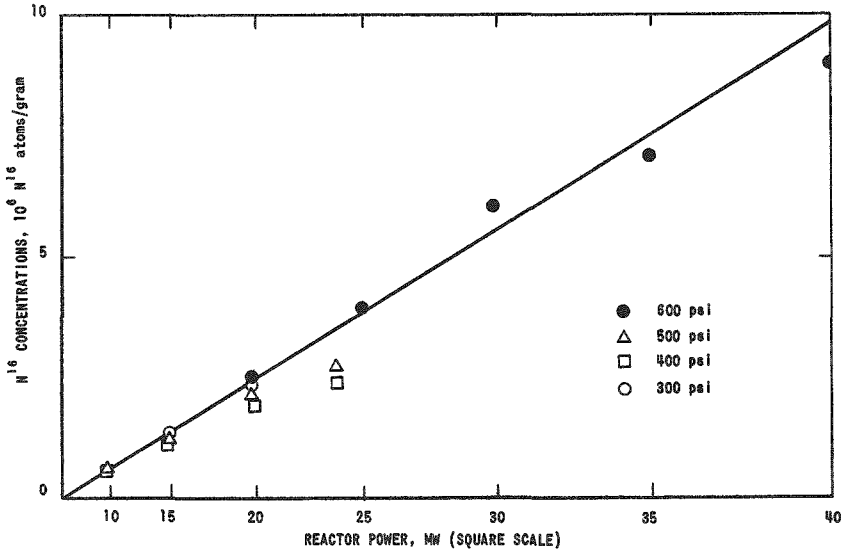

Fig. 6.16

N^{16} Concentrations in EBWR Steam at Various Operating Pressures 92 inches above Fuel

The effect, if any, of reactor operating pressure on the water and steam concentration of N^{16} and relative amount of anion and cation species in the water was not detectable. The activity of the steam in the system external to the reactor vessel increased with decreasing pressure due to increased steam velocities.

The amount of N^{16} present at a given elevation in the reactor water increased, and in reactor steam decreased, as the water level within the vessel was lowered. (This provided the basis for a method of determining the water and steam levels in the reactor and determining the thickness of the disengagement layer.(211)) These changes may be accounted for by consideration of the manner in which steam and water velocities within the vessel, and thus N^{16} decay, vary with reactor water level.

(c) N^{16} Distribution Between Steam and Water.

The ratio (α) of N^{16} contained in a gram of steam to N^{16} contained in a gram of water increases with the addition of certain chemicals and an increase in reactor power. Work at BORAX-III showed that decreasing reactor water pH increased α.(19)

The three conditions of reactor operation which caused an increase in α also caused an increase in the mass flow of hydrogen gas through the reactor water region above the core.

If it is assumed that the distribution of N^{16} between anion and cation species is a function of chemical equilibrium established in part by hydrogen gas concentration, it is possible to account for part of the variation in α.

Part of the N^{16} activity existing as cations is volatile permitting its appearance in the vapor phase. Opposed to this, N^{16} activity existing as anions remains in the liquid phase. If an increased amount of hydrogen gas results in the formation of more cations at the expense of anions, any condition of reactor operation that increases hydrogen concentration will increase α.

But this is not the only source of variations in α. An increase in reactor power is accompanied by an increased tendency for N^{16} cations to leave the liquid phase. The fraction (β),* by which the N^{16} cation concentration in water decreases upon formation of steam, varies with reactor power. This fraction (β) was shown to be independent of the absolute concentration of the cation form; at 20-Mw thermal, β remained unchanged during the addition of hydrogen gas which increased the absolute concentration of the cation form.

*Note: $\beta = \dfrac{N^{16} \text{ in cation form in the steam}}{N^{16} \text{ in cation form in the water}}$.

The value of β appears to be a function of a power dependent variable of this reactor. It is theorized that the amount of the cation form of N^{16} transported from the liquid to the vapor phase is related to the void fraction and to the probability that a cation species in water will approach a water-steam interface.

(3) Conclusions. Mittl and Theys concluded that in a boiling water reactor, the decontamination factor for N^{16} is a variable. It is a function of the hydrogen gas concentration and appears to be a function of the void fraction.

For EBWR, at 20 Mw and normal operating conditions, the average concentration of N^{16} was experimentally determined to be about 7.0×10^6 atoms per gram of water in the water 52 inches above the fuel, and 2.5×10^6 atoms per gram of steam in the steam phase 92 inches above the fuel. Because of the combined effect of the high recirculation ratio and the smaller than unity ratio of steam to water N^{16} concentration, the amount of N^{16} which leaves the reactor vessel with the steam at 20 Mw is less than 1% of the total N^{16} produced.

The addition of hydrogen gas to the reactor feedwater has indicated that it is possible to arrive at the condition where N^{16} concentration in steam equals or surpasses the concentration in water. No method is suggested to bring about the reverse, i.e. decrease the N^{16} in the steam below normal levels.

5. Tests of Defected Thoria-Urania Fuel Specimens

Robertson has described tests of defected thoria-urania fuel specimens in EBWR.(196)

a. Objectives. Tests were made in EBWR to:

(1) Study the rate of release of fission products from a defective 90: 10:: ThO_2: $UO_{2.1}$ fuel element.

(2) Study the distribution of these fission products throughout the reactor system.

(3) Evaluate the hazards involved in operating a boiling water reactor fueled with a ceramic fuel with defects in the cladding.

b. Experimental.

Test 1 was made on a small specimen, 5 pellets in a 3.1 in. long tube of stainless steel sealed at the ends but with a 0.01 in. diameter hole drilled through the wall at the center of the fuel. This test was run to determine the magnitude of the radiation levels to be encountered.

Test 2 was performed on a longer fuel tube 48 in. long containing 82 pellets, with a 0.02 in. diameter hole through the wall opposite the top pellet.

Burnups achieved in tests 1 and 2 were 1.2 and 3.2 atom % U^{235} respectively; and surface heat fluxes achieved were 1.65×10^5 and 1.52×10^5 Btu/hr ft^2 respectively.

The release rate of the fission gases was determined by taking samples of the exhaust gases from the air ejectors. When each sample was taken, the flow rates of the exhaust gases were measured. These samples were then analyzed for individual nuclides either by chemical means or by γ-ray spectrometry using a 200 channel γ-ray pulse height analyzer.

During test 1 only release rates of Xe^{138} and Kr^{88} were measured. During latter part of test 2 data were obtained on Xe^{138}, Kr^{88}, Kr^{85m}, Xe^{135} and Xe^{133}. During both tests samples of reactor water were analyzed by conventional radiochemical means for fission products. Samples of reactor water and ion exchanger effluent were taken throughout the test for gross β-γ count rate and decay was followed periodically on a gas flow proportional beta counter.

During both tests samples of various metals were placed both in the steam line and in the condenser to determine both the extent to which corrosion occurred and the extent to which fission products were deposited on their surfaces. At the completion of each test both sets of samples were removed and were counted in a 256-channel γ-ray pulse height analyzer.

Four stainless steel tubes were inserted through swagelock fittings in the head of the reactor vessel. Each tube was placed to withdraw water from a specific location, either from above the fuel element containing the defect specimen, or from adjacent or far removed fuel elements containing no defect.

Reactor water was passed through these tubes, cooled and passed either to a delayed-neutron monitor or to a cation ion-exchange bed. Beyond the bed the activity of the water could be monitored and measured by a NaI(Tl) scintillator connected to a photomultiplier tube and a single-channel γ-ray pulse height analyzer.

The delayed neutron monitor counted neutrons, after thermalization in a tank of water, by means of a BF_3 tube connected to a linear amplifier, discriminator, and count-rate meter.

The second monitor, the "Iodine Monitor," operated on the principle that the cation bed removed cationic and filterable activities from the water, leaving only rare gases and anionic species such as radio-iodines. Gamma rays from the rare gases, which are of low energy, could be discriminated against by setting the discriminator level to count only pulses with energies greater than 900 kev, and thus the monitor should "see" only radio-iodines or -bromines in the reactor water.

c. Results. The results are discussed below under ten different subdivisions as follows:

(1) General Plant Radiation Levels. During both tests, with one exception noted below, the radiation levels registered by various instruments throughout the system were no higher than normal. The air ejector monitor normally, when no defective fuel specimens were present, registered a smooth rise in counting rate to a new level as power was increased.

Behavior during test 1 was normal. In test 2, it was found that if the control rod nearest the defected specimen was moved so as to increase the neutron flux in that specimen, a burst of activity was emitted as indicated by a peak in the counting rate of the gamma-ray monitor at the air ejectors. This phenomenon was not observable on movement of any other rod.

(2) Fission Products in Reactor Water - Effect of Ion Exchange Resins. A flow of about 10 gpm was maintained through the ion exchange circuit. Actually in any one experiment this rate slowly fell off, due mainly to the clogging of filters located before the resins by corrosion products.

The decontamination factor (DF) across the resin may be defined as the ratio of the influent to effluent specific activity. The DF values for the resin were calculated from the water samples, which were counted for beta decay.

The efficiency of the resins (ϵ) for removing dissolved ions may be expressed as

$$\epsilon = \frac{\text{specific activity of influent - specific activity of effluent}}{\text{specific activity of influent}}. \quad (6.2)$$

For all the nuclides except the fission gases $\epsilon = 1$ in these tests.

In test 1 the DF for the ion exchanger was found to increase steadily as the test proceeded from 235 to greater than 5000.

In test 2 spot checks showed a DF of greater than 5×10^3 throughout.

The rate at which a given nuclide is removed from the reactor water is given by

$$(r\epsilon/v)N \tag{6.3}$$

where

N = number of atoms present in the reactor water;

r = flow rate to ion exchanger;

v = volume of circulating water in reactor;

ϵ = efficiency of resins = 1.

For a given nuclide which is released to the reactor water at a rate R atoms/sec

$$\frac{dN}{dt} = R - \lambda N - \frac{r}{v}N \tag{6.4}$$

where

λ = decay constant.

The magnitude of r/v is about 5.6×10^{-5} sec^{-1} at 10-gpm flow. (This corresponds to a "cleanup half life" of about $3\frac{1}{2}$ hr.) This value is considerably larger than λ for all nuclides with half lives much longer than a few hours. This means that the rate of approach to steady-state activities in the reactor water will be governed, not by the rate of decay of that nuclide, but by the rate of clean-up on the resins. For a steady release rate R, all nuclides should have reached their steady-state levels after one day steady operation at a given power.

The above equation is integrated, with boundary condition $N = 0$, at $t = 0$ to give

$$N = \frac{R}{\lambda + \frac{r}{v}}\left(1 - e^{-\left[\lambda + \left(\frac{r}{v}\right)\right]t}\right) \quad . \tag{6.5}$$

For the case of I^{131} ($t_{1/2}$ = 8.05 days, $\lambda = 9.94 \times 10^{-7}$ sec^{-1}) if there were no ion exchange flow, I^{131} activities would build up slowly over a period of about 50 days to their saturation level, $N = R/\lambda$ atoms. For a flow of 10 gpm, a saturation level of $N = R/[\lambda + (r/v)]$ atoms would be reached in only one day.

Thus steady-state levels of activity are soon reached when the ion exchange is in operation. The magnitude of this steady-state level will depend on the ion exchange flow rate. During these tests this rate was changing slowly but continuously and hence, for proper intercomparison of results, all results must be adjusted for ion exchange flow rate.

All rates are corrected to zero ion exchange flow by multiplying the observed activity by the factor $[\lambda + (r/v)]/\lambda$. The activity so obtained is the ultimate steady-state activity which would be reached if the reactor were operated for long enough steady power with no ion exchange flow.

Activities analyzed for were Cs^{138}, I^{131}, I^{132}, Mo^{99}, Sr^{89} and Ba^{140}. The results indicated the following:

(a) All activities were extremely low in all tests. In fact they were several orders of magnitude below the level of activation products such as Na^{24}, Mn^{56}, and Co^{58} in the reactor water. Typical steady-state activities for these three nuclides at 20 Mw and at 10 gpm ion exchange flow were:

Na^{24} 2×10^5 dpm/ml

Mn^{56} 6×10^4 dpm/ml

Co^{58} 4×10^3 dpm/ml

(b) The results were very erratic, probably largely due to very low activity level.

(c) During test 1, corrected activities were not significantly higher than during operation without a defect. During test 2, activities due to I^{131} were in general higher; activities of Ba^{140} and Sr^{89} were slightly higher; and the activity of Mo^{99} was no higher than during operation without a defect.

(3) Metal Specimens from Steam Line and Condenser. These specimens showed only such activation products as Co^{58} and Co^{60}. No γ-ray peaks which could be ascribed to any fission products were observed. It was concluded that any fission product activities deposited on these specimens must be very small compared to Co^{58} activity.

(4) Examination of Fuel Specimens after Irradiation. All pellets in the element used in test 1 had cracked. In the element used in test 2, pellets from the top 12-inch length of tube were uncracked. From that point cracking became progressively worse until the point of maximum flux, approximately 18-inches above the bottom, was reached. At this point, only severe cracking was in evidence - there were no signs of melting or recrystallization.

(5) Release Rates of Fission Products.

(a) No Defect - Fission Product Gases. Release rates were determined when no defect was present to obtain background information. The low values obtained were attributed to uranium contamination on the surface of the fuel.

The rate of production of fission gas in the uranium oxide contamination is

$$R' = M^{235} FY \tag{6.6}$$

where

M^{235} = mass of U^{235} (mg);

F = fission rate/mg of U^{235};

[fission/(sec)(mg U^{235})];

Y = fission yield of nuclide in question.

Assuming the release rate to the reactor water

$$R = R'/4;$$

then

$$R = M^{235} FY/4;$$

or

$$R/Y = M^{235} F/4.$$

Since M^{235} and F are both constants, the ratio R/Y should be a constant value for all fission gases.

Calculation of the average release rates for various fission gases gave the quotients R/Y shown in Table 6.19. The values of R/Y for all five gases, ranging in half life from 17 min to 5.3 days, are constant within ± 15%.

Table 6.19

FISSION GAS RELEASE RATES IN EBWR
(No Defect)

Fission Gas	Release Rates at 20 MW		R/Y
	curie/day	atom/sec	
Xe^{138}	1.0	6.3×10^{8}	1.1×10^{10}
Kr^{88}	0.053	3.35×10^{8}	0.93×10^{10}
Kr^{85m}	0.012	1.17×10^{8}	0.90×10^{10}
Xe^{135}	0.034	6.98×10^{8}	1.1×10^{10}
Xe^{133}	0.0028	7.90×10^{8}	1.2×10^{10}
			Avg. $(1.05 \pm 0.15) \times 10^{10}$

In EBWR operating at 20 Mw the value of F was about 8.7×10^9 fissions/(sec)(mg U^{235}). Using this value the weight of U^{235} contamination in the reactor was calculated to be about 5 mg, if it is assumed that only 25% of the fission fragments reach the water.

(b) No Defect - Other Fission Products. Neither I^{131} nor Mo^{99} would be stripped from the water, but instead would decay there. Assuming that they were released at a rate corresponding to R/Y = 1.0×10^{10} fissions/sec, the calculated steady-state activities are compared with measured values in Table 6.20.

Table 6.20

STEADY-STATE I^{131} AND Mo^{99} ACTIVITIES IN EBWR

Nuclide	Y	Calculated Activity dpm/ml	Measured Activity dpm/ml
I^{131}	0.029	1500	200-400
Mo^{99}	0.061	3200	~1700

The measured Mo^{99} values were low by a factor of 2 as compared to the calculated value, and the I^{131} values were similarly low by a factor of 4-7. The reason for this discrepancy is not known but may be due to both nuclides depositing to a considerable extent on surfaces and not remaining in solution.

(c) During Defect Tests - Fission Gases.

Test 1 - It was observed that both Xe and Kr release rates fell steadily as the experiment progressed. This was attributed to a gradual plugging of the 0.010 inch diameter hole through the sheath. This effect was not observed in test 2 where the hole was 0.020 inch in diameter.

Test 2 - Steady release rates of the various fission gases at steady power during test 2 are listed in Table 6.21. Only values which were consistent over many days of operation were taken. For Xe^{135} and Xe^{133} no data for operation at 10 Mw could be obtained since the release rates fell steadily over the operating period.

Observed release rates are corrected by subtracting release rates observed when no defects were present. It was assumed that the background release rate was proportional to reactor power. The release rate at 20 Mw was used to determine the proportionality constant.

Release rates are very small when compared to formation rates of the fission gases in the oxide. This is illustrated in Table 6.22, where formation and release rates at 20 Mw are compared.

Table 6.21

FISSION GAS RELEASE RATES IN EBWR - TEST 2

Nuclide	Xe^{138}	Kr^{88}	Kr^{85m}	Xe^{135}	Xe^{133}
Fission Yield, per cent	0.057	0.036	0.013	0.064	0.065
Observed Release Rate, curie/day					
10 Mw	0.5	1.4	0.07	-	-
20 Mw	1.2	0.43	0.18	0.13	0.035
23 Mw	1.4	0.59	0.22	0.15	0.043
26 Mw	1.6	0.62	0.23	0.175	0.054
Release Rate - No Defect, curie/day					
10 Mw	0.5	0.027	0.006	0.017	0.0014
20 Mw	1.0	0.053	0.012	0.034	0.0028
23 Mw	1.15	0.061	0.014	0.039	0.0032
26 Mw	1.3	0.069	0.016	0.044	0.0042
Corrected Rate, curie/day					
10 Mw	-	0.113	0.064	-	-
20 Mw	0.2	0.377	0.168	0.096	0.0322
23 Mw	0.25	0.529	0.206	0.111	0.0398
26 Mw	0.3	0.551	0.214	0.131	0.0498
Corrected Rate x 10^8 atom/sec					
10 Mw	-	7.05	6.25	-	-
20 Mw	1.26	23.5	16.4	19.7	91.0
23 Mw	1.57	32.8	20.1	22.8	112
26 Mw	1.89	34.3	20.9	26.8	140
R/Y x 10^{10} fission/sec					
10 Mw	-	2.0	4.8	-	-
20 Mw	0.22	6.5	12.6	3.1	14.0
23 Mw	0.28	9.1	15.4	3.6	17.2
26 Mw	0.33	9.5	16.1	4.2	21.5
$1/\sqrt{\lambda}$, $sec^{1/2}$	38	120	151	*	812

*168 at 20 Mw.
159 at 25 Mw.

Table 6.22

COMPARISON OF FORMATION AND RELEASE RATES OF FISSION GASES IN EBWR AT 20 Mw REACTOR POWER

Nuclide	Half Life	Formation Rate atom/sec x 10^{-13}	Release Rate atom/sec x 10^{-9}	Release Rate / Formation Rate (x 10^4)
Xe^{138}	17 minutes	1.6	0.13	0.08
Kr^{88}	2.8 hours	1.0	2.4	2.4
Kr^{88m}	4.4 hours	0.36	1.6	4.5
Xe^{135}	9.2 hours	1.8	2.0	1.1
Xe^{133}	5.27 days	1.8	9.0	5.0

Obviously only an extremely small fraction (< 0.01%) of any fission gas formed in the fuel was escaping through the defect

This table indicates that the value of R/Y is no longer a constant as it was when no defect was present, and indicates a general trend that relatively more fission gas escapes as the half life increases. This is illustrated in Fig. 6.17 in which the quotient R/Y is plotted against $1/\sqrt{\lambda}$ in which λ is the decay constant for a particular nuclide. The figure shows that at 20 Mw the points for radio-xenons fall on a reasonably straight line passing through the origin. The points for radio-kryptons appear to fall on a separate line of higher slope. Similar behavior is seen at 26 Mw. Evidence is given to show that this relationship is consistent with release of gases through the oxide by a diffusion controlled mechanism.

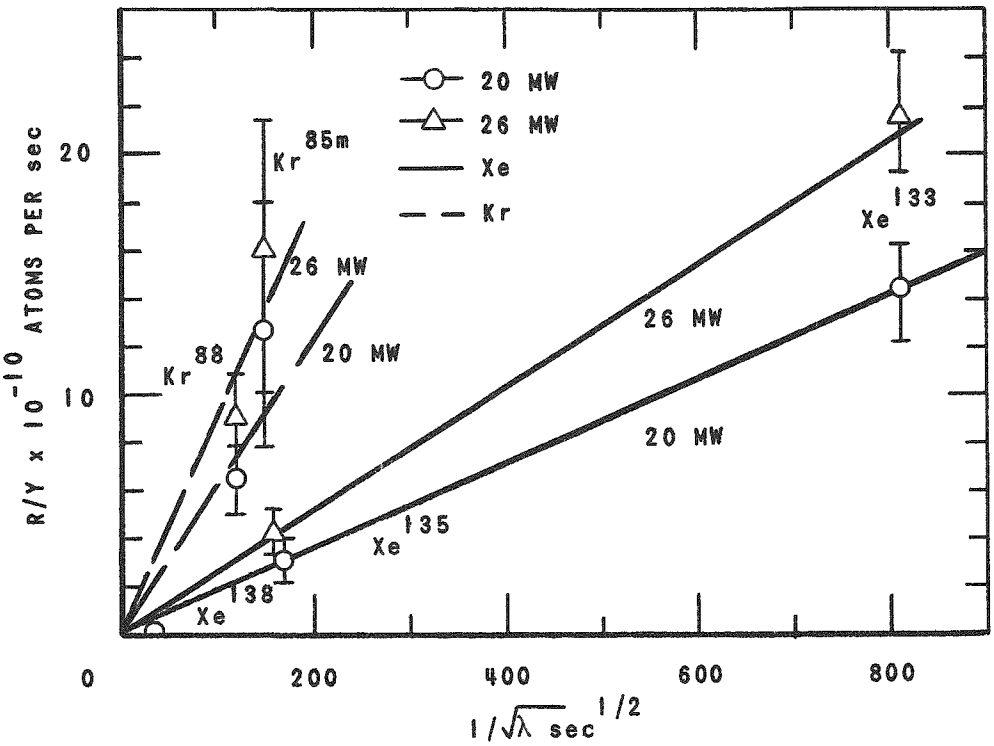

Fig. 6.17

R/Y vs $1/\sqrt{\lambda}$ EBWR Defect Test No. 2

(d) During Defect Tests - Other Fission Products. By assuming that I^{131} and Mo^{99} fit the plot of R/Y vs $1/\sqrt{\lambda}$ found to be true for the fission gases in the EBWR experiments, release rates R, can be calculated. From these R values saturation activity levels were calculated and compared with observed steady-state activities. Results showed that these two nuclides were released to the water at a rate 20 to 200 times more slowly than would be expected from fission gas release rates.

With no defect present the lower amounts of I^{131} and Mo^{99} were attributed to deposition of these nuclides on internal surfaces. Part of the discrepancy observed when a defective fuel element was present is probably due to this effect, but it is highly doubtful whether all of it is. Thus, it must be concluded that nuclides such as I^{131} and Mo^{99} without a fission gas precursor were released from the defect at a significantly lower rate than were the fission gases.

(6) Transient Effects After Power Changes. The short-lived fission gas release rates in the EBWR fuel defect tests were reasonably constant at a given power level and rose and fell with power changes in the manner expected. When reactor power was increased, the release rates of all fission gases showed the same transient behavior immediately after the power change that had been observed on the air ejector monitor. The magnitude of the peak increased as the half life of the nuclide increased.

When the reactor power was lowered, an additional effect was observed. Immediately after the power was lowered, all release rates fell to a very low level. Then the shorter-lived gases rose to their equilibrium levels, but the release rates of the long-lived gases rose over the next day or so to new levels which were much higher than the original levels. Then over the next few days the release rates fell off slowly to new values.

The sharp burst of activity released during reactor startup or after increases in power have been observed previously in irradiation of defective ceramic fuel elements. It is believed to be due to presence of a reservoir of fission gases in the space between fuel and sheath. Under steady conditions these fission gases are released at a steady state. With an increase in power, the temperature of the fuel was increased, and the pressure inside the sheath probably increased to a value above the reactor operating pressure for a short period, thus emitting a burst of fission product gases.

On startup, the space would be initially filled with water, and when this was turned to steam, there would be a corresponding pressure rise and escape of steam through the defect, carrying with it fission product activities leached from the oxide surface.

After power decrease, two effects were observed. Immediately after reduction in power, all release rates fell sharply. Then the release rates of shorter-lived gases returned soon to a level. Release rates of longer-lived gases continued to increase for a few days, then they fell back to new low steady rates.

The initial drop can be attributed to a brief contraction of gases within the sheath following a power decrease. However, equilibrium with operating pressure would soon be reached again and the gases should be released at a new steady rate depending on power level.

A possible explanation for the increasing then decreasing long-lived fission gas release rates might be that the fuel cracked during this transient. Another possibility is that the increased rate might be caused by escape of longer-lived gases from pores which were originally closed but were opened after the cracking.

(7) Comparison with Other Fuel Defect Tests.

(a) VBWR. Brutschy and Osborne[212] have reported results obtained during experiments similar to those performed in EBWR. Their results were obtained with UO_2 ceramic fuel sheathed in Zircaloy-2 and were obtained with naturally occurring defects. A comparison of the data with EBWR results indicates that the background activity due to uranium contamination was slightly higher in VBWR than in EBWR; and that radio-iodines were released to a far greater extent in VBWR than in the EBWR. In the presence of a defective fuel element, reasonably linear dependence of R/Y on $1/\sqrt{\lambda}$ was obtained as was found in EBWR. In contrast to results in EBWR, however, the kryptons and xenons apparently fall on the same line, the slope of which was considerably steeper than that found in EBWR.

The reason why kryptons are released more readily than xenons in EBWR but not VBWR is not known. The higher release rate of all gases in VBWR is believed due to the higher heat ratings of the fuel.

(b) PWR. P. W. Frank[213] analyzed the data obtained from one year of operation of the Shippingport, PWR, and concluded that one or more of the UO_2 blanket elements was defective during the latter part of the operation. In the PWR, of course, fission product gases are not stripped from the solution but remain in the coolant, where eventually steady-state activities result. Analysis of the data using the R/Y vs $1/\sqrt{\lambda}$ criteria again gave a reasonably linear relationship. Furthermore, qualitatively, the results agree with the EBWR results in that kryptons were released at a greater rate than the xenons. However, in the PWR the radio-iodines again appear much more predominantly than they did in the EBWR test.

There may be significance in the fact that in the EBWR and BORAX-IV experiments where the fuel was a ThO_2-UO_2 mixture, radio-iodines were not released to the coolant in any appreciable quantity, while in VBWR and PWR where UO_2 is used radio-iodine release rates were nearly equal to those of the fission gases.

It is suggested that perhaps ThO_2 retains iodine in the crystal lattice to a greater extent that does UO_2.

(8) Calculations of Long-Lived Contamination. Although long-lived fission product contamination was not observed in the EBWR condenser or in the stack effluent, calculations of steady-state fission product gas activities in various parts of the EBWR system illustrated several important points.

(a) The presence of one defective fuel rod, as used in test 2 actually released short-lived fission product gases (half life less than 17 min) at a slower rate than they were released by the 5 mg of U^{235} contamination in the reactor. Only the longer-lived Xe^{135} and Xe^{133} were released appreciably faster.

(b) Same was true for steady-state fission product gas activities in the condenser. It would take several defects to produce as much short-lived gas activity as that provided by uranium contamination.

(c) Release rates of short-lived gases from the stack, because of the delay involved, were very low and again several defects would be necessary to approach the emission rate from the contamination alone.

(d) None of the fission gases with half life greater than that of Xe^{138} have long-lived daughter products; all are either stable or short lived. Thus, even though the longer-lived gases may have been released to the condenser and from the stack in appreciable quantity, no contamination problem resulted. Because of the great dilution in the outside air, the activity due to the fission product gas itself was insignificant.

(e) Xe^{138} activities were fairly significant in the condenser. Within a few minutes after sampling, all of the shorter-lived activities had decayed and the daughter Cs^{138} was the predominant activity. Hence, the 33-minute half-life activity which was continually found can thus be explained.

(9) N^{16} Activities. Mittl and Theys[209,210] give the formation rate of N^{16} ($t_{1/2}$ = 7.4 sec) in EBWR as 3×10^{12} atoms/sec at 20 Mw. They showed that only about 10% of the N^{16} activity was released to the steam phase. Assuming that N^{16} is entering the steam at a rate of 3×10^{11} atoms/sec, it is possible to calculate the resulting N^{16} activity in the condenser by the methods of the previous section. This showed N^{16} activity in the condenser to be about 0.5 curie. Adding together all the calculated fission gas activities showed a total of only 0.02 curie of fission gas in the condenser, i.e. some 25 times less than N^{16} activity.

It is understandable why, under steady-state conditions, the presence of one defective specimen made no observable change to the counting rate of the monitor at the air ejector.

During startup or during periods when the neutron flux in the vicinity of the defective specimen was increasing, the fission gas evolution rate was increased by at least an order of magnitude during short periods and hence their activities were more significant and could be detected as a peak in the counting rate of the air ejector monitor.

(10) Long-Lived Contamination. The only decay chains which lead to significant long-lived activities are those starting with Kr^{90}, Kr^{89}, and Xe^{137}. Using conventional methods, and assuming a steady activity of fission gas in a given zone, the buildup of daughter products was calculated. Figure 6.18 shows the calculated buildup of long-lived activities outside the stack. The data in this figure were calculated on the assumption that one defective specimen in addition to 5 mg of U^{235} contamination were present.

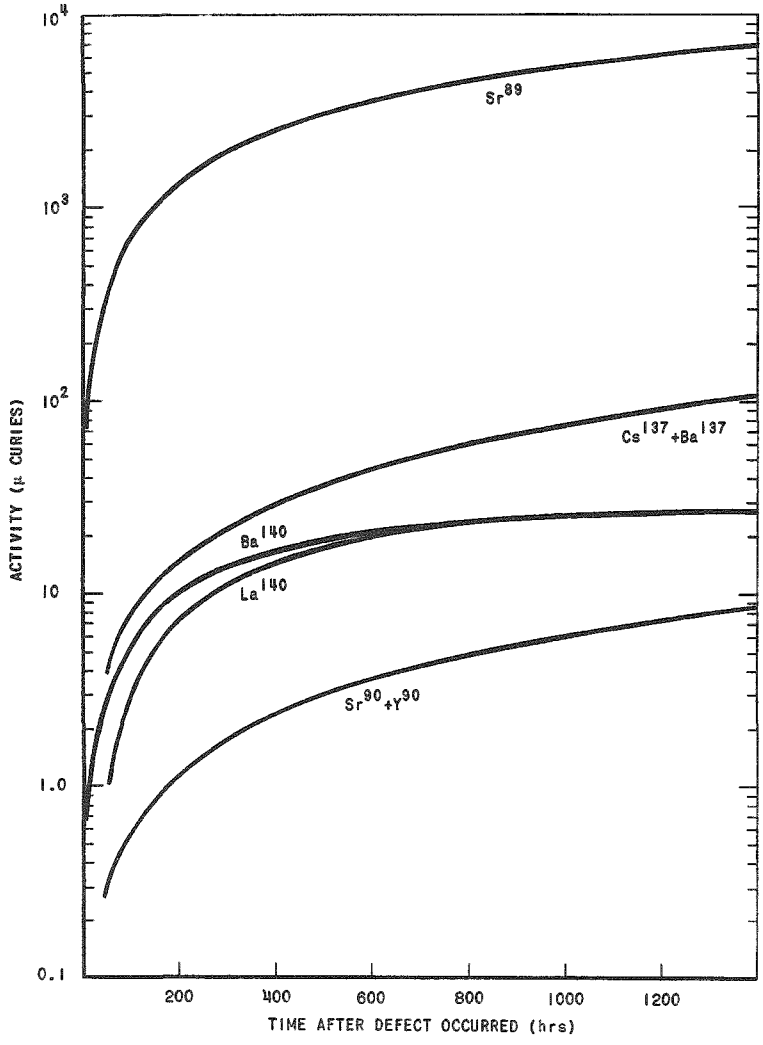

Fig. 6.18

Long-Lived Contamination from EBWR Stack

The same calculation was not done for the condenser because undoubtedly the cesiums and strontiums, which are decay products in the chain, would be washed from the condenser surfaces to the hotwell and would be returned to the reactor, whence they would eventually find their way to the ion-exchange resins. While nuclides, such as Sr^{89}, were found in the reactor water to a very small extent, none could be detected in the steam lines or in the condenser.

Obviously these amounts of activity scattered over the surrounding countryside would lead to negligible contamination levels. The highest contamination level in the EBWR, due to 51-day Sr^{89} after 1400 hours of steady operation, was roughly 7 millicuries. It must be remembered that 50% of this was a result of uranium contamination in the reactor and only the remaining 50% was due to the defect. Sr^{90} levels after the 1400 hours of steady operation amounted to less than 10 microcuries, and of this only 30% was due to the defect. Thus, it is obvious that EBWR could have been operated for long periods of time with only one defect such as that used in Test 2.

d. Conclusions. As a result of these tests the following conclusions may be drawn. They apply to ThO_2-UO_2 ceramic fuels of high density operating under the rather low heat ratings found in these tests. A small defect is presumed to be present in the sheathing.

(1) The main radioactive nuclides which escaped from the defect are fission product gases and the main radioactivities throughout the system are due to these gases or their decay products. The release of radio-iodines is apparently very small, much smaller, for instance, than from fuels made from UO_2.

(2) The rate of release of gases is controlled by a diffusion-type mechanism such that the shorter-lived gases escape through the defect at a much lower rate relative to the longer-lived ones. If R(atom/sec) is the release rate of a fission product gas from the defect, the quotient R/Y, where Y is the fission yield, has been found proportional to $1/\sqrt{\lambda}$ when λ is the decay constant of that fission product gas. The magnitude of R is a very small fraction (~0.01%) of the formation rate of the nuclide.

(3) With one defect present, activities throughout the reactor system are not distinguishably different from those when no defect and only slight amounts of uranium contamination are present. In the reactor steam and even in the condenser, N^{16} activities predominate, and in the reactor water, fission product activities are orders of magnitude lower than those from activation products such as Na^{24}, Mn^{56}, or Co^{58}.

(4) If a defective element is in the close vicinity of a control rod, its presence can be detected by movement of that control rod so that the flux in the defective element is increased. If this is done, a transient increase in activity will be observed on a monitor which is measuring activities in the vicinity of the air ejector.

6.5. VBWR

Activity investigations at VBWR have been described as follows:

1. Nitrogen-16.

At 40 Mw, radiation levels in the turbine building were 6 mr/hr or less except in the immediate vicinity of the condenser and the high pressure end of the turbine.(34) At these points, the level rose as high as 14 mr/hr. Contact levels as high as 100 mr/hr were measured at the air ejector. Gamma spectrometer analysis indicates that this activity is principally N^{16} which disappears almost immediately after shutdown. Experience indicates turbine personnel received less than 30 mr/week in the normal performance of their duties. Levels in the upper sections of the reactor building which are normally entered during operation, ranged up to 6 mr/hr, with levels in the reactor building basement, which was not intended to be accessible during operation, up to a few hundred mr/hr.

After operation, levels outside and inside the turbine casing quickly fall to a fraction of an mr/hr as predicted(191) so that regular maintenance procedures are entirely practical.

2. Fluorine-18.

F^{18} was found to dominate reactor water activity from a few minutes to a few hours after shutdown.(34) This isotope is produced in accordance with the following reaction:(193)

$$O^{18}(p,n)F^{18} - 2.45 \text{ Mev}$$

$$F^{18} \xrightarrow[112 \text{ min}]{\beta+} O^{18}$$

High energy protons necessary for this reaction are produced by moderation of neutrons in water. This isotope was identified by measurement of 0.51 Mev positron annihilation radiation. Well over 98% of all reactor water activity in the VBWR after 2 hours delay was due to F^{18}. The absolute amount of F^{18} in the VBWR system was measured at 12, 17 and 25 Mwt power levels to be 0.05, 0.05 and 0.09 curie per Mwt respectively, or an average of 0.06 ± 0.04 curie per Mwt calculated.(214)

3. Fission Products.

Traces of fission products have been found in the VBWR water, due, it is believed, to surface contamination of the fuel. Since non-gaseous water activities are removed by distillation, noble gases and their daughters predominate in the condenser off-gas system.(34) Noble gas daughters are principally alkali metals, which are readily soluble in water; and most of these activities are short-lived, facilitating decontamination and maintenance of equipment after a fuel failure.

4. Decontamination Factor.

Tests were made to determine the decontamination factor on boiling in the VBWR reactor.(35) In these tests small amounts of NaOH were added to the reactor water and the amount of Na^{24} activity in the steam and reactor water was measured. In this way a DF of 40,000 was found to exist for Na^{24}. But the value dropped suddenly below 100 when the water level in the reactor was allowed to rise too high. Traces of fission products in water, due to surface contamination of fuel, indicated comparable factors for other non-gaseous activities including halogens. Relative water and steam activity levels as measured by the distribution of radioactive isotopes of nonvolatile corrosion products during normal operation have confirmed the magnitude of the decontamination or separation factor for the VBWR as indicated in Table 6.23.

Table 6.23

CORROSION PRODUCT DECONTAMINATION FACTORS IN VBWR

Constituent	Activity Reactor Water $\mu\mu$c/ml	Activity Steam Condensate $\mu\mu$c/ml	Decontamination Factors
Cr^{51}	106	0.01	1×10^4
Mn^{54}	29	0.004	7×10^3
Co^{58}	18	0.006	3×10^3
Fe^{59}	10	0.008	1×10^3

Activities in micro microcuries per milliliter

It was noticed that the DF decreased with increasing time after sampling. This indicated that the foreign material in the steam was not representative of that in the reactor water, but had a lower ratio of short- to long-lived activities than the reactor water. This variation in ratios in VBWR was opposite to that found in the BORAX-III.(192) The latter, however, was heavily influenced by the Na^{24} content originating from the aluminum in the system.

5. High Purity Water.

High purity water, due to use of deionizers, contributes to the low residual activity levels in the VBWR. Condensate enters the reactor through a large mixed bed deionizer while reactor water is purified at a rate sufficient to clean up all the water in the reactor in two hours. The resistivity of the reactor water is generally maintained over one megohm, while the water entering the reactor has a resistivity over 5 megohms.

6. Turbine Activity.

The VBWR turbine was opened after 900 hours and after 3000 hours of operation.(35) The radioactivity changes noted between the two surveys were minor. The activity levels throughout the turbine were low, being on the average about 1-2 mr/hr gamma and 20 mrad/hr beta. The major activities identified were activated corrosion products including Co^{57}, Co^{58}, Co^{60}, Fe^{59}, Mn^{54}, and Cr^{51}. The higher pressure stages showed somewhat higher readings than the low pressure stages. A scan of the surface of the wheels has indicated that the outside surfaces were about three times more radioactive than the center of the wheels.

7. Radioactive Deposits.

The deposition of radioactive nuclides in the VBWR has been studied primarily by means of analysis of the deposits on the coupons exposed to various environments in the reactor.(57) In addition, some gross radiation measurements on specific components and the analysis of samples cut from the reactor piping are reported. Since the primary uncertainty at the time of initiation of the tests was the contamination to be expected in the turbine, the principal effort was directed toward measurement of the contamination in the steam system.

In VBWR, surfaces exposed to reactor water other than fuel, are largely 304L stainless steel. Steam piping and condensate piping are carbon steel. Condenser tubes are phosphorized admiralty metal. Fuel, originally predominantly clad with stainless steel, was gradually replaced with Zircaloy-2 clad fuel, until, when last operated, the core contained about half Zircaloy clad fuel.

Total system activity was found to be very low. For example, instrument ("Cutie Pie") readings after 8000 hours of power operation extending over a two-year period were as follows approximately four months after shutdown:

Turbine surfaces (1,000-20,000 CPM with GM)	1-3 mr/hr;
Steam piping adjacent to reactor (3 in. from 6 in. pipe)	9 mr/hr;
Water piping (3 in. from 2 in. pipe) clean-up system	10-40 mr/hr.

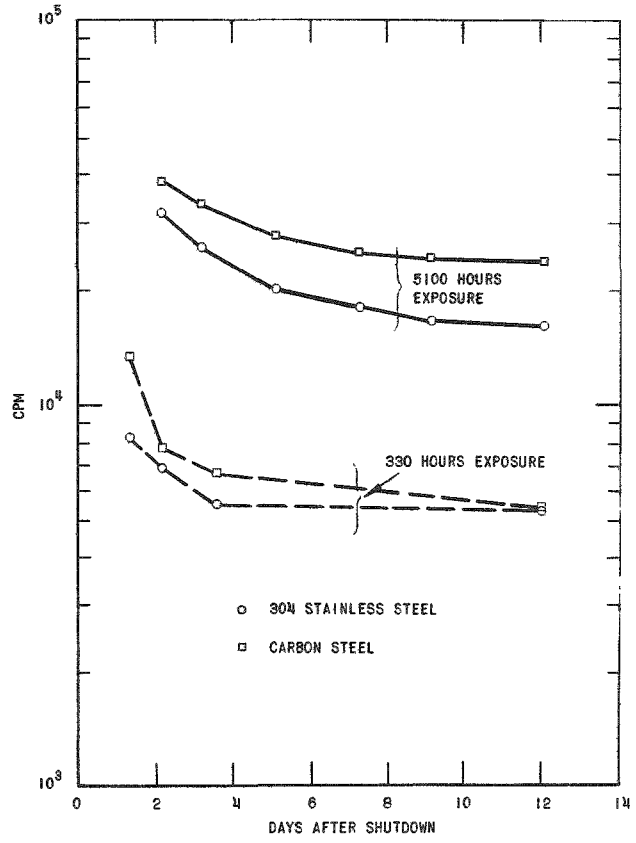

Fig. 6.19

Decay of Deposited Radioactivity in VBWR

Measurements of the gross radioactivity (counts per minute) deposited on coupons in the VBWR main steam line were made in a thin-window proportional counter. Figure 6.19 shows the rate at which this activity decayed, following reactor shutdown. Within the accuracy of the data, there was little difference in the rate of decay after 5100 hours exposure, as compared with the rate after 330 hours exposure. Likewise there was no significant difference in the rate of decay of the activity on stainless steel as compared to that on carbon steel coupons. The rate of decay was slow, and the activity level two weeks after reactor shutdown was about 60% of the level two days after shutdown.

The increase in total deposited contamination in the VBWR with continued exposure is shown in Fig. 6.20. The radiation from these coupons is increasing with approximately the square root of the exposure time. There was little difference between the contamination levels of stainless steel and carbon steel coupons.

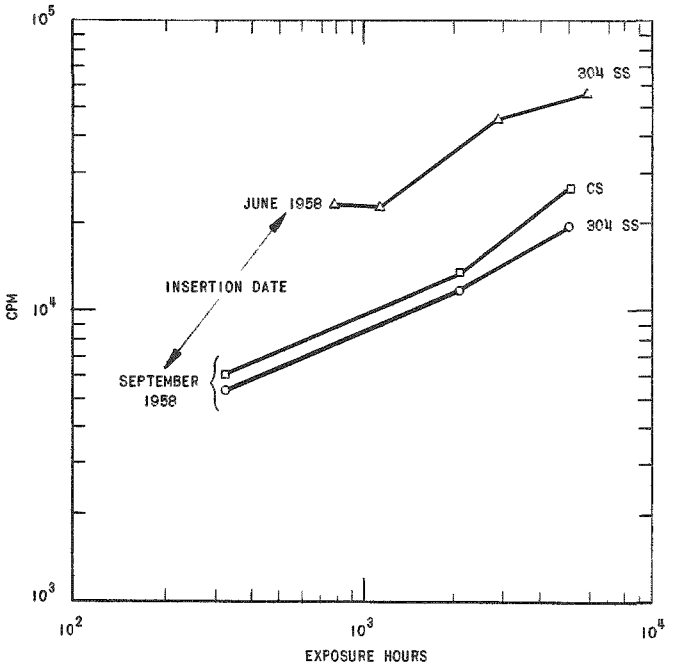

Fig. 6.20

Buildup of Deposited Radioactivity in VBWR

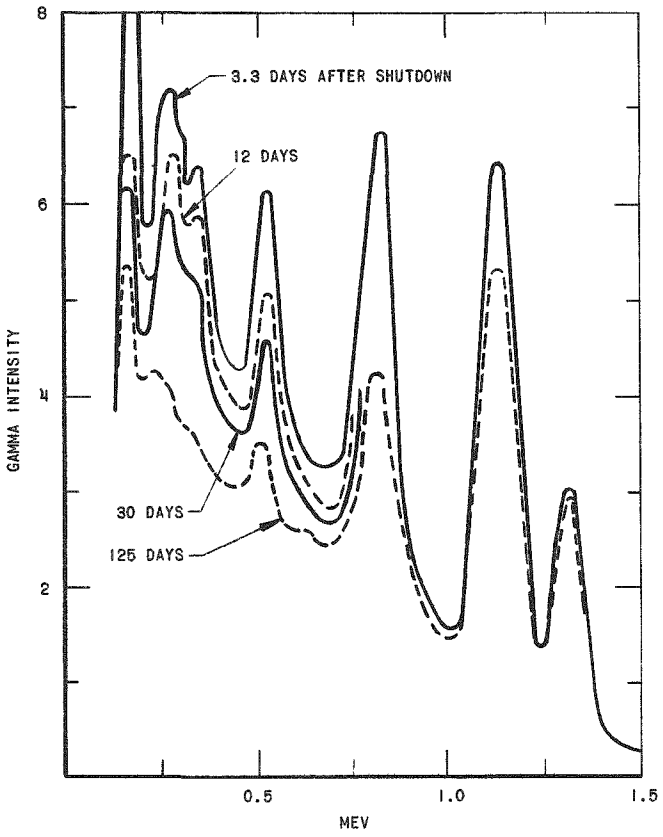

Fig. 6.21

Gamma Spectra of Deposited Radioactivity 5900 hours Exposure in VBWR

The radiochemical compositions of the deposits have been investigated by gamma spectrometer studies and radiochemical analysis. In general, the radioactivity on the steam system walls was similar in composition to that on the water system walls, but of lower level. Typical gamma spectrometer results are shown in Fig. 6.21 for the radioactivity on a coupon from the main steam line. The principal nuclides evident, which have been confirmed by radiochemical analysis, are Co^{60} (1.33 and 1.17 Mev), Zn^{65} (1.12 and 0.51 Mev), Co^{58} (0.81 and 0.51 Mev), Mn^{54} (0.89 Mev), and Cr^{51} (0.31 Mev). The nuclide responsible for the short-lived peak at 0.15 Mev was not positively identified, but was probably Mo-Tc^{99}. In spite of the fact that defected fuel was being tested in the reactor during a significant portion of its recent operation, fission products were not significant in the surface contamination.

A typical radiochemical analysis of the deposited radioactivity (microcuries per cm^2) experienced on the water piping is given in Table 6.24.

Table 6.24

DEPOSITED RADIOACTIVITIES IN VBWR

Nuclide	$\mu c/cm^2$	% Gross Gamma (of Listed Nuclides)
Co^{60}	0.54	69
Co^{58}	0.29	14
Zn^{65}	0.25	7
Mn^{54}	0.016	0.7
Cr^{51}	1.3	2
Fe^{59}	0.11	7
Sr^{90}	4×10^{-5}	0

Note: Activities in microcuries per square centimeter ($\mu c/cm^2$). 3700 hour exposure to reactor water calculated to 2 days after shutdown.

Analysis was made three months after reactor shutdown, so short-lived nuclides could not be determined. Two days after shutdown over 60% of the gross gamma radiation was attributable to the nuclides listed. The major active nuclide on pipe and vessel surfaces was Co^{60} even at this short a period after shutdown.

The relationships between Co^{60} and Zn^{65} concentrations and exposure time were studied by analysis of gamma spectra of coupons in the main steam line. The Co^{60} results are shown in Fig. 6.22. Although the levels of individual coupons varied by factors of up to 5, the increase with time was relatively uniform and proportional to the square root of the exposure time for most of the coupons studied. The Zn^{65} results, in Fig. 6.23, are more variable but show the same general trend.

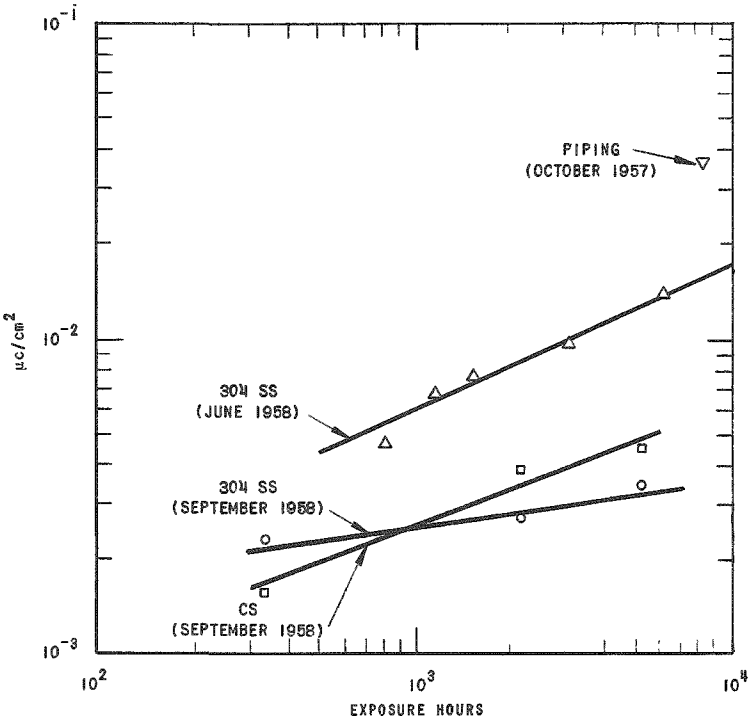

Fig. 6.22

Buildup of Co^{60}. Steam Line Coupons in VBWR

As seen in Figs. 6.22 and 6.23, the degree of surface contamination was less for the same number of exposure hours for coupons inserted later into the reactor. The reason is not completely clear. The extent to which it is attributable to improved steam water separation during recent operation, to reduced corrosion because of improved operating procedures, or to some other cause was to be investigated.

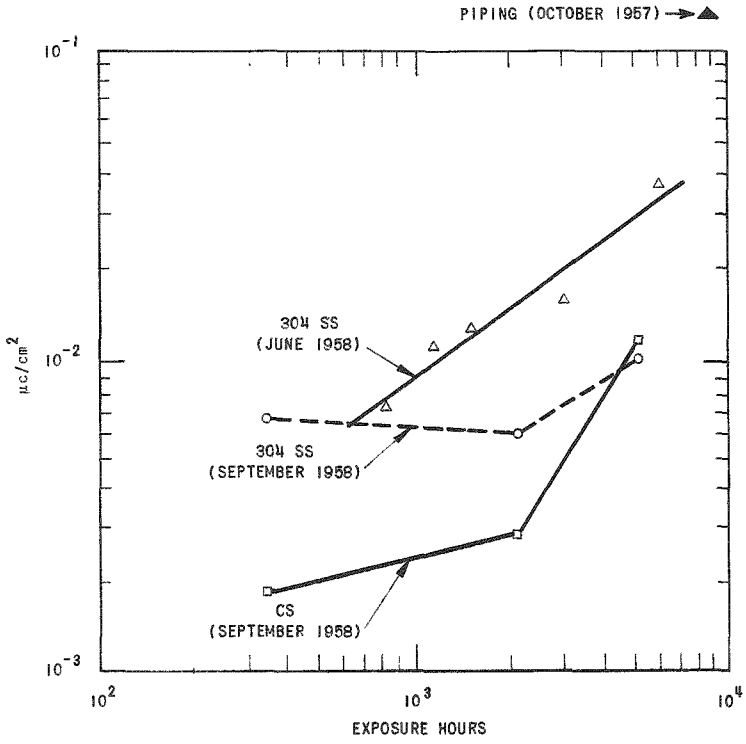

Fig. 6.23

Buildup of Zn^{65}. Steam Line Coupons in VBWR

Coupons exposed to VBWR reactor water were studied much less extensively than those in the steam line. Contamination levels were generally 10 to 100 times those of comparable steam line coupons, as compared to a decontamination factor greater than 10^4 reported for separation of water from steam in the VBWR.(35) The extent to which this small a difference is attributable to excess carryover during abnormal operation or transients requires further study.

The radiation levels observed in the VBWR turbine can serve as only a first approximation of the levels which will be found in other boiling water reactor turbines because of several unevaluated effects. First, the VBWR turbine is preceded by a pressure reducing station and steam purifier in which the initial, most radioactive, condensate is separated. Analysis of coupons in the high- and low-pressure steam lines indicates the contamination in the turbine may be reduced by about a factor of four as a result. Second, excessive carryover of liquid in the steam has occurred in the VBWR during the course of its experimental operation. Also, the steam-water separation provisions in the VBWR are not so elaborate as in full-scale power plants. How much the contamination levels in the steam system and turbine have been increased, as a result, is unknown. Third, the materials of construction and surface-to-volume ratios will undoubtedly be different in another plant. Fourth, the

corrosion rates in the VBWR have probably been greater than in a full-scale plant because of the intermittent operation of the reactor, owing to its experimental program. On balance, these factors provide encouragement that even lower surface contamination levels than observed here may be achieved in turbines of large scale, boiling water reactor plants.

6.6. ALPR (SL-1)

Activity investigations in ALPR were reported by Bailey and Gavin.(33)

1. Nitrogen-16.

In the course of the hydrogen additions to determine the effect on water decomposition described in Sec. 2, the effect on plant activities (essentially N^{16}) was observed. Results are given in Table 6.25. The increased activity resulting from hydrogen addition was similar to that observed in BORAX and EBWR.

Table 6.25

ALPR PLANT ACTIVITIES* DURING HYDROGEN ADDITION

H_2 Rate (%)	Feedwater Pumps		Simulated Heat Load Exchanger		Main Steam Line		Main Steam Line (Bemis panel)	Auxiliary Steam Line	Turbine	
	No. 1	No. 2	Pt. 1**	Pt. 2**	Pt. 1**	Pt. 2**			Pt. 1**	Pt. 2**
0	1.5	1	220	1.2	7	5	28	4.5	5	
32.8	2.2	1.5	300	1.5	15	10	55	12	8.5	4
32.8	4	3.5	700	4	+	17.5	50	+	9	18
26.1	4	4	100	2	8	4	22	6	4	5
51.0	1	2	265	2.5	18	15	55	15	10	11
4.18	4	1	100	1	7	4	25	8		5
11.7	1	1	140	1.5	10	6	24	9	5	7
11.7	2	2	350	2	16	9	55	15	7	8
43.0	2	2	225	2	11	9	55	15	7	9

*In mr/hr

**Points where survey meter readings were taken

2. The Decontamination Factor for Na^{24}.

The decontamination factor (the ratio of the concentration of the given isotope in one phase as compared to the concentration in another phase) between the reactor water and the steam was found to be approximately 1000. This is comparable to the values in BORAX and EBWR. The decay curves for reactor water and steam are given in Figs. 6.24 and 6.25, respectively. At this time the major long-lived activity in the reactor water was Na^{24}, corresponding to 6.27×10^5 dpm/ml.

The decontamination factor across the ion-exchange cleanup loop was found to be essentially infinite for all non-gaseous activities except for what is believed to be 2.6 hr Si^{31}. A decay curve for the effluent of the mixed bed is shown in Fig. 6.26. The presence of Si is not surprising since the fuel plates were silicon bonded, the X-8001 aluminum alloy contains about 0.2% silica as an impurity, and a weakly basic ion exchange resin, which does not remove silica, was used in the mixed resin bed.

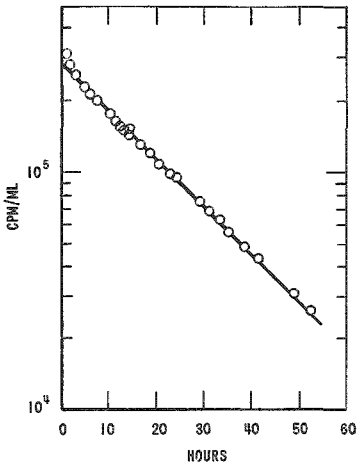

Fig. 6.24
ALPR Reactor Water Decay Curve

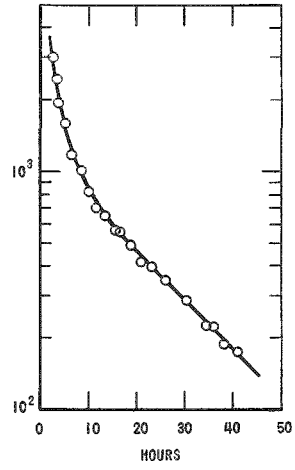

Fig. 6.25
ALPR Reactor Steam Decay Curve

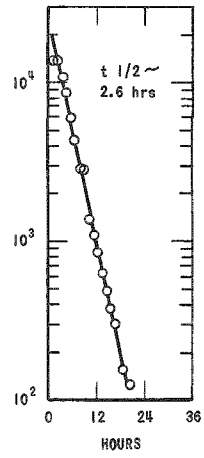

Fig. 6.26
Decay Curve of ALPR Mixed Bed Demineralizer Effluent Water

3. Fission Product Activities.

Fission product activities in the ALPR steam, the effluent gases from the condenser, and the reactor water were investigated by gamma spectroscopy. The following gases were detected in a sample of condensed steam: Xe^{133}, Xe^{135}, Xe^{138}, Xe^{140}, and Kr^{88}.

The emission rates of fission product gases Xe^{138}, Xe^{133}, and Kr^{88} in the exhaust gases leaving the reactor system are shown in Table 6.26.

Table 6.26

EMISSION RATES OF FISSION PRODUCT GASES IN ALPR

Emission Rate		Half Life	Theoretical Ratio of Gas to Xe^{133} if All Gas is Recoiled into Steam	Observed Ratio of Gas to Xe^{133}
Gas	Curies/day			
Xe^{138}	57×10^{-2}	17 minutes	392	41
Xe^{133}	1.5×10^{-2}	5.3 days	1	1
Kr^{88}	7×10^{-2}	168 minutes	25	5

One iodine analysis of the reactor water was made. The result obtained was 1.26×10^3 dpm/ml of I^{131}. Assuming that all of the I^{131} produced was released upon fission of U^{235} and, correcting for the ion exchange cleanup, one finds that approximately 1.4 mg U^{235} was required to produce this quantity of I^{131}. This is in agreement with a value of approximately 1 mg U^{235} to produce the observed Xe^{138}. However, approximately 11 mg of U^{235} are required to produce the observed Xe^{133}.

Part of the fission product activity at least can be accounted for by the presence of tramp* U^{235} on the surface of the fuel, since alpha activity was observed on the fuel elements before they were inserted into the reactor.

Both the I^{131} and Xe^{138} could be present from contamination alone, Kr^{88} and Xe^{133} however, are evolved at much greater rates than would be expected from about 1 mg U^{235} contamination, and would indicate that they are diffusing from some reservoir such as that between a fuel plate and the cladding. The data, however, are too limited to justify a definite conclusion that a defective fuel element was present.

6.7. Dresden

Activity investigations reported on Dresden include the following:

1. Plant Radiation Levels.

Early data on plant radiation levels released after Dresden reached full-power operation(215) are given in Table 6.27. The values indicate that design figures were quite conservative.

Table 6.27

DRESDEN RADIATION LEVELS AT RATED PLANT OUTPUT

Location	Neutron mrem/hr	Radiation Gamma mr/hr
Near air ejector		500
Feedwater heaters (four stages)		~0.5 - 225
Condensate demineralizers (end of cycle)		100
Feedwater pumps		~0.5
Turbine H.P. casing		300
Turbine H.P. front standard		19
Generator collector rings		0.3
Turbine building laydown area		1-4
Condenser (tube sheet)		5
Condenser (below hotwell)		11
Near primary steam line		700
Outside reactor shield (primary and secondary)	~0.5	~0.5
Above reactor top shield	40	175
Below reactor bottom	2000	2000
Steam generator compartment (operating)	~20	1500

*Contamination picked up during manufacturing process.

2. Activities.

Activity in the plant gases was consistently low; the principal activity was N^{13} with a half life of 10.5 min; the amount being about 1800 $\mu c/sec$ at full power. Fission gas release was very low, being about 100 $\mu c/sec$ at full power; all measurements being before holdup prior to stack discharge. (As a basis for comparison, the license limit for discharge of Xe and Kr is 700,000 $\mu c/sec$.)

A typical analysis of the reactor water showed less than 5×10^{-5} $\mu c/ml$ of iodine isotopes with significant half lives (I^{121}-I^{125}).

The subsequent(216) eight-fold increase in noble gas activity was interpreted as indicating a slight leakage of fission products into the reactor water. Confirming this was an increase of I^{135} in reactor water from a value of 120 cpm/ml (counts per minute per milliliter) on October 11, 1960 to 3000 cpm/ml on November 2. This small amount of activity, it was stated, could result either from leakage of a defective in-core fission chamber or from a fuel cladding defect.

A recent report(217) stated that the activity of the reactor water is dominated by the short-lived activation products of the water consisting primarily of N^{16}, N^{13} and F^{18}, which are found in all water-cooled reactors. The long-lived activities in the coolant arise from the activation of corrosion products. The significant corrosion product activities found in the reactor water are Cu^{64}, Co^{58}, Co^{60}, Cr^{51} and Mn^{56}, and are shown in Table 6.28.

Table 6.28

ACTIVATION PRODUCTS IN DRESDEN REACTOR WATER

Isotope	Probable Method of Production	Half Life	Type of Decay	Principal Gamma Energy
Nitrogen-16	O-n-p	7.35 seconds	Beta -	6.13 Mev
Nitrogen-13	O-p-α	10 minutes	Beta +	-
Fluorine-18	O-p-n	112 minutes	Beta +	-
Manganese-56	Mn-n-γ	2.58 hours	Beta -	0.82 Mev
Copper-64	Cu-n-γ	12.8 hours	Beta -	1.34 Mev
Chromium-51	Cr-n-γ	28 days	E.C.	0.32 Mev
Cobalt-58	Ni-n-p	72 days	Beta + E.C.	0.81 Mev
Cobalt-60	Co-n-γ	5.27 years	Beta -	1.33 Mev

These activities, except for Cu^{64}, are found in other water-cooled reactors constructed of similar materials. The source of the copper is the feedwater heaters.

The principal activity present after one day's shutdown is Co^{58}. The source of the nickel is the copper-nickel and monel tubes in the feedwater heaters and the stainless steel in the primary system. Cobalt-60 is attributed to the small amounts of Co^{59} present in the stainless steel. It is of concern because of its long half life. The short-lived corrosion product activities, such as 2.5 hour Mn^{56} and 12.5 hour Cu^{64}, are of lesser concern because of their shorter half lives, but do affect waste discharge, airborne activity due to valve packing leakage and short outage maintenance.

Thus far, radiation levels resulting from deposition of radioactive corrosion products have not unduly restricted maintenance at Dresden.

The reactor recirculating water system is provided with two cleanup demineralizers, each containing 80 cubic feet of mixed resin. In contrast with the condensate demineralizers which are regenerated, the reactor cleanup demineralizer resin is discarded upon exhaustion. The initial cleanup of the reactor system following each startup is accomplished by blow-down to the radioactive waste treatment system. The crud inventory is reduced in the first few days following startup to a turbidity level of less than 10 APHA (American Public Health Association) units. Subsequently, a reactor-water demineralizer is placed in operation at a flow rate of approximately 70,000 pounds per hour. A new charge of resin will further reduce turbidity, but will continue to effectively deionize long after the ability to remove crud is lost. However, once the plant is at load and crud inventories have stabilized, blow-down is no longer needed for control of turbidity.

In an attempt to control copper activity resulting from corrosion of the feedwater heaters, the pH of the secondary feedwater was maintained for two months between 8.5 and 9.0 by the addition of ammonia. The results indicate that while copper remains at a concentration which is barely detectable, nickel pickup has been reduced from 20 ppm to about 8 ppb. Ammonia, which is carried over to the turbine in the secondary steam, is prevented from entering the primary feedwater by the condensate demineralizers.

Investigations have been directed toward securing information on the long-term trends in the various activities in the system, including corrosion products. The specific activities of most of the nuclides were observed to increase rapidly at first, as expected, but have now apparently leveled off, indicating that a state of equilibrium has been reached. The crud has a specific activity of 1.5×10^7 cpm/mg Fe which compares to about 1.0×10^7 cpm/mg Fe for Shippingport at the same core life.

It was pointed out that the amount of copper and nickel pickup in the feed-water system (20 ppb) is extremely small and does not constitute a corrosion problem for the feedwater heaters. However, these small quantities can represent a real crud problem if not removed by cleanup or blowdown of the reactor water.

The major long-lived volatile activities present in the reactor steam are N^{13} and F^{18}. The major short-lived activities are N^{16} and O^{19}. The production rate of these activities has been shown to increase with the amount of air in-leakage, and is proportional to reactor power level. These and other non-condensable gases are carried in the steam and are removed from the condenser by the air ejectors. The total off-gas flow rate is about 20 cubic feet per minute. At this flow rate, approximately a 15-minute delay is afforded by a 450 cubic foot off-gas holdup pipe which reduces the short-lived activities to insignificant levels. The remaining N^{13} release rate varies from 500 $\mu c/sec$ to 1000 $\mu c/sec$. In addition to the N^{13} in the off-gas, a certain amount of noble fission gas accompanies this release. The amount of release thus far has been well within the release rate permitted by the AEC license for Dresden.

6.8. Conclusions

Radioactivity problems in Boiling Water Reactors originate from the same sources as radioactivity problems in other types of water cooled and moderated reactors. Primarily, they result from activation of water components, specifically the oxygen isotopes; activation of air components dissolved in non-deaerated water; activation of raw water impurities present as contaminants; activation of corrosion products; and fission products from fuel exposed to the water.

The phase change between water and steam characteristic of boiling water reactors provides a significant decontamination factor in restricting non-volatile radioactivity to the pressure vessel, and minimizing accessibility hazards in the external primary system. This characteristic affords an outstanding advantage of the boiling water reactor over the pressurized water reactor. It must be kept in mind, however, that excessive carryover or entrainment of water with the steam can reduce the decontamination factor otherwise possible in a boiling water reactor. Design provisions made to minimize this entrainment at higher powers constitute an important phase of Boiling Water Reactor Technology. Another factor that has tended to restrict the spread of fission product activity beyond the pressure vessel in event of cladding failure has been the development of ThO_2-UO_2 ceramic fuels. These mixed-oxide fuels appear to be even better than UO_2 fuels with respect to preventing release of fission products other than the gases.

The N^{16} activity in the steam constitutes the primary source of radiation hazard to personnel with respect to the steam system during reactor operations without fuel defects. The partition of this activity between water and steam has been shown to be a variable, some of the factors being susceptible to control. Although prospects for eliminating N^{16} activity from the steam appear dim, certain chemical additives and water conditions have been found to increase the amount in the steam. If these additives and conditions can be avoided, the amount of N^{16} in the steam can be minimized.

7. REFERENCES

1. A. O. Allen, "Radiation Damage to Water," Am. Inst. Chem. Engrs., Chem. Eng. Progr. Symposium Ser., 50, No. 12, 238-42, (1954).
2. H. O. Monson, "Water Decomposition," Chapter 1.10, Reactor Handbook, Vol. 2, 1st Ed., AECD-3646, May 1955.
3. A. O. Allen, "A Survey of Recent American Research in the Radiation Chemistry of Aqueous Solution," Proc. Intern. Conf. Peaceful Uses of Atomic Energy, Geneva, 1955, 7, 513, United Nations, New York, 1956.
4. R. F. S. Robertson, "The Radiolytic Behavior of Water in a Nuclear Reactor," Progress in Nuclear Energy, Vol. 1, Ser. IV, p. 265, Pergamon Press, New York, 1956.
5. C. J. Hochanadel, "Water Decomposition and Nitrogen Fixation," Reactor Handbook, Vol. 1, 2nd Ed., p. 878, Interscience Publishers, 1960.
6. C. J. Hochanadel, "The Radiation Induced Reaction of Hydrogen and Oxygen in Water at 25°C to 250°C," Proc. Intern. Conf. Peaceful Uses of Atomic Energy, Geneva 1955, 7, 521, United Nations, New York, 1956.
7. J. R. Humphreys, "Effects of Reactor Radiation Upon High Temperature Static Water Systems," Proc. Intern. Conf. Peaceful Uses of Atomic Energy, Geneva, 1955, 7, 583, United Nations, New York, 1956.
8. F. S. Dainton, et al., "Hydrogen Peroxide Formation in the Oxidation of Dilute Aqueous Solutions of Ferrous Sulphate by Ionizing Radiations," Trans. Faraday Soc., 49, 1011, (1953).
9. T. J. Sworski, "Yields of Hydrogen Peroxide in the Decomposition of Water by Cobalt Gamma Radiation. I. Effect of Bromide Ion," J. Am. Chem. Soc. 76, 4687, (1954).
10. J. A. Ghormley, "Lifetime of Intermediates in Water Subjected to Electron Irradiation," Radiation Research, 5, 247, (1956).
11. A. O. Allen, et al., "Decomposition of Water and Aqueous Solutions Under Pile Radiation," ORNL-130, 1949.
12. E. J. Hart, et al., "The Decomposition of Light and Heavy Water Boric Acid Solutions by Nuclear Reactor Radiations," Proc. Intern. Conf. Peaceful Uses of Atomic Energy, Geneva, 1955, 7, 593, United Nations, New York, 1956.
13. H. Fricke and E. J. Hart, "The Oxidation of the Ferrocyanide, Arsenite and Selenite Ions by the Irradiation of Their Aqueous Solutions with X-Rays," J. Chem. Phys. 3, 596, (1935).

14. H. A. Dewhurst, et al., "A Theoretical Survey of the Radiation Chemistry of Water and Aqueous Solutions," Radiation Research, 1, 62, (1954).

15. A. O. Allen, et al., "Decomposition of Water and Aqueous Solutions Under Mixed Fast Neutron and Gamma Radiation," J. Phys. Chem., 56, 575, (1952).

16. R. F. S. Robertson and N. G. Anderson, "Out-reactor Tests of the HTP Loop," CRDC 596 (AECL 195), 1955.

17. S. Gordon and E. J. Hart, "Radiation Decomposition of Water under Static and Bubbling Conditions," Proc. 2nd UN Intern. Conf. Peaceful Uses of Atomic Energy, Geneva, 1958, 3, 13, United Nations, New York, 1958.

18. T. Rockwell, III and P. Cohen, "Pressurized Water Reactor (PWR) Water Chemistry," Proc. Intern. Conf. Peaceful Uses of Atomic Energy, Geneva, 1955, 9, 423, United Nations, New York, 1956.

19. W. H. Zinn, et al., "Operational Experience with the BORAX Power Plant," Nucl. Sci. Eng. 1, 420-437, (1956).

20a. C. B. Zitek, "Study of BORAX-III Reactor Water Conditions during the Two Recent Startups Prior to Anticipated Continuous Operation," Unpublished internal memorandum to J. M. West, December 22, 1955.

20b. C. B. Zitek, "BORAX-III Operational Data during the Three Recent Continuous Runs," Unpublished internal memorandum to J. M. West, April 26, 1956.

21. C. B. Zitek, "Water Technology of EBWR during Initial Operation, TR 13A," EBWR Test Reports, V. Kolba, Ed., ANL-6229, November 1960.

22. R. E. Bailey, "Water Decomposition as a Function of Reactor Power, TR 22", EBWR Test Reports, V. Kolba, Ed., ANL-6229, November 1960.

23. R. E. Bailey, E. W. O'Keefe, "Water Decomposition at Varying Reactor Powers and Pressures, TR 22 A", EBWR Test Reports, V. Kolba, Ed., ANL-6229, November 1960.

24. J. M. Harrer, et al., "Performance Evaluation of Direct Cycle Boiling Water Nuclear Power Plants Based on Recent EBWR and BORAX Data," Proc. 2nd UN Intern. Conf. Peaceful Uses of Atomic Energy, Geneva, 1958, 9, 264, United Nations, New York, 1958.

25. G. E. Goring and A. P. Gavin, "Effect of H_2 Addition to Reactor Feedwater on Radiolytic Decomposition, TR 66," EBWR Test Reports, V. Kolba, Ed., ANL-6229, November 1960.

26. A. P. Gavin, et al., "Water Decomposition in a Direct-Cycle Boiling Water Reactor," Ind. Eng. Chem., 51, 1265, (1959).

27. R. E. Bailey, "Effect of Oxygen Addition on Water Decomposition," Reactor Engineering Division Quarterly Report Section II, April, May, June 1956, ANL-5601, December 1956.

28. P. I. Dolin and B. W. Ershler, "Radiolysis of Water in the Presence of H_2 and O_2 Due to Reactor Radiation, Fission Fragments and X-Radiation," Proc. Intern. Conf. Peaceful Uses of Atomic Energy, Geneva, 1955, 7, 564, United Nations, New York, 1956.

29. A. P. Gavin, Argonne National Laboratory "EBWR Air Ejector Gas Recombiner," June, 1958. (unpublished).

30. J. E. Draley and W. E. Ruther, "Experiments in Corrosion Mechanism: Aluminum at High Temperature," ANL-5658, April 1957.

31. C. B. Zitek, "Phosphoric Acid Addition to Reactor Water in BORAX-IV Reactor," Internal memo, September 24, 1957.

32. G. K. Whitham and R. R. Smith, "Water Chemistry in a Direct-Cycle Boiling Water Reactor," Proc. 2nd UN Intern. Conf. Peaceful Uses of Atomic Energy, Geneva, 1958, 7, 436, United Nations, New York, 1958.

33. R. E. Bailey and A. P. Gavin, "Water Chemistry, Appendix A, Initial Testing and Operation of the Argonne Low Power Reactor (ALPR), E. E. Hamer, Ed., ANL-6084, December 1959.

34. E. Beckjord, et al., "Operation of a High Performance Light Water Boiling Reactor," Proc. 2nd UN Intern. Conf. Peaceful Uses of Atomic Energy, Geneva, 1958, 9, 455, United Nations, New York, 1958.

35. F. J. Brutschy, et al., "Vallecitos Boiling Water Reactor Coolant Technology," Ind. Eng. Chem., 51, 1262-4, (1959).

36. D. C. Vreeland, et al., "Corrosion of Carbon and Low-Alloy Steels in Out-of-Pile Boiling Water-Reactor Environment," Corrosion 17, 269t-276t (1961).

37. J. W. Boyle, et al., "The Decomposition of Water by Fission Recoil Particles," Proc. Intern. Conf. Peaceful Uses of Atomic Energy, Geneva, 1955, 7, 576, United Nations, New York, 1956.

38. R. F. S. Robertson, "Experience With Heavy Water Systems in the NRX Reactor," Proc. Intern. Conf. Peaceful Uses of Atomic Energy, Geneva, 1955, 7, 556, United Nations, New York, 1956.

39. D. M. Wroughton, et al., "Water Technology for Primary Systems in Water-Cooled Power Reactors," Engineering Joint Council, Nuclear Congress, Cleveland, December 12-16 1955, AIChE, Nuclear Engineering, Part IV, 1956.

40. I. H. Welinsky, et al., "Chemistry of a Pressurized Water Nuclear Power Plant: A Review of Two Years Operating Experience," Proc. American Power Conference, 18, 559 (1956).

41. W. T. Lindsay, "Safeguards Aspects of PWR Reactor Coolant Chemistry," WAPD-SC-546, June 1957.

42. C. R. Bergen, "Activity Build-Up Control by High pH Coolant," APAE-MEMO-280, January 1961.

43. "Advanced PWR Study Phase 1," TID-8502, Stone and Webster, Combustion Engineering, 1959.

44. J. B. Vlanovski and Y. M. Karwin, "Crevice Corrosion of Stainless Steel," Zhur. Fiz. Chim 33, 148 (1959).

45. L. H. Vaughn and K. M. Ferguson, "Corrosion of Various Materials in High Temperature Water," BW-5250, June 1957.

46. Paul Cohen, "Shippingport Coolant Technology," WAPD-BT-12, April, 1959.

47. A. L. Medin, Editor, "Literature Survey for Activity Build-Up on Primary System Components," APAE-25, January 15, 1958.

48. C. C. Thomas and H. W. Lacock, "Corrosion Product Transport and Deposition Under Ionizing Radiation," YAEC-93, 1958.

49. D. J. DePaul, Editor, "Corrosion and Wear Handbook," TID-7006, 1957.

50. E. F. Stephan and P. D. Miller, "Solubility of Lithium Hydroxide in Water and Vapor Pressure of Solutions of Lithium Hydroxide Above 200°F," BMI-1329, March 19, 1959.

51. Paul Cohen, "Ammonia Synthesis Test," WAPD-CP-535, 1954.

52. "Shippingport Operations, From Start-Up to First Refueling, December 1957 to October 1959," DLCS-364.

53. R. J. Clark and A. L. Medin, "Corrosion and Water Purity Control For the Army Package Power Reactor," Corrosion, 14, 419-23, (1958).

54. N. R. Grant, "Summary of Corrosion Investigations of High-Temperature Aluminum Alloys, October 1957 to December 1959," ANL-6204, September 1961.

55. "The Experimental Boiling Water Reactor (EBWR)," ANL-5607, 1957.

56. C. R. Breden, et al, "Water Chemistry and Fuel Element Scale in EBWR," ANL-6136, November 1960.

57. E. E. Hamer, Editor, "Design of the Argonne Low Power Reactor (ALPR)," ANL-6076, May 1961.

58. E. E. Hamer, Editor, "Initial Testing and Operation of the Argonne Low Power Reactor (ALPR)," ANL-6084, December 1959.

59. A. Smaardyk, "Reactor Water Systems Analysis (ALPR)," Memo to ANL-RED Distribution, February 10, 1959.

60. N. R. Grant, Appendix IV, "Aluminum-Nickel Alloy Corrosion Testing," Ref. 57.

61. M. E. Gilwood, et al, "Silica Removal Characteristics of Highly Basic Anion Exchangers," Proceedings 12th Annual Water Conf., Engineering Society of Western Pennsylvania, October 22-24, p. 119-130, (1951).

62. L. Wirth, Jr., "The Expected Life of Anion Exchangers," Combustion, 25 49, May 1954.

63. D. W. Danielson, et al., "Corrosion and Contamination in the Vallecitos Boiling Water Reactor." Presented at ANS Meeting, Chicago, Illinois, June 15, 1960.

64. Shippingport Pressurized Water Reactor, Addison-Wesley, 1958.

65. D. M. Wroughton and P. Cohen, "Radioactivity Levels in Pressurized Water Reactor Systems," Proc. 2nd UN Intern. Conf. Peaceful Uses of Atomic Energy, Geneva 1958, 7, 427, United Nations, New York, 1958.

66. A. B. Sisson, et al., "High Flow Rate Demineralization of Condensate for Boiling Water Reactors," Proc. American Power Conf., 20 709-19, (1958).

67. Max Leva, "Correlation in Fixed Bed Systems," Chem. Eng. 64, 245, September 1957.

68. V. A. Elliott, et al., "The Dresden Nuclear Power Station," Proc. 2nd UN Intern. Conf. Peaceful Uses of Atomic Energy, Geneva 1958, 8, 508-534, United Nations, New York, 1958.

69. A. B. Sisson, et al., "Operating Experience With High Flow Rate Condensate Polishing Equipment at Dresden," Proc. American Power Conf., 23 600-610, (1961).

70. C. W. Elston, "First Large Turbine for Operation With a Boiling-Water Reactor," Proc. American Power Conf., 20 248-257, (1958).

71. H. D. Ongman, "Water Treatment Process for the Dresden Nuclear Power Station," Reprint 130, Session X, Nuclear Engineering & Science Conf., March 17-21, 1958, Chicago, Illinois.

72. R. J. Kremer, et al., "Chemical Cleaning of Boiling Water Reactors and Steam-Water System at the Dresden Nuclear Power Station," Proc. Annual Water Conf.,Engr. Soc. of Western Pennsylvania, 21 (1960).

73. Karl Smith, "Stainless Steels," Ch. 23, Reactor Handbook, 2nd Ed. Vol. I., Materials, C. R. Tipton, Jr., Editor, Interscience Publishers, New York, 1960.

74. R. F. Koenig, et al., "Corrosion," Section 2, Ch. 42, Reactor Handbook, 2nd Ed. Vol. I., Materials, C. R. Tipton, Jr., Editor, Intersience Publishers, New York, 1960.

75. T. J. Kettles, Argonne National Laboratory, Personal Communication, March 28, 1962.

76. B. Lustman and F. Kerze, Jr., Metallurgy of Zirconium, McGraw-Hill, 1955.

77. B. Lustman and J. G. Goodwin, "Zirconium and Its Alloys," Ch. 32, Reactor Handbook, 2nd Ed. Vol. I. Materials, C. R. Tipton, Jr., Editor, Interscience Publishers, New York, 1960.

78. R. E. Machery, et al., "Manufacture of Fuel Plates for the Experimental Boiling Water Reactor," ANL-5629, June 1957.

79. J. E. Draley, et al., "The High Temperature Aqueous Corrosion of Uranium Alloys Containing Minor Amounts of Niobium and Zirconium," ANL-5530, April 1957.

80. S. Greenberg, "Corrosion of Irradiated Uranium Alloys," Nuclear Science and Engineering, 6, No. 2, 159, August 1959.

81. J. H. Kittel, et al., "Effects of Irradiation on Some Corrosion - Resistant Fuel Alloys," Nuclear Science and Engineering, 2, 431-449 (1957).

82. J. H. Kittel and S. H. Paine, "Effects of Irradiation on the Corrosion Resistant EBWR Reference Fuel Alloy, U-5 w/o Zr-1.5 w/o Nb," ANL-5639, March 1961.

83. C. R. Breden, "Properties of Fuel Materials," Appendix C of "EBWR, The Experimental Boiling Water Reactor," ANL-5607, May 1957.

84. C. F. Reinke and R. Carlander, "Examination of Irradiated EBWR Core 1 Fuel Elements," ANL-6091, July 1960.

85. N. Balai, "Boron Stainless Steel Development," Reactor Engineering Division Quarterly Report, Section I, October-November-December, 1955, ANL-5561, April 1956; and Section I, January-February-March, 1956, ANL-5571, July 1956.

86. L. C. Hymes and N. Balai, "The Effect of Manganese and Silicon Content on the Hot Workability of Type-304 Stainless Steel Containing 2 w/o Boron," ANL-6393, October 1961.

87. N. R. Grant, "Corrosion of Boron Stainless Steel," unpublished.

88. L. B. Prus, "Hafnium," Ch. 36, Reactor Handbook, 2nd Ed., Vol. I, Materials, C. R. Tipton, Jr., Editor, Interscience Publishers, New York, 1960.

89. W. E. Ruther and N. R. Grant, "Examination of EBWR Dummy Assemblies," ANL Internal Memo, December 9, 1957.

90. W. E. Ruther, "EBWR Dummy Fuel Assemblies," ANL Memo to J. E. Draley, January 29, 1959.

91. N. R. Grant, "Corrosion of EBWR Steam Line Samples," TR-79, EBWR Test Reports, V. Kolba, Ed., ANL-6229, November 1960.

92. Reactor Engineering Division Quarterly Report on the Power Reactor Program, January 1, 1955 through March 31, 1955, ANL-5461, April 1955.

93. N. R. Grant, "Corrosion of Nickel-Plated Steel Specimens," ANL Memo, January 5, 1959.

94. J. M. Harrer and E. A. Wimunc, "EBWR Turbine Blade Failure Summary Report," ANL-5941, November 1958.

95. R. E. Bailey, "Examination of the Kanigen Plating in the EBWR Main Steam Line, TR-58," EBWR Test Reports, V. Kolba, Ed., ANL-6229, November 1960.

96. W. L. Pearl, "Carbon Steel for a Dual Cycle Boiling Water Reactor Plant," GEAP-0812, February 20, 1956.

97. D. E. Tackoff, et al., "Review of Carbon Steel Corrosion Data in High-Temperature, High-Purity Water in Dynamic Systems," WAPD-LSR (C)-134, October 14, 1955.

98. R. U. Blaser and J. J. Owens, "Special Corrosion Study of Carbon and Low Alloy Steels," ASTM Symposium on High Purity Water Corrosion, June 28, 1955. Special Technical Publication No. 179.

99. H. A. Cataldi, et al., "Investigation of Erosion and Corrosion of Turbine Materials in Wet Oxygenated Steam," Trans. A.S.M.E., 80, 1465-1478, October 1958.

100. M. C. Bloom and M. Krulfeld, "Hydrogen Effusion Method for the Determination of Corrosion Rates in Aqueous Systems at Elevated Temperature and Pressure," J. Electrochem Soc., 104, 264-269 (1957); also Corrosion 13 297-302 (1957).

101. D. L. Douglas and F. C. Zyzes, "Corrosion of Iron in High Temperature Water," Corrosion 13 361-374 (1957).

102. C. R. Breden, "Evaluation of Al-Alloys for Reactor Applications." Appendix B, "Study of 40 Pressurized Water, Boiling Water, and Organic Moderated Reactors for Production of Process Steam," ANL-6009, June 1959.

103. J. E. Draley and W. E. Ruther, "Aqueous Corrosion of 2S Aluminum at Elevated Temperatures," ANL-5001, February 1953.

104. J. E. Draley and W. E. Ruther, "Aqueous Corrosion of Aluminum, Part I, Behavior of 1100 Alloy," Corrosion, 12, 441t-448t, September 1956.

105. W. E. Ruther, "Corrosion Experiments with 2S Aluminum at 200°C," ANL-5500, March 1956.

106. J. E. Draley and W. E. Ruther, "Corrosion Resistant Aluminum Above 200°F," ANL-5430, July 1955.

107. J. E. Draley and W. E. Ruther, "Aqueous Corrosion of Aluminum, Part III - Methods of Protection Above 200°C," Corrosion 12, 4805, September 1956.

108. "Reactor Engineering Division Quarterly Report, October 1, 1954 through December 31, 1954, ANL-5371," January 1955.

109. "Reactor Engineering Division Quarterly Report, Section II, April 1, 1955 through June 30, 1955," ANL-5471, September 1955.

110. "Reactor Engineering Division Quarterly Report, Section II, July, August, September, 1955," ANL-5511, January 1956.

111. "Reactor Engineering Division Quarterly Report, Section I, October-November-December, 1955," ANL-5561, April 1956.

112. "Reactor Engineering Division Quarterly Report, Section I, January-February-March, 1956," ANL-5571, July 1956.

113. "Reactor Engineering Division Quarterly Report, Section II, April-May-June, 1956," ANL-5601, December 1956.

114. C. R. Breden and N. R. Grant, "Summary of Corrosion Investigations on High Temperature Aluminum Alloys," ANL-5546, February 1960.

115. R. A. U. Huddle and N. J. M. Wilkins, "The Corrosion of Commercially Available Pure Aluminum in Demineralized Water Between 125°F and 300°F," AERE M/R 1669, May 1955.

116. R. L. Dillon, et al., "High Temperature Aqueous Corrosion of Commercial Aluminum Alloys," HW-37636, January 1956.

117. C. Groot and R. E. Wilson, "The Intergranular Corrosion of Aluminum in Superheated Steam," HW-51797, May 1956.

118. R. A. U. Huddle and N. J. M. Wilkins, "The Resistance of Binary Aluminum Alloys to Corrosion by Water at High Temperatures and Pressures," AERE M/R 1669A, May 1956.

119. F. H. Krenz, "Corrosion of Aluminum Nickel-Type Alloys in High Temperature Aqueous Service," Corrosion, 13, 575t, (1957).

120. N. J. M. Wilkins and C. F. Britton, "Aluminum Alloys Resistant to Water at High Temperatures and Pressures," AERE M/R 1669B, May 1958.

121. Aluminum Alloy Task Group Reports, 1955-1959.

122. F. H. Krenz, et al., "Chalk River Experience with Zircaloy-2 and Aluminum-Nickel-Iron Alloys in High Temperature Water," Proc. 2nd UN Intern. Conf. Peaceful Uses Atomic Energy, Geneva, 1958, 5 241, United Nations, New York, 1958.

123. J. E. Draley, et al., "High Temperature Aqueous Corrosion of Aluminum Alloys," Proc. 2nd UN Intern. Conf. Peaceful Uses Atomic Energy, Geneva, 1958, 5 113, United Nations, New York, 1958.

124. J. E. Draley and W. E. Ruther, "Corrosion Resistance and Mechanical Properties of Aluminum Powder Products," ANL-5927, March 1959.

125. D. E. Johnson and W. H. Ellis, "A Preliminary Study of the Mechanical Properties of M-388 (X-8001), An Aluminum - 1% Nickel Alloy," HW-41859, March 1956.

126. R. S. Kemper and K. F. Powell, "Mechanical Properties of Aluminum Alloy M-388 (X-8001), Effect of Fabrication Variables," HW-54364, January 1958.

127. V. H. Troutner, "High Temperature Aqueous Corrosion Product Films on Aluminum," HW-53389, November 1957.

128. R. L. Dillon and V. H. Troutner, "Observations on the Mechanism and Kinetics of Aqueous Aluminum Corrosion," HW-51849, September 1957.

129. C. Groot and R. M. Peekmea, "The Corrosion of Aluminum and Its Alloys," HW-36692, May 1955.

130. R. J. Lobsinger and J. M. Atwood, "Corrosion of Aluminum Jacketed Fuel Elements in Reactor Cooling Water," HW-47778, January 1957.

131. R. M. Hoag and F. C. Zyzes, "Corrosion of Aluminum in High Temperature Water, Part III - Inhibition of Corrosion by Sodium Silicate," KAPL-1741, February 1957.

132. V. H. Troutner, "Uniform Aqueous Corrosion of Aluminum - Effects of Various Ions," HW-50133, January 1957.

133. J. A. Ayres, "Corrosion Rates of Aluminum in Nuclear Reactors Cooled by High Temperature Water," HW-52844, October 1957.

134. M. D. Ferrier, "Minutes of a Conference on the Corrosion of Aluminum in Water at High Temperatures," Chalk River, Ontario, Canada, December 18 and 19, 1957, CR Met.-700, June 1957.

135. J. E. Draley, S. Greenberg, and W. E. Ruther, "Corrosion of Some Reactor Materials in Dilute Phosphoric Acid," ANL-6206, April 1961.

136. R. E. Bailey, Internal ANL Memorandum to C. R. Breden, August 2, 1957.

137. C. F. Reinke, Internal ANL Memorandum to J. H. Kittel, September 2, 1956.

138. R. J. Lobsinger, "Summary Report on the Corrosion of Aluminum in High-Temperature Dynamic Water Systems," HW-59778 Rev., February 1961.

139. K. Riskevics, "Investigation of the Corrosion Aspects of Selected Aluminum Alloys, Final Report," ACNP-6009, January 1961.

140. J. E. Draley, "Aqueous Corrosion of 1100 Aluminum and of Aluminum-Nickel Alloys," TID-7587, AEC-Euratom Conference on Aqueous Corrosion of Reactor Materials, October 14-17, 1959, p. 165-187.

141. J. E. Draley, W. E. Ruther and S. Greenberg, "Aluminum Alloys with Improved High Temperature Aqueous Corrosion Resistance," J. Nuclear Materials, 6, p. 157-171 (1962).

142. H. C. Bowen, "Development of Corrosion-Resistant Aluminum Alloys for High-Temperature Water Service," HW-68253 March, 1961.

143. M. H. Brown, R. H. Brown, W. W. Binger, "Aluminum Alloys for Handling High Temperature Water;" Preprint for National Association of Corrosion Engineers Meeting, Dallas, March 14-18, 1960.

144. R. L. Dillon, "Dissolution of Aluminum Oxide as a Regulating Factor in Aqueous Aluminum Corrosion," HW-61089 August 31, 1959.

145. J. E. Draley and W. E. Ruther, "The Corrosion of Aluminum Alloys in High Temperature Water," International Atomic Energy Agency Conference on Corrosion of Reactor Materials, Salzburg, June 4-8, 1962 (to be published).

146. D. R. Dickinson, R. J. Lobsinger and R. B. Richman, "Corrosion of Aluminum-Clad Fuel Elements," Research Reactor Fuel Element Conference, Gatlinburg, September 17-19, 1962 (to be published).

147. A. P. Gavin, "Irradiation of an Aluminum Alloy-Clad Ceramic Pellet Fueled Plate," ANL-6143, May 1960.

148. A. P. Gavin and C. C. Crothers, "Irradiation of an Aluminum Alloy-Clad, Aluminum-Uranium Alloy-Fueled Plate," ANL-6180, July 1960.

149. J. H. Kittel, A. P. Gavin, C. C. Crothers and R. Carlander, "Performance of Aluminum-Uranium Alloy Fuel Plates under High Temperature and High Burnup Conditions," Research Reactor Fuel Element Conference, Gatlinburg, September 17-19, 1962 (to be published).

150. C. F. Reinke, et al., "Metallurgical Evaluation of Failed BORAX-IV Reactor Fuel Elements," ANL-6083, May 1961.

151. "SL-1 Accident," Atomic Energy Commission Investigation Board Report, Joint Committee on Atomic Energy, Congress of the United States, June 1961.

152. J. L. English, et al., "The Corrosion of Aluminum Alloys in High Velocity Water at 170° to 290° C," ORNL-3063, June 1961.

153. J. G. Griess, et al., "Effect of Heat Flux on the Corrosion of Aluminum by Water, Part III, Final Report on Tests Relative to the High-Flux Isotope Reactor," ORNL-3230, December 1961.

154. S. C. Datsko, "Metal Transport in Liquid-Water Systems and Effect on Heat Transfer," Trans. A.S.M.E., 78, 1223-7, August 1956.

155. C. Wohlberg and F. Kleimola, "Factors Which Affect Formation and Deposition of Transport Corrosion Products in High-Temperature Recirculation Water Loops," ANL-5195, December 1953.

156. I. H. Welensky, "Corrosion, Transport and Fouling in Water Cooled Reactors," WAPD-C-200, 1957.

157. D. M. Wroughton and D. J. DePaul, "Structural Materials for Use in the Pressurized Water Power Reactor, Nuclear Metallurgy - A Symposium on Behavior of Materials in Reactor Environment," American Inst. of Mining and Met. Engineers, IMD Special Report Series No. 2, 1956.

158. F. W. Pement, "Calculated Deposited Crud Activity in the PWR Primary System Due to Corrosion of Core Materials," WAPD-PWR-CP-2995, 1957.

159. "SM-1 (APPR-1) Research and Development Program, Activity Build-up Program, Task 1, Status Report - February to November, 1958," APAE-Memo 180, 1959.

160. "Long-Lived Circulating Activity in the Army-Package Power Reactors," APAE No. 20, August 28, 1957.

161. "Corrosion Product Activity in the Primary System of the Army-Package Power Reactor," APAE No. 29, April 15, 1958.

162. C. A. Bergmann, "SM-1 Research and Development Program. Long-Lived Induced Activity Buildup During SM-1 Core 1 Lifetime, Task XVIII. Phase I," APAE No. 77, November 1960.

163. W. S. Brown, et al., "SM-1 Research and Development Activity Buildup Program, Task 1, Final Report," APAE-51, August 1959.

164. N. R. Grant, "Measurement of Suspended and Dissolved Solids in EBWR Water, TR-73A," EBWR Test Reports, V. Kolba, Ed., ANL-6229, November 1960.

165. C. B. Zitek, "Deposits on Steam Side of EBWR Condenser and Steam Dryer, 30," EBWR Test Reports, V. Kolba, Ed., ANL-6229, November 1960.

166. E. A. Wimunc, ANL, Internal Memo, Incident Report No. 9, "Startup Heater Leak," June 12, 1958.

167. H. L. Gann, et al., "Turbine Inspection, TR's 36, 53, 53A," EBWR Test Reports, V. Kolba, Ed., ANL-6229, November 1960.

168. E. A. Wimunc, "Radioactive Crud Cleanup in Nozzles Below EBWR Reactor, TR-56," EBWR Test Reports, V. Kolba, Ed., ANL-6229, November 1960.

169. J. F. Matousek, "Modification of the Experimental Boiling Water Reactor (EBWR) For Higher-Power Operation, (Supplement to ANL-5607)," ANL-6552, April 1962.

170. C. B. Zitek, "Deposits From a Fuel Element and Dummy Fuel Elements, TR-29," EBWR Test Reports, V. Kolba, Ed., ANL-6229, November 1960.

171. R. F. S. Robertson, Chalk River, on loan to ANL, personal communication, June 18, 1958.

172. C. F. Reinke, ANL, personal communication, August 1, 1958.

173. K. H. Vogel, Westinghouse Atomic Power Division, personal communication, January 20, 1958.

174. A. P. Gavin, ANL, unpublished.

175. R. E. Bailey, "Flux Plot of N. W. Quadrant of the EBWR Core Loading, No. 46, TR-25A," EBWR Test Reports, V. Kolba, Ed., ANL-6229, November 1960.

176. R. H. Leyse, "Scale on Fuel Elements in EBWR, TR-29A," EBWR Test Reports, V. Kolba, Ed., ANL-6229, November 1960.

177. Ira Charak, "Visual Inspection of EBWR Fuel Assemblies During Core Loading, TR-29D," EBWR Test Reports, V. Kolba, Ed., ANL-6229, November 1960.

178. S. B. Skladzien, ANL, unpublished.

179. T. L. Kettles and N. Balai, "EBWR Reactor Pressure Vessel Changes, Revisions for Instrumentation and Increased Steam Output," USAEC Report ANL-6162, January 1962.

180. R. J. Armani, "Radiochemical Analysis of Samples from EBWR Shock Shield, TR-104," EBWR Test Reports, V. Kolba, Ed., ANL-6229, November 1960.

181. S. Vogler, et al., "Chemical Engineering Division Summary Report for July, August, and September, 1958," ANL-5924, 109-112, December 1958.

182. S. Vogler and H. Tyler, "Chemical Engineering Division Summary Report for October, November, and December, 1958," ANL-5959, 104-108, March 1959.

183. C. R. Breden, "Corrosion Product Deposits in the EBWR," Proceedings of the Tripartite Conference on Transport of Materials in Pressurized - Water Nuclear Systems, G. R. Vavasour, Editor, AECL-1265, June 1961.

184. E. A. Wimunc and J. M. Harrer, "Hazards Evaluation Report Associated with the Operation of EBWR at 100 Mw," ANL-5781 (Addendum), December 1958.

185. J. H. Kittel, Argonne National Laboratory, Personal Communication.

186. Ira Charak, "Removal of EBWR Fuel Element Scale by Slurry Honing," ANL-6216, September 1960.

187. Clarence Jacklin and Harris Thompson, "Experimental Studies of Iron Oxide Deposits in Boilers," Proceedings Midwest Power Conference 12, 108-113 (1950).

188. J. R. Dietrich, et al., "Design and Operating Experience of a Prototype Boiling Water Power Reactor," Proc. Intern. Conf. Peaceful Uses Atomic Energy, Geneva, 1955, 3, 70, United Nations, New York, 1955.

189. C. J. Zitek, "Coolant Activation and Decomposition," Appendix E, "The EBWR Experimental Boiling Water Reactor," ANL-5607, May 1957.

190. S. Untermeyer, "Direct Steam Generation for Power," Nucleonics 12, No. 7, 43-47, July 1954.

191. S. Untermeyer, "With Boiling-Water Reactors, Turbine Contamination Causes Only Small Problem," Nucleonics 13, 8, 52, 54, 56, 58, 60, August 1955.

192. A. J. Shor, et al., "Radioactive Carryover from Borax III and Test Systems," Nuclear Science and Engineering, 2, 126-142, (1957).

193. N. Faull, "An Experimental Study of Neutron Induced Activities in Water," AERE R/R 1919 (1957).

194. T. Rockwell, III, "Reactor Shielding Design Manual," TID-7004, March 1956.

195. R. F. S. Robertson and V. C. Hall, Jr., "Fuel Defect Test - Borax IV," ANL-5862, October 1959.

196. R. F. S. Robertson, "Tests of Defected Thoria-Urania Fuel Specimens in EBWR," ANL-6022, May 1960.

197. J. D. Eichenberg, et al., "Effects of Irradiation on Bulk UO_2," WAPD-183, October 1957.

198. J. A. L. Roberson, et al., "Behavior of Uranium Oxide as a Reactor Fuel," Paper No. 193, Proc. 2nd UN Intern. Conf. Peaceful Uses Atomic Energy, Geneva 1958, 6, 655, United Nations, New York, 1958.

199. C. B. Zitek, "Plant Radiation Levels, TR-7," EBWR Test Reports, V. Kolba, Ed., ANL-6229, November 1960.

200. S. J. Goslovich, et al., "Scintillation Counter Analysis of EBWR Radioactivity," Nucleonics, 16, No. 5, 94-97, (1958).

201. R. F. S. Robertson, "First Defect Test in EBWR, TR-55", EBWR Test Reports, V. Kolba, Ed., ANL-6229, November 1960.

202. P. A. Roys and K. Shure, "Production Cross Sections of N^{16} and N^{17}," Nuclear Science and Engineering, 4, 536-545, (1958).

203. W. J. Henderson, P. R. Tunnecliffe, "The Production of N^{16} and N^{17} in the Cooling Water of the NRX Reactor," Nuclear Science and Engineering, 3, 145, (1958).

204. J. Barrett and H. Cadoff, "Reactor Steam Purity by Radioactive Sodium Tracer, TR-37," EBWR Test Reports, V. Kolba, Ed., ANL-6229, November 1960.

205. H. C. Martin, "Cross Sections for the O^{16} (n,p) N^{16} Reaction from 12 to 18 Mev," Physical Review, 93, No. 1, 498-499, (1954).

206. J. R. Stehn, "Table of Radioactive Nuclides," Nucleonics, 18, No. 11, 186, (1960).

207. W. H. Zinn, "Heterogeneous Power Reactors," Nucleonics, 12, No. 12, 54, December 1954.

208. A. Gibson and N. A. Kershaw, "Prediction of N^{16} Gamma Activity in the Experimental Boiling Water Reactor, TR-34," EBWR Test Reports, V. Kolba, Ed., ANL-6229, November 1960.

209. M. H. Theys and R. L. Mittle, "Distribution of N^{16} in EBWR, TR-34A," EBWR Test Reports, V. Kolba, Ed., ANL-6229, November 1960.

210. R. L. Mittle and M. H. Theys, "N^{16} Concentration in EBWR," Nucleonics, 19, No. 3, 81 (1961).

211. R. L. Mittle and M. Theys, "Water Level Measurements in the Reactor Vessel, TR-62, -62A, -62B," EBWR Test Reports, V. Kolba, Ed., ANL-6229, November 1960.

212. F. J. Brutschy and R. N. Osborne, "Release of Fission Products From Uranium Dioxide Fuel," Trans. American Nuclear Society, 2, No. 2, Paper 10-13, November 1959.

213. P. W. Frank, "Evaluation of the Fission Product Activities in the Primary Coolant of Shippingport," Bettis Technical Review, WAPD-BT-12, April 1959.

214. J. L. Russel, Jr. and B. F. Rider, "Fluorine-18 Production in Water Moderated Reactors," Trans. American Nuclear Society, 1, No. 1, 36, June 1958.

215. "Dresden, Full Power Operation," Nuclear Eng. 5, 440-441, (1960).

216. "Dresden Nuclear Power Station, First Quarterly Report of Station Operation," NP-9793, January 25, 1961.

217. G. L. Redman, "Power Generation Statistics, Load Schedules, and Water Chemistry," (Dresden) Presented at the 24th Annual Meeting of the American Power Conference, March 27-29, 1962.